



**Power Quality Improvement in the Distribution
Network using Optimization of the Hybrid Distributed
Generation System**

Mohammad Jafar Hadidian Moghaddam

A thesis is submitted in fulfillment of the requirements of the degree of

Doctor of Philosophy

March- 2021

Principal Supervisor: Professor Akhtar Kalam

Co-supervisor: Associate Professor Juan Shi

Institute for Sustainable Industries and Liveable Cities
College of Engineering and Science
Victoria University

Abstract

Due to increase in population growth and industrialization process, energy requirements have multiplied. Because of gradual depletion of energy sources resulting from fossil fuels as well as low efficiency and environmental concerns arising from these sources, much attention has been paid to the use of renewable energy sources. The use of resources such as wind and sun that are nominated as clean energy sources has been examined. However, due to the uncertainty of solar radiation and wind speed, their energy production has an unpredictable nature. Therefore, renewable energy resources are used appropriately to form a hybrid system consisting of wind turbines and solar arrays that meets network requirements. A group of power generation systems that are supplied from different sources are known as Hybrid Distributed Generation (HDG). In other words, they work together as complementary group and connect to the distribution network in both the stand-alone and grid-connected ways to supply the load. The presence of DGs in the distribution network has advantages and disadvantages. Voltage support, power loss reduction and reliability improvement are some of the benefits of DGs if their site and size are properly selected in the distribution network. On the other hand, Power Quality (PQ) problem can be defined as any power problem manifested in voltage, current or frequency deviations that fails to meet the requirements of customer equipment. Poor PQ causes tremendous financial losses in deregulated power systems. Today's electric power systems are connected to many non-linear loads. One PQ problem is harmonic distortion, which is the result of the presence of non-linear loads in the network. Harmonics can cause improper performance in protective equipment, such as relays and fuses. Furthermore, due to the generated heat by the harmonic currents, many consumers and distribution companies are sometimes forced to decrease the amount of output from the transformers. Determination of appropriate location and optimal size of HDG in the distribution network is a main challenge in the changing regulatory and economic scenarios.

In this thesis, design and placement of a HDG based on photovoltaic (PV) panel, wind turbines and battery storage (PVWTBAHDG) is proposed to improve the loss reduction and PQ in an unbalanced 33-bus radial distribution network. Further, in this research, improvement of voltage sag, voltage swell, Total Harmonic Distortion (THD) and voltage

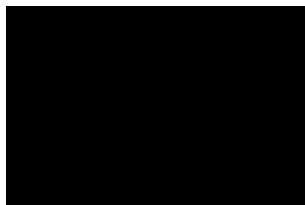
unbalance are considered as PQ indexes. The HDG system is designed to supply a residential load and it is able to inject its excess power into the distribution network. The PVWTBAHDG system has been designed to minimize the energy generation costs including initial investment costs and maintenance and operation costs. Therefore, the site and size of PVWTBAHDG components are optimally determined considering the total objective function of the system which includes decreasing the losses, reducing the cost of energy generation by the HDG and improving the power quality indexes. In this research, based on the social and intelligent behavior of crows, a hybrid meta-heuristic method named Crow Search Algorithm-Differential Evolution (HCSADE) is proposed to determine the location and size of PVWTBAHDG components in the network. In order to avoid the Crow Search Algorithm (CSA) from trapping in the local optima and increase the convergence speed of the algorithm, the crossover and mutation operators of the Differential Evolution (DE) method are employed to improve the CSA performance. Simulations have been implemented in several scenarios of single and multi-objective optimizations. Multi-objective results are obtained by compromising the results of single-objective optimization. The simulation results show that the HCSADE method presents a desirable performance in optimal sizing and siting the PVWTBAHDG in the network and also causes loss reduction and PQ improvement. The superiority of the HCSADE is confirmed in comparison with CSA and DE methods in terms of better objective function. Moreover, the results prove that increasing the number of PVWTBAHDG causes further reduction in the PQ indices and losses.

Student Declaration

“I, Mohammad Jafar Hadidian Moghaddam, declare that the PhD thesis entitled Power Quality Improvement in the Distribution Network using Optimization of the Hybrid Distributed Generation System is no more than 80,000 words in length including quotes and exclusive of tables, figures, appendices, bibliography, references and footnotes. This thesis contains no material that has been submitted previously, in whole or in part, for the award of any other academic degree or diploma. Except where otherwise indicated, this thesis is my own work”.

“I have conducted my research in alignment with the Australian Code for the Responsible Conduct of Research and Victoria University’s Higher Degree by Research Policy and Procedures.

Signatur



Date: 15/03/2021

Acknowledgements

“In the name of God”

Firstly, I would like to thank my supervisors Professor Akhtar Kalam and Associate Prof. Juan Shi for their consistent support and guidance during the running of my Ph.D study and related research, for their patience, motivation, and immense knowledge. Their guidance helped me in all the time of research and writing of this thesis.

I gratefully acknowledge the Australian Government Research Training Program (RTP) stipend scholarship received towards my PhD from Victoria University.

I am also thankful to the College of Engineering and Science of Victoria University and all its member's staff for all the considerate guidance.

To conclude, I cannot forget to thank my father and mother (**God rest their soul**) for supporting me spiritually throughout my life in general.

Table of Contents

Contents

Abstract	ii
Student Declaration	iv
Acknowledgements	v
Table of Contents	vi
Authorship Declaration: Co-Authored Publications	xix
List of tables	xxiv
List of figures	xxviii
List of Abbreviations	xxxiii
Chapter1. Introduction	1
1.1 Motivation	2
1.2 Research Objectives	3
1.3 Scientific Contribution	4
1.4 Thesis outline	6
Chapter2. Literature Review	8
2.1 Introduction	9
2.2 Distribution network	9
2.3 Distributed generation (DG).....	12
2.3.1 DG application in the distribution network.....	14
2.3.2 Distributed generation benefits	14
2.3.3 Distributed generation limitations	15
2.3.4 DG types.....	17

2.3.4.1 Micro-turbine	17
2.3.4.2 Diesel generator	17
2.3.4.3 Photovoltaic cell.....	17
2.3.4.4 Wind turbine.....	18
2.3.4.5 Fuel cell.....	19
2.3.4.6 Geothermal energy	19
2.3.4.7 Biomass.....	20
2.3.5 DG effects	20
2.3.5.1 The effects of DGs on power flow components.....	22
2.3.5.1.1 The effect of DGs online currents	23
2.3.5.1.2 The effect of DGs on voltage profile	24
2.3.5.1.3 The effect of DGs on network loss.....	26
2.3.5.2 The effect of different operation modes of DGs on power flow	26
2.3.5.2.1 Constant power factor operation mode	26
2.3.5.2.1 Voltage control mode.....	27
2.3.5.3 The effect of DG on voltage regulation devices.....	29
2.3.5.3.1 Control method	30
2.3.5.3.2 Tap adjustment.....	30
2.3.5.4 The effect of DG on capacitors	32
2.3.5.4.1 Reactive power flow	32

2.3.5.4.2 Capacitor control methods	33
2.3.5.5 The effect of DG on voltage regulators.....	33
2.3.6 Study of different loadings in the network.....	34
2.3.6.1 Without DGs and with maximum loading	34
2.3.6.2 With DGs and with maximum loading	35
2.3.6.3 With DGs and with minimum loading	35
2.3.7 DG application in distribution system based on optimization algorithm .	35
2.3.7.1 Particle Swarm Optimization (PSO)	36
2.3.7.2 Genetic Algorithm (GA)	38
2.3.7.3 Ant Colony Optimization (ACO).....	39
2.3.7.4 Artificial Bee Colony Algorithm (ABC).....	40
2.3.7.5 Fireworks Algorithm (FWA)	41
2.3.7.6 Backtracking Search Optimization Algorithm (BSOA).....	41
2.3.7.7 Ant Lion Optimizer (ALO)	41
2.3.8 Analysis of Power Quality (PQ) Features with DGs in the network.....	42
2.3.8.1 PQ problems in distribution systems with DGs	43
2.3.8.1.1 Gradual changes in the voltage	43
2.3.8.1.2 Flicker and rapid changes in voltage.....	45
2.3.8.1.3 Harmonics and inter harmonics	46
2.3.8.1.4 Power flow and power loss	48
2.3.8.1.5 Short circuit current.....	49

2.3.8.1.6 Analysis of ubalance	49
2.3.9 Determining the maximum power generation by DGs in radial distribution systems considering harmonics limitations.....	50
2.4 HDG design as renewable energy system	53
2.4.1 Graphic structure	54
2.4.2 Probabilistic approach.....	55
2.4.3 Deterministic Method.....	55
2.4.4 Iterative Approach.....	55
2.4.5 Artificial Intelligence (AI)	55
2.4.6 Literature Review on HDG design.....	56
2.5 HDG application in the distribution system.....	59
2.6 Limitation of previous studies and how the proposed work will overcome this.....	60
2.7 Conclusion.....	60
Chapter3. Design of Photovoltaic panel/Wind Turbine/Battery Hybrid Distributed Generation (PVWTBAHDG) system.....	61
3.1 Introduction	62
3.2 HDG system.....	62
3.3 Types of HDG system.....	62
3.3.1 PVBAHDG System.....	62
3.3.2 WTBHDG System	63
3.3.3 PVWTBAHDG System	64
3.4 Storage system in HDG system.....	66
3.5 Design of PVWTBAHDG renewable energy system	66

3.6 Objectives in PVWTBAHDG system designing.....	67
3.6.1 Loss of Power Supply Probability (LPSP).....	67
3.6.2 Expected Energy Not Supplied (EENS).....	68
3.6.3 Levelized Cost of Energy (LCE).....	68
3.6.4 Net Present Value (NPV)	69
3.6.5 Annualized Cost of System (ACS).....	69
3.7 Optimization of HDG system using PSO Algorithm	69
3.8 Optimization of the HDG System using the Big-Bang Algorithm.....	73
3.9 Optimization methods in PVWTBAHDG system designing	78
3.10 Conclusion.....	80
Chapter 4. Concepts and Definitions of Power Quality (PQ) in the Distribution Network	81
4.1 Introduction	82
4.2 PQ Definition	83
4.3 PQ =Voltage quality.....	86
4.4 A general classification of PQ problems.....	86
4.5 Transients	87
4.5.1 Impulsive transient.....	87
4.5.2 Oscillatory transient wave.....	90
4.6 Long-duration voltage oscillations.....	91
4.6.1 Long-duration overvoltage.....	92
4.6.2 Long-duration under-voltage.....	93
4.6.3. Sustained interruptions.....	93

4.7. Short-duration voltage oscillations.....	93
4.7.1 Short-duration interruption.....	93
4.7.2 Sag.....	94
4.7.2.1 Magnitude and duration of sag.....	95
4.7.2.2 Impacts of voltage sag.....	96
4.7.3 Voltage swell.....	96
4.8 Voltage unbalance.....	98
4.9 Waveform distortion.....	99
4.9.1 DC offset.....	100
4.9.2 Harmonics.....	100
4.9.2.1 Harmonic generation sources.....	101
4.9.2.2 Adverse effects of harmonics.....	103
4.9.3 Interharmonics.....	104
4.9.3.1 Interharmonics generation sources.....	104
4.9.3.2 Interharmonic effects.....	105
4.9.4 Notching.....	105
4.9.5 Noise.....	106
4.10 Voltage fluctuation.....	106
4.10.1 Causes of voltage fluctuation.....	108
4.10.2 Effects of voltage oscillation.....	108
4.11 Power frequency oscillation.....	109

4.12 PQ terminology	110
4.13 Main indexes of PQ.....	116
4.13.1 Voltage sag and interruption	116
4.13.1.1 Causes of voltage sag	118
4.13.1.1.1 Voltage sag arising from short circuit	118
4.13.1.1.2 Voltage sag arising from motor starting.....	119
4.13.1.2 Estimation of different voltage sag characteristics.....	120
4.13.1.2.1 Estimation of the voltage sag amplitude arising from motor starting with a complete voltage	120
4.13.1.2.2 Estimation of the voltage sag arising from short circuit	120
4.13.1.2.2.1 Voltage sag amplitude.....	120
4.13.1.2.2.2 Duration of voltage sag	122
4.13.1.2.2.3 Voltage sag occurrence frequency	122
4.13.1.2.2.4 Vulnerability zone.....	123
4.13.1.2.2.5 Classification of voltage sags.....	123
4.13.1.3 The sensitivity of equipment to voltage sag	124
4.13.1.4 The relationship between voltage sag and equipment operation	125
4.13.1.4.1 Reporting voltage sags	126
4.13.1.4.1.1 The number of phases	126
4.13.1.4.1.2 Reclosing issue.....	127

4.13.1.4.1.3 Voltage sag duration	128
4.13.1.4.2 Coordination curves of the voltage sag	128
4.13.2 Long-term voltage variations, voltage unbalance and frequency deviations	128
4.13.2.1 Long-term voltage variations	128
4.13.2.1.1 The roots of long-term voltage variations	128
4.13.2.1.2 Principles of voltage regulation	129
4.13.2.1.3 Voltage regulation equipment	129
4.13.2.1.3.1 Step-voltage regulators.....	130
4.13.2.1.3.2 Ferro-resonance transformers.....	130
4.13.2.1.3.3 Electronic regulator	131
4.13.2.1.3.4 Motor-generator set.....	132
4.13.2.1.3.5 Static Var Compensators (SVCs).....	132
4.13.2.1.3.6 Capacitors for voltage regulation	133
4.13.2.1.4 The allowed range of long-term voltage variations	134
4.13.2.2 Voltage unbalance	134
4.13.2.2.1 The causes of voltage unbalance	134
4.13.2.2.2 The effects of voltage unbalance.....	135
4.13.2.2.2.1 The effects on the normal operation of three-phase motors	135

4.13.2.2.2.2 The effects on the operation of contactors	135
4.13.2.2.2.3 The effect on the safety of customers... 135	
4.13.2.2.2.4 The effect on power loss	136
4.13.2.2.3 The allowed range of voltage unbalance on buses	136
4.13.2.2.4 Voltage unbalance measurement method and determining its index.....	136
4.13.2.3 Frequency deviations	136
4.13.2.3.1 Damages to turbo-generators	137
4.13.2.3.2 Frequency control systems.....	137
4.13.2.3.2.1 Frequency control under normal conditions.....	137
4.13.2.3.2.2 Frequency control under emergency conditions.....	137
4.13.2.3.3 Adopting control decisions	138
4.13.2.3.4 The effect of frequency changes on the equipment available on LV systems	139
4.13.2.3.5 Allowed frequency range	139
4.13.3 Voltage of flicker	139
4.13.3.1 Causes of voltage flicker.....	139
4.13.3.2 Methods of determining flicker index.....	139
4.13.3.2.1 The SCVD index	140
4.13.3.2.2 Equivalent 10-Hz flicker-meter.....	140

4.13.3.2.3 The IEC flicker-meter	141
4.13.3.3 The allowed range of flicker at different voltage levels.....	141
4.13.4 Harmonics	141
4.13.4.1 An introduction to harmonics.....	141
4.13.4.2. Harmonic distortion	143
4.13.4.3 Current and voltage distortion.....	145
4.13.4.4 RMS values and the THD	147
4.13.4.5 Power and power factor	148
4.13.4.6 Third-order harmonics	151
4.13.4.7 Harmonic sources.....	153
4.13.4.7.1 Arcing equipment.....	154
4.13.4.7.2 Saturable elements	155
4.13.4.8 The effect of harmonic distortion on the operation of equipment and power system.....	156
4.13.4.8.1 The effects on capacitors.....	157
4.13.4.8.2 The effects on transformers.....	157
4.13.4.8.3 The effects on motors.....	160
4.13.4.8.4 Telecommunication interferences	161
4.13.4.9 Identifying the locations of harmonic sources	162
4.13.4.10 Harmonic study methods.....	163
4.13.4.10.1 Symmetric components.....	164

4.13.4.10.2 Modeling of harmonic sources.....	166
4.13.4.10.3 Computer programs for harmonic calculations..	167
4.13.4.10.4 Capabilities of harmonic analysis programs	169
4.13.4.11 General principles and requirements for harmonics.....	169
4.13.4.11.1 The accumulate effect of harmonics	171
4.13.4.11.2 Acceptable harmonic production level for customers	173
4.13.4.12 Regulations of some countries on accepting harmonic producing customers	174
4.13.4.12.1 Germany.....	174
4.13.4.12.2 Australia.....	175
4.13.4.12.3 England	175
4.14 Conclusion.....	177
Chapter 5. Problem Formulation.....	178
5.1 Introduction.....	179
5.2 Problem Formulation.....	179
5.2.1 HDG System Modeling.....	179
5.2.2 Objective Function.....	181
5.2.3 Constraints.....	184
5.3 Suggested Optimization Technique	185
5.3.1 Overview of Proposed Hybrid Crow Search Algorithm Differential Evolution (HCSADE).....	185

5.3.2 Using HCSADE for Problem Solution.....	189
5.4 Conclusion.....	191
Chapter6. Simulation Results and Discussions	192
6.1 Introduction.....	193
6.2 Simulation Results	193
6.2.1 The Proposed Distribution System.....	193
6.2.2 Load, Solar and Wind Profile.....	193
6.2.3 Technical and Economic Data of HDG.....	196
6.2.4 Simulation Scenarios.....	197
6.2.4.1 Results of Scenario 1 (Single objective-one HDG)	198
6.2.4.2 Results of Scenario 2 (Multi objective-one HDG).....	208
6.2.4.3 Results of Scenario 3 (Comparison the single and multi- objective results-one HDG).....	213
6.2.4.4 Results of Scenario 4 (Multi objective designing-two HDGs).....	215
6.2.4.5 Results of Scenario 5 (Comparison of the results-one and two HDGs)	219
6.2.4.6 Results of Scenario 6 (Performance evaluation of HCSADE).....	219
6.2.4.7 Results of Scenario 7 (Impact of HDG load decreasing-one HDG).....	222
6.2.4.8 Results of Scenario 8 (Impact of network load increasing-one HDG).....	223
6.2.4.9 Results of Scenario 9 (Multi objective designing-HDG combinations).....	223

6.2.4.10 Results of Scenario 10 (Impact of battery cost variations-one HDG).....	224
6.2.4.11 Results of Scenario 11 (Impact of battery cost variations-two HDG).....	232
6.2.4.12 Results of Scenario 12 (Superiority of HCSADE to past researches).....	241
6.3 Conclusion.....	241
Chapter7. Conclusion and suggestion	243
7.1 Conclusion.....	244
7.2 Suggestion for future work.....	247
References	248

Authorship Declaration: Co-Authored Publications

This thesis contains work that has been published and prepared for publication.

Details of the work:
Moghaddam, M. J. H., Kalam, A., Shi, J., Nowdeh, S.A., Gandoman, F.H. and Ahmadi, A., 2020. A new model for reconfiguration and distributed generation allocation in distribution network considering power quality. IEEE Systems Journal, p. 1-9.
Location in thesis: Chapters: 5, 6
Student contribution to work:
This article proposed a new model for reconfiguration and distributed generation (DG) allocation in the distribution network by considering network loss reduction and power quality improvement. The objective function aims to minimize losses and improve power quality indices by using the new antlion optimizer (ALO) algorithm.
Co-Authored signatures and dates:

Details of the work:
Moghaddam, M.J.H., Kalam, A., Nowdeh, S.A., Ahmadi, A., Babanezhad, M. and Saha, S., 2019. Optimal sizing and energy management of stand-alone hybrid photovoltaic/wind system based on hydrogen storage considering LOEE and LOLE reliability indices using flower pollination algorithm. Renewable Energy, 135, pp.1412-1434.
Location in thesis: Chapters: 5,6
Student contribution to work:
In this paper, the optimal design and energy management of the hybrid systems including PV panels, WT and fuel cell (FC) based on hydrogen storage (HS) (PWFHS) are presented to minimize the total net present cost (TNPC) using intelligent flower pollination algorithm (FPA). The reliability indices that are considered simultaneously as technical constraints are the loss of energy expected (LOEE) and the loss of load expected (LOLE).
Co-Authored signatures and dates:

<p>Details of the work:</p> <p>Moghaddam, M.J., Kalam, A., Shi, J. and Gandoman, F.H., 2018. A Model for Reconfiguration and Distributed Generation Allocation Considering Reduction of Network Losses. Journal of Scientific & Industrial Research, 77, pp. 615-620.</p>
<p>Location in thesis: Chapters 5, 6</p>
<p>Student contribution to work:</p> <p>This paper proposes a new model for reconfiguration and distributed generation allocation in distribution network to reduce network losses. The objective function minimizes power loss by using the new Ant Lion Optimizer (ALO) algorithm. The proposed reconfiguration has been investigated on the unbalanced 33-bus IEEE network with and without Distributed Generation Sources (DGRs) as well as the use of capacitors.</p>
<p>Co-Authored signatures and dates:</p>

<p>Details of the work:</p> <p>Hadidian Moghaddam, M.J., Kalam, A., Miveh, M.R., Naderipour, A., Gandoman, F.H., Ghadimi, A.A. and Abdul-Malek, Z., 2018. Improved voltage unbalance and harmonics compensation control strategy for an isolated microgrid. Energies, 11(10), p.2688.</p>
<p>Location in thesis: Chapters 5, 6</p>
<p>Student contribution to work:</p> <p>This paper suggests an enhanced control scheme for a four-leg battery energy storage systems (BESS) under unbalanced and nonlinear load conditions operating in the isolated microgrid. Simplicity, tiny steady-state error, fast transient response, and low THD are the main advantages of the method. Firstly, a new decoupled per-phase model for the three-phase four-leg inverter is presented.</p>
<p>Co-Authored signatures and dates:</p>

<p>Details of the work:</p> <p>Naderipour, A., Abdul-Malek, Z., Miveh, M.R., Hadidian Moghaddam, M.J., Kalam, A. and Gandoman, F., 2018. A harmonic compensation strategy in a grid-connected photovoltaic system using zero-sequence control. <i>Energies</i>, 11(10), p.2629.</p>
<p>Location in thesis: Chapters 5, 6</p>
<p>Student contribution to work:</p> <p>This paper deals with the control method of a three-phase Grid-Connected Inverter (GCI) PV system, which is based on the zero-sequence current adjuster. The proposed method is capable of removing the harmonic current and voltage without using any active and passive filters and without the knowledge of the microgrid topology and also impedances of distribution bands and loading conditions.</p>
<p>Co-Authored signatures and dates:</p>

<p>Details of the work:</p> <p>Moghaddam, M.H., Kalam, A., Shi, J., Miveh, M.R. and Peidaee, P., 2017, November. Supplying the load by the optimization of a stand-alone hybrid power system using firefly algorithm considering reliability indices. In 2017 Australasian Universities Power Engineering Conference (AUPEC) (pp. 1-5). IEEE. Melbourne, Australia.</p>
<p>Location in thesis: Chapters 3, 5</p>
<p>Student contribution to work:</p> <p>In this study, the main purpose is to develop an effective method for optimizing the size of hybrid power system (HPS) by considering reliability indices and power balance constraint. A new metaheuristic nature-inspired algorithm, called firefly algorithm (FA) is utilized to achieve these objectives.</p>
<p>Co-Authored signatures and dates:</p>

<p>Details of the work:</p> <p>Peidaee, P., Kalam, A. and Moghaddam, M.H., 2017, November. Developing a simulation framework for integrating multi-agent protection system into smart grids. In 2017 Australasian Universities Power Engineering Conference (AUPEC) (pp. 1-6). IEEE. Melbourne, Australia.</p>
<p>Location in thesis: Chapter 2</p>
<p>Student contribution to work:</p> <p>In this study, a simulation framework is developed through interfacing between MATLAB/SIMULINK with Java Agent Development Environment (JADE). Furthermore, based on the proposed simulation framework a multi-agent protection system (MAPS) has been identified where different agent types collaborate in system protection tasks. The main objective of this paper is to highlight the requirements for an effective simulation framework to integrate MAPS into future smart grids.</p>
<p>Co-Authored signatures and dates:</p>

<p>Details of the work:</p> <p>Nowdeh, S.A., Moghaddam, M.J.H., Babanezhad, M., Davoodkhani, I.F., Kalam, A., Ahmadi, A. and Abdelaziz, A.Y., 2019. A Novel Maximum Power Point Tracking Method for Photovoltaic Application Using Secant Incremental Gradient Based on Newton Raphson. In Solar Photovoltaic Power Plants (pp. 71-96). Springer, Singapore.</p>
<p>Location in thesis: Chapter 5</p>
<p>Student contribution to work:</p> <p>In this chapter, some common methods of maximum power point tracking (MPPT) of the photovoltaic system such as perturb and observe, particle swarm optimization and grey wolf optimizer are described to solve the MPPT problem. Also, a novel method is proposed for MPPT of PV system titled secant incremental gradient based on Newton Raphson (SIGBNR) method. SIGBNR uses the chord slope passing through two points of the function instead of using the explicit derivative of the function, which is equal to tangent line tilt of the function.</p>
<p>Co-Authored signatures and dates:</p>

<p>Details of the work:</p> <p>Nasri, S., Nowdeh, S.A., Davoodkhani, I.F., Moghaddam, M.J.H., Kalam, A., Shahrokhi, S. and Zand, M., 2020. Maximum Power Point Tracking of Photovoltaic Renewable Energy System Using a New Method Based on Turbulent Flow of Water-based Optimization (TFWO) Under Partial Shading Conditions. In <i>Fundamentals and Innovations in Solar Energy</i>, Springer.</p>
<p>Location in thesis: Chapter 5</p>
<p>Student contribution to work:</p> <p>In this chapter, turbulent flow of water-based optimization (TFWO) inspired based on whirlpools created in turbulent flow of water is used to solve the maximum power point tracking (MPPT) of photovoltaic systems in partial shading conditions. The TFWO is used to determine the optimal duty cycle of the DC/DC converter with the objective of maximizing the extracted power of the photovoltaic system.</p>
<p>Co-Authored signatures and dates:</p>

<p>Details of the work: (Submitted book chapter)</p> <p>Nowdeh, S.A., Moghaddam, M.J.H. and Kalam, A., 2021. Sizing of Solar Pumping System Integrated with Water Storage using Improved Water Cycle Algorithm Considering Life Cycle Cost and Reliability. In <i>CRC Taylor and Francis</i>.</p>
<p>Location in thesis: Chapter 5</p>
<p>Student contribution to work:</p> <p>In this chapter, optimization of solar pumping system integrated with water storage tank (WST) is presented to supply the drinking water of customers for remote area application based on real annual data of solar radiation and water demand. In this study, instead of a battery bank storage or fuel cell, the WST is used to avoid an excessive increase in the system costs. The objective function is defined as minimization of life cycle cost (LCC) including initial capital cost and maintenance and operation costs and the reliability constraint is considered as water supply probability (WSP).</p>
<p>Co-Authored signatures and dates:</p>

List of tables

Table 2.1. Classification of DG sources [24].	14
Table 2.2. The order of elimination of different harmonics in LV, MV, and HV systems [71-72].	47
Table 2.3. The impedance characteristics of the bus and feeders of the distribution system [73-75].	52
Table 2.4. The bus current magnitude (Ampere) for the 7th and 9th order harmonics of distribution systems with different loadings on feeders [73-75].	53
Table 2.5. The ratio between the power generation by DGs and the whole loads of the system without leading to unallowable harmonics [73-75].	53
Table 3.1: Comparison of intelligent methods in the optimal design of the PVWTBAHDG	80
Table 4.1. Classification of main events that lead to electromagnetic distortion in the system [116].	88
Table 4.2. Classification and characteristics of electromagnetic phenomena in the power system [115].	89
Table 4.3. Sample fault clearance times [133].	123
Table 4.4. The allowed range of voltage unbalance percentages [140].	136
Table 4.5. Frequency control methods [115].	140
Table 4.6. The allowed range of flicker in different networks [143-144].	141
Table 4.7. Evaluation of capacitors [115].	158
Table 4.8. Calculation of K factor for transformers [115-146].	159
Table 4.9. Sample values of P_{EC-R} [115].	161
Table 4.10. Adaptation limit of voltage harmonics in LV and MV networks in percentage [150].	171
Table 4.11. Design levels of voltage harmonics in different networks in percentage [151].	172

Table 4.12. The allowed limit of voltage harmonics in Australia.....	176
Table 4.13. Maximum capacity of converters for automatic acceptance in England [115].	176
Table 4.14. The allowed limit of voltage harmonics in England [115].....	177
Table 6.1. PV panel data [90, 152].....	196
Table 6.2. WT data [90, 152]	196
Table 6.3. Battery data [90, 152].....	197
Table 6.4. Economic data of system design [90, 152]	197
Table. 6.5. Results of one HDG placement in unbalanced 33- bus network by considering min Ploss as objective function.....	199
Table 6.6. Optimal sizing and siting of one HDG in unbalanced 33- bus network by considering min Ploss as objective function	199
Table. 6.7. Results of one HDG placement in unbalanced 33- bus network by considering min Vsag as objective function	201
Table 6.8. Optimal sizing and siting of one HDG in unbalanced 33- bus network by considering min Vsag as objective function.....	201
Table. 6.9. Results of one HDG placement in unbalanced 33-bus network by considering min Vswell as objective function	203
Table 6.10. Optimal sizing and siting of one HDG in unbalanced 33-bus network by considering min Vswell as objective function	203
Table. 6.11. Results of one HDG placement in unbalanced 33- bus network by considering min THD as objective function.....	205
Table 6.12. Optimal sizing and siting of one HDG in unbalanced 33- bus network by considering min THD as objective function.....	205
Table. 6.13. Results of one HDG placement in unbalanced 33- bus network by considering min Un as objective function.....	207
Table 6.14. Optimal sizing and siting of one HDG in unbalanced 33- bus network by considering min Un as objective function.....	207

Table. 6.15. Results of one HDG placement in unbalanced 33- bus network considering multi objective function	209
Table 6.16. Optimal sizing and siting of one HDG in unbalanced 33-bus network considering multi objective function.....	209
Table. 6.17. Results of one HDG placement in unbalanced 33- bus network by considering multi objective function.....	213
Table 6.18. Optimal sizing and siting of one HDG in unbalanced 33- bus network by considering multi objective function.....	213
Table. 6.19. Results of two HDG placement in unbalanced 33-bus network by considering multi objective function	216
Table 6.20. Optimal sizing and siting of two HDG in unbalanced 33-bus network by considering multi objective function.....	216
Table. 6.21. Results of two HDG placement in unbalanced 33-bus network by considering multi objective function	219
Table. 6.22. Optimal sizing and siting of two HDG in unbalanced 33- bus network by considering multi objective function.....	219
Table. 6.23. Results of one HDG placement in unbalanced 33-bus network by considering multi objective function with C_{HDG}	221
Table 6.24. Optimal sizing and siting of one HDG in unbalanced 33- bus network by considering multi objective function with C_{HDG}	221
Table. 6.25. Results of two HDG placement in unbalanced 33-bus network by considering multi objective function with C_{HDG}	221
Table 6.26. Optimal sizing and siting of two HDG in unbalanced 33-bus network by considering multi objective function with C_{HDG}	222
Table 6.27. Results of one HDG placement in unbalanced 33-bus network by considering multi objective function with C_{HDG} using HCSADE.....	222
Table 6.28. Optimal sizing and siting of one HDG in unbalanced 33-bus network by considering multi objective function with C_{HDG} using HCSADE.....	222
Table 6.29. Results of one HDG placement in unbalanced 33-bus network by considering multi objective function with C_{HDG} using HCSADE.....	223
Table 6.30. Optimal sizing and siting of one HDG in unbalanced 33-bus network by considering multi objective function with C_{HDG} using HCSADE	223

Table 6.31. Results of one HDG placement in unbalanced 33- bus network by considering multi objective function with C_{HDG} using HCSADE.....	224
Table 6.32. Optimal sizing and siting of one HDG in unbalanced 33- bus network by considering multi objective function with C_{HDG} using HCSADE.....	224
Table. 6.33. Results of one HDG placement in unbalanced 33-bus network by considering battery cost variations.....	225
Table 6.34. Optimal sizing and siting of one HDG in unbalanced 33-bus network by considering battery cost variations.....	225
Table. 6.35. Results of two HDG placement in unbalanced 33-bus network by considering battery cost variations	232
Table 6.36. Optimal sizing and siting of two HDG in unbalanced 33-bus network by considering battery cost variations.....	232
Table 6.37. Comparison to last research for unbalanced 33-bus network.....	241

List of figures

Fig. 2.1. Basic structure of a power system [22].	10
Fig. 2.2. Radial distribution network [22].	10
Fig. 2.3. Network configuration of a distribution network [22].	11
Fig.2.4. Loop configuration of a distribution network [22].	11
Fig. 2.5. Concentrated and distributed power generation [24].	13
Fig. 2.6. Connection of a DG to a sub-branch of a distribution feeder.	24
Fig. 2.7. Connection of a DG to the load bus.	25
Fig. 2.8. Voltage profile of a distribution network at minimum and maximum loads. .	31
Fig. 2.9. The changes in the voltage with respect to the system angle and power factor [71-72].	44
Fig. 2.10. The changes in the voltage with respect to the short circuit ratio for different values of power factor [71-72].	44
Fig. 2.11. The schematic of a radial distribution system with equal loadings for all feeders [73-75].	51
Fig. 2.12. The schematic of a radial distribution system with increasing linear loadings of the feeder when departing from the substation [73-75].	51
Fig. 2.13. The schematic of a radial distribution system with decreasing linear loadings of the feeder when departing from the substation [73-75].	52
Fig.3.1. Block diagram of a stand-alone PVBAHDG system [90].	63
Fig.3.2. Block diagram of a stand-alone WTBAHDG system [90].	63
Figure 3.3. Block diagram of an islanded PVWTBAHDG system [90].	64
Fig.3.4. Solar and wind power capacity over the world from 2000 to 2023 [107].	64
Fig. 3.5. Solar-wind-battery-diesel hybrid system [112].	70
Fig. 3.6. The HDG system under study [90].	74
Fig. 4.1. A survey data related to the roots of power quality issues [115].	84

Fig. 4.2. Transient surge wave due to a lightning strike [115].	90
Fig. 4.3. The oscillatory transient current wave created due to the switching of a back-to-back capacitor [115].	91
Fig. 4.4. The oscillatory low-frequency transient wave created due to capacitor bank energizing [115].	92
Fig. 4.5. An oscillatory low-frequency transient wave created by a Ferro resonance event in an unloaded transformer [115].	92
Fig. 4.6. Temporary interruption of a line and reclosing operation [115].	94
Fig. 4.7. Typical sag [115-118].	95
Fig. 4.8. Sag with a complicated form [115-118].	95
Fig. 4.9. Sag due to a single-phase to ground short circuit [115-119].	97
Fig. 4.10. Sag due to starting of a motor [115-119].	97
Fig. 4.11. Instantaneous voltage sag due to a single-phase to ground short circuit [115].	98
Fig. 4.12. Voltage unbalance for a residential feeder [115].	99
Fig. 4.13. Input current waveform and the harmonic spectrum in a motor drive with the speed-adjustability capability [115].	101
Fig. 4.14. Representation of voltage harmonic drop [115].	102
Fig. 4.15. A voltage notching created by a three-phase converter [115].	106
Fig. 4.16. Type A voltage fluctuation [126].	106
Fig. 4.17. Type B voltage fluctuation [126].	107
Fig. 4.18. Type C voltage fluctuation [126].	107
Fig. 4.19. Type D voltage fluctuation [126].	107
Fig. 4.20. An example of voltage flicker due to electric arc operation [115].	109
Fig. 4.21. Voltage sag following a fault and when the fault is cleared [115].	119
Fig. 4.22. An impedance divider to calculate sag amplitude [115].	121

Fig. 4.23. The impedance diagram and voltages of different points [115].	121
Fig. 4.24. Description of the vulnerability zone of a transmission system [119]......	124
Fig. 4.25. Types of voltage sags [119].	124
Fig. 4.26. Voltage drop on the system impedance, causing many voltage regulation problems [115].	130
Fig. 4.27. Schematic diagram of a voltage regulator [115].	131
Fig. 4.28. Characteristics of a Ferro-resonance transformer [115]......	131
Fig. 4.29. Electronic regulator [115].	132
Fig. 4.30. Motor-generator set [115].	132
Fig. 4.31. Two types of SVCs [115].	133
Fig. 4.32. Current distortion caused by a nonlinear resistor [115].	144
Fig. 4.33. Fourier series representation of a distorted waveform [115].	145
Fig. 4.34. Harmonic currents flowing from the system impedance and produce voltage harmonic on the load [115].	146
Fig. 4.35. The relationship between different components of apparent power [115]..	151
Fig. 4.36. High neutral current in supply circuits of single-phase nonlinear loads [115].	152
Fig. 4.37. Flow of third-harmonic current in a three-phase transformer [115].	153
Fig. 4.38. The equivalent circuit of an arcing device [115].	155
Fig. 4.39. Magnetic characteristic of an iron core [115].	156
Fig. 4.40. The general path of harmonic currents in radial networks [115].	162
Fig. 4.41. Power factor correction capacitors are able to change the path of one of the current harmonic components [115].	163
Fig. 4.42. The effect of transformer connection type on modeling requirements for network harmonic analysis [115].	165
Fig. 4.43. Representation of a nonlinear load using a harmonic current source to analyze the system [115].	167

Fig. 4.44. Replacement of a simple model of the current source with a Thevenin or Norton equivalent circuit to improve and model the system under resonance conditions [115].	167
Fig. 4.45. A simple circuit that can be solved by hand [115]......	168
Fig. 5.1. The off-grid HDG system under study [16]......	179
Fig. 5.2. Structure of CSA [18]......	186
Fig. 5.3. The flowchart of CSA.....	187
Fig. 5.4. The flowchart of HCSADE.....	190
Fig. 6.1. 33-bus IEEE standard (unbalanced) distribution network [153]......	193
Fig. 6.2. Solar radiation curve for 24 hours.....	194
Fig. 6.3. Ambient temperature curve for 24 hours	194
Fig. 6.4. Wind speed curve for 24 hours	195
Fig. 6.5. Load demand of HDG for 24 hours	195
Fig. 6.6. Normalized load curve of 33- bus unbalanced network for 24 hours	196
Fig. 6.7. Convergence curve of HCSADE by considering min Ploss objective function (one HDG).....	199
Fig. 6.8. Active loss of unbalanced 33- bus network by considering min Ploss as objective function (one HDG)	200
Fig. 6.9. Convergence curve of HCSADE by considering min Vsag as objective function (one HDG).....	201
Fig. 6.10. Voltage sag of unbalanced 33-bus network considering min Vsag as objective function (one HDG)	202
Fig. 6.11. Convergence curve of HCSADE by considering min Vswell as objective function (one HDG)	203
Fig. 6.12. Voltage swell of unbalanced 33-bus network considering min Vswell as objective function (one HDG).....	204
Fig. 6.13. Convergence curve of HCSADE by considering min THD as objective function (one HDG).....	205

Fig. 6.14. Voltage THD of unbalanced 33-bus network by considering min THD as objective function (one HDG).....	206
Fig. 6.15. Convergence curve of HCSADE by considering min U_n as objective function (one HDG).....	207
Fig. 6.16. Unbalance voltage of unbalanced 33- bus network by considering min U_n as objective function (one HDG).....	208
Fig. 6.17. Convergence curve of HCSADE by considering multi objective function with and without C_{HDG} (one HDG).....	208
Fig. 6.18. Active loss of unbalanced 33-bus network by considering multi objective function, one HDG (with C_{HDG}).....	210
Fig. 6.19. Voltage sag of unbalanced 33- bus network by considering multi objective function, one HDG (with C_{HDG}).....	210
Fig. 6.20. Voltage swell of unbalanced 33- bus network considering multi objective function, one HDG (with C_{HDG}).....	211
Fig. 6.21. Voltage THD of unbalanced 33- bus network considering multi objective function, one HDG (with C_{HDG}).....	211
Fig. 6.22. Voltage unbalance of unbalanced 33- bus network considering multi objective function, one HDG (with C_{HDG}).....	211
Fig. 6.23. SOC of battery by considering multi objective function (one HDG)	212
Fig. 6.24. Energy contribution of units for multi objective function a) with and b) without C_{HDG} (one HDG).....	212
Fig. 6.25. Convergence curve of HCSADE considering multi objective function (two HDG).....	215
Fig. 6.26. Energy contribution of units for multi objective function, HDG 1, a) with and b) without C_{HDG} , (two HDG).....	217
Fig. 6.27. Energy contribution of units for multi objective function, HDG 2, a) with and b) without C_{HDG} , (two HDGs)	218
Fig. 6.28. Convergence curve of optimization method by considering multi objective function (one HDG)	220
Fig. 6.29. Convergence curve of optimization method by considering multi objective function (two HDGs).....	220

Fig. 6.30. Active loss of unbalanced 33-bus network by considering battery cost variations	a) 50\$, b) 100\$ (base study) and c) 200\$ [One HDG].....	226
Fig. 6.31. Voltage sag of unbalanced 33-bus network by considering battery cost variations	a) 50\$, b) 100\$ (base study) and c) 200\$ [One HDG].....	227
Fig. 6.32. Voltage swell of unbalanced 33-bus network by considering battery cost variations	a) 50\$, b) 100 \$ (base study) and c) 200 \$ [One HDG].....	228
Fig. 6.33. Voltage THD of unbalanced 33-bus network by considering battery cost variations	a) 50\$, b) 100 \$ (base study) and c) 200 \$ [One HDG].....	229
Fig. 6.34. Voltage unbalance of unbalanced 33-bus network by considering battery cost variations	a) 50\$, b) 100 \$ (base study) and c) 200 \$ [One HDG].....	230
Fig. 6.35. Energy contribution of units by considering battery cost variations	a) 50\$, b) 100\$ (base study) c) 200\$ [One HDG].....	231
Fig. 6.36. Active loss of unbalanced 33-bus network by considering battery cost variations	a) 50\$, b) 100\$ (base study) and c) 200\$ [Two HDG].....	233
Fig. 6.37. Voltage sag of unbalanced 33-bus network by considering battery cost variations	a) 50\$, b) 100\$ (base study) and c) 200\$ [Two HDG].....	234
Fig. 6.38. Voltage swell of unbalanced 33-bus network by considering battery cost variations	a) 50\$, b) 100\$ (base study) and c) 200\$ [Two HDG].....	235
Fig. 6.39. Voltage THD of unbalanced 33-bus network by considering battery cost variations	a) 50\$, b) 100\$ (base study) and c) 200\$ [Two HDG].....	236
Fig. 6.40. Voltage unbalance of unbalanced 33-bus network by considering battery cost variations	a) 50\$, b) 100\$ (base study) and c) 200\$ [Two HDG].....	237
Fig. 6.41. Energy contribution of units considering battery cost variations	a) 50\$, b) 100\$ (base study) and c) 200\$ [Two HDG].....	240

List of Abbreviations

AACO	Adaptive Colony Optimization Algorithm
ABC	Artificial Bee Colony

AC	Alternating Current
ACO	Ant Colony Optimization
ACS	Annualized Cost of System
AI	Artificial Intelligence
AIS	Artificial Immune Algorithm
ALO	Ant Lion Optimizer
ANN	Artificial Neural Networks
AP	Awareness Probability
ASD	Adjustable Speed Drive
AVR	Automatic Voltage Regulator
BBA	Big Bang Algorithm
BBO	Biogeography-based Optimization
BIIL	Basic Impulse Insulation Level
BSOA	Backtracking Search Optimization Algorithm
CBEMA	Computer Business Equipment Manufacturers Association
COE	Cost of Energy
CRF	Capital Recovery Factor
CSA	Crow Search Algorithm
DC	Direct Current
DE	Differential Evolution
DG	Distributed Generation
DHSA	Discrete Harmony Search Algorithm
DIN	Distortion Index
DNO	Distribution Network Operator
EENS	Expected Energy Not Supplied
EHV	Extra High Voltage
EMF	Electromotive Force
ENS	Energy Not Supplied
FC	fuel cell
FGA	Fuzzy Genetic Algorithm
FL	Flight Length
FWA	Fireworks Algorithm
GA	Genetic Algorithm
GW	Gigawatts
GWO	Gray Wolf Optimizer

CSADE	Crow Search Algorithm-Differential Evolution
HDG	Hybrid Distributed Generation
HID	High-Intensity Discharge
HV	High Voltage
HVDC	high-voltage direct current
ICA	Imperial Competitive Algorithm
IHSA	Improved Harmony Search Algorithm
IVESTC	Investment Cost
LCE	Levelized Cost of Energy
LDC	Line Drop Compensator
LG	Line to Ground
LL	Line to Line
LPSP	Loss of Power Supply Probability
LSF	Loss Sensitivity Factor
LV	Low Voltage
MANIC	Maintenance Cost
MHA	Modified Heuristic Approach
MV	Medium Voltage
NPV	Net Present Value
OPF	Optimal Power Flow
PCC	Point of Common Connection
PLC	Power Line Carrier
PQ	Power Quality
PSO	Particle Swarm Optimization
PV	Photovoltaic
PVBAHDG	Photovoltaic/Battery Hybrid Distributed Generation
PVWTBAHDG	Photovoltaic / Wind Turbine with Battery Hybrid Distributed Generation
PVWTHDG	Photovoltaic/Wind Turbine Hybrid Distributed Generation
PWM	Pulse Width Modulation
REPLACEC	Replacement Cost
RES	Renewable Energy Source
RF	Renewable Factor
RLC	Resistive-Inductive-Capacitive
RLF	Repetitive Load Flow
RMS	Root Mean Square

SCVD	Short Circuit Voltage Depression
SOC	State of Charge
SVC	Static Var Compensator
SVR	Step Voltage Regulators
TDD	Total Demand Distortion
THD	Total Harmonic Distortion
TPC	Transaction Processing Performance
TV	Television
UPS	Uninterruptible Power Supply
VA	Volt-Amp
VSI	Voltage Stability Index
VT	Voltage Transformer
WT	Wind Turbine
WTBAHDG	Wind Turbine/Battery Hybrid Distributed Generation

Chapter1. Introduction

1.1 Motivation

Advances in technology and the global trend towards the use of renewable energy have introduced distributed generation (DG) units in the distribution network as one of the sources of energy supply. Further, some factors such as reliability improvement, pollution and loss reduction have expanded the influence of DG resources in the distribution network [1]. These resources are sited at the end of the network and close to the customers. Also, the generation of these resources is associated with very low pollution and the cost of their primary fuel is minimal [2-3]. In recent years, renewable energy sources based on DGs have been widely welcomed by network operators, as these types of resources can provide clean and intelligent generation to meet the demand. The most commonly used renewable energy sources are Photovoltaic (PV) energy and Wind Turbine (WT) that are considered by the operators of the energy systems. PV and wind sources, along with the cheap and clean energy that can generate these resources have other benefits when properly deployed in the distribution network. Some of these benefits can be the reduction of network losses, improvement of network voltage profile, active and reactive power sale, improvement of Power Quality (PQ), etc. [4]. All the benefits of DG sources are available for distribution networks if these resources are placed in a suitable location and have optimum generation capacity. However, an important issue with regard to all DG sources in the radial distribution network is the issue of determining the location and capacity of these resources in the network. The lack of proper location of distributed generation sources can affect the network performance adversely in terms of network losses and network voltage stability. Therefore, determining the location and size of DG is one of the most important aspects related to the installation and operation of DGs. Determining the location and capacity of DGs can usually be accomplished for different purposes, among which the most important goals can be as follows [2-3]:

- loss reduction;
- voltage profile and reliability improvement; and
- PQ improvement.

One of the applications of renewable sources is in hybrid distributed generation (HDG) for off-grid applications that have been welcomed by energy engineers in the last decade. PV/ WT with Battery HDG (PVWTBAHDG) is one of the most commonly used systems. In this system, PV panels and wind turbines are the main sources of load supply. The battery storage in the PVWTBAHDG is used for energy management and compensation

of power fluctuations to improve the system reliability. In some cases, these types of energy generation systems are considered as connected to the network to provide power injection to the network and receive power from the network in certain condition. Also, PVWTBAHDG systems can be used to provide specific load, and in addition, the excess energy generated by this type of systems is also injected into the distribution network. In recent years, several studies have been done on the application of PV panels and WTs without energy storage system, rather than in the form of a PVWTBAHDG in the distribution network. In all studies, the best location and capacity of these energy sources are optimally determined for maximizing their advantages in the network considering the objective function and operation constraints. One of the important issues that are not well addressed is the effect of using PVWTBAHDG on PQ indices in the distribution network. The effect of using only PV panels and only WTs without storage system is studied in few cases for improving the network PQ. With the use of HDG systems in the distribution network and injection of power in network lines, the impedance of the power path is changed, so the voltage sag is also subject to change. Voltage fluctuations as PQ indices can cause outage of some critical loads, so improving voltage sag and voltage fluctuations can improve the PQ, as well as reduce system loss and thus improve the reliability [5-6]. The injection of power through DGs in the distribution network change the lines of load flow, nodes voltage and the unbalance and even the distortion level of the bus voltages including harmonics. Also, changing the effective load impedance of the load flow path and conversely inducing voltage because of changes in line of load flow in the distribution network will change the harmonic of the node voltage. So, an optimal application of PVWTBAHDG systems in the network can solve these problems and make the advantage of using these types of power generation systems in the distribution networks. Therefore, the objectives of using PVWTBAHDG systems in the network can be to minimize network power losses, improve the voltage sag (decreasing in effective voltage amplitude) and voltage swell over the network during fault or switching, minimize the harmonic distortion of nodes voltage and minimize network voltage unbalances. In recent years, quality problems such as voltage sag, harmonics and network voltage unbalance have drawn the attention of researchers and network engineers [7-10].

1.2 Research Objectives

One of the best methods to improve network characteristics is the use of renewable resources in the distribution network. The use of PVWTBAHDG systems is a highly

desirable option for exploiting the distribution networks with the aim of improving network distribution features and in particular, improving network PQ. Non-optimal application of PVWTBAHDG systems may have unsuitable impacts on network PQ indices, and it will weaken the indices. Therefore, improving the PQ indices, based on the application of PVWTBAHDG systems, the optimal location and capacity of this type of system should be determined in the distribution network. In addition, PVWTBAHDG systems must be designed to minimize their energy generation costs by achieving desirable reliability. The optimal capacity of PVWTBAHDG system refers to optimal size of the system components, including the PV panels, wind turbines and the capacity of the battery bank. Therefore, in this study, the effect of applying the PVWTBAHDG systems on active power losses and PQ indices of radial distribution network has been evaluated. In this study, PQ indices include voltage sag, voltage swell, harmonic and voltage unbalance.

In addition, the optimal application of PVWTBAHDG system, which is an optimization problem with multiple factors, cannot be solved using traditional methods due to its complexity. For this reason, the use of artificial intelligence methods based on intelligent methods of optimization has been adopted in recent years and is proposed in this research for optimization problem solution.

In this research, the main aims of PVWTBAHDG utilization in the distribution network are as follows:

- Optimal design of PVWTBAHDG system;
- Reduction of network power losses;
- Reduction of PVWTBAHDG generation cost;
- Improvement of power quality and network reliability;
- Improvement of voltage sag;
- Improvement of voltage swell;
- Reduction of harmonics in the network;
- Reduction of voltage unbalance; and
- Utilization of a new meta-heuristic method.

1.3 Scientific Contribution

In this thesis, the optimization of PVWTBAHDG systems is studied with the aim of reducing active power loss and PVWTBAHDG generation cost as well as improving PQ

indices in distribution network. So far, the effects of the use of PV and wind systems with battery storage in the form of PVWTBAHDG and optimal location and size have not been studied in the unbalanced distribution network as multi-objective optimization problem [11-17]. The innovations of this thesis are as follows:

- Optimization of the PVWTBAHDG system based on battery storage in the radial distribution network;
- Optimization of the PVWTBAHDG system to reduce power losses and improve PQ indices as multi-objective problem;
- Provision of intelligent approach to solve the optimization problem; and
- Single and multi-objective problem solution based on weighted coefficients.

The main objective of the problem is PQ indices improvement of the distribution network considering minimizing the cost of PVWTBAHDG application in the network. The costs of PVWTBAHDG include capital cost, operation and maintenance cost and replacement cost. The PVWTBAHDG system is seen from the distribution network as a power source, so it is appropriate to determine its optimal location in the network to maximize its benefits. Hence, two issues are solved simultaneously. The first issue is the design of the PVWTBAHDG system and determination of optimal capacity of PVWTBAHDG system components by considering the objective function of minimizing energy costs and relevant constraints. The design of the PVWTBAHDG is such that the load is fully provided by itself and the excess power is injected to the distribution network. For the second issue the optimal location and capacity of PVWTBAHDG is determined optimally. This issue highlights the effect of excess power injected by PVWTBAHDG system to the distribution network on PQ indices considering network utilization constraints. Therefore, two problems are solved simultaneously by the meta-heuristic method. In particular, the optimal capacity of PV panels and WTs, as well as the battery storage along with the optimal location of PVWTBAHDG in the distribution network as decision variables is determined with the objective of minimizing energy costs, reducing active power losses and improving the PQ indices by considering the constraints. In this thesis, a meta-heuristic algorithm, named hybrid crow search algorithm- differential evolution (HCSADE), is used to solve the optimization problem. The crow search algorithm (CSA) was presented by Askarzadeh in 2016 inspired based on the social and intelligent manner of the crows [18]. The CSA algorithm is formulated based on intelligent behavior of crows in tracking and finding other crows food caches [19]. In

order to avoid trapping, the conventional CSA in local optimal and increasing the convergence speed of the algorithm, when increasing the dimensions of the optimization problem, the crossover and mutation operators of differential evolution (DE) method [20-21] are used to improve the performance of the CSA in problem solution. The proposed method is implemented on an unbalanced 33- bus network. The problem is done as multi-objective optimization based on the weighted coefficients method. The simulation results included active power losses, voltage sag, voltage swell, harmonics and voltage unbalance, which are investigated before and after the optimization of PVWTBAHDG systems in the network. The effect of increasing the PVWTBAHDG load demand, as well as increasing the network load, is also evaluated on the problem solution. The capability of the HCSADE is compared with the conventional CSA and DE algorithm. In addition, in order to verify the HCSADE, the results are compared with previous studies.

1.4 Thesis outline

In this thesis, the optimization of the PVWTBAHDG system with battery storage is presented in an unbalanced 33-bus network with the goal of reducing power losses, reducing the energy generation costs and improving the PQ indices of the distribution network using HCSADE meta-heuristic method.

In chapter 2, previous studies on Distributed Generation optimization (DGs) in distribution networks are evaluated. The objective functions used along with the optimization methods are investigated. The optimal design of HDG systems are investigated considering economic and technical indicators. Also, studies on connected HDG systems to the network are described. The limitations of past studies and the proposed approach to cover these limitations are presented.

In Chapter 3, the structure of HDG systems is presented with storage systems. Also types of different HDG systems are demonstrated. The principles of energy systems optimization are evaluated in view of objective functions and designing constraints. Also, the intelligent methods used for optimal designing of HDG systems are described.

In Chapter 4, PQ concepts and indices classification are presented. Important indices of PQ include voltage sag, voltage swell, harmonic and voltage unbalance are described. Also, methods for improving the PQ in the distribution network are presented.

In Chapter 5, the formulation of the optimization problem of the PVWTBAHDG in the distribution network is presented, to reduce energy costs and power losses and improve the network PQ indices. The objective function is presented considering the operation

constraints. The HCSADE meta-heuristic method is described and its implementation steps are presented in the problem solution.

In Chapter 6, simulation results of the PVWTBAHDG optimization in the distribution network are presented with the goal of reducing energy costs, reducing power losses and improving the 33-bus unbalanced network PQ indices using the HCSADE method. The simulation results are compared with and without the optimal PVWTBAHDG application in the distribution network. The best installation site and size of the PVWTBAHDG system in the distribution network and the optimal design effect of the PVWTBAHDG system are presented, in order to improve the PQ indices of the distribution network. In addition, the capability of the proposed optimization method is compared with the traditional CSA and DE method, as well as previous studies. The effect of increasing the number of PVWTBAHDG systems is evaluated on problem solution. The effect of increasing the PVWTBAHDG load demand and network load is studied on system optimization, loss values and the PQ indices.

In chapter 7, highlights and conclusions from the research are presented and the results are summarized. There are also suggestions for future research.

Chapter2. Literature Review

2.1 Introduction

Several studies have been investigated so far to exploit distributed networks based on distributed generation resources, especially renewable energy sources [22-106]. Different indices have been investigated to evaluate the effect of distributed generation resources on the distribution network. In the operation of distribution networks, various methods are proposed to find the optimal location and size of the energy resources, and different objective functions are provided. Among the analytical methods, optimization methods are proposed based on their intelligent characteristics. In this chapter, some research items are reviewed based on the optimization process of distributed generation (DG) and its impact on various parameters such as power loss, power quality (PQ), etc. in the distribution network. Moreover, in this chapter, recent studies are analyzed based on the optimization of the hybrid distributed generation (HDG) systems in both islanded and grid-connected operations. Furthermore, the limitations of these methods and the techniques of overcoming these limitations are presented.

2.2 Distribution network

A power system is expected to supply customers with proper voltage and frequency and without any interruptions. To this end, the generation system must produce the required power, the transmission system must transfer the huge amount of power on the transmission line over long distances with no overheating, and distribution networks must deliver the electricity to the input node of the customers' internal systems. Conventionally, generation means the injection of power into the transmission system, which can be defined as the carrier of power from the generating stations to the sub-transmission system at voltage levels of 230 kV and above. The sub-transmission system then transfers the power to distribution networks. Finally, the distribution network at voltages typically below 34.5kV supplies electricity to the consumer. Fig. 2.1 shows a conventional bulk electrical power system.

An important characteristic of distribution networks is the configuration or how their lines are connected. There are three conventional configurations for distribution networks: radial, ring (loop), and network (interconnected). In radial configurations, the lines are sequentially branched out and the power flow is unidirectional as shown in Fig. 2.2. This configuration imposes the lowest cost; however, it has the minimum reliability, because any fault in the feeders will cause service interruptions at all downstream locations.

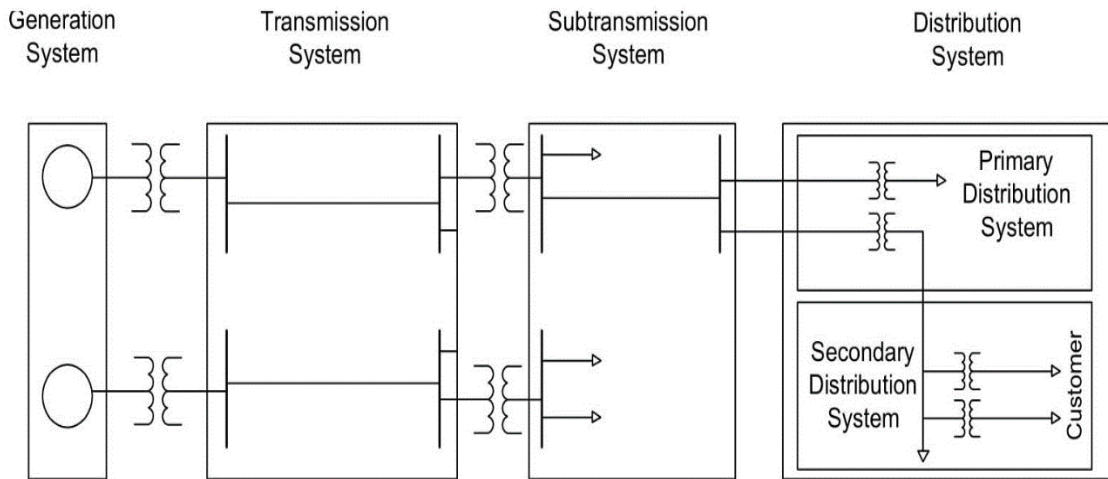


Fig. 2.1. Basic structure of a power system [22].

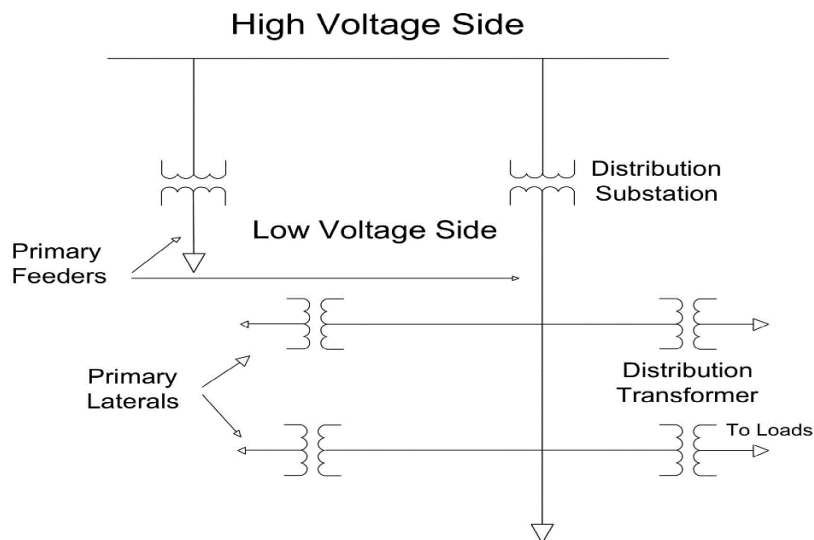


Fig. 2.2. Radial distribution network [22].

In a network configuration, the number of connections is greater, meaning that the two points are usually jointed through more than one path, forming some loops within the system. Fig. 2.3 illustrates a network configuration of a distribution network.

Loop configuration distribution networks are between the two abovementioned cases in terms of cost and reliability. As can be seen in Fig. 2.4 the loop configurations can be described as two radial systems separated by a normal-open switch. With the failure of one of the two substation transformers, the switch can be closed and part of the distribution network is energized through another transformer [22].

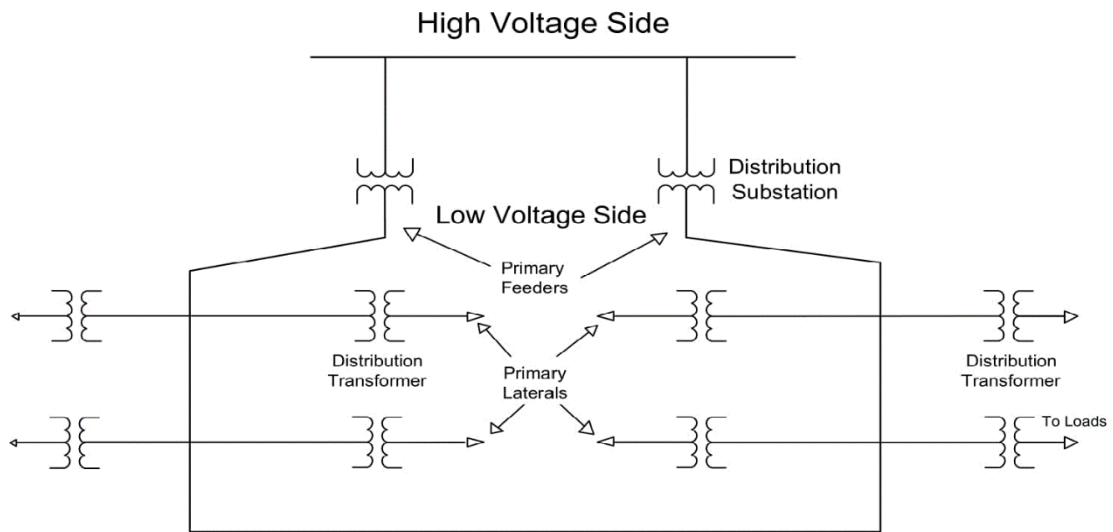


Fig. 2.3. Network configuration of a distribution network [22].

Design and planning of the distribution network envisage a major challenge in the model due to the restructuring of the power industry, policy changes, and advances in distributed generation (DG) technologies. Proper planning and design of the distribution network is the best approach for network development to provide reliable services and reduce economic costs for customers. Today, the rapid advances in DG technology and its numerous benefits have made it a viable and attractive option for distribution companies in their planning tasks.

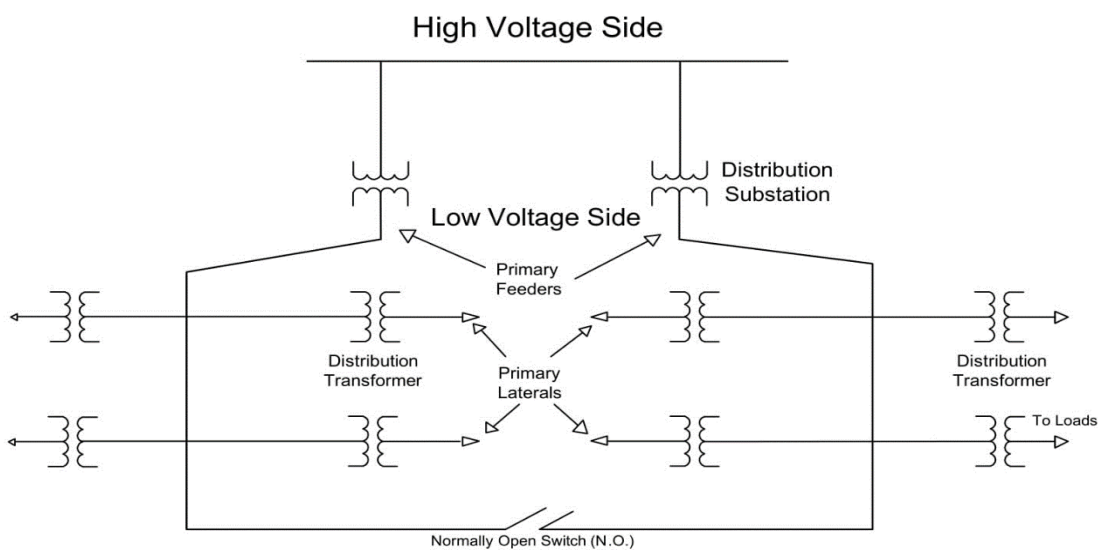


Fig.2.4. Loop configuration of a distribution network [22].

2.3 Distributed generation (DG)

A distributed generation is called locally generated or distributed energy. In this type of electrical energy generation method, electricity is generated by small sources. Recently, industrialized countries are producing large amounts of their electricity usage from fossil fuels such as coal, gas, nuclear power plants, and large hydroelectric plants. However, the new restructured system can provide this feature by using renewable sources such as solar, wind, and other resources. Concentrated DG units based on renewable energies are economically cost-effective and have no negative environmental impacts. DG resources are small-scale power technologies that have been used to improve PQ in traditional electrical networks. DGs can improve network characteristics including PQ by injecting active and reactive power into the network, which requires them to be located in the right place with optimal capacity [23]. DGs are an alternative to electricity transmission to rural areas, thus reducing transmission and distribution costs. Small DGs throughout the power system are responsible for supplying incremental load demand changes. In other words, these types of resources supply the demand shortage.

The technology adapted to DG includes small gas turbines, micro-turbines, fuel cells, wind and solar energy, biomass power plants, hydroelectric power, and more. DG can be used in an isolated mode, supplying local customer demand, or in an integrated electrical system with the grid. In the distribution network, DG can be employed to meet the needs of customers, especially in places where the power transmission system is faulty. Fig. 2.5 illustrates the difference between the conventional centralized generation and today's distributed generation.

The main reasons behind the widespread application of DGs in the conducted studies include the following [24]:

- Power generation by DG in the load site reduces distribution and transmission costs;
- In an integrated restructured system including the network and DGs, distribution and transmission costs increase as DG costs decrease;
- Recent energy resources technology has made it possible for different DGs to have access to power plants with higher efficiency and capacity ranging from a few KW to several 100 MW;
- In the restructured system, it is crucial to determine the optimal location and size of the DG resources;

- DGs usually require less installation time than traditional power plants or transmission lines to supply remote loads and have low investment risk; and
- DGs have relatively good efficiency, especially in hybrid combustion and combined cycle (larger power plants).

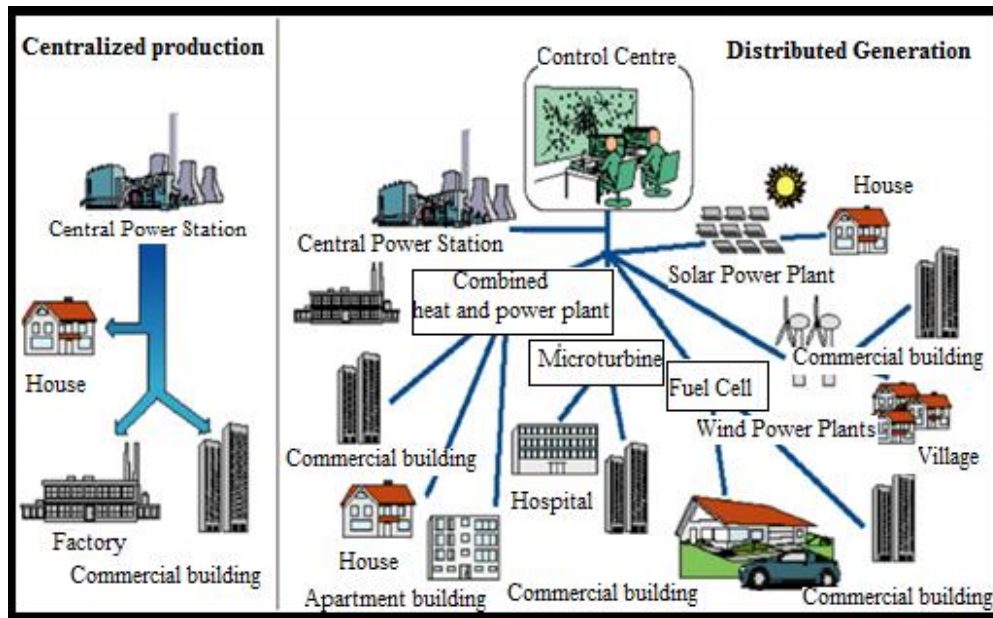


Fig. 2.5. Concentrated and distributed power generation [24].

When the operation of distribution networks and the impact of DG are considered, the greatest attention is paid to location and sizing of DG units because, installing them in suboptimal locations can increase power loss and reduce the reliability level of supplying the customer demand [25-26]. In other words, it weakens the PQ of the network. Therefore, using the appropriate tools can help locate and size the DG units in an optimal way so that the system costs are reduced and PQ is improved. At the power consumption endpoint level, many DG technologies can be used, one of which is the internal combustion engine. At this level of technology, DG can produce power as an "island" or can be used as a small member of a grid. Most studies confirm that DG penetration up to 10-15% peak load can be easily received by the power grid without major structural changes. The classification of DGs in terms of generation capacity is presented in Table 2.1, which is based on various parameters such as fuel used, capacity, electrical efficiency, installation cost, maintenance cost, peak load correction, reliability, and power quality [24].

2.3.1 DG application in the distribution network

The application of different DG technologies is determined by various factors. Some of these factors are as follows:

- *Base load:* The system is operated in parallel with the distribution network. It is, therefore, able to inject energy into the grid and also sell energy to the grid. Under these conditions, the system is constantly running and reduces network energy consumption;
- *Peak load Supply:* Since energy costs are usually higher during the peak load period, DG is used to supply electricity during this period, thereby reducing peak demand;
- *Distribution network Support:* To strengthen their power grid and avoid congestion at different times of the year or network failure, power companies or large customers sometimes support the grid in a distributed or periodic way by installing small power plants;
- *Power Supply Quality:* DGs are used to compensate for power shortages if the quality of power supply in the distribution network is lower than the electricity customers' demand; and
- *Energy storage:* DGs are used as alternative sources when the cost of using this technology is low or when the network has frequent interruptions. Therefore, they are also used as backup resources.

Table 2.1. Classification of DG sources [24].

Classification	Generation level
Micro DG	1 W to 5 kW
Small DG	5 kW to 5 MW
Average DG	5 MW to 50 MW
Large DG	50 MW to 300 MW

2.3.2 Distributed generation benefits

Distributed power generation has provided many opportunities. By DGs, clean energy can be produced free from environmental pollution because many DG sources are some kind of renewable sources operating on the cogeneration of electric power and heat. Renewable energy sources, such as wind and solar, are obtained from nature for free, and

this also applies to thermal power plants. Therefore, regarding their high efficiency and environmentally-friendly nature, they help reduce greenhouse gas emissions. Many of the benefits of deploying DG in existing distribution networks have economic and technical implications and are interdependent. As such, the benefits of DGs are categorized into three categories: technical, economic, and environmental [24]. The technical benefits cover a wide range of issues such as peak load correction, proper voltage, continuous load, and overcoming some PQ problems. System loss reduction can be addressed by some installations in developing countries, where they lose 15 to 20% of their generation as losses. The figure for a developed power system is 10%. However, the optimal location and sizing of DGs are two critical factors in reducing loss that has been investigated [24]. Some of the technical benefits of employing DG are as follows:

- Reduction of distribution network losses;
- Improvement of voltage profile in the distribution network;
- Improvement of energy efficiency;
- Improvement of network reliability and security;
- Improvement of PQ; and
- Minimizing transmission and distribution costs.

The economic benefits include saving on fuel consumption, saving on transmission and distribution costs, and reducing electricity sales prices. The major economic benefits of utilizing DG are as follows:

- Deferred investment to upgrade facilities;
- Reduced maintenance and operation costs of some DG technologies;
- Reduced healthcare costs due to environmental improvements;
- Reduced fuel costs due to increased overall efficiency;
- Reduced storage requirements and associated costs;
- Lower operating costs due to load peak correction; and
- Increased security for critical loads.

2.3.3 Distributed generation limitations

When the DG penetration level is noticeable, the dynamics of the system can be affected. DG connection analysis becomes complicated, especially given the wide range of DG technology and distribution network configuration designed to operate with unidirectional power flow. When large-scale DG is connected to the grid, researchers and

operators of distribution networks face the following challenges and limitations [26]:

- *Reverse power flow:* Connection of a DG to the system disrupts the protective circuits in the network configuration;
- *Reactive power:* Many DG technologies use synchronous generators that do not inject reactive power into the grid;
- *System frequency:* The frequency deviation from the system's nominal frequency is due to an imbalance between supply and demand. Increasing the DG capacity affects the frequency of the system, and these generators complicate the control process;
- *Voltage levels:* Installed DG improves the voltage profile of the distribution network due to changes in load distribution value. Usually, the voltage profile will tend to increase, which is not a problem in congested networks with low-voltage problems;
- *Protection design:* Most distribution networks are configured in a radial or loop form. This structure permits unidirectional power flow. Thus, the protection system is designed accordingly. The installation and start-up of DGs makes the power flow bidirectional. As a result, new security equipment and network resizing are necessarily applied;
- *Islanding protection:* This is a very important security issue. A situation in which a part of the system includes load and distribution of resources; while isolated from the rest of the system, it is still energized and is supplied by a DG. The utilization of DG may inject energy into the part of the network where workers are repairing and create irreparable risks. One solution is to use protective devices (electronics and mechanical) such as relays and transition switches;
- Injecting harmonics into the system by asynchronous DG sources that use inverters for connection;
- Network instability;
- Increased fault currents depending on the location of DG units;
- High financial costs per kW of power generation; and
- PQ is an issue that is at risk with the use of power electronics for controlling wind energy technologies.

2.3.4 DG types

2.3.4.1 Micro-turbine

The micro-turbine is a mechanism that uses gas flow to convert thermal energy into mechanical energy. The combustible fuel (usually gas) pumped by the compressor is mixed in the air combustion chamber [27]. The resultant gases from combustion cause the turbine to rotate, which rotates the generator and compressor at the same time. In the most used design, compressors and turbines are mounted on the same shaft with the generator.

The output voltage of the micro-turbines cannot be directly connected to the grid or urban facility and must be converted to direct current (DC) in order to have rated voltage and frequency and then converted back to alternating current (AC). The main advantage of micro-turbines is a clean operation with low gas emission and suitable performance. Other features of the micro-turbine include fast response time, moderate startup time, high availability, and convenient dispatching capability. On the other hand, the disadvantages are the high maintenance costs and lack of experience in this field. Very few micro-turbines are deployed for a sufficient time to create a database in the reliability domain. In addition, load control and power flow methods have not been developed for a large number of micro-turbines and for the sale of remaining energy.

2.3.4.2 Diesel generator

Diesel generators are used as an Uninterruptible Power Supply (UPS) or backup source for low to large public and industrial uses [27]. A diesel generator is a combination of a diesel engine with an electric generator (often called a dynamo) that is used to generate electricity. Diesel generators are used in situations of network failure or as expressed as emergency power in conditions connected to the power grid. Diesel generators are utilized in many cases, including construction (auxiliary electricity) as well as mobile residential electricity. The diesel generator set is a combination of a diesel engine, generator, and a variety of auxiliary devices such as stand or chassis, control systems, circuit breakers, and water heaters to operate the system. Diesel generators with rated power from 8 to 30 kW are normally used for homes, shops and small offices, and for large office complexes, factories, and industrial centers.

2.3.4.3 Photovoltaic cell

The solar cell is considered an essential part of the photovoltaic system [28]. In this system, solar radiation energy is converted to electricity by photovoltaic (light energy) effects. Solar cells are often electrically coupled and considered as a module. Today,

electricity generation from a few watts to as much as a conventional power plant is made possible by solar power technology. Advances in solar technologies as a result of research activities have made it possible for solar power to compete with other electricity generation methods. Solar power generation and consumption will play an important role in reducing greenhouse gas emissions.

Solar power systems are used in both grid-connected and grid-independent modes. In the former case, the electrical energy from the photovoltaic system is converted from AC to DC using the inverter and is injected into the grid at a given voltage and frequency level. In grid-independent mode, without the need for the main grid, the solar power system directly supplies the electricity needed for the load. In this case, the required electrical energy is provided by PV panels, energy storage system, and energy control system with high reliability. The major advantage of solar power plants includes:

- No required for fossil fuel and refueling ability to install and operate different capacities to meet the needs of consumers;
- Longevity;
- Ease of operation;
- Ability to install and operate on the roof of homes; and
- storage capability.

2.3.4.4 Wind turbine

To generate electrical power by wind kinetic energy, a specific cycle must be made between the input and output of the wind turbine. This cycle is such that when the turbine blades are driven by wind energy, the mechanical power is transmitted to the gearbox by the main shaft [29]. The gearbox output is transmitted to the generator by a coupling mechanism, and electrical energy is generated by the rotation of the generator. The wind turbine consists of a tower, a yoke, a generator, and a compartment. The power flow path starts from wind, mechanical energy, and electrical energy. The tower holds the main parts of the wind turbine. Part of the wind power is initially lost and does not enter the system because the turbine is not ideal, and another part of the power is lost mechanically in the turbine, shaft, and generator. The other part, which is dependent on the speed changes, is stored in the form of inertia in the mechanical system. Finally, the other part is lost to the electrical loss in components such as generators, cables, brushes, etc.

2.3.4.5 Fuel cell

The performance of the fuel cells [30] is similar to a battery that is continuously charged with high-hydrogen gas fuel; the fuel cell charging includes air, which provides the oxygen needed for the chemical reaction. The fuel cell uses a reaction of hydrogen and oxygen to generate DC voltage using an electrolytic conductive ion. The DC voltage is converted to AC voltage using an inverter and then delivered to the grid. A fuel cell generates heat and water along with electricity but has high operating costs, which is a major disadvantage. The main advantage of a fuel cell is that there is no moving part, which increases the reliability of the technology and produces electricity with no noise. In addition, it can operate more efficiently than any other electricity generation device by employing a wide range of fossil fuels. On the other hand, it is necessary to evaluate the effect of rapid contamination and hardening of the electrolyte properties, as well as its effect on cell efficiency and longevity.

2.3.4.6 Geothermal energy

The thermal energy present in the earth's solid crust is called geothermal energy [31]. The center of the earth is a huge source of thermal energy that exists in many forms, including volcanic eruptions or warm waters. According to existing hypotheses, the earth was a fiery mass that formed more than 4 billion years ago and has gradually cooled to freezing and cooling, and this cooling continues. At present, geothermal energy, which is free to obtain, is widely used in many parts of the world and used in various forms. Researchers have evolved new methods of energy supply, as new energy technologies are introduced, and future efforts to develop them in the field of technology transfer will be essential. The exploitation of geothermal energy, as a potential energy source in the depths of the earth, is independent of climate conditions and is capable of responding to current and future human needs.

Areas with geothermal energy potential correspond to volcanic and earthquake-prone areas of the world. The first attempts to generate electricity from this energy were made in Italy in 1904 and there have been many activities around the world since then. In general, areas of the earth that have three important properties can have good potential for exploiting geothermal energy. These three features include a heat source, intermediate fluid, and porous media. It is possible to utilize geothermal energy using both power plant and non-power plant methods. Non-power plant method can be used in greenhouse centers, fishponds, thermal pumps, and ice prevention in the passageways as well as for

home heating and snow melting. The process of electricity generation at a geothermal power plant is divided into two groups: two-phase and single-phase geothermal power plants. In some countries, it is also important to use it in areas of the earth that have the geothermal potential. On the other hand, most of these generation methods in these countries are restricted to DG studies, and their application in the main grid should be examined by locating them, considering the appropriate objective function and the effects of their presence on the power system.

2.3.4.7 Biomass

One of the most appropriate energy sources for environmental protection is biomass [32], which in addition to being renewable, contributes to environmental cleanliness and health. Since energy generation reduces environmental pollution, biomass technology as a source of energy is available in various forms and methods. Biomass is the result of the collection, conversion, and storage of solar energy by plants and other surplus residues from nature. The efficiency of this process is low, but as its raw material (fuel) is free, and due to the additional benefits they provide, it is increasingly used. Today, many efforts are being made to increase efficiency and make progress in this technology. Various technologies have been developed to convert biomass to heat in thermal power plants. The efficiency of these technologies typically ranges from 36 to 47%.

2.3.5 DG effects

Distribution systems are designed assuming that the electrical charge is flowing from the power system to the load. Therefore, output fluctuations or a reverse current flow from the generator occurs due to the presence of DG, it is likely to have effects on the distribution system. These impacts may include power losses, voltage profile, reliability, power quality, protection, and safety. Some of the important effects of DGs are as follows [24, 33]:

Due to its proximity to the load center, the DG has a significant impact on electrical losses. The DG unit should be in sites requiring further reduction in losses. Similar to capacitor placement, the DG location process is carried out to reduce losses. The main difference is that the DG unit affects both the active and reactive power, while the capacitor bank only affects the reactive power flow. In a feeder with high loss, if a small amount of DG is reasonably located (10-20% load of the feeder), it can significantly reduce network losses.

The voltage of the distribution systems is usually regulated by tap changer on the substation transformer and by using a regulator voltage and capacitor in the feeder. In this form of voltage regulation, it is assumed that the power flows from the substation to the loads. DG offers continuous power flow, which may interfere with the conventional voltage regulation method. Since voltage regulation control is usually based on radial power flow, inappropriate DG placement can cause an under-voltage or overvoltage in the network. On the other hand, DG installation can have a positive effect on the distribution network by providing reactive power for voltage control, loss reduction, frequency regulation, and operation as a spinning reserve [34].

PQ refers to the degree of power characteristic, in line with the ideal sinusoidal waveform of current and voltage, with balanced current and voltage. To protect the system from PQ loss, the system operator must guarantee the minimum specified short circuit capacity [35]. The relationship between DG and PQ is ambiguous. On the one hand, many authors emphasize the effects of DG on the issue of power quality. For example, in areas where voltage support is difficult, DG can be helpful, because the connection of DG generally leads to an increase in voltage of the grid. It also has potentially positive effects on voltage support and power factor corrections. If there are many DG connections in a given line, the power flow distance among feeder lines widens due to the backward current flow of the DG. This difference may cause the voltage profiles of the feeder line to exceed the acceptable range. The voltage of the distribution lines is controlled by a programmable timer or Line Drop Compensator (LDC) [36].

Generally, a distribution transformer has several feeder lines and the voltage for these lines is set as a block. If the DG output changes within a short time, the system voltage fluctuates. These oscillations will cause overvoltage and under-voltage on the end-user side. When the generation system is dependent on natural conditions, such as wind and PV generators whose inputs include the uncertainty of wind speed and solar radiation intensity, there are concerns regarding the voltage fluctuations caused by changes in the power output of the wind and solar units [37].

As the interruptions in power supply highly affects power distribution companies and end-users; and causes significant economic loss, the employed power supply source needs to have high reliability and be economically justifiable. In the past, the outages and power interruptions at the distribution systems were less catastrophic than those occurring at the generation and transmission systems. Yet, according to the information collected with

many years, it has been unquestionable that the power interruption at the users' location, i.e. at the distribution level, dramatically affects the power supply chain and this is all because of interruption at the distribution network. As a result, DGs are usually embedded in distribution networks hoping to enhance the power supply reliability [38]. Further, DGs can be considered as support and backup systems or sometimes can be utilized as the main power source to feed the load. The other aim of using DGs is to reduce costs at the peak hours.

Providing an estimation of the influence of the service given in the past is among the important problems when assessing the reliability at distribution level. To tackle this, the impacts of service deficiencies on the performance indices of the system should be determined. Operators use reliability indices to enhance the service level and satisfy the users' needs. Other applications of reliability indices are in finding the needs of generation and transmission systems and the added capacity to the distribution level, besides being used to check the robustness of the system against harmful faults and events. Additionally, reliability indices have extensively been utilized by power engineers and operators to decide on the operation of the system and make changes in case of emergency [39].

2.3.5.1 The effects of DGs on power flow components

Distribution networks are, in fact, designed based on this assumption that the primary side of sub-transmission substations connected to the transmission system is the only power source that short circuit capacity of the system can be obtained based on characteristics of this side. DGs dispersed within the distribution network violate the previous assumption. Therefore, new paradigms of the operation are formed that have never occurred in traditional systems. Accurate engineering can overcome the potential disadvantages of DGs and employ them with maximum efficiency possible [40]. Some of these disadvantages are as follows [41]:

- Increase probability of failure in system equipment and customers;
- Reduction of PQ (especially overvoltage);
- Reduction of reliability;
- Increased substation -fault restoration time; and
- Reduced safety of the system and personnel.

This subsection addresses the impacts of DGs on different power flow components such as line currents, voltage profile, and system loss in the distribution network. Noting that systems employ several specific equipment to adjust the voltage profile, the following

deals with the effect of DGs on voltage regulation devices. Different loading scenarios are extracted based on the studies conducted focusing on the influence of DGs. Traditional unidirectional radial distribution networks have one power supply (from the primary side of the substation connected to the transmission network). By changing this structure due to the presence of DGs, new problems arise in these networks that affect the power flow components.

2.3.5.1.1 The effect of DGs on line currents

As they supply loads locally, the presence of DGs usually reduces network loading and releases the capacity of different lines, which is one of the benefits of these resources. Nonetheless, under poor engineering design conditions, some lines may overload. Therefore, investigating the network with DGs in terms of overcurrent of lines is one of the studies that should be conducted in the presence of DGs. In a traditional network, the conductors of the network usually become weaker as they make a distance from the substation. In fact, by increasing the distance from the substation, the line currents decrease and the conductors with the less cross-sectional area can be used. This type of design is based on the same initial assumption of these networks that the radial network is radial and unidirectional and its power supply is located at the beginning of the substation. Normally, the DG will reduce the line currents by feeding part of the network load. However, given the size and condition of the network, it is possible for the DG current to flow in the opposite direction. If the DG is larger than the load after it, then part of the current returns to the substation. This, by itself, cannot pose a particular problem unless the current flow toward the substation exceeds the conductor capacity. Of course, this can happen under certain conditions, one of which may be to curtail (removal) of loads after the DG, which may occur due to unpredictable faults. In this case, the entire DG current flows to the substation. That is, if the size of the DG is large and the network is designed based on the same traditional network defaults, an overcurrent problem may appear.

One of the other cases that may cause an overcurrent problem is when a dedicated DG is embedded to feed certain customers. In these cases, if conductors leading to the DG are selected based on the released capacity of the line, it can cause challenges in the load outage mode. In this case, the DG current that flows toward the beginning of the feeder may be greater than the maximum conductor current. For example, in Fig. 2.6, the DG is connected to bus a to feed the three-phase load. When the load is disconnected the DG

current flows towards point *b*. As a result, if the line between *a* and *b* is selected based on the released capacity of the line, it will not be able to transfer DG energy to point *b* and experiences overloading.

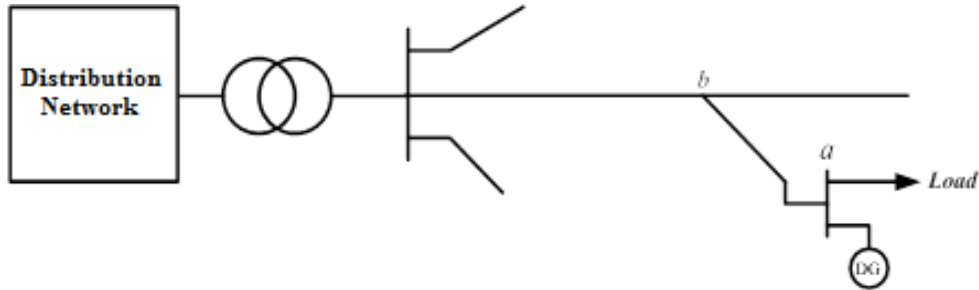


Fig. 2.6. Connection of a DG to a sub-branch of a distribution feeder.

Therefore, although in most cases DG can reduce line current and release capacity of the line, in some cases poor design can cause overloading. This issue can be investigated under the maximum and minimum loading of the DG and the network, respectively, which will be addressed in the study of different scenarios for studying network loadings.

2.3.5.1.2 The effect of DGs on voltage profile

DGs located near the load centers in distribution networks can improve voltage profile due to the following reasons:

- Because of the proximity to the load, the impedance of the load feeding path is thus reduced, DGs reduce the voltage drop according to the impedance reduction;
- By supplying the loads, DGs reduce the power transfer from the sub-transmission substation or distribution substation toward the end of the feeders, thereby reducing the voltage drop by reducing the active and reactive power supply; and
- By operating in the PV mode, DGs can regulate the voltage of the network.

At the same time, these resources can cause some disadvantages in the grid. Since most of DGs deliver constant power to the network and improve voltage profile during peak load hours, they increase voltage at low loads by reversing the power flow. In Fig. 2.7, a DG is connected to the load bus. The amount of injection power of the distribution substation is obtained as follows:

$$S_s = P_s + jQ_s = (P_L - P_{DG}) + j(Q_L - Q_{DG}) \quad (2.1)$$

where, S_s is apparent power, P_s and Q_s , are active and reactive powers respectively, j is an imaginary number and Q_L and Q_{DG} are reactive powers of the load and DG respectively.

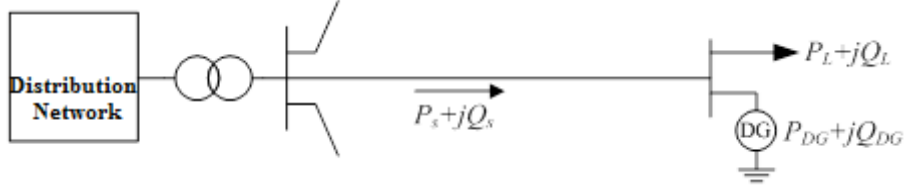


Fig. 2.7. Connection of a DG to the load bus.

Therefore, the voltage drop in the feeder is calculated as follows:

$$\Delta V = (r(P_L - P_{DG}) + x(Q_L - Q_{DG}))/V_S \quad (2.2)$$

Where, ΔV is voltage difference, r and x are resistance and reactance from the primary point of view of the circuit respectively and V_S is considered as the reference voltage of the network.

During the peak consumption hours, if the amount of power injected by the DG is lower than peak power consumption by the loads, ΔV is positive and as a result, the DG acts to improve the voltage profile and bring the load busbar voltage closer to the substation voltage.

However, if at low-load hours the injected power of DG exceeds the load demand, ΔV is negative and the busbar voltage will be higher than the substation voltage, which indicates the load experiences overvoltage.

It will be difficult to adjust the transformer tap-changers. When the DG is installed on one of the feeders, the transformer tap-changer should be set on the low taps to avoid overloading the feeder at low-load hours. Setting the transformer tap-changer on the lower taps causes the other feeders to experience voltage drop at peak loads. As a result, it will be challenging to find a balance point for this transformer tap-changer.

When the DG operates in the PV mode, it injects/absorbs reactive power to/from the network to maintain the voltage level. If its size is large and operates in the lag mode, then it receives a large reactive power from the network. The DG should, therefore, suggest a solution to offset this reactive power drawn from the network. The absorption of such reactive power from the network has an impact on the network losses and loads that should be considered by distribution utilities. On the other hand, the effect of a sudden

power outage of the source, which will cause transient overvoltage; and also the duration the primary side of the transformer can react to this event and restore the network should be taken into account. In such circumstances, the distribution utility shall employ switching capacitors and other reactive power compensation devices to recover the voltage of the network.

2.3.5.1.3 The effect of DGs on network loss

DGs typically reduce network loss by reducing the load supply path. When a DG is selected proportional to a local load and is installed near it, it can significantly reduce losses by reducing injected powers. The effect of DG on the voltage profile is not separate from its effect on network losses and these two components are closely correlated. However, in some situations, inadequate DG size and its inappropriate location may increase network losses. If the DG is too far from the substation and delivers power to the substation, or even if the power is returned to the transmission network then the distribution network losses increase but the transmission network losses are reduced [41].

2.3.5.2 The effect of different operation modes of DGs on power flow

A DG connected to the circuit, depending on the DG's nature and the common goals of the seller and buyer (distribution utility), can usually operate in two different modes as follows:

2.3.5.2.1 Constant power factor operation mode

In this case, the DG is connected to the circuit with a constant power factor. Since the purpose of this mode is to investigate the synchronous generator DGs and active power produced by this type of DGs is constant, the reactive power of DGs is determined by assuming a constant power factor. Therefore, they can be modeled as PQ buses or loads in power flow equations. On the other hand, in most power systems, the buses are operated in such an operating mode. The most convincing factor in using such a mode is the ease of operation and the reduced number of control devices. In this case, the active and reactive powers of the bus are specified. The unknowns include the magnitude and phase angle of the voltage of the bus. Therefore, these quantities can be obtained using conventional power flow equations. The amount of drop or increase in the voltage of the bus can also be discussed.

One of the main disadvantages of this operating mode is that there is no control over the bus voltage. Thus, in cases where the DG power injection is greater than the local load consumption power, by having a reversed current flow, the voltage of the bus is increased.

In fact, this operating mode is the main cause of the voltage increase. However, according to the IEEE P1547 standard [42], the DG should not be used for voltage control, this operation mode is the most common operating mode of DGs.

2.3.5.2.1 Voltage control mode

In some cases, the voltage control mode is used to improve the voltage profile. In this case, with the help of control devices, the voltage magnitude and active power injection of the bus are determined. The bus unknowns include the amount of reactive power injected into the bus and the phase angle of the bus voltage. As the voltage of the bus to which the DG is connected must be constant, the voltage drop calculations will be somewhat different. In the case, according to Fig. 2.7, the magnitude of the load voltage can be written as:

$$V_S = |V_L| + (r(P_L - P_{DG}) + x(Q_L - Q_{DG}))/V_S \quad (2.3)$$

where, $|V_L|$ is the magnitude of the bus voltage. Now, if $|V_L|$ is assumed to be equal with the reference bus voltage, Equation (2.3) changes to the following equation:

$$r(P_L - P_{DG}) + x(Q_L - Q_{DG}) = 0 \quad (2.4)$$

In this case, the following situations can occur:

- If the injected power by the DG is less than the active power of the load and the load is also inductive then, the load consumes reactive power or on the other hand, reactive power of DG will be positive as follows:

$$Q_{DG} = (r(P_L - P_{DG}) + x(Q_L))/x > 0 \quad (2.5)$$

- If the injected power by the DG is greater than the active power of the load and the load is also capacitive, which means it produces reactive power as follows:

$$Q_{DG} = -r \frac{(P_{DG} - P_L)}{x} + Q_L < 0 \quad (2.6)$$

- If the active power injection by the DG is less than the active power of the load and the load is capacitive, depending on the value of the parameters, the sign of Equation (2.6) can be positive or negative.
- If the active power injection by the DG is greater than the active power of the load and the load is inductive, depend on the value of the parameters the sign of Equation (2.6) can be positive or negative.

The advantage of this operation mode is that the DG can adjust the voltage profile by injecting reactive power, but can cause problems when it absorbs reactive power. On the other hand, each DG has some limitations relevant to reactive power generation, which must be observed and when the reactive power injection by DG exceeds these limitations, the DG changes from the PV operation mode to the PQ operation mode.

The disadvantages of DG operation in this mode can be described as follows:

- Unavailability of DG control by the network operator; and
- Feeding the fault location. Suppose that a three-phase symmetric ground fault occurs near the DG. The voltage of the fault location is assumed to be zero. Thus, the relevant Equation will be as follows:

$$|V_{DG}| - 0 = (r_{sc} P_{DG} + X_{sc} Q_{DG}) / |V_{DG}| \quad (2.7)$$

where, r_{sc} and X_{sc} are short circuit resistance and reactance respectively. Apart from the reactive power, all other parameters of Equation (2.7) are constants, so it is possible to obtain the reactive power of DG as follows:

$$Q_{DG} = (|V_{DG}|^2 - r_{sc} P_{DG}) / X_{sc} \quad (2.8)$$

In the aforementioned Equation, the real and imaginary terms of the impedance are small, and on the other hand, if DG is considered a synchronous generator then, the voltage of the DG bus is obtained as follows:

$$V_{DG} = E_f - j X_s I_a \quad (2.9)$$

where, E_f is the electromotive force of the generator and I_a is the injection current of the generator that feeds the fault location. In Equation (2.9), if the voltage of the generator bus is to remain about one p.u., then the reactive power injection will be as follows:

$$Q_{DG} = 1 / X_{sc} \quad (2.10)$$

that will be a large amount, which means the generator will strongly feed the fault location. By following Equations (2.8) and (2.9), the electromotive force according to the fault is obtained as follows:

$$I_a = \frac{E_f}{r_{sc} + j(X_s + X_{sc})} \quad (2.11)$$

Certainly, in order to make the voltage of the generator terminal or V_{DG} remain on one p.u., the electromotive force must be greater than one p.u. In order to the electromotive force to be more than one p.u., the injection current, as given in Equation (2.11), must be greater than one p.u., which means the generator intensively feeds the fault point.

In practice, not only the terminal voltage but also the electromotive force (EMF) will drop sharply and become much less than one p.u.. In fact, the voltage control system increases the excitation current when the terminal voltage is less than the desired value. With respect to Equation (2.11), the generator current increases if the electromotive force is increased. According to Equation (2.9), the increase in the generator current leads to more drop in the terminal voltage, and this cycle can be repeated. Therefore, a closed loop will be formed that will intensively feed the fault point.

With the agreement of the distribution operator and the owner of the DG, these sources can be used as voltage regulators. In this case, they can help regulate grid voltage by injecting or absorbing reactive power. However, in general, any attempt by the DG to control voltage can interfere with the voltage regulation scheme applied by the grid operator to control the same bus or a bus nearby [41]. The network operator's voltage control scheme may include the use of capacitor banks, Step Voltage Regulators (SVRs), or online tap-changers on sub-transmission transformers.

When the use of DG as a voltage regulator is permitted, the reactive power output of the DG can be varied to regulate the voltage (stabilizing the voltage of a point at a specified limit). However, the range of DG variations may not be sufficient to control large voltage variations. In these cases, the DG changes its operation mode similar to any other PV bus. In fact, the efficiency of the voltage control of the generator's common connection point depends on the ratio between the short-circuit powers of the DG and the grid. If this ratio is small, the effect of the DG on the voltage change will be low and causes the DG to require high reactive power injection or absorption to stabilize its bus voltage near below or above standard voltage levels. Hence, the DG should operate at a low power factor by limiting its ability to generate active power. In actual applications, the DGs for voltage control should not operate at low power factors [41].

2.3.5.3 The effect of DG on voltage regulation devices

Voltage regulation equipment mostly operates based on traditional distribution network structures, so the introduction of DGs can affect their performance. Usually, for control

devices that control the voltage of the network, the presence of DG can be very effective because it supplies the network in a bidirectional way and can affect the control method of the voltage control devices. This subsection tries to investigate the effect of DG on the important voltage profile adjustment devices as an automatic tap-changer of sub-transmission substations. The penetration of DGs to distribution networks affects the tap-changer of sub-transmission transformers in two ways as follows:

2.3.5.3.1 Control method

Online tap-changers of sub-transmission substations use a variety of methods to control the secondary voltage, where the presence of DGs can influence some of these methods. Tap-changers that use the line-drop compensation and/or negative reactance compounding methods for voltage control may have problems in the presence of DGs [43].

2.3.5.3.2 Tap adjustment

In traditional methods, the tap-changer of the sub-transmission transformer is so adjusted that the voltage drop at the end of feeders is not lower than the acceptable range. In this case, the main concern is the voltage drop of the buses. Therefore, the decision to set the transformer tap depends only on the voltage drop of the feeders. The value is usually set to the maximum permissible voltage to ensure that the voltage at the end of all feeders is within the allowable limit.

The penetration of DG into distribution networks also affects the regulation of transformer taps. By generating active power, and thus reducing the bus voltage drops, these sources (i.e. DGs) improve the voltage profile. On the other hand, they can lead to over voltages during low load durations, when they cause reverse power flow. As a result, in this case, in addition to considering the lower voltage drop of the feeders, for the feeders on which the DG is located, the overvoltage must also be considered. In fact, an optimal condition should be considered for the transformer tap so that the voltage of all feeders is within the permissible range under different loading conditions.

Utilizing DGs at their maximum power generation capacity needs to manage the voltage profile and prevent unacceptable over voltages. One of the most important and effective ways to increase DG power in the network is to set the sub-transmission transformer taps on the lower steps. However, due to the voltage drop problems in the adjacent feeders, it

may not be possible for the operator to use such conditions. Yet, in any case, it can be said that the adjustment of sub-transmission transformer taps is one of the effective ways to increase DG power in the network without generating over voltages [44-45].

Fig.2.8 presents a typical mode of voltage profile in the distribution network. In this figure, the voltage of the sub-transmission transformer tap is adjusted to 1.04 p.u. Also, according to this figure, the minimum voltage at the end of the feeder during peak and low load hours is 0.96 p.u. and 1.03 p.u., respectively. This indicates that if a DG is placed in the network, it is only permitted to increase the network voltage to 0.02 p.u. during low load hours. In the Medium Voltage (MV) section, the minimum voltage at maximum and minimum loads is 0.99 p.u. and 1.02 p.u., respectively. Therefore, in this stage, the DG is only allowed to increase the voltage by 0.03 p.u.

Now if the same transformer tap is set to 1.0 p.u. on the same network, then the permissible increase in voltage in the MV and Low Voltage (LV) sections would be 0.04 p.u. and 0.03 p.u., respectively. Correspondingly, on the MV side, the minimum value of the voltage at the minimum and maximum loads will reach 1.01 p.u. and 0.98 p.u., respectively. These values in the LV side are 1.02 p.u. and 0.95 p.u., respectively.

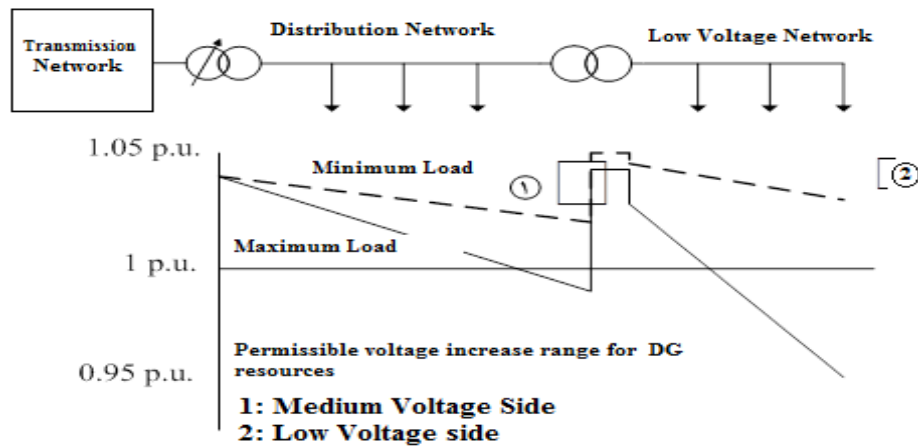


Fig. 2.8. Voltage profile of a distribution network at minimum and maximum loads.

These numbers are approximate and are used only to show that proper tap settings can increase DG penetration in the network. The difference in the amount of power generated by a DG in a case that is allowed to increase the voltage by 0.04 or 0.03 p.u. is very high compared to the case that it is allowed to increase the voltage by 0.02 p.u. Therefore, the

most important factor for increasing DG penetration in the network is the appropriate lowering of transformer taps.

Fig. 2.8 illustrates a different problem arising from setting the distribution transformer tap and may cause problems to the network. In Fig. 2.8, it is assumed that the distribution transformer tap will always regulate the voltage to 1.0 p.u. obviously, such a situation cannot be the case for non-automatic taps, and it is shown in the figure only for studying the LV network conditions at high voltage levels. The figure illustrates that it is not possible to set the automatic distribution transformer tap without coordination with the offline distribution transformer tap. Suppose the distribution transformer tap is set to 0.05 p.u. Then, on the MV side, neglecting the transformer voltage drop, the maximum voltage should be 1 p.u. In a similar way, when the DG is implemented on the LV side it should not increase the voltage further than this value.

2.3.5.4 The effect of DG on capacitors

Capacitors, as one of the most important reactive power compensation elements, play a key role in reducing voltage drop and power loss in traditional distribution networks. When installed on the DG network its application will face a challenge as the DG is not only a voltage drop compensating element but can also cause over voltages in the network. The effects of DG on capacitors can be examined in two parts.

2.3.5.4.1 Reactive power flow

One of the important parameters that can control the voltage is the reactive power flow. Thus, when DGs are installed in distribution networks, the reactive power flow is converted from a quantity that always need to be compensated and an undesirable quantity in the network to a quantity that its flow is sometimes beneficial and its further flow is demanded. In fact, because of the voltage increase by the DG, this increase should be compensated by using a quantity and this quantity can be the reactive power flow. On the other hand, one of the simplest methods of voltage control used by DGs is to change the reactive power flow that they adopt in the PV mode. Therefore, reactive power flow control is one of the simplest methods of voltage control in the presence of DGs.

Usually, in the presence of DGs, the increased penetration of which generally increases the voltage, the placement of capacitor to compensate reactive power will be meaningless, or in other words, capacitor placement will increase the voltage. Thus, in these networks, instead of compensating the reactive power, it must be consumed so that the voltage drop

caused by this reactive power consumption falls within the permissible range. Reactive power consumption of the network can be increased by installing a reactor. By increasing the reactive power consumption and the resulting voltage drop, it is possible to increase the DG penetration level in the network. In this case, however, the network losses will increase with the increase in the amount of reactive power flow of the network, and problems such as overvoltage and the possibility of network recovery will occur after DG's sudden outage.

On the other side, when the DG operates in the voltage control mode, the generator can generate or consume reactive power to control the voltage. The generator usually consumes reactive power when there is the possibility of overvoltage. In this case, the increased reactive power flow can increase network losses and cause problems for the network in the event of a sudden outage of DG. Capacitors, reactors, and other reactive power compensation devices in the network should be highly coordinated and studied to prevent overvoltage or voltage drop below the acceptable range.

2.3.5.4.2 Capacitor control methods

The impact of DGs on capacitive banks depends on the type, operation mode and location of the DG, as well as the methods of control methods of switching capacitor banks. Voltage-controlled capacitors should not be affected by the DG, if the DG does not operate in the voltage control mode. To prevent the voltage from moving rapidly between the DG and the capacitors, the set-point should be adjusted, and the time delay increased. If the line current control method is used, the DG can affect the capacitor because it can change the line current and even reverse it sometimes. Therefore, the current monitored by the capacitor does not reflect the current of the downstream network. The switching set-point is adjusted by assuming that the current at any location on the feeder has a reasonable ratio to the current at the control site [41]. If the DG operates at the unity power factor, the reactive power flow control method of the capacitors will not be affected. However, the DG with a non-unit power factor can have a great influence on this control mode [41].

2.3.5.5 The effect of DG on voltage regulators

Due to the similarities between automatic tap-changer and voltage regulators, the control method of these regulators can be affected by the presence of DG. As aforementioned for automatic tap-changer, the LDC method, which is one of the common control methods of

voltage regulators, can be problematic in the presence of DGs. However, capacitors can also affect the performance of voltage regulators and may sometimes cause them to malfunction.

2.3.6 Study of different loadings in the network

Distribution network loading varies according to the load characteristics. This loading changes depends on the time of day and the weather. Usually in the early evening due to the need for lighting, the load is the maximum; and at the last night hours, it reaches its minimum value. In traditional distribution networks, network power flow analysis is performed for maximum load conditions, which causes the highest voltage drop and line currents, and since the network is unidirectional, this is the worst case for the network. As a result, if the voltage profile and line currents are within the standard range, these standards will apply to other loadings as well.

The presence of DGs changes the nature of the network from unidirectional to multi-directional supply. This change in the configuration changes the nature of the current direction in the lines and consequently the voltage profile varies as well. Therefore, it can no longer be said with certainty that if the voltage profile in the overload is within the standard limit, then the network load will also fall within the standard range. From another point of view, it can be said that the active injection power by a DG is usually constant and can be returned to the substation due to the reduced overload consumption by the DG. Under these conditions, the current flowing in the opposite direction will change the voltage profile and, in some cases, create overvoltage. In fact, in the worst case, the network should also be solved even in the worst case to ensure that the voltage profile or line current exceeds the permitted limit. Usually, the power flow of the network in the presence of DGs should be carried out in three different cases as follows:

2.3.6.1 Without DGs and with maximum loading

This case is used to study the network in a situation where DGs are disconnected. However, this mode can be employed to analyze the state of the network before the introduction of the DGs. The DG disconnection can occur due to repairs, vendors withdrawing from sales to the network, unpredictable faults, and so on. If the network is designed based on the permanent presence of DGs, it may experience voltage drop or line over currents after the outage of the DGs, i.e. when the DGs are disconnected. Due to the

increase in current flow from the beginning of the substation to the end of the feeders, the voltage drop will be high and may cause the aforementioned problems.

2.3.6.2 With DGs and with maximum loading

In this case, the network is studied at peak hours and in the presence of DGs. This is a state in between. On the one hand, the voltage drop increases, as does the consumption. On the one hand, the presence of DGs can somehow reduce this voltage drop. If there is no proper coordination between the automatic tap-changer of the sub-transmission substation, the offline tap-changer of the substation, the location, and operation mode of the DGs, there can be an overvoltage in one feeder and a high voltage drop in the other feeder.

2.3.6.3 With DGs and with minimum loading

DGs and network loads adversely affect the voltage profile. In fact, the DGs act to increase the voltage profile, while the network load acts in reverse to reduce the voltage profile. Therefore, when the network load is reduced to a minimum, the network may face an increase in voltage. Reducing the load causes the current flow by DGs toward the beginning of the feeder, and since the reverse flow causes an inverse voltage drop, the buses near these DGs may encounter increased voltages. However, considering the outage of some loads, several studies have considered the lost load in the network as the minimum network load.

2.3.7 DG application in distribution system based on optimization algorithm

The entry of DGs into the electricity industry has made major changes to the design of distribution networks. The use of DGs reduces the number of newly installed feeders in the next periods. In addition, they cause delays in system upgrades or installing new posts in subsequent periods, which reduce losses and even free up the capacity of the network. Grid-connected distributed generation systems are integrated into the distribution network by transferring the power to it. So, like the other generation units and electrical network components, they affect the network characteristic and variables such as voltage, loss, reliability, etc. On the other hand, in designing and developing of distribution networks, the cost of DGs is very high. Therefore, designing and developing of distribution networks, considering DGs are done based on the constraints of distribution and to spend the least investment, operation and maintenance. In the design and network operation, the problem optimal siting and sizing of these resources has been investigated.

To optimize the optimal siting and capacity of DGs, various methods have been used in distribution networks. An optimization method is an intelligent approach applied to determine the optimum solution to a problem. This response can be a minimum or a maximum value. To make effective and efficient method, it is necessary to formulate a proper function for the problem [46]. The meta-heuristic methods also include a repetitive intelligence algorithm that is under computational intelligence. In these methods, using specific rules and methods, it is searched for the best site and the size of DGs in the distribution network. The optimization method is a repetitive production process that applies the search approach to effectively identify near-optimal responses by using different intelligent computing methods and help to search and explore the searching space. This approach is employed to find perfectly optimal or near-optimal solutions. This subsection describes the desirable methods used in the problem of HDG application. In recent years, meta-heuristic algorithms are considered for the optimization of DG resources in distribution networks. Some of these methods are presented in subsections 2.3.7.1-2.3.7.4.

2.3.7.1 Particle Swarm Optimization (PSO)

The meta-heuristic PSO algorithm is applied in many optimization problems solutions. The PSO is based on birds or fish manner. The PSO's main idea is the generation of particles randomly considering positions and velocities. The positions and velocities of particles are updated considering the search experience in comparison with the other particles. The optimal solution is obtained with the repetition of this process [47]. In [47], the PSO method is applied to find the optimum site and size of DGs units in a multi-phase imbalanced distribution grid. While in actual experiments, a combination of DGs is used. The results are investigated with the results of the Repetitive Load Flow (RLF) method, which has found that the method was more suitable in finding the location of DGs and was faster in terms of computational time. Also, the optimized distributed generation has amplified the voltage profile and also has reduced the losses. The method presented in [48] has used two networks of 33- and 69-bus. At first, the optimization base on the PSO algorithm has been applied to two systems and then the analysis approach has been applied. Results have shown that the PSO method provides lesser encapsulations in optimizing problem-solving. Also, methods and the results of the PSO for the 69-bus system are compared with the genetic algorithms and artificial bee colony (ABC)

algorithm have shown that all the methods have received approximately the same calculations in the viewpoint of losses.

Wind turbines are generally connected to the network to reduce power loss, prevent accumulation, and improve the voltage condition and the power supply in peak load conditions. Suitable sizing and siting of wind turbines play a significant role in minimizing losses in distribution networks. In [49], PSO is applied to find the installation site of wind turbines considering power maximum capacity to reduce losses. The site and maximum allowable size of wind units are calculated with minimizing the power loss and considering operational constraints. In this approach, there are at first the optimum location of wind units as optimization variable. And then, the value of the losses is calculated considering some cases with respect to the number of wind units. The feasibility of the proposed method is confirmed using two samples of 84- and 32-bus networks. The results cleared with the determination of the optimum size of wind units the losses are reduced and the voltage deviations are decreased. Increasing the turbine numbers also has a positive impact on loss reduction and improving the voltage profile. The results showed that when the capacity of wind turbines is considered instead of taking into account the maximum capacity allowed for their production as a variable, a greater reduction in losses and improvement of the voltage profile is accrued.

In [48], the location of wind units and PVs is done to reduce the losses and voltage stability improvement using the PSO. The problem of optimization is done as a multi-objective method and using weight coefficients. The optimum site and size of wind and PV sources are found by the optimization method with minimizing the losses and also provide the best voltage stability. The results have showed that this method can reduce the losses by employing optimal PV panels and wind turbines with the capability of reactive power injection, and to improve the voltage stability of the network, the voltage profile has improved in the network. In [50], the PSO is proposed to investigate optimal responses to the problem of capacitors sitting in a 16-bus IEEE-based wind energy distribution network considering the cost function. The siting and sizing of the capacitors lead to loss reduction and voltage improvement. In this study, the PSO method is used to obtain an optimal response to the problem. The results showed the performance of the losses cost. Also, the use of the PSO for the 16-bus network has less cost of power losses and voltage deviations than the genetic algorithm.

In [51], a method is proposed to find the optimum size and location of renewable distributed and non-distributed sources in a network. In this study, DG units based on wind energy and PV are non-DGs, while biomass energy-based DGs are defined as distributed units. The multi-objective approach consists of power losses, branches allowable current, voltage, environmental and economic indices. Suitable weight coefficients for different indices are determined by the analytical hierarchical process. To solve the extended formula, the PSO-based method has been applied to the 51-bus network. The results are compared with the results of the other multi-objective methods, in which different weight coefficients have assigned to the indices and this method is simple and efficient.

2.3.7.2 Genetic Algorithm (GA)

The GA is a technique for optimization, uses a direct simulation of the behavior of nature. This algorithm works with a population of "unique members", which defines "fitness" for each member. Obviously, those members who are more fit will find more opportunities for "fertility" through "blending" with other people in the population. By choosing the best members of the current population and performing a mix of them, a new set of members is created, which has higher population characteristics than the previous population. By continuing this process, after multiple reproductions and generating sequential populations, members' attributes are gradually published in populations and members are modified in a desirable way. Thus, if the algorithm is well designed, then the population is converged toward an optimal solution [52]. In [52], the goal of the optimal siting of DGs is to minimize DG investment and utilization costs, minimizing the cost of purchasing electric power for the main grid, and minimizing the voltage deviation. Pareto optimization strategy using fuzzy theory method is used for extracting solutions as a multi-objective problem. However, the allocation and determination of the optimal capacity of DG units have been done using a GA. The invertebrate of voltage deviation constraints, the generating power of DG units, and overloads for lines have added to the target function using penalty coefficients. In this study, an improved GA is proposed to solve the multi-objective problems and has been used to find the optimum site and capacity of DG units. The improved GA changes DG's locations and capacities and evaluates their fitness using objective functions. Then, using a number of solutions, it creates the Pareto front. Here, using the fuzzy method, arbitrary results are extracted from the solutions in the Pareto front. In [53], determining the optimal wind turbine capacity

has been presented for minimizing the losses in the distribution network. The optimization was performed by the GA and load flow is applied to calculate the energy losses. The characteristic of the load and the profile of the variable power of the turbine has been considered. For optimization, a weight coefficient is selected for each candidate bus. These coefficients determine the number of turbines per bus. The method is employed to the 30-bus network and it is assumed there are candidate buses for placing the wind units. A comparison is performed among different states for 4 days as well as one year. The results have shown that the amount of losses has decreased with the use of wind turbines. Also, by clustering, the energy losses are slightly increased. In [54], a hybrid optimization method is proposed to calculate the best place and size of wind turbines that combine GA and Optimal Power Flow (OPF) method based on the electricity market. In this method, overall energy losses are minimized considering the combination of wind production and load, simultaneously. The GA is used to select the optimal capacity, while the optimal load distribution based on the electricity market has been used to determine the number of optimal wind turbines per candidate buses.

In [55], a method is proposed for the optimal siting of wind turbines in the distribution network. The GA and PSO are combined to optimize the cost of investments made by wind turbine developers as well as social welfare in the distribution network operator (DNO) benefit market environment simultaneously. The GA has been used to select optimal capacities between the different capacities of wind turbines, while the market has been used to find the number of wind units to maximize social welfare, taking into account network constraints. The results have shown that wind turbine developers can improve their benefit by optimizing the location of wind units and the consumers' benefit will also be increased with decreasing the energy cost.

2.3.7.3 Ant Colony Optimization (ACO)

The ACO is an inspiration and mimic of the relationships and behaviors happening in real ant colonies. Ants follow an interesting and optimized way of forage such that they innately discover the optimal path to reach the food source. This means that ant colonies have the potential and ability to explore and reach the food supply. The fundamental step of the ant colony optimization is to mimic and simulate the same trend followed by ants [56-57]. The ACO algorithm is defined as a wildly inspired new meta-heuristic method for solving complex combinatorial optimization (CO) problems. This method is used to obtain suitable solutions for difficult combinatorial optimization problems at a proper

computational time. ACO is one of the evolutionary methods based on the implementation of finding the shortest way for the ants when they search for food. Ants determine the shortest way from the nest to the place of food by placing a chemical called the pheromone [58]. The ACO is used for several optimization problems in electrical engineering [59-60]. Based on the ACO, losses reduction, and increase of load balancing for distributed radial distribution networks are presented [61]. The results showed lower losses and better load balance when the network is compared in the presence and absence of distributed generation. However, this study only focuses on the impact of distributed generation on losses, while the distributed generation's site and size are already constant values. The results illustrated that the ACO is converted into a highly perfect method, and its performance is better than the genetic method. It is clear that when DG is located on a network, the average loss of 44.626% is achieved by the ACO, while this average is 43.803% using GA.

2.3.7.4 Artificial Bee Colony Algorithm (ABC)

The ABC method is a collective intelligence-based optimization that follows the behavior of bee honey swarm with the fact that bees seeking food sources [62-63]. The pursuit model election that causes the convergence of social intelligence consists of three essential elements: job seeker bees, non-worker seeker bees, and source of food. The two manners also define the movement toward a source of nectar and drop insignificant food sources. Comprehensive studies have been conducted in various fields using the ABC algorithm to solve the problems of practical optimization [63]. In [64], the ABC is applied for losses reduction with the determination of DG optimum capacity. The proposed method has been implemented on networks containing three distributed generation units. The results show that the process simultaneously reduces power losses and computational time, while not in local optimizations. In [65], the location and planning of DG-based on hybrid diesel-photovoltaic resources in the distribution network have been performed using the ABC. The objective function of the optimization problem is minimizing the cost of investment, replacement, operation, and maintenance of the system equipment, minimizing losses, reducing the amount of power transferred to the network, and reducing unsupplied loads. This method is applied to radial systems of 33- and 45-bus. In this study, the PSO algorithm has been used to compare the ability of the ABC algorithm. The simulation results show that the ABC optimization method has a higher ability in

problem-solving than the PSO method and it receives lower system costs with higher convergence rates.

2.3.7.5 Fireworks Algorithm (FWA)

The FWA is a randomized search based on collective intelligence. It can be applied for optimization problems solution because it can be employed to search for areas that are prone to be allocated as a response space. This method is inspired by the firefighting explosion phenomenon and sparks created inside the space around the explosion of crackers in the sky. The firing algorithm is considered as a new algorithm, the reason for this is the explosive nature of crackers and its inspiration when searching for a response. This algorithm can also divide resources into a hierarchical community when it comes to searches for solutions [66]. In [67], a new hybrid method is proposed for minimizing the losses and voltage stability improvement by installing DGs in a network. Using the FWA, the location, and optimal capacity of the DGs are determined optimally based on the Voltage Stability Index (VSI).

2.3.7.6 Backtracking Search Optimization Algorithm (BSOA)

The site of DGs is determined considering losses minimization and voltage profile improvement using the BSOA [68] based on fuzzy rules and loss sensitivity factors [68]. The fuzzy expert rules are responsible for determining the initial locations and priorities of the candidate buses of the DGs. The loss sensitivity factor has also been applied to illustrate the critical bus for DGs siting as well as reduced computational time. The Loss Sensitivity Factor (LSF) is able to predict where active and reactive power injections have the highest loss of life at which buses. And normalize it to use LSF in fuzzy logic. The proposed method in this study is applied to the 33-bus system and two scenarios are considered for DG units. In Scenario A, DGs have only the ability of active power injections, and in scenario B, in addition to active power injections, the DGs have the ability of reactive power injections. The results show that the consideration of two DGs can improve the voltage, reduce the losses and improve the power factor. However, considering the three DGs does not change much about the state of the two DGs. Also, the results show that employing two DGs with the capability of active and reactive power injection reduces the losses effectively as well as improves the voltage.

2.3.7.7 Ant Lion Optimizer (ALO)

The optimization of the siting and sizing of PV and wind units in the network is presented based on ALO in [69]. The purpose of this study is to determine the optimal location and

capacity of distributed wind and PV using the intelligent approach. The problem is optimized by multi-objective and using weight factors. In this study, the proposed method is implemented on the radial distribution network using 33-bus and 69-bus IEEE standard system. In resolving the problem of using renewable sources in the distribution network, their optimal location and capacity should be determined in the distribution network. In this research, a new algorithm called the ALO optimization algorithm is used for solving the problem of hybrid DGs based on PV and wind resources in the network. The loss sensitivity index is presented to show the cascade-sensitive buses. The search area and thus the time of the optimization process can also be reduced by using this factor. In other words, the buses that are in problem in the viewpoint of losses are identified by this factor and the site of DG installation is determined among these buses. The objective function is aimed to reduce the losses and voltage, as well as voltage stability improvement of the network. The proposed problem is implemented based on multi-objective optimization and using the sum of weighted factors using the ALO algorithm. The results clearly shows that the ALO resulted in less loss. ALO also operates better than the others in the viewpoint of voltage profile improvement and achieving the minimum voltage. It is also shown from the comparisons that the ALO has reached significant aims in terms of losses and saving due to loss reduction.

2.3.8 Analysis of Power Quality (PQ) Features with DGs in the network

The utilization of DGs with the help of renewable energy resources in medium- and low-voltage distribution systems are among the fundamental approaches to energy generation. With the widespread use of DG resources in distribution systems, it is essential to consider various technical parameters of the system. The exploitation of renewable energy resources such as solar and wind plants in distribution systems to provide part of the system's demand is essential regarding today's concerns in terms of environmental pollution and fuel consumption reduction. However, the analysis of PQ issues and an attempt to improve it under normal and faulty operating conditions is critical [70].

This subsection addresses PQ problems in distribution systems due to the presence of DGs and examines the reasons for each of the causes such as harmonics, voltage waveform oscillation, voltage flicker and increased short circuit level of the system. Furthermore, as individual DGs produce harmonics in the distribution system and to prevent the harmonics and the system voltage oscillations from exceeding the determined standard limits, it is necessary to use a method to determine the maximum value of the

power generated by DGs. This will avoid the excessive use of DGs and maintain PQ against severe disruptions.

2.3.8.1 PQ problems in distribution systems with DGs

By analyzing distribution systems with DGs, PQ problems can be identified in these systems, including oscillations and changes, distortion and harmonics in voltage and current waveforms, and increased short circuit level of the system. In general, the connection of DGs to LV distribution systems may cause the following problems [71-72]:

- Increase or decrease in the voltages of conductors;
- Increase in the voltage harmonic distortions;
- Increase in the system short circuit level;
- Disoperation of protective systems; and
- Increase in the temperature of LV system conductors.

These cases are true for radial and ring distribution systems.

2.3.8.1.1 Gradual changes in the voltage

Steady-state analysis of the voltage at the connection point between DGs and overhead line feeders or underground cables of distribution systems is one of the fundamental parameters in studying such systems. Therefore, standards have been regulated for the changes in the voltage magnitudes in LV and MV systems with DGs. One method is to analyze the average values of voltage change ($\varepsilon\%$) at 10-min intervals at the connection point. The voltage magnitude at the connection point in steady-state conditions is calculated as follows [71-72]:

$$\varepsilon\% = 100 S_n / S_k \cos(\phi_K + \phi) = 100/R \cos(\phi_K + \phi) \leq 3\% \quad (2.12)$$

where S_n is the rated power of the DG source, S_k is the short circuit capacity at the connection point, ϕ_K represents the network impedance angle, ϕ is the output current angle of the DG, and $R = S_k/S_n$ is the short circuit ratio at the connection point. According to the standards of European countries, the value given in Equation (2.12) should not exceed 2-3% in MV systems so that the changes in the voltage of LV systems remain less than 10%. The magnitude of changes in the voltage at the connection point of DGs to the distribution system in terms of power factor ϕ , system angle ϕ_K , and short-circuit ratio R is shown in Fig. 2.9 for different values. Moreover, the power factor of the DG

influences the Root Mean Square (RMS) voltage. Fig. 2.10 illustrates the changes in the voltage with respect to the short circuit ratio at the connection point for different power factors of the DG.

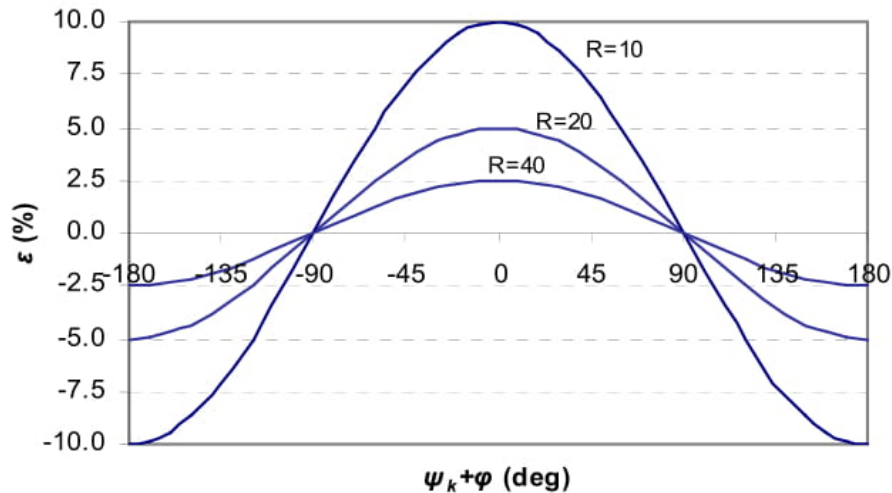


Fig. 2.9. The changes in the voltage with respect to the system angle and power factor [71-72].

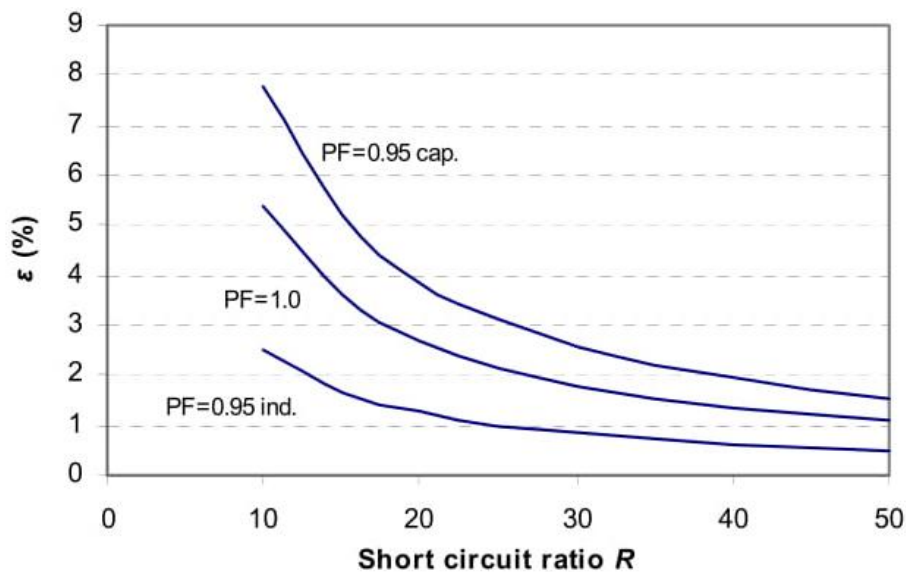


Fig. 2.10. The changes in the voltage with respect to the short circuit ratio for different values of power factor [71-72].

In the case of using multiple DGs in the system and connecting them to a single feeder, the changes in the voltage due to all DGs should be considered. Hence, an accurate power flow analysis is essential for the system. When the power generated by DGs is the maximum (minimum) and the power consumed by the system loads is the minimum (maximum) the changes in the voltage of the connection point will be maximum

(minimum). The average voltage at the connection point should not exceed 5% of the rated voltage so that it can be compensated by setting the tap-changers of MV to LV transformers as follows [71]:

$$0.95 V_n < V_{med} = \frac{V_{min} + V_{max}}{2} \leq 1.05 V_n \quad (2.13)$$

where, V_n , V_{med} and V_{max} are rated voltage, medium voltage and maximum voltage respectively. The change in the voltage of the connection point around the average voltage should not exceed 3% of the rated voltage so that the voltage changes in the LV system is maintained less than 10% that is presented as follows [71]:

$$2\Delta V = V_{max} - V_{min} \leq 0.06 V_n \quad (2.14)$$

2.3.8.1.2 Flicker and rapid changes in voltage

The flicker coefficient shows the range of variation and voltage oscillation caused by small power sources and it can be calculated or measured for real systems. The coefficient depends on the short circuit current of that point, the rated power generation, and the flicker coefficient of equipment, which gives the flicker generation capability of the equipment. Gas and thermal turbine generators have a flicker coefficient of 20, but the value for wind turbines is 40. The large value of the flicker coefficient in wind turbines causes oscillations on voltage and current waveforms of the distribution system easily. Rapid changes in voltage at the point DGs are connected to the distribution system may be the result of switching the power source on/off or abrupt changes in the output power of the power source. The magnitude of these changes and its resultant flicker should be bounded to prevent the damage to equipment and consumption loads available in the system. In the case of power source switching, it is important to consider the system type (LV or MV), the size of equipment, and the operating frequency. Thus, the values of such limitations are specified in different standards. For instance, the maximum changes in the voltage for an MV distribution system with DGs must be less than 2%, 3%, and 4% for cases the power source switching per hour is more than 10 times, less than 10 times and more than 1 time, more than 1 time, and less than one time, respectively.

The corresponding values for LV distribution systems must be less than 4%, 5.5%, and 7%. Equation (2.15) presents the magnitude of rapid change in the voltage when switching the power source on [71]:

$$\varepsilon_{max} \% = 100 * k * \frac{S_n}{S_k} = \frac{100}{R} * k \quad (2.15)$$

where S_n is the rated power of the DG source, S_k is the short circuit capacity at the connection point and k is voltage change factor. However, the more accurate equation is obtained by considering the dependency of k to the power factor of the system and is given as $k(\phi_K)$. For simplicity, this quantity can be assumed equal to the ratio between the power source starting current to the rated current, a value between 1-8, where it depends on the start-up method and the type of the DG source. The voltage flicker magnitude caused by switching of DGs in distribution systems in short-term P_{st} and long-term P_{lt} periods is provided by (2.17) and (2.18) [71]:

$$P_{st} = 18/S_k \left(\sum_{i=1}^N N_{10,i} (K_i(\phi_K) S_{n,i})^{32} \right)^{1/32} \quad (2.17)$$

$$P_{lt} = 8/S_k \left(\sum_{i=1}^N N_{120,i} (K_i(\phi_K) S_{n,i})^{32} \right)^{1/32} \quad (2.18)$$

where, N is the number of parallel DG sources in the system, $S_{n,i}$ expresses the rated power, and $K_i(\phi_K)$ is the flicker step coefficient of unit i . Moreover, $N_{10,i}$ and $N_{120,i}$ are the maximum number of switching of DGs at periods of 10 min and 120 min for unit i . The voltage flicker magnitude for an LV distribution system for short-time and long-term durations is less than 0.75 and less than 1, respectively. However, these values for an MV system considering the system parameters are less than 0.7 and less than 0.9, respectively. The flicker of the whole system is obtained by switching all DGs available in the distribution system.

2.3.8.1.3 Harmonics and inter harmonics

Using power electronics devices in the form of converters to connect DG sources such as wind turbines and solar cells to the distribution system causes harmonics and distortion in voltage and current waveforms of the distribution system. In the MV system, voltage harmonics may be produced due to the connection of equipment to LV or High Voltage (HV) systems. That is why individual devices need to limit specific harmonics so that the voltage harmonic level of the whole system does not exceed the regular limit. Therefore, when utilizing DGs in the distribution system, attention has to be paid to the potential of producing harmonics and inter harmonics caused by such equipment. In a distribution

system with nonlinear loads equipped with converters at their input, constituting mainly the industrial loads, the voltage waveform harmonics increase due to the use of DGs, where the increase in harmonics at the bus connected to the DG source is more severe. As a result, filters are required to eliminate harmonics. The order of harmonics elimination control for different LV, MV, and HV levels form one voltage level to another is provided in Table 2.2.

Table 2.2. The order of elimination of different harmonics in LV, MV, and HV systems [71-72].

Odd multiples and multiples of 3				Odd multiples and multiples of 3				Even multiples			
Order	Magnitudes of voltage harmonics			Order	Magnitudes of voltage harmonics			Order	Magnitudes of voltage harmonics		
	LV	MV	HV		LV	MV	HV		LV	MV	HV
5	6	5	2	3	5	4	2	2	2	1.5	1.5
7	5	4	2	9	1.5	1.2	1	4	1	1	1
11	3.5	3	1.5	15	0.3	0.3	0.3	6	0.5	0.5	0.5
13	3	2.5	1.5	21	0.2	0.2	0.2	8	0.5	0.4	0.4
17	2	1.6	1	higher	0.2	0.2	0.2	10	0.5	0.4	0.4
19	1.5	1.2	1					12	0.2	0.2	0.2
23	1.5	1.2	0.7					higher	0.2	0.2	0.2
25	1.5	1.2	0.7								
The THD of the values given in this table for HV, MV, and LV systems is 3%, 6.5%, and 8%, respectively.											

Therefore, the amount of distortion in the MV system for the harmonic of order h is obtained according to (2.19) [71]:

$$\sqrt[\alpha]{L_{hMV}^\alpha - (T_{hHM} * L_{hMV})^\alpha} \quad (2.19)$$

where, L_{hMV} and L_{hHV} are the magnitudes of the harmonic order h for MV and HV systems, T_{hHM} represents the transfer factor of harmonic order h from HV to MV side, and α is a coefficient equal to 1 for harmonics orders $h < 5$, 1.4 for $5 \leq h \leq 10$, and 2 for $h > 10$.

Using G_{hMV} , the voltage distortion range of $E_{Vh,i}$ can be obtained for each DG in proportion to its output power as follows [71]:

$$E_{Vh,i} = G_{hMV} \alpha \sqrt{\frac{S_{n,i}}{S_i}} = G_{hMV} \alpha \sqrt{S_i} \quad (2.20)$$

where, S is the total power of the system and S_i is the ratio between the power generation by each DG and the total power of the system.

Considering DGs as harmonic current sources, it is possible to calculate the current harmonics of the system using the system impedance for each harmonic order as follows [71]:

$$V_{hi} = Z_h * I_{hi} \leq E_{Vh,i} \Rightarrow I_{hi} \leq E_{Ih,i} = \frac{E_{Vh,i}}{Z_h} \quad (2.21)$$

where, V_{hi} and I_{hi} are the voltage and current values of harmonic h of the unit and $E_{Ih,i}$ gives the range of current distortion in the distribution system [71-72].

2.3.8.1.4 Power flow and power loss

To study the amount of change in the power loss of a distribution system with DGs, power flow calculations should be performed first. The aim of power flow analysis in distribution systems with DGs is to analyze the voltage at any connection point. This increased voltage caused by the presence of synchronous or induction generator of DGs is found:

$$\Delta V = \frac{PR + XQ}{V} \quad (2.22)$$

where, R and X are the resistance and reactance of the overhead line feeder and P and Q are transient active and reactive power at that point.

As resistance is more effective than reactance in LV systems, active power will be more impactful than reactive power in a distribution system. In the power flow analysis of such a distribution system, the effective parameters include the active and reactive power output of the DG and its connection point to the system, loading of the system, the number of sources connected to a single line, and the impedance of the system.

Power flow results for such distribution systems indicate the voltage increase at the connection point, but if the power factor of DGs is unity or very close to unity, the voltage increase is reduced and reaches smaller than 2%. These analyses show that power loss in MV distribution systems with DGs is less than a distribution system without DGs. On the other hand, if the conditions for using DGs with a unity power factor is met, the power loss will increase compared to the case with a smaller power factor. Thus, the best case

of using DGs considering voltage changes and power loss is to employ DGs with the power factor in the range of 0.95 to 1. With such a selection, the increase in power loss and voltage at the connection point of DGs to the distribution is prevented.

2.3.8.1.5 Short circuit current

In distribution systems with DGs, depending on the impedance of the system, the more the number of DGs, the higher is the value of the short circuit current of the system. The value of this current is higher for lines connected to DGs than those without connection. The reason for such a fact is that in the case of a fault at each of overhead line feeder or underground cable, the relays will detect the fault and disconnect the DG connected to the feeder at that substation, the reconnection of which is subject to fault clearance. However, in distribution systems with DGs, in the case of a fault at each of the feeders they are connected to, DGs are still connected to the system despite the disconnection of the main grid. This may help continue feeding the faulty feeder, the consequences of which are the consistency of arc at the fault location and an increase in the system's short circuit level. In the case during a fault, DGs directly connected to the faulty feeder are automatically disconnected from the system, not only the short circuit level of the system is not increased but this also prevents de-energizing the loads supplied by these sources. Hence, it is essential to analyze the voltage system of distribution systems with DGs and the coordination between relay settings. Thereby, relays connected to DGs are required to trip the source in the case of a fault in the related feeder and avoid the wrong tripping of the source and disconnecting part of the loads due to a fault occurrence on another feeder [71-72].

2.3.8.1.6 Analysis of unbalance

As three single-phase conductors are used in distribution systems and the loads are generally single- or three-phases, the imbalance can be reduced to establish rather balanced arrangements between each of the phases. The connection of DGs in a three-phase form to the system or in a single-phase form with balanced arrangements has a negligible impact on the imbalance of current and voltage waveforms of the distribution system such that the system imbalance can be maintained at less than 2% by establishing appropriate arrangements.

2.3.9 Determining the maximum power generation by DGs in radial distribution systems considering harmonics limitations

Voltage oscillations and harmonics in distribution systems with DGs are the sums of oscillations and harmonics injected into the system by individual DGs. Therefore, to maintain the PQ of distribution systems within the standard range, the power generation by such sources is expected to be limited. To determine the maximum power generation by DGs in distribution systems along with maintaining the level of oscillations and its harmonics within a determined range the following method can be used [73]:

In this method, to maintain the voltage oscillations of the LV system within the range of 10%, it is necessary to prevent the oscillations increase of the MV system from exceeding 3%. Thus, considering the loading of feeders and calculating the current of the main bus, the increase in harmonics and its oscillations is avoided. Since, there is no voltage harmonics at the farthest points of the radial distribution system feeders, the main current at the feeder is the maximum load that can be supplied by DGs along the feeders before the magnitude of voltage harmonics exceeds the allowed 3% level. The simplest analysis for a distribution system with equal loadings is its feeders, shown in Fig. 2.11.

In this case, by assuming I_{sub} as the substation current in Fig. 2.11, x is the distance from the substation location in miles, L is the length of the feeder in miles, $\bar{Z}_{sub} = R_{sub} + jhX_{sub}$ (h is harmonic number) is in ohms, and $\bar{Z}_{line} = R_{line} + jhX_{line}$ is in ohm/mile, then the line current at any location X on the feeder and the worst voltage with the highest harmonic content at the feeder, which is equal to the voltage drop at the farthest point on each feeder caused by the line current, $V_{dist.}$, are obtained as follows [73]:

$$I_{line}(X) = I_{sub} \left(1 - \frac{X}{L} \right) \quad (2.23)$$

$$V_{dist.} = I_{sub} * \bar{Z}_{sub} + \int_0^L \{ \bar{Z}_{line} * I_{line}(x) \} dx \quad (2.24)$$

Then, the substation current is found from Equation (2.25), which can be used for determining the amount of power DGs can inject to supply the system loads without causing unallowable oscillations [73].

$$I_{sub} = V_{dist.} / (\bar{Z}_{sub} + 0.5 * L * \bar{Z}_{line}) \quad (2.25)$$

By assuming the increase of linear loading of the feeder in the distribution system, by departing from the substation, according to Fig. 2.12 the magnitudes of $I_{line}(x)$ and I_{sub} are

found as follows [73]:

$$I_{line}(X) = I_{sub} \left(1 - \frac{X^2}{L^2} \right) \quad (2.26)$$

$$I_{sub} = V_{dist.} / (\overline{Z_{sub}} + 0.6667 * L * \overline{Z_{line}}) \quad (2.27)$$

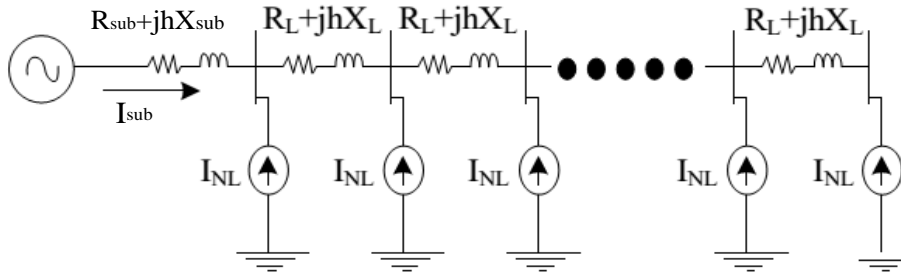


Fig. 2.11. The schematic of a radial distribution system with equal loadings for all feeders [73-75].

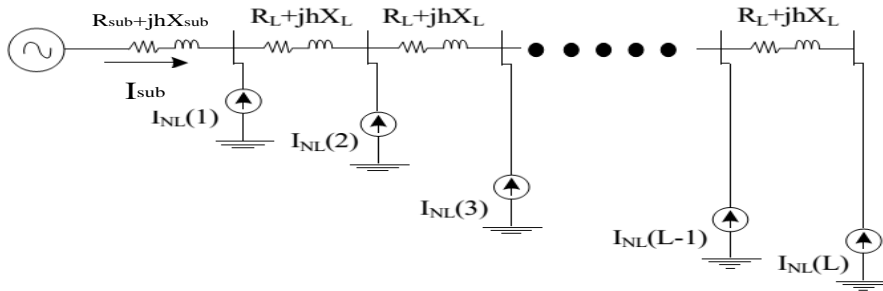


Fig. 2.12. The schematic of a radial distribution system with increasing linear loadings of the feeder when departing from the substation [73-75].

For a distribution system with decreasing linear loading of the feeder, by departing from the substation, as given in Fig. 2.13, the magnitudes of $I_{line}(x)$ and I_{sub} are as follows, respectively [73].

$$I_{line}(X) = I_{sub} \left(\frac{X^2}{L^2} + 1 - \frac{2X}{L} \right) \quad (2.28)$$

$$I_{sub} = V_{dist.} / (\overline{Z_{sub}} + 0.3334 * L * \overline{Z_{line}}) \quad (2.29)$$

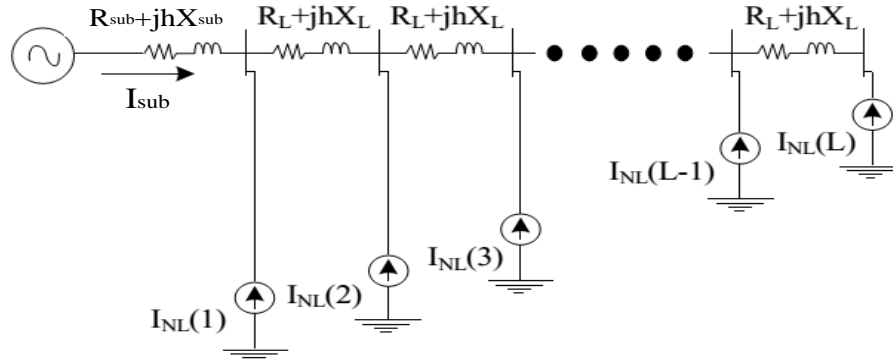


Fig. 2.13. The schematic of a radial distribution system with decreasing linear loadings of the feeder when departing from the substation [73-75].

Now, as an example, consider a distribution system with three feeders. The impedance characteristics of the feeder and the substations are given in Table 2.3. The substation currents for the above three systems are calculated using Equations (2.25), (2.27), and (2.29) and listed in Table 2.4.

Table 2.3. The impedance characteristics of the bus and feeders of the distribution system [73-75].

Impedance	Feeder 1	Feeder 2	Feeder 3
Z_{line+}	0.592+j0.816	0.258+j0.581	0.126+j0.631
Z_{line0}	0.893+j2.211	0.686+j2.058	0.430+j2.026
$Z_{sub,+}$	0.754+j3.017	0.377+j1.058	0.2514+j1.005
$Z_{sub,0}$	0.226+j0.905	0.132+j0.528	0.1005+j0.402

Once the values of the bus current for different harmonic orders are found and the ratio between the bus current and the maximum current required by the loads is calculated as

$\frac{I_{sub}}{I_L * I_{h,limit}}$ assuming a 3% limitation for current distortion, the amount of load supplied by

DGs without the increased distortion of the system violating the allowed limit can be determined [73-75]. A ratio of 100% means that DGs can supply the whole load of the system without violating the allowed harmonics limit. These ratios for positive and zero sequence harmonics of the above distribution system are shown in Table 2.5.

Table 2.4. The bus current magnitude (Ampere) for the 7th and 9th order harmonics of distribution systems with different loadings on feeders [73-75].

Feeder	Length (mile)	Equal loading		Increasing loading		Decreasing loading	
		Harmonic	Harmonic	Harmonic	Harmonic	Harmonic	Harmonic
		7	9	7	9	7	9
Feeder 1	2	8.038	7.695	7.503	6.222	8.654	10.078
	5	6.086	3.727	5.363	2.879	7.035	5.222
	10	4.332	2.004	3.634	1.532	5.362	2.896
Feeder 2	2	14.750	9.274	13.496	7.329	16.261	12.623
	5	10.402	4.227	8.938	3.246	12.439	6.059
	10	6.974	2.217	5.718	1.683	8.938	3.246
Feeder 3	2	18.843	9.880	16.695	7.730	21.624	13.687
	5	11.934	4.388	9.914	3.352	14.987	6.349
	10	7.408	2.278	5.912	1.724	9.915	3.353

Table 2.5. The ratio between the power generation by DGs and the whole loads of the system without leading to unallowable harmonics [73-75].

Feeder	Length (mile)	Equal loading		Increasing loading		Decreasing loading	
		Positive sequence	Zero sequence	Positive sequence	Zero sequence	Positive sequence	Zero sequence
Feeder 1	2	100	100	100	100	100	100
	5	100	93.17	100	74.42	100	100
	10	100	50.10	90.85	38.30	100	72.40
Feeder 2	2	100	100	100	91.61	100	100
	5	100	52.83	100	40.57	100	75.73
	10	87.17	27.71	71.47	21.03	100	40.57
Feeder 3	2	100	82.33	100	64.41	100	100
	5	99.45	36.56	82.61	27.93	100	52.90
	10	61.73	18.98	49.26	14.36	82.62	27.94

In conclusion, economic and environmental features of RESs are among the main factors of the tendency to employ DGs in the distribution systems. Nonetheless, it is essential to consider differential technical parameters of distribution systems with DGs because DGs can cause PQ problems in such systems. In [73-75], PQ problems has been investigated in distribution systems with DGs. Also, problems such as gradual and rapid changes in

the system voltage, harmonics of current and voltage waveforms, voltage flicker, increased short circuit level, and power loss in the case of using DGs and their effectiveness were analyzed. An analytical method was also proposed to determine the maximum power generation of DGs in distribution systems with different loadings on their feeders, which can prevent the oscillations and voltage harmonics if the power generation by DGs exceeds the allowed range [73-75].

2.4 HDG design as renewable energy system

One of the uses of HDG is for off-grid applications and supplying critical loads that have been considered by energy engineers in the last decade. One of the popular HDG systems is the solar-wind-powered system which has been used in numerous studies to provide the off-grid loads. In order to achieve the reliable energy of HDG systems and power balance between generation and consumption of energy, the optimal design is necessary to calculate the optimum size of their equipment to minimize energy costs. More research has been implemented on the HDG systems designing based on objective, constraints, and various optimization methods, which are discussed below. Before the implementation and installation of the HDG, it is necessary to determine the equipment capacity by using the design methods to optimize the cost of initial investment and feasibility studies. Determining the capacity of the equipment is mainly based on the experimental capacity calculation of the hybrid equipment for minimizing the cost of the system while maintaining the reliability of the loads. In an HDG system based on battery storage, the correct capacity should be determined based on the capacities of wind unit, PVs, and battery bank [76]. This is important to maintain optimal energy management in an HDG system to prevent inappropriate capacity determination. The large capacity of the equipment system will raise the cost of the system, while if it is considered a small capacity, this may result in the failure of the power supply sources to meet the load requirements [76]. Different methods of optimization such as graphical structure, probabilistic approach, repetitive method, dynamic and linear programming, and many other objective methods are applied to design the HDG systems.

2.4.1 Graphic structure

The optimization problem considering two decision variables is solved using the graphical structure of how they change each other. By visualizing the possible area, the optimized problem on the image or graph can be identified after plotting the contours of

the objective function. In [77], a data set of PV radiation has been used, in which the optimal size is determined using the overlap of the daily solar radiation cycle. In [78], a method to find the optimum value of the HDG system is presented. The function of this system is set to an hour which is done by maintaining the capacity of the wind generators. The probability of non-delivery of ancillary loads with various capacities of the PV and the battery is determined and the optimum combination of the system is determined by calculating the amount of production cost and the probability of non-delivery of the system load.

2.4.2 Probabilistic approach

In the probabilistic method, the inputs such as radiation and wind velocity are randomly considered. Therefore, probabilistic data are described instead of definite values using a statistical tool. The HDG's optimum value can be calculated as the average hourly or daily power of each month, the day with the lowest PV power for a month with the lowest power per month. The two benefits of this approach are achieving a minimum amount of cost and minimum time to collect environmental and load data [76-79-80].

2.4.3 Deterministic Method

In the deterministic method, each set of state variables is determined uniquely by the parameters in the model and with the aid of a set of different states of variables, so there is a response to the parameters, which is not like this in the probabilistic method. In the deterministic method, in designing an HDG, there is a unique value in the output instead of a set of solutions for cost and reliability values [76-79-80].

2.4.4 Iterative Approach

Iterative-based methods are a mathematical approach that is generally implemented using computer systems, which generates a sequence of improvements in the approximate response for the optimization problem until the end-of-term criterion is satisfied. In this method, when the optimization variables number increases, the calculation time expands [79-80].

2.4.5 Artificial Intelligence (AI)

The AI is a field of intelligent science that investigates and organizes the smart machines. AI is described considering intelligent agents design, in which a smart operating system causes the chances of success to be maximized.

AI includes artificial neural networks (ANNs), GA, fuzzy logic, and hybrid systems that combine two or more of the mentioned approaches. The proper application of smart technologies helps useful and improved performance of the systems and other features that are difficult or impossible to achieve through traditional methods [80].

2.4.6 Literature Review on HDG design

Optimal design of the HDG system, which is a problem of optimization with multiple parameters considering the problem complexity, traditional methods are not capable of solving this problem desirably, and because of this, various intelligent methods for designing HDGs have been used. In [81], the optimal design of a distributed photovoltaic-wind turbine with battery storage (PVWTBAHDG) is designed using non-linear programming with the aim of minimizing energy costs and considering reliability constraints as a probability of non-supplying of the load. In [82], the optimal design of the PVWTBAHDG system is presented using non-linear programming on a diesel generator in islanded operation to minimize system power shortages and the present worth of cost of the network. In [83], the optimal design of the PVWTBAHDG system is conducted using the GA with the objective of minimizing annual energy costs and considering the reliability constraint of the probability of non-supplying of the load. The results show that by increasing the reliability of the system, the cost of system energy generation increases. In [84], the optimal design of the PVWTBAHDG system with the goal of minimizing the annual costs of the system and considering the power balance problem has been studied. The purpose of this study is to determine the number of solar panels, wind turbines, and the number of batteries using the discrete harmony search algorithm (DHSA). In [85], the optimal design of the PVWTBAHDG system is proposed by minimizing total costs and environmental pollution using the GA as a multi-objective. In [86], the achievement of the capacity of the PVWTBAHDG system with a diesel generator is presented using the Improved Harmony Search Algorithm (IHSA) with the aim of achieving the optimum supply reliability and the lowest annual cost of the system. In [87], an objective function of three-parameter optimization with minimizing the total cost, environmental emissions of fuel, and load power shortages are presented using the Pareto-evolutionary algorithm for the determination of the optimal size of the PVWTBAHDG system. In [88], the combination of particle swarm algorithm (PSO) and optimization constraints are presented to determine the optimal size of the PVWTBAHDG system equipment. In this study, the overall system costs are defined as

the objective function of the optimization problem and environmental pollution and load energy shortage as constraints. The optimal design of the PVWTBAHDG system with a diesel generator is aimed at minimizing the annual costs of the system and considering the reliability and fuel constraints of the pseudo-evolutionary algorithm [89]. In [90], the Big Bang Algorithm (BBA) is used to design an optimal PVWTBAHDG system. In this study, the minimization of initial investment costs, maintenance, and replacement is considered as the objective function of the problem, and the reliability index is considered as the technical constraint of the problem. In [91], an assessment of Photovoltaic/Wind Turbine Hybrid Distributed Generation (PVWTHDG) system based on reliability and cost of the fuel cell has been investigated to reduce the annual cost of the system by considering the energy cost of non-supplied load and the reliability constraints of the probability of non-delivery of the load. In this study, PSO is used to minimize the system cost. In [92], the optimal design of the PVWTBAHDG system was studied by using Evolutionary Algorithm (DE) algorithm, minimizing initial investment costs, maintaining and replacing equipment, and limiting the probability of non-delivery of load, and the effect of the changes of the constraints in optimal capacity Equipment and cost of the HDG. In [93], the optimization of a PVWTBAHDG system to minimize the annual cost of the system with regard to the power balance constraint using the Gray Wolf Optimizer (GWO) algorithm has been investigated. In this study, the effect of equipment availability has been evaluated by providing a reliability model. In [94], the optimal design of the battery PVWTHDG system is provided using the Cuckoo Search Algorithm (CSA), minimizing system cost, and improving load reliability. In [95], the optimal design of the PVWTHDG system with a hydroelectric power plant is proposed using the Biogeography-based Optimization (BBO) considering minimizing the not supplied load cost and determining the optimal capacity of the equipment.

The design of a PVWTBAHDG system for feeding an off-grid radio system with the goal of minimizing system costs is presented in [96]. The results have shown that the use of solar arrays is not technically and economically feasible because there will be a large number of solar arrays and batteries that will not be economically feasible. The results also indicate that the wind power system is technically and economically feasible for this purpose. Moreover, long-time wind fluctuations require a backup power source, in which case diesel generator is considered. The battery minimizes the initial demand from diesel, which in turn reduces the required storage capacity of the battery.

In [83], a model is proposed based on the PVWTBAHDG system design. The purpose of the design is to determine the optimal capacity of the equipment with the aim of minimizing the energy costs of the system and considering the probability of non-supplying of the load. System costs have been considered as investment costs, maintenance, and replacement of equipment.

In [97], determining the optimal capacity of a wind-solar system is presented in the form of a single-objective design problem. The battery backup system is used to compensate system power shortages and increase reliability. The goal of the study is to minimize system costs, including the cost of the number of employed equipment, including the number of solar panels, wind turbines, and the number of batteries. On the other hand, reliability constraints also indicate the inability of the system to supply the load.

A model for a single-objective design of a PVWTBAHDG system is proposed in [98]. The goal of the study is to minimize the cost of energy production, and supplying the load, desirably. The optimum capacity of the equipment is calculated considering the cost and reliability indices. The results show that when the capacity of the batteries increases, the capacity of the solar arrays is reduced and the system costs increase.

The design of the PVWTBAHDG system for supplying a residential home is presented in [99]. In this study, the optimum equipment capacity of the system is determined based on the proposed model considering the objective function of minimizing investment and maintenance costs. On the other hand, the inability of the system to supply the load has been expressed as a probability index of the probability of shortage of load power. In this study, the equipment capacity is calculated for minimizing the total annual cost of the system, and the power shortage is kept within a certain range.

A model for determining the optimal capacity of the PVWTHDG system along with the fuel cell with the objective function is presented to minimize initial investment costs and maintain the system in the form of a single-objective design using the bee colony algorithm in [100]. Also, the index of the probability of non-delivery of loads is also considered as a constraint. In this study, the number of solar arrays, wind turbines, and reservoir capacity of the hydrogen storage tank is optimally determined by considering the load demand. The results show that supplying the system with higher probability requires more costs.

The optimal capacity of the PVWTBAHDG equipment system is determined to minimize the annual cost of the system and the probability of non-delivery of load, considering the

loads in three levels: low load, intermediate load and high load periods in [100]. In this study, the effects of different load times on system design have been investigated. The results show that according to the load situation in each period, the capacity of the equipment, especially the system costs, also varies. Therefore, the type of load cycle has a direct effect on the optimization of system equipment capacity. The results show that, as the load increases, the cost of the energy system increases.

2.5 HDG application in the distribution system

In [101], a model for designing a grid-connected PVWTBAHDG system has been introduced for the roof of a residential building. This system is evaluated to supply the demand of the load, taking into account the index of the probability of non-delivery of a certain load. Various parameters of system reliability, power quality, lack of load, and probabilistic features of wind speed and solar radiation on the design of the system have been studied. The results have shown that the wind and the sun cover each other and thereby increase the reliability of the system.

In [102], the design of a grid-connected PVWTHDG system for single-use residential demand is aimed to minimize energy costs using Homer software. The design has been done for different interest rate and the results show that the Energy efficiency in this system is not economical for interest rates up to 80% .In [103], Optimal design of the PVWTHDG system with a fuel cell system is presented for islanded and grid-connected operations to the local network and buying and selling the electricity from or to the network with the goal of minimizing system energy costs and the cost of energy-unsupplied system load using the Imperial Competitive Algorithm (ICA) provided.

In [104], the PVWTHDG control strategy is presented based on a multi-input transformer coupled with a DC/DC converter. The purpose of the study is to provide reliable times, manage the power of various resources and inject excess power to the network.

In [105], the design of a PVWTHDG system is presented with and without battery storage for different combinations of the system for a variety of capacities of solar and wind resources for residential applications in hot areas. The annual performance of energy is explained based on the balance of production and consumption for different combinations of the system.

In [106], the effect of dynamic phenomenon is evaluated on the operation and voltage stability of the PVWTBAHDG system. To determine the performance of the

PVWTBAHDG system, the wind and solar power potential are presented based on the balance of power between production and energy consumption.

2.6 Limitation of previous studies and how the proposed work will overcome this

By investigation of previous studies on the application of PVWTHDG systems, it has been found that most studies are done as a stand-alone system and to supply the loads to reduce energy costs and very few studies have been done as a grid-connected of these types of systems. In a few cases, the connection of these types of systems to local networks is studied and aimed at the purchase and sale of electricity. In the past studies, the improvement of power loss, network losses cost, network voltage profile and network voltage stability, and network PQ have been investigated but the reliability and network PQ indices have not been investigated, comprehensively. In the past studies, most distribution networks are considered to be balanced, that due to the unbalanced load of the network phases, it does not seem reasonable considering load as balanced. One of the distribution network challenges, in addition to high network losses, is the low PQ. The use of the PVWTBAHDG system is a highly desirable option for distribution networks operation, with the aim of improving the distribution network characteristics and in particular improving the network power quality, which is the motive for this research work. In addition to supplying its own load, the PVWTBAHDG system can improve network characteristics, in particular, reducing power losses and improving the PQ indices including voltage sag, voltage swell, harmonics, and voltage unbalance through the power injection to the radial network. However, this advantage requires the selection of the optimal site and size of the PVWTBAHDG system in the network.

2.7 Conclusion

This chapter presents studies on the application of DG and HDG in distribution networks including analytical and bio-inspired methods. Researches on the optimal design of grid-off HDG systems as well as grid-connected HDG to the network are investigated. The studies are evaluated in terms of objective functions, constraints, and optimization methods. Finally, the limitations of previous studies and the proposed method for overcoming these limitations are presented.

**Chapter3. Design of Photovoltaic panel/Wind
Turbine/Battery Hybrid Distributed Generation
(PVWTBAHDG) system**

3.1 Introduction

The power system engineers aim to design hybrid distributed generation (HDG) systems to supply the load demand. To design photovoltaic-wind-battery hybrid systems (PVWTBAHDG), the capacity of solar panels, wind turbines as well as battery capacity should be optimally determined. The aims of determining the optimal capacities of PVWTBAHDG systems are to minimize the economic costs of the energy by considering technical standards of the supplied load as well as optimize the technical and economic indices in the system. Therefore, finding the optimal size of the equipment along with the specific standards is important to design the optimal HDG systems. Several methods have been used to optimize the HDG system design. In this chapter, some of the traditional methods along with relevant standards are presented in HDG system designing.

3.2 HDG system

HDG systems are mainly used to supply power to remote areas of the network and in rural areas. The application of HDG systems has grown due to cost reduction in PV, wind and inverter technologies. The HDG systems can be widely deployed in both grid-connected and islanded operation modes [76]. Nearly all the HDG systems which are designed and optimized to provide the power in remote areas operate in islanded mode. Such a system is disconnected from the main power grid. Islanded HDG systems are used to provide critical loads, especially for loads in which the transmission and development of the network impose exorbitant costs and have many problems [76]. Therefore, the islanded systems do not import or export energy with the grid. Further, a grid-connected HDG system is connected to a larger independent grid and is usually connected to the main power grid, which directly injects the electrical energy into the network. Converting a direct current (DC) to alternative current (AC) is done through grid-connected synchronized inverters (which is called interfaced inverters). Therefore, in grid-connected systems, there is an ability to exchange power between the HDG system and the grid. Also, in peak conditions, the HDG system can inject power into the grid and absorb power from the main grid during a power shortage [76].

3.3 Types of HDG system

3.3.1 PVBAHDG System

In Figure 3.1, a PV/Battery Hybrid Distributed Generation (PVBAHDG) system has been shown in islanded operation mode [90]. The PV panel is the main source of energy supply.

Solar panels generate DC power, in which the maximum power is extracted by utilizing a DC/DC converter and the power changes with the irradiation level. The DC power is converted to AC power using an inverter and this power is injected to the AC load. The battery is also used for charging and discharging (energy management by charging the regulator) in the condition of low and high power (due to the deviation of the photovoltaic panels) and, consequently, it is used for supplying load without interruption.

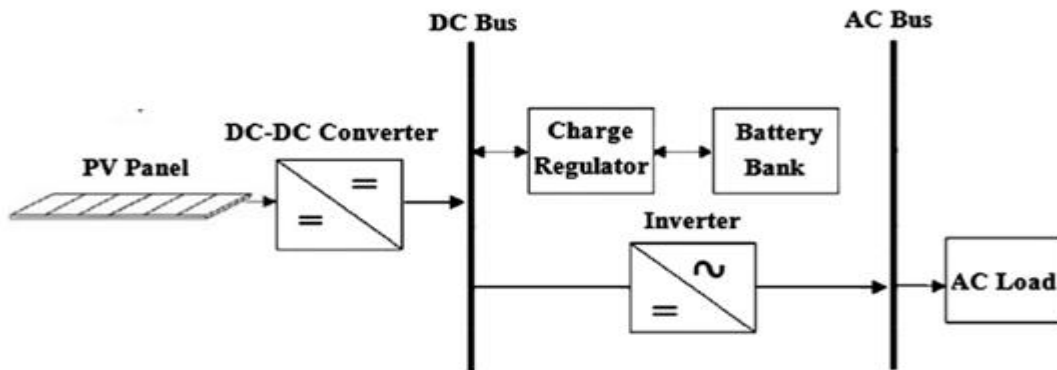


Fig.3.1. Block diagram of a stand-alone PVBAHDG system [90].

3.3.2 WTBHDG System

In Figure 3.2, a wind hybrid-battery system (WTBAHDG) is depicted in islanded operation mode. Wind turbine produces the required power of the system. The produced AC power by the wind turbine is rectified by an AC/DC converter and injected into a DC bus. The DC power produced by the AC inverter is injected into an AC load. Here the battery is also used to control the energy of the system due to the wind turbine power fluctuations. Therefore, to achieve optimum reliability, the use of a battery backup system is critical [90].

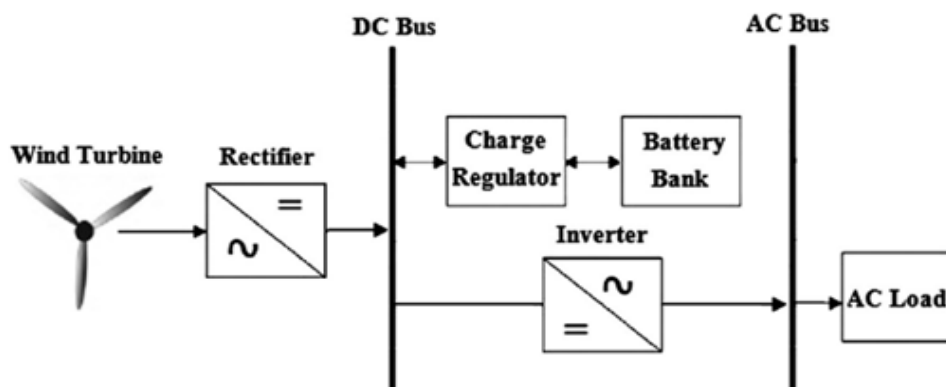


Fig.3.2. Block diagram of a stand-alone WTBHDG system [90].

3.3.3 PVWTBAHDG System

The schematic of a PVWTBAHDG system is depicted in Figure 3.3. Here, solar and wind units are cooperating with each other as power generators and used to supply the system. Here, the battery is used to provide continuous load power and improve the reliability of load demand [90]. In the PVWTBAHDG system, when the total photovoltaic and wind power is more than that required by the load, the excess power comes into the batteries and the batteries are charged. If the power produced by the units is smaller than the load demand, then the system's load deficiency is compensated by discharging the battery. As seen in Figure 3.4, in recent years, the use of renewable solar and wind resources has been widely considered and, according to the predictions, they will increase to 238 Gigawatts (GW) by 2023 [107].

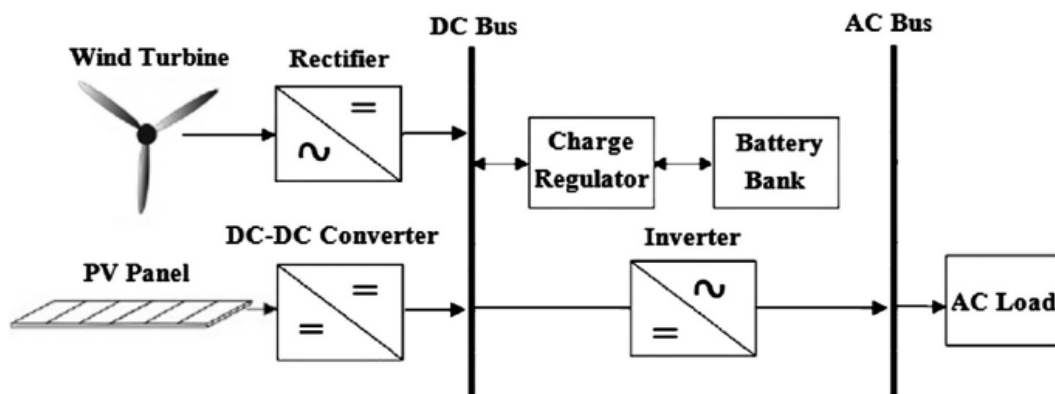


Figure 3.3. Block diagram of an islanded PVWTBAHDG system [90].

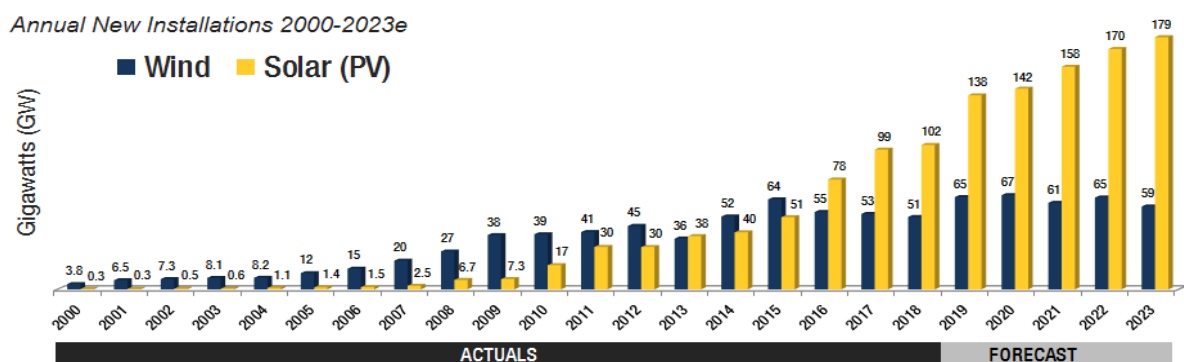


Fig.3.4. Solar and wind power capacity over the world from 2000 to 2023 [107].

The power output of PV panels are obtained using (3.1) taking into account the radiation and ambient temperature parameters [90].

$$P_{PV}(t) = N_{PV} \times P_{PV,Rated} \times \left(\frac{S(t)}{1000}\right) \times [1 - N_T (T_C(t) - T_{ref})] \quad (3.1)$$

$$T_C(t) = T_A(t) + \left(\frac{NOCT-20}{800}\right) \times S(t) \quad (3.2)$$

where, P_{PV} represents the power output of the solar panel, N_{PV} shows the number of solar panels, T_C is the temperature of the solar cell in degree Centigrade at time t, N_T is the temperature coefficient of the photovoltaic panel. T_{ref} expresses the temperature of the solar panel under standard conditions (which is 25°C), $S(t)$ gives the irradiation at time t, $T_A(t)$ is the temperature of the surrounding environment in °C at time t, and $NOCT$ provides the nominal temperature of the panel.

Wind turbine power is found in (3.3) [90]:

$$P_{WT} = \begin{cases} 0 & v \leq V_{ci} \\ P_{Rated} \times \frac{v - V_{ci}}{v_r - V_{ci}} & v_{ci} \leq v \leq v_r \\ P_{Rated} & v_r \leq v \leq v_{co} \\ 0 & v \geq v_{co} \end{cases} \quad (3.3)$$

where, v_{co} is the cut-off speed, v_{ci} is the cut-in speed, v_r expresses the rated speed, v represents the wind speed, P_{Rated} shows the rated power, and P_{WT} is the output power of the wind turbine.

In the PVWTBAHDG system, because of power fluctuation in the PV and wind turbines, a battery storage system has been used to manage supply the loads, continuously. The capacity of the battery bank constantly varies in the PVWTBAHDG system as the power oscillates and changes in the PV and WT. Thus, the stored energy in the battery bank at time t will be obtained as [90]:

$$E_{storeBat}(t) = E_{storeBat}(t-1) + [(N_{PV} \times P_{PV}(t) \times \eta_{con DC/DC} + N_{WT} \times P_{WT}(t) \times \eta_{con AC/AC}) - P_{Load}(t) / \eta_{Inv DC/AC} \times \eta_{Bat ch}] \quad (3.4)$$

here, $E_{storeBat}(t)$ and $E_{storeBat}(t-1)$ are the values of battery charge at times t and $t-1$. $\eta_{con DC/DC}$, $\eta_{con AC/AC}$, and $\eta_{Inv DC/AC}$ are the efficiencies of the converter, rectifier, and inverter, respectively. $P_{Load}(t)$ gives the charging efficiency of the battery bank.

In the case of power produced by renewable units is less than the load, the battery discharges. Therefore, the battery charge at time t will be [90]:

$$E_{storeBat}(t) = E_{storeBat}(t-1) - [P_{Load}(t)/\eta_{Inv DC/AC} - (N_{PV} \times P_{PV}(t) \times \eta_{conDC/DC} + N_{WT} \times P_{WT}(t) \times \eta_{con AC/AC})]/\eta_{Bat disch} \quad (3.5)$$

where, $\eta_{Bat disch}$ is the discharge efficiency of the battery bank.

3.4 Storage system in HDG system

Recently, storage systems including batteries and fuel cells have become widespread in HDG systems. As hybrid systems, particularly in islanded systems, aim for high reliability, the capability of demand is evaluated in the studies of HDG systems. Because of output power oscillations in the wind and solar units, energy storage is utilized in HDG systems to enhance reliability. In the case when the output of the renewable energy units is larger than the demand level the extra energy is stored, and if the output of the renewable units cannot meet the demand, this is compensated by the storage system [93-103].

The common storage systems which are used frequently include batteries and fuel cells (FC). Batteries are short-time storage systems with the following features [93-103]:

Short-time storage

- Low cost;
- Proper reliability; and
- Save energy directly.

On the other hand, features of fuel cells as long-time storage systems are as follows [93-103]:

- Long-time storage;
- High cost;
- High reliability; and
- Indirect energy storage in the form of hydrogen.

Therefore, the storage system can improve the HDG reliability in the viewpoint of supplying the load and reducing or preventing the load shedding. It should be noted that in recent years, batteries have been used more often in PVWTHDG systems due to lower investment costs.

3.5 Design of PVWTBAHDG renewable energy system

In HDG systems, which consist of new energy resources and battery storage, the reliability and cost factors are very important. The index of reliability is a criterion of the

system's capability of provision and the cost is associated with the power generation cost. In the optimal design of a PVWTBAHDG system, the number of wind unit, PV arrays, and storage system should be calculated to enhance the load reliability level and minimize the cost, i.e., the demand energy should be continuously and sufficiently supplied. Also, the storage system as the backup should be large enough so that the load requirements are met even in the absence of wind and solar radiation. The grid-connected systems can buy or sell electricity from/to the main grid. Calculation of the optimal size of the generation units, the storage system, and the power purchased from the grid is very difficult. Since the costs of electrical energy purchasing from and selling to the main grid are usually tariffed, it is necessary to optimize computing at all the hours of the day, despite the existence of the main grid. Therefore, it seems essential to obtain the optimal size of the equipment, considering the indices in the optimal design of the system. Because, if the system designing is done properly, the reliability is achieved and energy costs are also minimized and designed renewable energy system can compete with other methods of generating energy [76].

3.6 Objectives in PVWTBAHDG system designing

Optimization of PVWTBAHDG system has been studied for specific purposes using technical and economic indicators. There are several economic and technical indicators for energy efficiency systems which can be used to estimate the reliability and cost of the system. Therefore, PVWTBAHDG system designers can determine the optimal capacity of the system by using appropriate methods. In subsections 3.6.1- 3.6.5, some of the economic indicators that have been used in different studies have been introduced.

3.6.1 Loss of Power Supply Probability (LPSP)

Owing to fluctuations in solar radiation and wind speed, the reliability of PVWTBAHDG systems is very important. A power generating system is desirable when it is capable to provide enough energy for the loads in a period. LPSP as a technical indicator shows the inability of the PVWTBAHDG system to demand supply. The energy shortage ratio of the PVWTBAHDG system is considered as the load demand and is defined as shown in (3.6) [83, 92]:

$$LPSP = \sum_{t=1}^T DE(t) / \sum_{t=1}^T P_{load}(t) \cdot \Delta t \quad (3.6)$$

where, $DE(t)$ is the energy shortage of the system or energy unsupplied, $\sum_{t=1}^T P_{load}(t)$ is the overall demand for the given study period.

3.6.2 Expected Energy Not Supplied (EENS)

EENS represents a probability index of reliability. This indicator represents the mathematical expectation of not-supplied energy as a technical index. By considering the electric charge (L) and the output power of the energy-recovery system (P_h), EENS index is found in (3.7) [108]:

$$EENS = \begin{cases} L > P_{h \max} & ; L - \int_{P_{h \min}}^{P_{h \max}} P_h \times f_{ph}(P_h) dP_h \\ P_{h \min} \leq L \leq P_{h \max} & ; \int_{P_{h \min}}^{P_{h \max}} (L - P_h) \times f_{ph}(P_h) dP_h \\ L < P_{h \min} & ; 0 \end{cases} \quad (3.7)$$

where, $P_{h \max}$ represents the maximum power produced by the PVWTBAHDG, $P_{h \min}$ gives the minimum power provided by the hybrid energy system, and $f_{ph}(P_h)$ shows the probability density function for the output power of the hybrid energy-system. Therefore, if the PVWTBAHDG system fails to provide part of the load, it should pay a penalty per kWh. Therefore, the cost of not-supplied energy is defined in (3.8):

$$C_{EENS} = EENS \times C_{kWh} \quad (3.8)$$

where, C_{kWh} expresses the cost per kWh of the unloaded energy.

3.6.3 Levelized Cost of Energy (LCE)

LCE refers to the fixed cost of each unit of energy. LCE is the Indicator Energy Estimates Energy system used in the design of the PVWTBAHDG system, which involves the total costs in the system's lifetime. LCE is shown in (3.9) [109]:

$$LCE = TAC / E_{tot} \quad (3.9)$$

Where, TAC refers to the annual cost, and E_{tot} is the annual energy. Further, TAC is based on the initial cost and the capital recovery factor (CRF) of the hybrid energy system. CRF is obtained from (3.10):

$$CRF = d(1 + d)^t / ((1 + d)^t - 1) \quad (3.10)$$

here d shows the depreciation rate of capital, and t gives the system's useful lifespan.

3.6.4 Net Present Value (NPV)

NPV is calculated by adding the present value of reduced income by reducing the lifetime cost of the system. The NPV can be obtained from (3.11) [110]:

$$NPV = \sum NPV_{sale-k} + \sum NPV_{end-k} + C_{investment} - \sum NPV_{r-k} - \sum NPV_{O\&M-k} \quad (3.11)$$

where, NPV_{sale-k} gives the present value of the benefit from sales of K. NPV_{end-k} is the present value of reduced benefits due to the remainder of equipment K when the lifespan of the PVWTBAHDG system is finished, $C_{investment}$ is of the initial cost, NPV_{r-k} is the lifetime replacement equipment costs, $NPV_{O\&M-k}$ are the operating costs and maintenance of equipment K during the life of the system.

3.6.5 Annualized Cost of System (ACS)

Another function for optimizing the PVWTBAHDG system, i.e. the ACS index, is the annual cost of the system, including initial investment cost (C_{cap}), annual replacement cost (C_{rep}), and annual maintenance cost (C_{main}) [92]. In a PVWTBAHDG, the costs are assigned to individual equipment. The ACS index is expressed in (3.12):

$$ACS = C_{cap}(PV + Wind + Bat + \dots) + C_{rep}(Bat) + C_{main}(PV + Wind + Bat + \dots) \quad (3.12)$$

3.7 Optimization of HDG system using PSO Algorithm

By employing particle swarm optimization (PSO) algorithm, the authors in [111-112] present the optimal design of an off-grid HDG system for load supply to minimize energy generation cost by achieving the desired reliability of the system's load. Normally, three subsystems are interconnected to form an HDG system. Subsystems encompass generation, distribution, and demand and they experience significant variations concerning specific parameters such as availability of RESs, desirable services, and the demand. These parameters affect decision making and thus the cost and reliability. The design of a wind/solar/diesel/battery system as a generation subsystem for three cities in Iran, namely Nahavand, Rafsanjan, and Khash, has been studied. The hybrid configuration of the distribution subsystem is shown in Figure 3.5 and is designed in the form of a low-voltage (LV) single-phase distribution network to generate 220V, 50 Hz AC electricity [112]. The intermittent innate of RESs highly complicates the power management strategy in hybrid generators, particularly when a reliable source of energy is required for accommodating the temporal distribution of the demand.

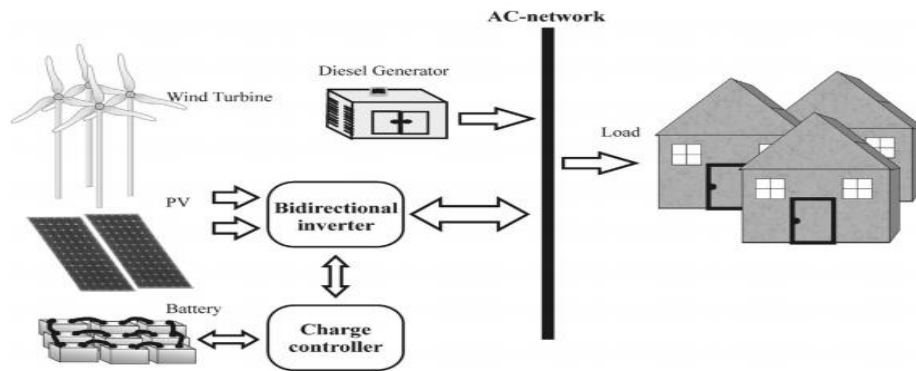


Fig. 3.5. Solar-wind-battery-diesel hybrid system [112].

Concerning the limited capacity of RESs, generator capacity can be increased immediately to accommodate increased demand. Additionally, in some cases the electricity produced by the units is greater than the demand; in such cases, a dump load should be used to consume the excess energy, this prevent the overcharging of the batteries. As a result, a power management strategy becomes an important factor when designing the discussed systems.

The operation of the HDG system is determined by its operating conditions. At any given time, one of the following conditions may apply:

- The sum of energy produced by RESs equals demand. Consequently, the whole power generated by RESs is injected into the load through the inverter.
- The whole energy generated by RESs is larger than the demand. Thus, the surplus power generated by the wind and solar units is stored in the battery, and if the power injected into the battery is exceeded, the excess power is lost using a dump load.
- The whole energy generation by RESs is smaller than the demand. Thus, the demand is fed using the battery. In the case this power deficiency is greater than the rated capacity of the battery it is compensated by the diesel generator as a backup.
- The whole energy produced by RESs, batteries, and diesel is smaller than the demand. In this case, part of the load demand will be curtailed, where the reliability index is referred to as the energy not supplied (ENS) probability.

For each country or region that is located in the solar belt of the earth and receives most of the irradiation during the year, it is a more preferred region to establish photovoltaic systems (PVs). Almost 240 to 250 days annually with solar radiation provides 4.5 to 5.4

kWh/m² daily horizontal radiation on average. The power produced by each solar panel unit is found as a function of irradiation [112]:

$$P_{PV-out} = P_{N-PV} \times \left(\frac{G}{G_{ref}} \right) \times [1 + K_t ((T_{amb} + (0.0256 \times G)) - T_{ref})] \quad (3.13)$$

where, P_{PV-out} shows the PV output power, P_{N-PV} denotes the rated power under standard conditions, G is the irradiance (W/m²), G_{ref} is 1000 W/m², T_{ref} is 25°C, K_t is -3.7×10^{-3} (1/°C), and T_{amb} shows the ambient temperature. It is worth noting that, in this study, the temperature is considered constant. Also, a solar panel with 1 kW rated power is assumed for the HDG [93].

The wind source, as a free energy source can be utilized to produce electrical energy. Wind energy is also favorable in the north and northwest of Iran. Iran is regarded as an average area of the globe in terms of wind speed; however, continuous winds with adequate speed in some areas can generate electricity. In 2006, 37 MW of wind energy was produced in Iran, ranking among the top thirty countries in the world from the wind energy generation aspect [112]. In the current study, a 1 kW wind turbine is used in the design of the HDG.

As the speed of wind depends on the height, the wind speed measured by an altimeter must be converted to the desired polar heights [112]:

$$V_2 / V_1 = (h_2 / h_1)^\alpha \quad (3.14)$$

where, V_2 represents the speed at the pole height (h_2), V_1 is the speed at the reference height (h_1), and α is the friction coefficient (known as Hellmann exponent, wind slope, or power law exponent). Parameter α relies on wind speed, stiffness of the ground, height from the ground level, temperature, the hour of the day, and the day of the year [112].

(3.15) gives the approximate output power of each wind turbine unit [95]:

$$P_{WT} = \begin{cases} 0; & v \leq V_{cut-in} \text{ or } v \geq v_{cut out} \\ (V)^3 \times \left(\frac{P_r}{(V_r)^3 - (V_{cut-in})^3} \right) - P_r \times \left(\frac{(V_{cut-in})^3}{(V_r)^3 - (V_{cut-in})^3} \right); & v_{cut-in} \leq v \leq v_{rated} \\ P_r; & v_{rated} \leq v \leq v_{cut-out} \end{cases} \quad (3.15)$$

where, P_r is the rated power, V shows the wind speed at the current time step, and $V_{cut-out}$, V_{rated} , and V_{cut-in} are the cut-out speed, rated speed, and cut-in speed, respectively.

Assuming N_{PV} and N_{wt} as the number of solar panels and wind turbines used in the design of the HDG system, the sum of energy generated by the RES units of the system can be found by:

$$P_{RES} = N_{wt} \times P_{wt} + N_{PV} \times P_{pv} \quad (3.16)$$

Diesel generators in remote areas and rural industries help reduce the energy storage needed, leading to a reliable and cost-efficient system. Diesel plays the role of a secondary energy source when the battery is depleted during peak hours. Yet, no-load operation mode or even an operation with light loading of the diesel generator should be avoided [112].

Efficiency and hourly fuel consumption by the diesel generator need to be taken into account when designing the hybrid system [112]:

$$q(t) = a \times P_{diesel}(t) + b \times P_r \quad (3.17)$$

where, $q(t)$ denotes the fuel consumption (lit/h), $P_{diesel}(t)$ is the generated power (kW), P_r shows the rated power, a and b are constants (lit/kW) showing fuel consumption coefficients, which are approximately 0.246 and 0.08415, respectively [112]. The current study uses diesel units with 1 kW capacity.

Battery capacity is defined based on the load demand. Design of the battery bank in the solar-wind-battery HDG system is performed in (3.18) [112]:

$$C_B = EL \times AD/DOD \times \eta_{inv} \times \eta_b \quad (3.18)$$

where, EL shows the demand, AD represents the number of off-grid days (3 to 5 days), DOD is the depth of discharge, η_{inv} denotes the inverter's efficiency, and η_b is the battery efficiency.

Investigating the load profile of an area during the design of a reliable, high-efficiency system is vital. Choosing the size and model of the batteries depends on the load profile. Furthermore, pick load periods and customers' behavior are effective on the system's reliability, the size of components, and the electricity price. This study has considered the hourly load profile of a conventional rural region. To design a low-cost, high-efficiency HDG, the priority must be given to finding the size of the system elements. The mixture of energy sources plus the use of high-quality components significantly impacts the system lifelong and may further reduce the electrification cost in remote areas. Therefore,

the current study presents the objective function as the Cost of Energy (COE) reduction [112]:

$$\min COE (\$/kWh) = TNPC(\$) \times CRF / \sum_{t=1}^{8760} P_{Load}(t) \quad (3.19)$$

here, $TNPC$ is the total net present cost and CRF denotes the capital recovery factor. $TNPC$ is one of the most popular and widespread economic profitability indices of HDG RESs. NPC of an off-grid HDG system includes the capital cost, replacement cost, and operation and maintenance costs, and is obtained using (3.20) [112]:

$$NPC_i = N_i \times (CC_i + RC_i + O\&MC_i) \quad (3.20)$$

where, i represents the considered device, N shows the number of units or capacity of the device, CC , RC , and $O \& MC$ show the capital cost, replacement cost, and operation and maintenance costs in \$/unit, respectively. In Equation (3.10), CRF expresses the capital recovery factor of system components for the given time considering the interest rate that is obtained from (3.21) [112]:

$$CRF = \frac{i(1+i)^n}{(1+i)^n - 1} \quad (3.21)$$

where, i indicates the real interest rate and n represents the system's lifetime.

Renewable Factor (RF) is used to calculate the energy produced by the diesel generator in comparison with renewable units. An RF equal to 100% indicates an ideal system based on only RESs. Nevertheless, a 0% RF value shows that the power generated by the diesel generator equals that of supplied by the RESs. RF is obtained from (3.22) [112]:

$$RF(\%) = \left(1 - \frac{\sum P_{diesel}(t)}{\sum (P_{pv}(t) + P_{wt}(t))}\right) \times 100 \quad (3.22)$$

This study excludes the RF in the objective function, but it is presented to evaluate the participation of the diesel generator compared to renewable units. The results obtained from the design of the HDG system demonstrate that the COE of an area as well as the participation of RESs differ in proportion to irradiance pattern and wind speed in that area.

3.8 Optimization of the HDG System using the Big-Bang Algorithm

A method for solving the optimal design of an HDG system which includes PV panels, wind turbines and battery banks is presented in [90] using a combined Big-Bang

algorithm. The objective function is considered as the minimization of Transaction Processing Performance (TPC) council cost that includes the total costs during the useful lifelong of the system. The energy not supplied (ENS) index is considered as the reliability index so that a reliable system is achieved. The numbers of PV panels, wind turbines, and batteries are assumed as the optimization parameters. The study was carried out to electrify a remote region in Qazvin province, Iran. The HDG system under study is comprised of photovoltaic systems (PVs) and wind turbines (WTs) as primary power sources, the battery bank as the backup system, an inverter, and a regulator that are shown in Figure 3.6 [90].

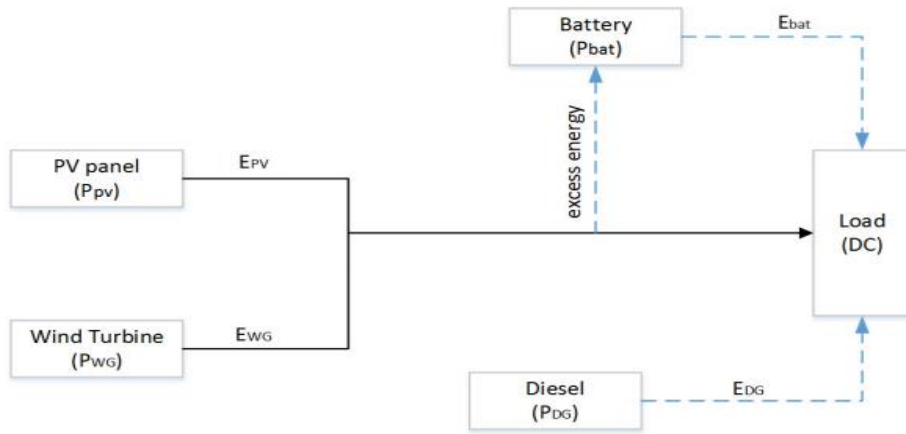


Fig. 3.6. The HDG system under study [90].

The power outputs of PV panels regarding the irradiance are obtained using (3.23) [90]:

$$P_{PV} = P_{PV,Rated} \left(\frac{G}{1000} \right) \times \eta_{MPPT} \quad (3.23)$$

where, G is the vertical irradiance (W/m^2), $P_{PV-rated}$ denotes the rated power of individual PV panel for $G = 1000 W/m^2$, and η_{MPPT} represents the efficiency of the DC/DC converter at maximum power point tracking (MPPT) mode. In the present study, $\eta_{MPPT} = 95\%$ is set.

For a WT, if the wind speed is higher than the V_{cut-in} , the WT's generator starts to produce power. In the case the wind speed is greater than the rated speed of the WT, the output power will be constant. If the wind speed is greater than the $V_{cut-off}$, the WT's generator stops operation for protective reasons. The output power of each wind generator can be obtained based on the wind speed [90]:

$$P_{WT} = \begin{cases} 0 & v \leq V_{ci} \text{ or } v \geq v_{co} \\ P_{WT-rated} \times \frac{v - V_{ci}}{v_r - V_{ci}} & v_{ci} \leq v \leq v_r \\ P_{WT-rated} & v_r \leq v \leq v_{co} \end{cases} \quad (3.24)$$

where, v is the wind speed, V_{ci} , V_{co} , and V_r represent the cut-in, cut-out, and rated speeds of the WT. P_{WT} is the rated power of the WT's generator.

In the case the overall output power of PV panels and WTs is larger than the demand the battery bank will be operating in the charging mode. The remaining charge in the battery bank at time t is [90]:

$$P_{BA}(t) = P_{BA}(t-1) \times (1 - \alpha) + [(N_{PV} \times P_{PV}(t) \times \eta_{con} + N_{WT} \times P_{WT}(t) \times \eta_{REC}) - \frac{P_{Load}(t)}{\eta_{INV}}] \times \eta_{BA} \quad (3.25)$$

where, $P_{BA}(t)$ and $P_{BA}(t-1)$ are the battery's charging values at times t and $t-1$, respectively. Parameter α denotes the hourly self-charging value, η_{con} , η_{REC} , and η_{INV} show the efficiencies of the converter, rectifier, and inverter, respectively. Moreover, $P_{Load}(t)$ gives the load level and η_{BA} shows the charging efficiency of the battery bank. When the overall output power of the PV panels and WTs is greater than the load, the battery bank will be in the charging mode. The amount of battery bank charge at time t is [90]:

$$P_{BA}(t) = P_{BA}(t-1) \times (1 - \alpha) - [(N_{PV} \times P_{PV}(t) \times \eta_{con} + N_{WT} \times P_{WT}(t) \times \eta_{REC}) - \frac{P_{Load}(t)}{\eta_{INV}}] \times \eta_{BA} \quad (3.26)$$

where, $P_{BA}(t)$ and $P_{BA}(t-1)$ are the battery charging values at times t and $t-1$, respectively. Parameter α denotes the hourly self-charging value, η_{con} , η_{REC} , and η_{INV} show the efficiencies of the converter, rectifier, and inverter, respectively. Moreover, $P_{Load}(t)$ is the load and η_{BA} is the charging efficiency of the battery bank.

When the overall output power of the PV panels and WTs is smaller than the demand, the battery bank will operate in the discharging mode. The current study sets the discharging efficiency of the battery bank equal to 1. The amount of battery bank charge at time t will be obtained from (3.27) [90]:

$$P_{BA}(t) = P_{BA}(t-1) \times (1 - \alpha) - \left[\frac{P_{Load}(t)}{\eta_{INV}} - (N_{PV} \times P_{PV}(t) \times \eta_{con} + N_{WT} \times P_{WT}(t) \times \eta_{REC}) \right] / \eta_{BA} \quad (3.27)$$

The objective function aims to minimize the TPC of the system. TPC equals the sum of Investment Cost (INVESTC), Maintenance Cost (MANIC), and Replacement Cost (REPLACEC) during the useful lifelong of the system. TPC is known as capital investment. The optimization is performed in a way that the load demand is continuously supplied regarding the ENS reliability index. The formulation of the problem is given using (3.28) [90]:

$$\text{Minimize } TPC = INVESTC + MAINC + REPLACEC \quad (3.28)$$

The investment cost that includes the costs of WTs, PV panels, battery bank, rectifier, charge regulator, inverter, and converter is obtained from (3.29):

$$INVESTC = (C_{PV} \times N_{PV}) + (C_{WT} \times N_{WT}) + (C_{BA} \times N_{BA}) + (C_{REC} \times N_{REC}) + (C_{REG} \times N_{REG}) + (C_{INV} \times N_{INV}) + (C_{CON} \times N_{CON}) \quad (3.29)$$

where, C_{PV} , C_{WT} , C_{BA} , C_{REC} , C_{REG} , C_{INV} , and C_{CON} denote the costs of the PV panel, WTs, battery bank, rectifier, regulator, inverter, and converter, respectively. Also, N_{PV} , N_{WT} , N_{BA} , N_{REC} , N_{REG} , N_{INV} , and N_{CON} are the number of the mentioned devices, respectively. The maintenance cost of the equipment can be calculated using (3.30):

$$MAINC = CPV(C_{PV,M} \times N_{PV} + C_{WT,M} \times N_{WT} + C_{BA,M} \times N_{BA}) \quad (3.30)$$

where, $C_{PV,M}$, $C_{WT,M}$, and $C_{BA,M}$ show the annual maintenance costs of PV panels, WTs, and batteries, respectively. It should be noted that the maintenance costs of rectifier, charge regulator, inverter, and converter have been discarded. CPV represents the cumulative present value, which transforms the total costs during the useful lifelong of the system into the initial moment of investment [90]:

$$CRV(f) = f \sum_{t=1}^T \frac{(1+InfR)^t}{(1+IntR)^t} \quad (3.31)$$

In (3.31), $IntR$ gives the interest rate, $InfR$ shows the inflation rate, and T indicates the economic lifelong of the hybrid system. The replacement cost concerning the equipment's lifelong is given in (3.32):

$$REPLACEC = CPV(C_{BA} \times N_{BA} + C_{REC} \times N_{REC} + C_{REG} \times N_{REG} + C_{INV} \times N_{INV} + C_{CON} \times N_{CON}) \quad (3.32)$$

where, the lifelong of PV panels and WTs are considered equal to the useful lifelong of the system, hence no replacement costs are assumed.

The present study uses the following constraints:

- Minimum and maximum numbers of components of the hybrid system;

$$N_{i-min} < N_i < N_{i-max} \quad (3.33)$$

N_i shows the number of equipment i and N_{i-min} and N_{i-max} indicate the minimum and maximum numbers of equipment i .

- The amount of annual ENS;

The ENS index has to be taken into account to provide a reliable hybrid system:

$$ENS(\%) \leq ENS_{max}(\%) \quad (3.34)$$

$ENS_{max}(\%)$ is the allowed percentage for energy not-served annually and $ENS(\%)$ shows the percentage of energy not-supplied annually [90]:

$$ENS(\%) = \frac{ENS}{\sum_{t=1}^{8760} P_{Load}(t)} \times 100 \quad (3.35)$$

where, ENS is the energy not-supplied annually [90]:

$$ENS = \sum_{t=1}^{8760} [P_{Load}(t) - (N_{PV} \times P_{PV}(t) + N_{WT} \times P_{WT}(t) + P_{BA}(t))] \quad (3.36)$$

- Minimum and maximum charges of the battery bank [90]:

$$P_{BA-min} \leq P_{BA} \leq P_{BA-max} \quad (3.37)$$

where, P_{BA-max} is the maximum charge of the battery which is set equal to the rated capacity of the battery bank (S_{ba}). Also, P_{BA-min} shows the minimum charge in the battery bank, given based on the maximum DOD [90]:

$$P_{BA-min} = (1 - DOD) \times S_{BA} \quad (3.39)$$

The numbers of PV panels, WTs, and batteries in the employed algorithm have been taken into account as optimization variables. The Big-Bang algorithm is used for the optimal designing of the HDG system and the optimal determination of the system equipment.

The proposed algorithm has been used for the optimal design of a hybrid power system in a rural region in Qazvin city, Iran. Because of economic and geographic problems the

region has no access to electric power. The empirical data related to the wind speed and irradiance in this region has been extracted from the data for the year 2011 available in the meteorological organization.

The design results verify the suitability of the suggested method in determining the optimal size of the HDG system. Concerning the obtained results, the HDG system includes both PVs and WTs along with a cost-effective and reliable battery storage system.

3.9 Optimization methods in PVWTBAHDG system designing

The purpose of optimization methods for optimizing the PVWTBAHDG system is to find the best system equipment with the least cost. GA is a meta-heuristic method inspired based on biological organisms [113-114] applied to the design to find the size of the PVWTBAHDG. Input data for a GA-based method can include atmospheric conditions and system prices, including initial cost and operation costs. For example, limiting the maximum PV numbers or limiting the wind numbers, or batteries number, etc. can be cited. Some constraints are presented according to the type of use in the problem. In addition, an objective function must be presented as an input for the GA. By using the initial data, the GA-based optimal capacity determination method provides a repeat process using GA operators, and repetitions continue until the pre-defined stopping criteria or the maximum number of repetitions is met. Initially, by generating random populations, the GA provides random capacities for PVWTBAHDG components that satisfy the balance between demand and produced power. Each response is calculated according to the objective function [113]. The most important advantage of GA to be used in finding the optimal capacity of the PVWTBAHDG system is that it is able to avoid local optima and can determine the overall optimal points. In addition, the algorithm can be programmed for an unlimited number of parameters in a given chromosome, making it desirable for optimum capacity studies.

PSO is based on transferring and smart congestion [113]. Similar to the GA, the initial data of the PSO-based method includes the climate conditions, the unit price of the PVWTBAHDG equipment including investment and operation costs. The PSO performance is based on population and is selected randomly. On each repetition, the particle moves to the optimal solution using its current speed, the best personal answers ever obtained by themselves and the best solutions obtained by all particles. GA and PSO are performing well with the repeat search method; PSO has more benefits than GA.

The simulated refrigeration method (SA) is a method to solve the problems of PVWTBAHDG [113]. In each repetition, the motion of the candidate is chosen randomly, and the movement is suitable if an answer with a value of the fitness is better than the present one. Otherwise, motion is dependent on the decay of the fitness. If the value of the new problem objective function is better than the best answer in the current community, new answers are saved. On the other hand, if the value of the new problem objective function is worse compared to the best solution of the current community, the new one might be acceptable depending on the difference in the value of its fitness function with the best function of fitness in the next iteration and considered for the new population. The dependence of the refrigeration method on the temperature reduction allows the temperature to be faster at the beginning of the process of repeating the search in a wide area and then in the next steps of the algorithm, with slower reduction of temperature at the number of steps, local searches around the best solution can be obtained. The temperature reduction method is called the "cooling program", which is the main SA structure [58]. The SA application in optimizing the PVWTBAHDG system, such as GA and PSO, is not popular, but today, the use of SA has increased. ACO is an intelligent method based on the ant colony. Based on this method, initially, in the search space, each ant is located in a random location. In the next repetition, the pheromone is smelled around an ant position and transfer from the second position to the large level of the pheromone. Depending on the level of the pheromone, the next move can be achieved. All ants look for their positions around the pheromone and choose their next move. Therefore, the entire search space is determined and the colony commences moving in groups on the repeating routine. The algorithm ends when predetermined conditions are satisfied such as the desired amount of food found on the ants or the maximum number of repetitions.

The artificial immune algorithm (AIS) is inspired by the function of the immune system and observing principles in nature [113]. The solution in searching space is programmed as a population in the method. The population of antigen in each replication varies with the investigation of the population's capability during the removal of irreversible (pathogens). To maximize the objective function values, the old antigen is replaced by new objective function values with new ones. Like GA, the AIS has some operators that can increase the likelihood of the method to determine the optimal overall point [113]. Given the similarity to GA in terms of the possibility of suitable operation for the optimal

solution of complicated problems, AIS is a method with perfect capability to use in future measurement studies. However, with its capability to handle many parameters, GA is still used more than AIS. Table 3.1 shows the comparison of the intelligent methods in the optimal design of the PVWTBAHDG system.

3.10 Conclusion

This chapter describes the stand-alone and grid-connected HDG. A variety of photovoltaic-wind HDG systems is presented. In addition, the principles of designing the HDG systems with objective function and constraint are discussed. Designing optimization methods for PVWTBAHDG systems is also presented. Comparison of intelligent methods in the optimal design of the PVWTBAHDG system is presented in Table 3.1.

Table 3.1: Comparison of intelligent methods in the optimal design of the PVWTBAHDG

Disadvantages	Advantages	Energy Management Approach
Hard programming	Effective performance in determining the general optimal, used in problems with many parameters	Genetic Algorithm
Relatively low performance in general optimum determination, not desirable in problem-solving with many parameters	Easy programming with few equations	Particle Swarm Algorithm
Relatively low performance in general optimum determination, not desirable for problem-solving with many parameters	Easy programming	Simulated Annealing Algorithm
High speed of computation and inappropriate problem-solving with many parameters	Easy programming with few equations	Ant Colony Algorithm
Desirable capability to determine the overall optimum point	Easy programming	Artificial immune algorithm

Chapter 4. Concepts and Definitions of Power Quality (PQ) in the Distribution Network

4.1 Introduction

Today, electric utilities and their customers are concerned even more about electrical energy quality. The term Power Quality (PQ) has found numerous applications in industrialized countries and the electric industry. The subjects related to PQ are considered to be old conventional concepts. Yet, engineers make an effort to collect these concepts and categorize them in specific patterns. To put it simply, a new insight into power system distortions has introduced itself as a subject exploring which is turning into one of the prime item in the study of power systems. Additionally, regarding a large number of problems caused by undesired PQ, using appropriate methods to enhance electrical PQ seems necessary and this requires suitable novel solutions. Consequently, it is necessary to grasp PQ problems and concepts to find proper solutions. This will be realized only if these concepts are appropriately defined and evaluated [115].

Generally, the following reasons are provided to justify the ever-increasing focus on PQ.

- With the focus on improving the efficiency of the power system, devices such as adjustable-speed motor drives and shunt capacitors are widely being utilized to improve power factor. System loss is reduced using shunt capacitors, but this type of capacitor changes the impedance-frequency characteristics of the system, leading to the resonance phenomenon and results in the increase of distortions temporarily and especially in increasing the harmonic distortion level of the system. Besides, motor speed controllers increase the harmonics level in the power system and impact on the system's capabilities. To put it another way, the application of novel devices and equipment that provide the essential need of a modern power system (in the perspective of both customers and power companies) helps create a new type of problem. Therefore, the mutual effect of the equipment and the system appears unavoidable;
- Due to the integrated and interconnected nature of the system, the failure of an element of the system will adversely affect the system's equipment and lead to even more devastating consequences. As power systems are extended networks exposed to distortions caused by low PQ, the propagation of problems in such an interconnected system at any moment may lead to undesirable event;
- The sensitivity of modern electrical equipment to variations of PQ has increased. Most of the modern electrical appliances use microprocessor controllers and power electronics elements. These devices are sensitive to most types of

distortions in the power system and these results in an inappropriate operation of the equipment. As the number of these devices is large, especially at industrialised centres, hospitals, laboratories, etc., many problems may occur;

- The customer's and power companies' lack of protective and fault alarming devices associated with low PQ may lead to misunderstanding between customers and utilities because of the ambiguity of limitations;
- Awareness of PQ problems has increased for customers. Subjects including power interruption, under voltage, and switching transient phenomena have gained more attention by customers day by day and this makes utilities to think about enhancing PQ. This means that end-users are dissatisfied with merely benefiting from electricity, but they look for high-quality power such that all modern equipment is suitably utilized; and
- The main and ultimate reason for considering PQ is its association with economic issues, which highly impact power companies, customers, and producers of electrical devices. PQ can bear a direct economic effect on the power consumption of most of the customers, especially industry customers. As was noted recently, using modern and automatic devices for improving industries has highly been emphasized. These devices are controlled electronically, so they are more sensitive to PQ. Therefore, industrial customers are highly affected by power system distortions. On the other hand, large investments are lost and costs are increased because of dealing with such distortions. For instance, the failure of one switch in a factory will disconnect a production line and consequently pecuniary loss, compensating for which is not an easy task for factories [115].

Utilities pay attention to the aforementioned problems because of two major reasons. On the one hand, by resolving the low PQ problems, the number of customers of utilities will increase. Using high efficient electrical devices, on the other hand, will reduce the amount of investment required for power generation centers and substations. The interesting point is that devices used for increasing efficiency are damaged more than other devices due to power interruption and sometimes they become the origin of popular PQ problems [115].

4.2 PQ Definition

Different definitions of PQ have been presented in various references. For instance, utilities may assume the PQ term is a synonym of power interruption, and using the

available statistics, they may show that the level of power interruption is very low. However, manufacturers of electrical devices may provide another definition of PQ as follows [115]:

"The features of the power system that provide devices with proper operation".

This definition might differ from various equipment and different manufacturers. Nonetheless, the common agreement between customers on PQ is of high importance and priority. Thus, achieving a specific definition of PQ before addressing the main topic is important so that PQ is evaluated based on the aforementioned definition. In general, the following definitions can be used in regards to PQ [115]:

"Any change in voltage, current, and frequency quantities that cause failure and/or failed operation of the consumers' equipment".

There are different views on the reasons behind PQ issues. Fig.4.1 illustrates the results of a statistical analysis performed in an industrialized country, where the personnel of Electricity Company and customers participated in commenting on the causes of PQ issues [115].

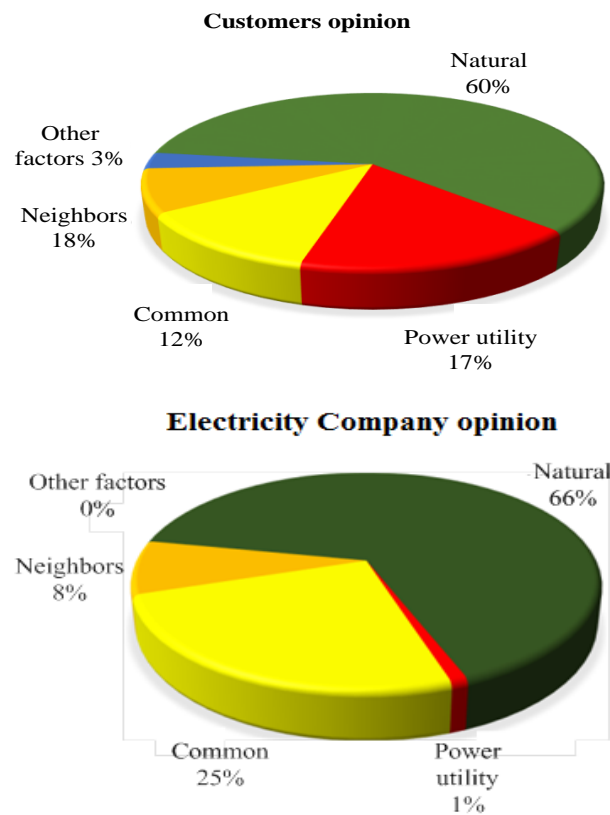


Fig. 4.1. A survey data related to the roots of power quality issues [115].

While opinion polls from other companies may provide different results, Fig.4.1 clearly demonstrates a common idea and that is the different lines of thoughts of electricity companies and customers. Both companies and customers attribute more than two-third of these events to the natural phenomena (like lightning). However, customers, more than the personnel of electricity companies, are of the opinion that the poor performance of electricity companies is the origin of this problem. Anyhow, it is worth noting that the result of most of the events occurring in the power system will lead to problems for customers and never will be recorded in the electricity company statistics.

An example of these problems is capacitor switching, which is a common occurrence for electricity companies but can cause transient overvoltage or even disconnect some of the modern equipment. Another example is the occurrence of an instantaneous short circuit, which will reduce the voltage of customers and may lead to the interruption of a motor drive with speed regulation capability. Nonetheless, the electricity company will not sense any sign of a problem in the related feeder, except when a PQ monitoring device is mounted on the feeder beforehand. Practically, because of the exorbitant cost of monitoring devices, mount the required devices on all feeders is not economically justified [115].

Besides the aforementioned problems, there are other challenges in the power system concerned with the mis operation of control systems, hardware, and software. Because of transient voltages occurring repeatedly in the system, electronic devices become degraded during their lifespan and it is most likely to be useless after an event with rather a low magnitude. Therefore, sometimes attributing a failure or a fault to a given origin is challenging. Overall, some of the events occurring in the power system may not have been predicted in the control software. Concerning the above statements and regarding the ever-increasing focus of customers on PQ, electricity companies are obliged to propose special plans. The philosophy of the plans can be divided into two different types. It can be either reactive, meaning that the company replies complains of its customers, or educational, where the company educates its customers and beside it, it tries to create services to help customers find solutions for PQ problems and this way help the company. Additionally, economic issues must also be taken into account when analyzing a PQ problem. It might be that an optimal solution is to lower the device's sensitivity to PQ problems. The required level of PQ is that it helps the appropriate operation of the device in special facilities [115].

In summary, it is difficult to quantify PQ similar to the quality of other assets and services. Although guidelines and manuals are available to sense voltage and other parameters, determining the final value of PQ will be realized according to the operation of the customer's equipment. In other words, among the factors affecting the proper or improper PQ is the type of consumption and this should be taken into special consideration [115].

4.3 PQ =Voltage quality

Although the general title of the present chapter is PQ, it is voltage quality that is discussed in most of the cases. The major problem here, as mentioned before, is the definition of the PQ. In general, in a power system, only the quality of voltage is controllable and currents cannot be appropriately controlled. Thus, PQ standards in industrialized countries have been specified as the acceptable voltage limits. Alternative current (AC) power systems operate with rather sinusoidal voltage with specific frequency and magnitude. Considerable deviations in magnitude, frequency, or waveform will emerge as a PQ issue [115].

Voltage and current are almost interrelated in most cases. Even though generators generate a rather pure sinusoidal voltage, the flow of current on the system impedance may create various types of voltage distortions in the system as follows [115]:

- Current produced by the occurrence of a short circuit will significantly reduce the voltage or make it zero;
- Currents entering the system due to the lightning strike can cause large wave voltages that mostly lead to arc on insulators and finally transform into other phenomena like short circuits; and
- Distorted currents produced by harmonic-generating loads create distortions in the voltage and this voltage is applied to customers. This problem, particularly in interconnected systems is a challenging one as it makes it difficult to take appropriate actions for improving PQ [115].

4.4 A general classification of PQ problems

The IEC standard divides different electromagnetic phenomena into six groups as given in Table 4.1 [116].

Various active teams in the power industry in the area of PQ monitoring have added other groups, besides the available six groups, to the IEC standard [117]. For instance, the short-duration changes group can be included voltage dips and short-duration interruptions

groups of the IEC. In addition, the group of distortions in the waveform is introduced as a group that includes harmonics (interharmonics), the DC offset related to the IEC standard, and the notching phenomenon in the IEEE standard. At last, Table 4.2 tabulates the general categories of PQ issues. This table presents the information about the spectrum content, duration, and magnitude that are necessary to describe each group. These groups and the corresponding characteristics are required for classifying different measurement results and explain electromagnetic phenomena causing PQ problems [115].

4.5 Transients

The term "transients" has been extensively employed for a long time in the area of unsteady conditions analysis of power system to specify undesirable yet instantaneous phenomena. The classical example is that of the damping oscillatory behavior of a Resistive-Inductive-Capacitive (RLC) circuit.

A commonly-used definition of the term "transient" is given as follows:

"Part of a variable's changes that disappears during transitions between two separate steady states" [115].

This definition can also cover other abnormal events of a power system as well. Another term that is often used as a synonym for the term "transients" is "surge".

Generally, the term transient is divided into two groups: impulsive and oscillatory, which describe the transient waveforms of currents or voltages.

4.5.1 Impulsive transient

An impulsive transient is an aberration in steady states of voltage, current, or both current and voltage, with a non-power frequency and its polarity is unidirectional (positive or negative). Besides its magnitude, an impulsive transient is normally determined using peaks and valleys. For instance, a 2000 V, 1.2/50 μ s wave is a wave that reaches its peak (2000 V) within 1.2 μ s and drops to half of the peak during 50 ms. Lightning and switching are considered as the main reasons for the occurrence of the transient impulsive phenomenon.

Fig. 4.2 depicts an impulsive transient current wave created due to the lightning strike. Owing to the existence of high frequencies in an impulsive wave, its waveform changes quickly by the system parameters and it may exhibit various features when observed from different positions of the system.

Table 4.1. Classification of main events that lead to electromagnetic distortion in the system [116].

<p>Conducted low-frequency phenomena</p> <p>Harmonics, interharmonics</p> <p>PLC signals</p> <p>Voltage fluctuation (flicker)</p> <p>Voltage dips and interruptions</p> <p>Voltage unbalance</p> <p>Power frequency variations</p> <p>Induced low-frequency voltages</p> <p>DC offset</p>
<p>Radiated low-frequency phenomena</p> <p>Magnetic fields</p> <p>Electric fields</p>
<p>Conducted high-frequency phenomena</p> <p>Induced continuous-wave voltages or currents</p> <p>Unidirectional transients</p> <p>Oscillatory transients</p>
<p>Radiated high-frequency phenomena</p> <p>Magnetic fields</p> <p>Electric fields</p> <p>Electromagnetic fields</p> <p>Continuous waves</p> <p>Transients</p>
<p>Electrostatic discharge phenomenon</p>
<p>Nuclear electromagnetic pulse</p>

Table 4.2. Classification and characteristics of electromagnetic phenomena
in the power system [115].

Category	Typical spectrum content	Typical duration	Typical voltage magnitude
1. Transients 1.1. Impulsive 1.1.1. Nanosecond 1.1.2. Microsecond 1.1.3. Millisecond 1.2. Oscillatory 1.3. Low frequency 1.4. Medium frequency 1.5. High frequency	5 ns rise 1 μ s rise 0.1 ms rise less than 5 kHz 5-500 kHz 0.5-5 MHz	less than 50 ns 50 ns-1 ms more than 1 ms 0.3-50 ms 20 μ s 5 μ s	up to 4 p.u. up to 8 p.u. up to 4 p.u.
2. Long-duration variations 2.1. Lasting interruption 2.2. Undervoltage 2.3. Overvoltage		more than 1 min more than 1 min more than 1 min	0 p.u. 0.9 p.u. 1.05 p.u.
3. Short-duration variations 3.1. Immediate 3.1.1. Interruption 3.1.2. Sag 3.1.3. Swell 3.2. Instantaneous 3.2.1. Interruption 3.2.2. Sag 3.2.3. Swell 3.3. Temporary 3.3.1. Interruption 3.3.2. Sag 3.3.3. Swell		0.5-30 cycles 0.5-30 cycles 0.5-30 cycles 30 cycles-3 s 30 cycles-3 s 30 cycles-3 s 3 s-1 min 3 s-1 min 3 s-1 min	less than 0.1 p.u. 0.1-0.9 p.u. 1.1-1.8 p.u. less than 0.1 p.u. 0.1-0.9 p.u. 1.1-1.2 p.u. less than 0.1 p.u. 0.1-0.9 p.u. 1.1-1.2 p.u.
4. Voltage unbalance		Steady state Steady state	0.5-2% 0-0.1%
5. Waveform distortion 5.1. DC offset 5.2. Harmonics 5.3. Interharmonics 5.4. Notching 5.5. Noise	1 st to 100 th harmonics 0 to 6 kHz Broadband	Steady state Steady state Steady state Steady state	up to 20% up to 2% up to 1%
6. Voltage oscillation	Less than 25 Hz	Intermittent	0.1% to 7%
7. Power frequency variations		Less than 10 s	

NOTE: s: second, ns: nanosecond, μ s: microsecond, ms: millisecond, kHz: kilohertz, MHz: megahertz, min: minute, p.u.: per unit.

These waves usually have a great impact at the distances close to their input place and the impact becomes weaker as the wave moves away from the place. An impulsive transient may stir the natural frequencies of the circuits and create an oscillatory transient wave which is described in subsection 4.5.2 [115].

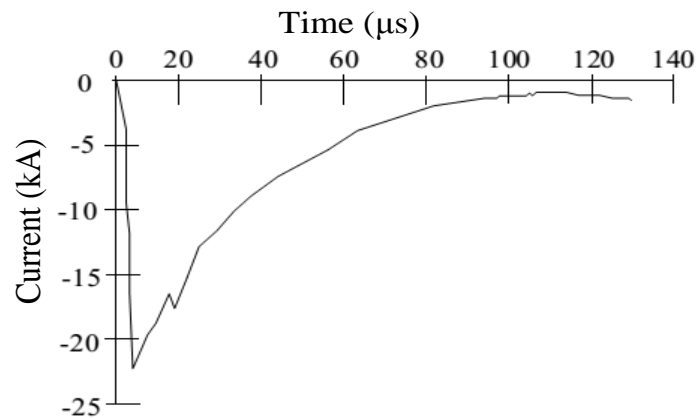


Fig. 4.2. Transient surge wave due to a lightning strike [115].

4.5.2 Oscillatory transient wave

Oscillatory transient wave is the result of an abrupt deviation from steady states of voltage, current, or both voltage and current, with a non-power frequency and its value possesses positive and negative polarities. Oscillatory transient wave is a voltage or current wave in which the polarity of its instantaneous value changes abruptly. This type of wave is specified by its spectrum content (dominant frequencies), duration, and magnitude and can be classified into the following sub-groups [115]:

- A wave with a fundamental frequency above 500 kHz with a duration of μs , is known as a high-frequency oscillatory transient wave. This transient phenomenon is often the system's response to an impulsive transient wave;
- A transient with a fundamental frequency between 5 Hz and 500 kHz with duration of tens of μs , is called medium-frequency transient. Back-to-back capacitor energizing may lead to the establishment of such a wave, a sample of which is shown in Fig. 4.3. By back-to-back capacitor two sets of capacitor banks close to each other are connected to the system via independent switches. Cable switching creates oscillatory voltage transients in the mentioned frequency range. A medium-frequency wave may also appear because of the system response to an impulsive transient wave [115]; and

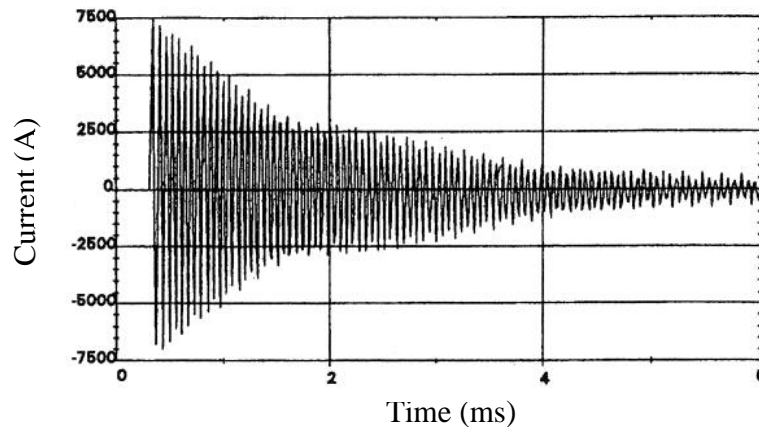


Fig. 4.3. The oscillatory transient current wave created due to the switching of a back-to-back capacitor [115].

- A transient wave with a fundamental frequency below 5 kHz with a duration of 0.3-50 ms is named a low-frequency transient wave. This group of the impulsive transient event is often discussed in transmission and distribution networks, which results in various type of events. The most famous type of such phenomenon is capacitor bank energizing, which produces an oscillatory voltage transient with a fundamental frequency in the range of 300-900 Hz. The peak magnitude of this wave may reach 2.0 p.u. However, it is normally in the range of 1.3 to 1.5 p.u. and duration of 0.5-3 cycles (this depends on the damping situation in the system).

Fig. 4.4 depicts a typical oscillatory low-frequency transient wave [115].

An oscillatory transient wave with a fundamental frequency smaller than 300 Hz can also appear in distribution systems. These transient waves are generally associated with Ferro resonance and transformer energizing, as shown in Fig. 4.5. Transient phenomena caused by series capacitors can fall into this category [115].

4.6 Long-duration voltage oscillations

Long-duration voltage oscillations include any deviation in the root-mean-square (RMS) value of the voltage at the nominal frequency for a duration longer than 1 min.

In other words, voltage oscillation is an event the voltage exceeds its acceptable range for a duration longer than 1 min. Long-duration voltage oscillations appear in the form of either overvoltage or under-voltage emerging due to the variations in the load and/or disconnecting power generation resources from the system [115].

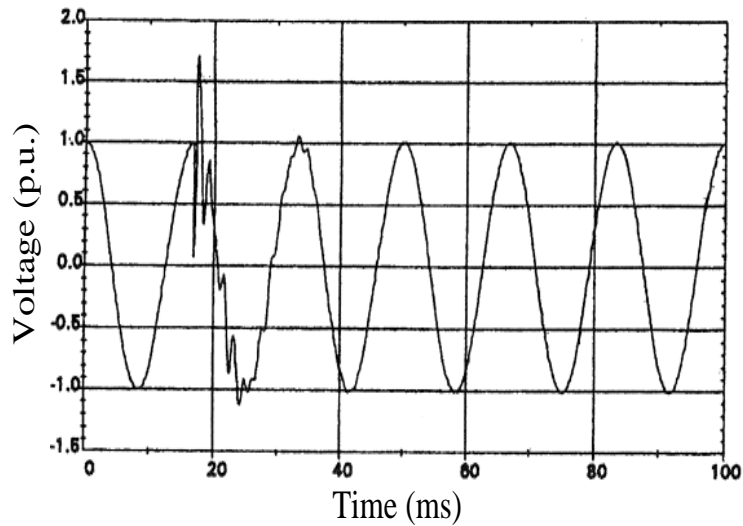


Fig. 4.4. The oscillatory low-frequency transient wave created due to capacitor bank energizing [115].

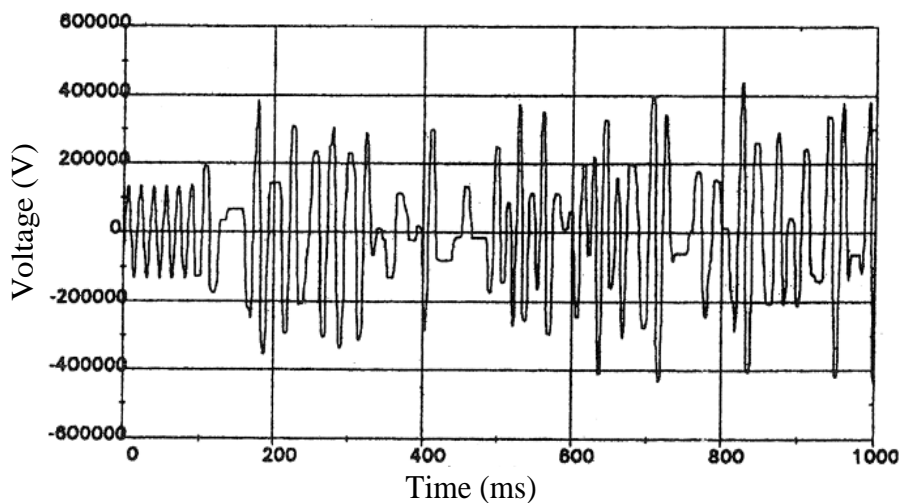


Fig. 4.5. An oscillatory low-frequency transient wave created by a Ferro resonance event in an unloaded transformer [115].

4.6.1 Long-duration overvoltage

A long-duration overvoltage is defined as an increase in the RMS value of the voltage above 5% at the nominal frequency for a period longer than 1 minute. The following items provide some of the factors that create over-voltages [115]:

- Disconnecting a large load;
- Switching on a capacitor bank;
- Incorrect voltage control; and
- Incorrect position of the transformer's tap.

4.6.2 Long-duration under-voltage

A long-duration under voltage is defined as a decrease in the RMS value of the voltage above 10% at the nominal frequency for longer than 1 minute. The reasons for under-voltages are the same factors mentioned in over-voltages. For instance, the circuit's overload or switching off the capacitors may lead to under-voltages [115].

4.6.3. Sustained interruptions

Sustained interruption occurs when the value of the supply voltage is zero for longer than 1 minute. Such interruptions are mostly permanent interruptions and system restoration requires personnel to bring it back to the steady state. The term "sustained interruption" alludes to a particular event in power systems and, generally, is not correlated with the term "outage". Nonetheless, the similar meaning of these two terms is confusing for customers and they may consider outages as power interruptions. On the other hand, "outage" is the state of a device when it fails to perform its expected operation [115].

4.7. Short-duration voltage oscillations

As given in Table 4.2, these variations are categorized into three groups according to their durations: instantaneous, momentary, or temporary. Short-duration voltage oscillations occur due to the following reasons [115]:

- Short-circuits
- Energizing large loads with high starting currents.

A fault can cause either temporary voltage drops (sag), voltage rises (swell), or a complete loss of voltage (interruptions), which relies on the location of short-circuits and the system conditions. The fault may be in the neighborhood of or distant from the point under-study. Regardless of the fault location, its occurrence has a short-duration impact on voltage, which continues until protective devices operate [115].

4.7.1 Short-duration interruption

A short-duration interruption appears at the time the supply voltage or the load current decreases below 0.1 p.u. during a period shorter than 1 minute. Interruptions may emerge due to power system short-circuits, failures of devices, and malfunction of controllers. Short-duration interruptions are determined only by their duration because its amplitude is invariably below 10% of the rated value. The duration of an interruption caused by a short circuit in the system is specified by the operating time of the system's protective

devices. One solution in case of transient short circuits normally is to reclose the breakers, which helps limit the interruption period within thirty cycles. The duration of an interruption caused by mis operation of devices is random and undetermined [115].

There are interruptions that may appear following voltage sag. This usually happens when faults occur. The voltage sag continues from the time a short circuit occurs until protective devices operate. Figure 4.6 illustrates such a momentary interruption, in which case the voltage reduces to one-fifth of its initial value during three cycles and falls to zero during roughly 1.8 s before the recloser operates again [115].

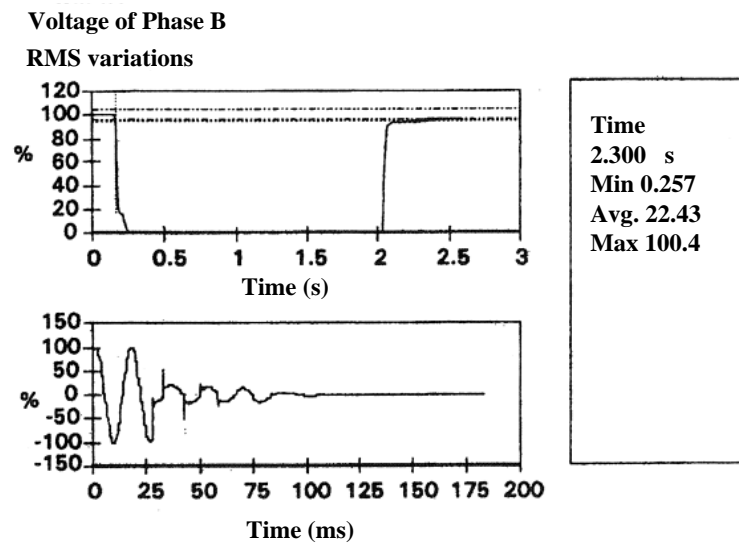


Fig. 4.6. Temporary interruption of a line and reclosing operation [115].

4.7.2 Sag

Sag (dip) is a reduction in the voltage/current from 0.1 to 0.9 p.u. at the fundamental frequency that continues half a minute to one minute. The IEC uses the term "dip" as a synonym for "sag". In general, when 20% sag appears, it means the voltage has decreased to 0.8 p.u., where the base or nominal voltage must be known. Sag can be determined using two parameters: its magnitude ΔU and its duration Δt (Fig. 4.7). In Fig. 4.7, ΔU_C denotes the deviation between two steady-state voltages, where one voltage variation has happened. Also ΔU_{max} shows the deviation between the maximum and minimum characteristics values of voltage changes. Voltage sag with a complicated shape (Fig. 4.8) can be specified using two or more values (Δt and ΔU). Voltage sag with a complicated form rarely happens, and in general, it can be determined using its maximum magnitude and its total time duration [115-118].

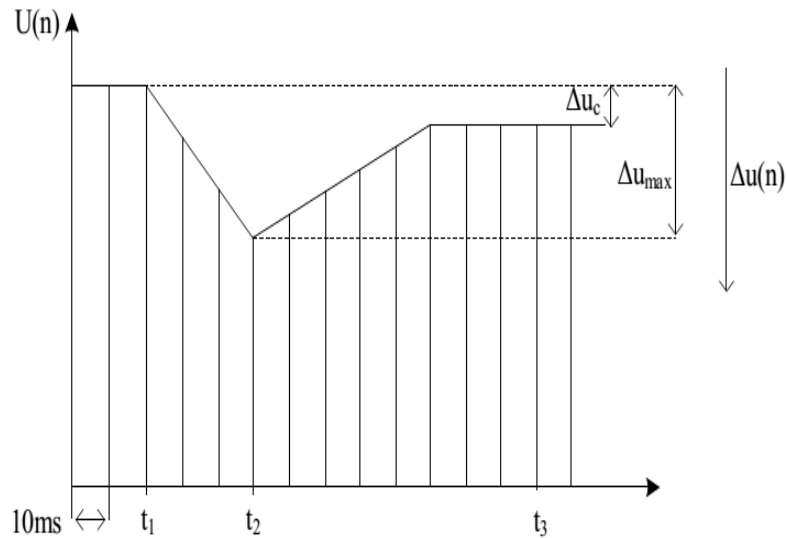


Fig. 4.7. Typical sag [115-118].

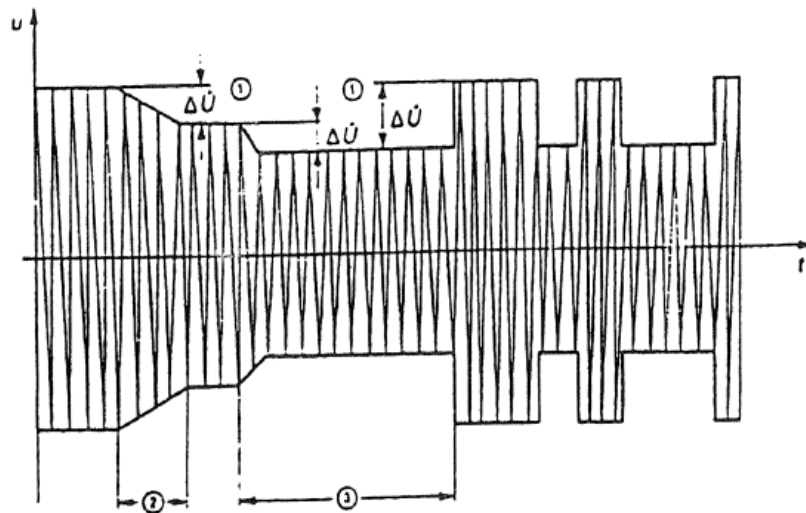


Fig. 4.8. Sag with a complicated form [115-118].

4.7.2.1 Magnitude and duration of sag

As previously noted, voltage variations with a voltage magnitude greater than 0.9 p.u. are not considered voltage sags. Voltage reduction for a duration shorter than half a cycle is not considered in this group but are taken into account as transients [115-118].

It is worth noting that, in general, sags happen in a system all the time. Therefore, most of the equipment should accept the risk of several misoperations due to this type of distortion. Parameters ΔU (magnitude) and Δt (time) cannot be limited in practice. In other words, all values of magnitude between 10% and 100% and Δt values longer than half of a cycle are expected. It is worth noting that voltage sag is not the same for all three phases [115-118].

4.7.2.2 Impacts of voltage sag

Voltage sag may damage the equipment connected to the system or lead them to mis operation, and consequently, the following problems appear [119]:

- Glow-discharge lamp turn off;
- Malfunction of regulators;
- Motor speed change or motor stop;
- Wrong turn on/off commands to contactors;
- Error in computer calculations and/or measurement devices that are accompanied by electronic devices;
- Asynchronism of synchronous motor and generators; and
- Commutation failures of the thyristor bridge in the inverter mode.

Voltage sag mostly occurs due to system short circuits. However, energizing large loads or starting large motors can also help this phenomenon occur. Fig. 4.9 shows voltage sag on a feeder caused by a single-phase fault on the other feeder. According to Fig. 4.9, an 80% sag has continued for three cycles until a substation breaker clears the short-circuit current. Fig. 4.10 exhibits starting current of a large induction motor which draws current 6 to 10 times greater than the nominal current at the direct starting. In this case, starting current becomes comparable to the short circuit current, the resultant sag will be a great value. Normally, voltage regulation devices are used to control an under-voltage that continues for longer than one minute. Such an under-voltage might not originate from short circuits in the system. Thus, such events are considered as long-duration variations [115-119].

4.7.3 Voltage swell

Voltage swell is defined as a rise in the RMS value of the voltage from 1.1 to 1.8 p.u. at the fundamental frequency for time intervals between half a cycles to one minute. Similar to voltage sag, swells also occur due to short circuits.

Swell may appear because of a single-phase to ground short circuit in healthy phases, as shown in Fig. 4.11. Moreover, energizing a large capacitor bank or disconnecting a large load may result in swells [115]. Swells are specified using the amplitude (RMS value) and duration. The intensity of a swell when a fault occurs depends on the fault location, system impedance, and the grounding method. In ungrounded systems (isolated neutral point), the voltages of the healthy phases are 1.73 p.u. in case of a single-phase to ground fault. Short circuits at different locations in a four-wire multi-grounded system will result

in different values of swells in the healthy phases. For instance, Fig. 4.11 depicts a 15% voltage swell. Instead of "swell", "Momentary overvoltage" is sometimes used by many engineers [115].

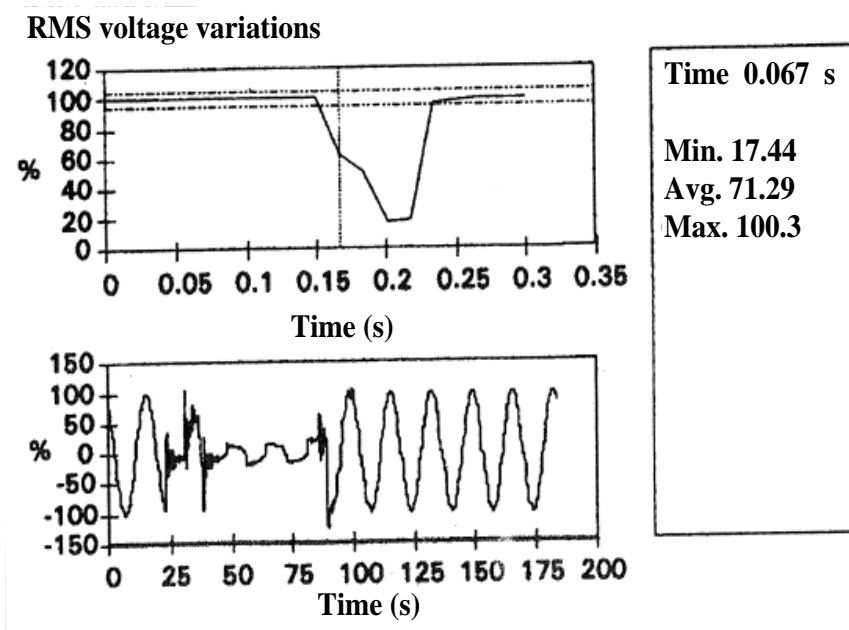


Fig. 4. 9. Sag due to a single-phase to ground short circuit [115-119].

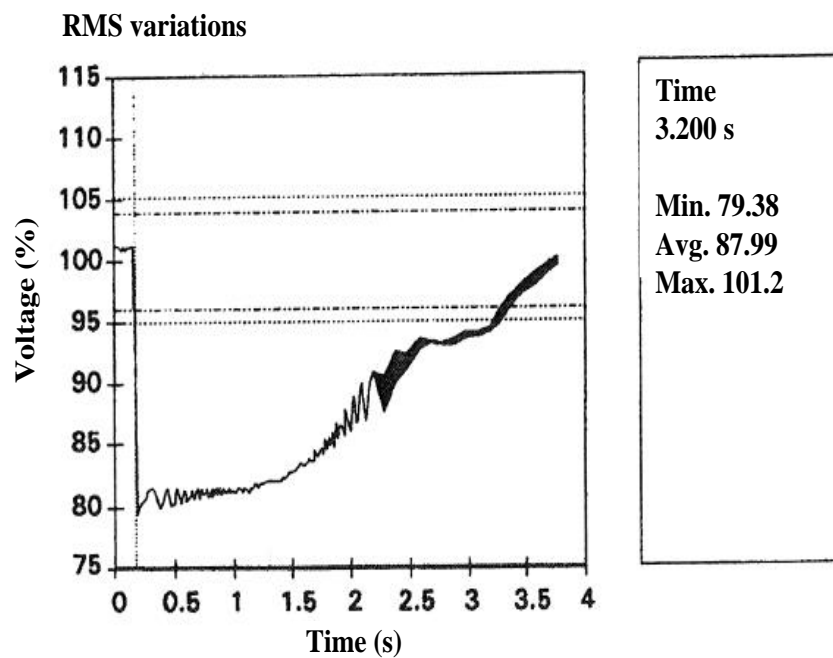


Fig. 4. 10. Sag due to starting of a motor [115-119].

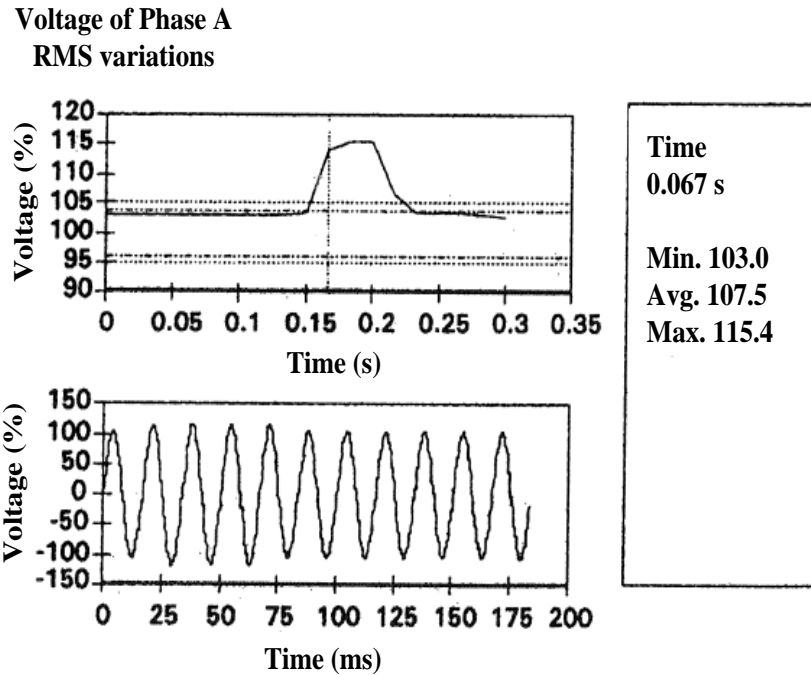


Fig. 4.11. Instantaneous voltage sag due to a single-phase to ground short circuit [115].

4.8 Voltage unbalance

Voltage unbalance refers to conditions where the voltage values of the three phases are different and/or phase shifts between the three phases are not 120° . These two conditions can happen at the same time [122-125]; this situation is also called voltage unbalance. Simply put, voltage unbalance is the maximum change from the average value of three phase voltages divided by the average value of three phase voltages expressed in percentage. Symmetrical components may sometimes be used to describe and define voltage unbalance. The negative- or zero-sequence component divided by the positive-sequence component determines the percentage of asymmetry. Figure 4.12 shows a sample of the above two ratios for a feeder connected to residential load during one week [115].

The main origin of voltage unbalances below two percent is the presence of single-phase loads in a three-phase network. This phenomenon may happen because of fuse cut-off in one phase of a three-phase capacitor bank. In low-voltage (LV) networks, single-phase loads are often connected in a phase-to-neutral way but their distribution on the three-phase network is almost balanced. One of important single-phase loads that cause voltage unbalance is single-phase induction furnaces. It should be said that transmitting zero-sequence voltages from lower to higher voltage levels is accompanied by high attenuation.

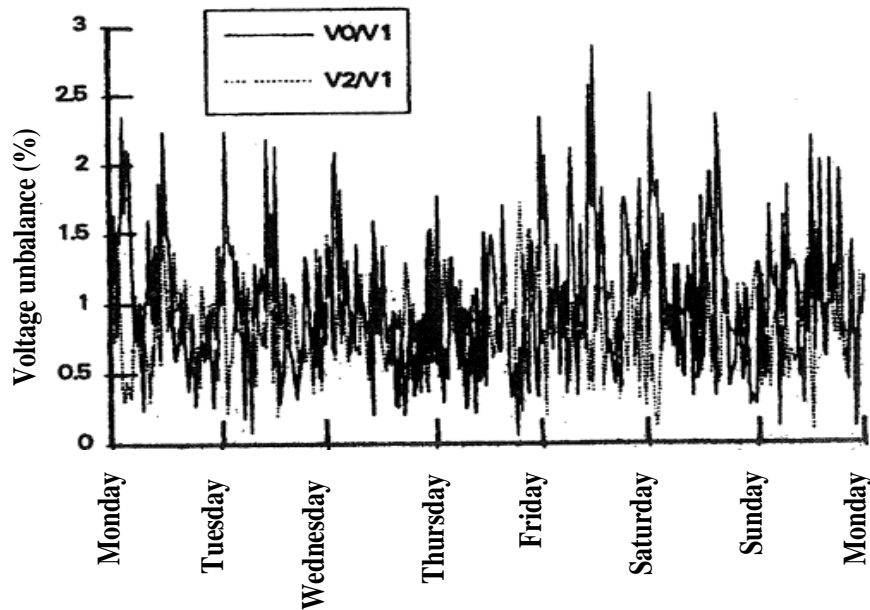


Fig. 4.12. Voltage unbalance for a residential feeder [115].

Voltage unbalance leads to some problems, which are summarized as follow [120]. The negative-sequence impedance of three-phase machines equals that in the starting mode. As a result, a machine fed by an unbalanced source will draw an unbalanced current from the network, the percentage of which is several times of voltage unbalance. Consequently, three-phase currents significantly differ from each other. Under such conditions, higher current in one or several phases increases the machine's temperature. This increase is neutralized with reduced heat caused by the reduced current of other phases. However, in general, the machine's temperature will increase in such conditions and may damage the machine. Motors and generators, especially the expensive types, should be protected using protective devices. The devices will separate the motor from the network under severe voltage unbalance conditions [115].

In multi-phase converters, where the amplitude of input voltages is effective on the output DC voltage, the unbalanced voltage will impact the performance of the converter and create undesirable components on the DC side, besides establishing harmonics on the AC side [115].

4.9 Waveform distortion

Waveform distortion is a deviation from a pure sinusoidal waveform with fundamental frequency, which is described by the spectral content of that waveform. Some main kinds of waveform distortion include [115]:

- DC offset;
- Harmonics;
- Interharmonics;
- Notching; and
- Noise.

4.9.1 DC offset

DC offset refers to the case when DC voltages or DC currents are present in an AC system. The main cause of this phenomenon is rectifiers. This DC component in AC networks can saturate transformer cores under normal operating conditions, reduce the transformer's lifespan, and even lead to its burning. Moreover, Direct current can lead to the electrolytic erosion of grounding electrodes and its other related connections [115].

4.9.2 Harmonics

Harmonics refer to sine wave voltages or currents with frequencies equal to integer multiples of the nominal frequency (50 Hz) of the system. Distorted waveforms can be decomposed into the fundamental frequency and several harmonics. The nonlinear nature of equipment and loads causes harmonic distortions. The complete harmonic spectrum can be used to describe the harmonic distortion level, where each harmonic component is determined separately using its magnitudes and phase angle. THD is a quantity to give the effective value of harmonic distortion. Figure 4.13 shows the waveform and harmonic spectrum of an input current of a sample speed-adjustable drive. As mentioned earlier, the current distortion level is described using a THD parameter. However, it is rather confusing! As an instance, in most adjustable-speed drives, the THD level of the input current in low loads is very high. This is a minor concern from the system's perspective since the harmonic current has a small value, although its relative distortion is large.

Total Demand Distortion (TDD) has been defined to address this issue. TDD is similar to the THD but, in the former, distortion value is divided into the nominal current of the load instead of being divided into the magnitude of the fundamental frequency current [115].

The harmonic distortion appears when devices with nonlinear voltage-current characteristics start to operate. Such devices are conceived of as harmonic current sources. The current harmonic generated by different devices results in a harmonic voltage drop at both sides of the network impedance.

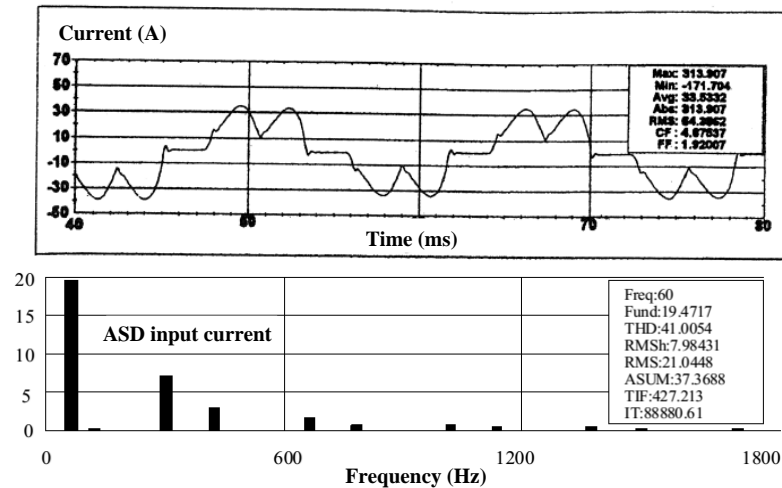


Fig. 4.13. Input current waveform and the harmonic spectrum in a motor drive with the speed-adjustability capability [115].

This phenomenon is shown in Fig. 4.14. On the other hand, connecting reactive loads (like power factor correction capacitors) and the capacitive effect of cables can create series and shunt resonances, the result of which is the significant increase in the voltage at a point far away from the harmonic generator device [115].

4.9.2.1 Harmonic generation sources

Small harmonic currents with low harmonic levels are produced in the generation, transmission, and distribution systems. As a result, it can be said that a rather high level of the generated distortions is due to some of the residential or industrial loads.

The following are harmonic current generation factors in a system [115]:

- Phase control and high power devices; and
- Uncontrolled rectifiers, especially those using a capacitor at the DC side (like rectifiers used in Televisions (TVs), frequency converters, and ballast lamps).

- *The equipment used in generation, transmission, and distribution*

This category includes devices employed by the utility for power delivery to customers. These mainly include generators and transformers and lately, although in a low number, static compensators and frequency converters [115].

Since the generation of a pure sine voltage by generators is not practically possible, rotating machines are also among the factors that generate harmonics. Anyhow, by proper selection of the number of slots under each pole and winding pitch we can reduce the harmonics level and turn the generated waveform into a sine wave.

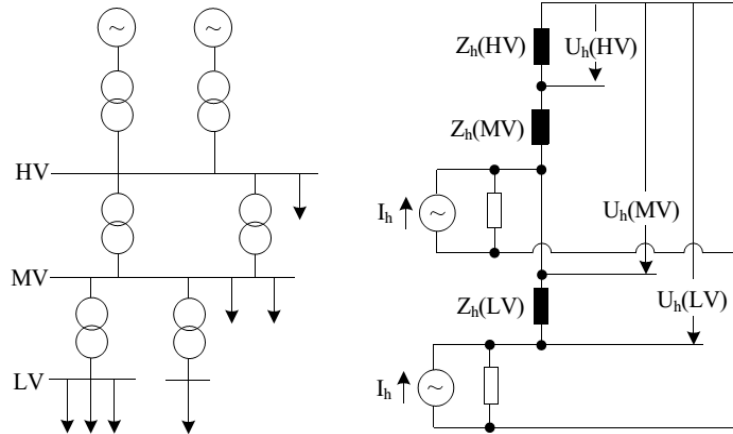


Fig. 4.14. Representation of voltage harmonic drop [115].

However, unbalanced operation generates 3rd or higher-order harmonics. The distortion caused by a transformer is due to its nonlinear magnetic curve [115].

- Industrial loads

Industrial loads are among the main reasons for the generation of harmonics. These loads include rectifiers, induction furnaces, and electric arc furnaces. Power electronics devices have a considerable impact on the distortion of the system. Using this type of device is increasing every day. By "increase", both the increase is contained in the number and the rated power of equipment. In theory, current characteristics harmonics of a power converter have the following values [121]:

$$n = p \times m \pm 1 \tag{4.1}$$

where, n is the harmonic order, p shows the number of pulses in the converter and m is an integer (1, 2, 3 ...)

In practice, non-characteristic harmonics are produced due to inaccuracy in the firing angle, unbalanced voltage source, and any factor affecting the balance of the rectifier. In theory, the harmonics level in rectifiers reduces as the harmonic order increases. This is stated by the following law [121]:

$$I_n = I_1/n \tag{4.2}$$

where, I_n is current harmonic of order n and I_1 indicates amplitude of the fundamental component.

The value of the current harmonic depends on the inductive voltage drop caused by the source inductance and firing angle. Electric arc furnace is another factor of

current harmonic generation and it can be modeled using an internal impedance that consists of an inductance and a damping resistor. The current spectrum generated by these furnaces presents a discrete spectrum mounted on a continuous spectrum [121].

- Residential loads

Residential loads are low power consuming appliances. Nonetheless, the high number of such appliances that operate simultaneously might be considered as a main cause of distortions in the system. The most important types of these appliances include TVs, devices using thyristor in their structure, fluorescent lamps, and power-saving lamps.

TV receivers are normally fed through a rectifier beside a large capacitor on the DC side. In such a case, the current drawn from the network includes short-duration pulses with a high percentage of harmonics [121].

Today, using thyristor-controlled loads is ever-increasing. Even though the power of each individual load is low, their superposition effect creates distortion in the voltage source [121].

4.9.2.2 Adverse effects of harmonics

The determining and major effects of harmonics include [115]:

- Misoperation of controllers;
- Misoperation of signal generators and protective devices;
- Additional loss in capacitor banks and electrical machinery;
- Additional noise in motors and the rest of the equipment; and
- Telephone interruptions.

Adverse effects of harmonics on equipment can be classified as momentary and steady [115]:

- Momentary effects

Momentary effects cause damage and misoperation of the devices that use zero-crossing time of the voltage wave. Regulators, electronics devices, and computers are more prone to these effects. On the other hand, a high level of harmonics may result in mis operation of protective relays.

- Steady effects

Steady effects are basically in thermal form. Additional loss and heat reduce the lifespan and damage capacitors and machines [115].

4.9.3 Interharmonics

Interharmonics are sine wave voltage or current signals with frequencies that are not integer multiples of the fundamental frequency. Interharmonics can appear in systems with different voltage levels. The fundamental roots of interharmonics include frequency converters, cycloconverters, and induction furnaces. Power Line Carrier (PLC) signals are other forms of interharmonics [115].

4.9.3.1 Interharmonics generation sources

Interharmonics generation factors can be found in LV, MV, and HV networks. Those generated by LV sources can significantly impact the neighboring devices. Those produced in MV and HV networks propagate into LV networks [115].

- *Static frequency converters*

Static frequency converters convert the system voltage to an AC voltage with a frequency smaller or greater than the system frequency. This device includes AC-DC (rectifier) and DC-AC (inverter) sides. The output frequency of the rectifier modulates the DC voltage and consequently, voltage interharmonics appear. Static frequency converters are used in devices that need variable frequency, and these converters are employed increasingly. Various type of static frequency converters with different characteristics are available. Harmonics and their interharmonics are given by the following equation [115]:

$$f_v = [[p_1 \times m) \pm 1]] \times f_1 \pm [p_2 \times n] \times F \quad (4.3)$$

where, p_1 is the number of pulses in the rectifier, p_2 declares the number of pulses in the converter, m and n are is an integer, 0, 1, 2, 3, ..., F is output frequency, f_1 shows the fundamental frequency of the supply network (50 or 60 Hz) and f_v demonstrates generated harmonic or interharmonic

The mixture of p_1 and m gives harmonics. These harmonics along with p_2 , n , and F result the interharmonics [115].

- *Cycloconverters*

Cycloconverters are high-power (several MWs) electronic converters that draw a balanced three-phase power from the electrical network to supply single- or three-phase output with low-frequency (usually less than 15 Hz) to low-speed motors. These converters consist of two or more rectifiers connected in the bridge

configuration. The formula that helps calculate the frequency of harmonics and interharmonics is similar to that of static frequency converters [115].

- *Induction motors*

Induction motors draw irregular magnetic currents because of slots in their rotors and stators. In LV networks, this current along with iron saturation effect creates interharmonics. Such motors when placed at the end of an LV overhead line longer than 1 km produce more distortion. Voltage interharmonics caused by induction motors up to 1% of the rated voltage have also been measured [115].

- *Arc welding machines*

Welding machines establish a wide range of frequency spectra. Welding is a turning on and off process where the duration of the operation is variable and may take from one to several seconds [115].

- *Electric arc furnaces*

Due to their irregular input current, electric arc furnaces produce variable and random interharmonic frequency spectrum. These devices are high-power (50 MVA to 100 MVA) equipment but are mainly connected to MV or HV networks. The maximum interharmonic voltage appears in the start step of the welding process [115].

4.9.3.2 Interharmonic effects

This phenomenon adversely impacts control ripple receivers and its effects on induction motors and electric arc furnaces are sensible [115].

4.9.4 Notching

The notching phenomenon is the presence of a periodic voltage distortion created by power electronic equipment when commutating between different phases. The components of the frequency related to notching have large values which are not detected using common harmonic measurement equipment. Figure 4.15 shows how a voltage notching occurs in a three-phase converter, which continuously generates DC currents. As mentioned, notches happen in the case where current commutation occurs between different phases. In this interval, a momentary fault occurs between two different phases, which brings the voltage value as close to zero as allowed by the system impedance [115].

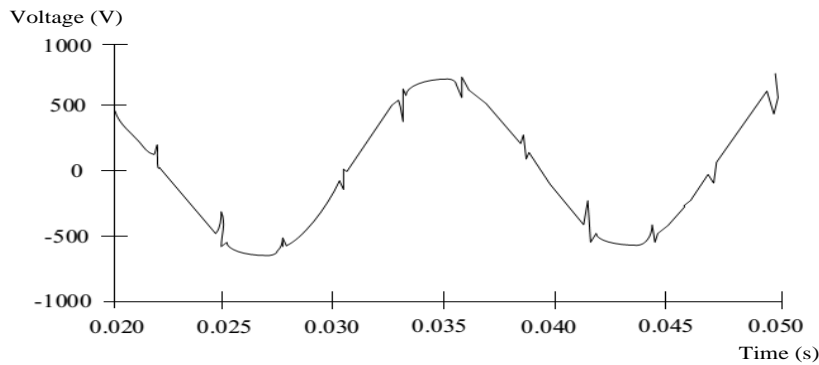


Fig. 4.15. A voltage notching created by a three-phase converter [115].

4.9.5 Noise

Noise refers to undesirable signals that appear on voltage or current waveforms of phase conductors, nulls, or carrier lines. There are various reasons for the appearance of noise, including power electronics devices, control circuits, arcing devices, loads with solid-state rectifiers, and switching power supplies. Improper grounding of the power system significantly boosts noise. Fundamentally, noise is composed of undesirable distortions differing from harmonic distortion or transient. This phenomenon affects electronic equipment, including microcomputers and programmable controllers. One solution to remove noise is to utilize filters, isolation transformers, etc. [115].

4.10 Voltage fluctuation

Voltage fluctuation refers to regular changes in the voltage envelope or a set of stochastic voltage variations. Various types of voltage oscillations can be classified as follows [126]:
 Type A) Rectangular and periodic (equal size step changes) voltage fluctuation due to turning on/off single-phase resistive loads (Fig. 4.16).

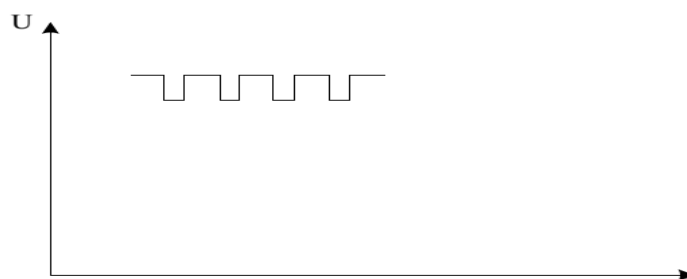


Fig. 4.16. Type a voltage fluctuation [126].

Type B) a series of voltage step changes that occur irregularly in terms of time and values of its step changes can be equal to different value. Also, the changes can happen in either

positive or negative directions. This case occurs due to switching several loads at the same time (Fig. 4.17).

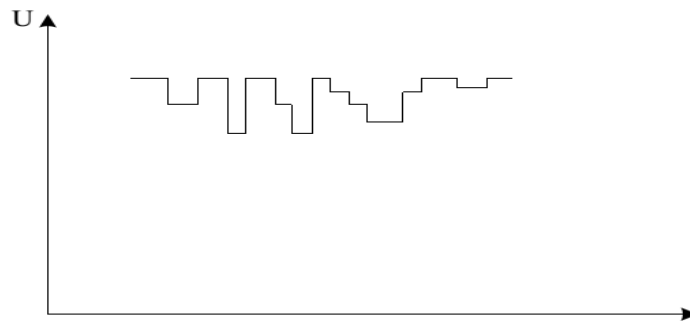


Fig. 4.17. Type B voltage fluctuation [126].

Type C) This type of fluctuation consists of a series of voltage fluctuations that not all of them are step changes. This is caused by switching non-resistive loads (Fig. 4.18).

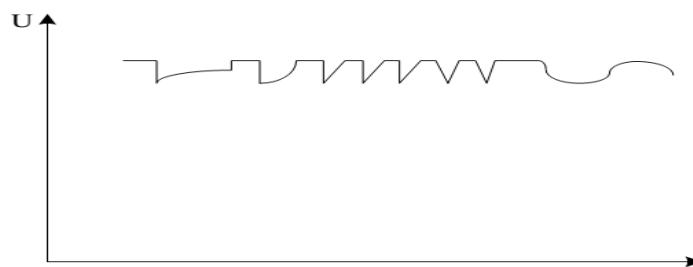


Fig. 4.18. Type C voltage fluctuation [126].

Type D) a series of continuous or random voltage fluctuations caused by random or periodic changes in the loads (Fig. 4.19).

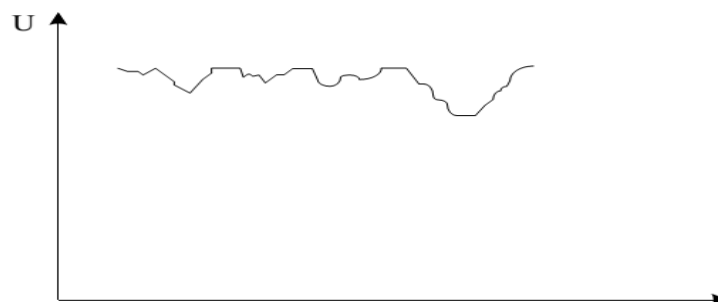


Fig. 4.19. Type D voltage fluctuation [126].

All types of voltage fluctuations can be characterized using the load characteristic and/or by observing the sensed waveform [126].

4.10.1 Causes of voltage fluctuation

In LV networks, residential appliances are the main cause of voltage fluctuation. However, any device can individually impact several customers. In general, the main factor behind the generation of this phenomenon is industrial loads that include as follows [115]:

- Resistive welding machines;
- Metal rolling factories;
- Electric arc furnaces; and
- Strong welding facilities.

Step voltage fluctuations might originate from switching of capacitor banks and large loads. It is worth noting that voltage fluctuations caused by industrial loads affect a great number of customers feeding from one feeder [115].

4.10.2 Effects of voltage oscillation

The most important potential problem due to voltage fluctuation is voltage flicker. The problem caused by this phenomenon depends on its magnitude, frequency, occurrence rate, and duration. In any case, small flickers are not observable. Some devices, particularly those with large time constants, are rarely impacted by the voltage fluctuation. Nonetheless, other devices, such as TV receivers, electronic controllers, personal computers, and light lamps are intrinsically sensitive to voltage fluctuations. Continuous changes in the voltage fluctuation (caused by electric arc furnaces and cycloconverters) also have adverse effects. In this case, voltage fluctuation will have a frequency modulation spectrum in the 0-30 Hz band. Normally, the effect of the superposition of several frequencies can be measured by using a flicker-meter [127]. Additionally, the modulation level relies on the proportion of feeding network impedances and distortion-generating equipment [115].

As mentioned earlier, fast changes in the amplitude of the load current can cause voltage fluctuations, referred to as flicker. Anyhow, there is a subtle difference between these two terms. Technically, voltage oscillation can be assumed as an electromagnetic event, but the flicker is the adverse result of voltage fluctuation. Nonetheless, these are interchangeably used in this study [115].

Fig. 4.20 shows a voltage waveform which results in voltage flicker. This flicker has been created by electric arc furnaces that are among the prevalent reasons for voltage

oscillations in transmission and distribution networks. Flicker may refer to the ratio between the RMS to the fundamental magnitudes [115].

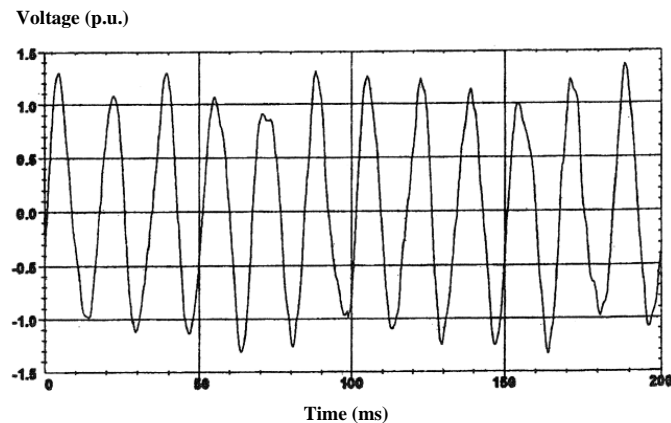


Fig. 4.20. An example of voltage flicker due to electric arc operation [115].

4.11 Power frequency oscillation

Power frequency oscillation refers to the change in the fundamental frequency from the rated frequency. The fundamental frequency has respectively direct and reverse relations with the rotational speed and poles of the generators that feed the power system. The system frequency changes when the dynamic equilibrium between supply and demand varies. The frequency change and its duration are proportional to the characteristics of the load and the response of the control system in power plants. Frequency variations beyond the allowed limits can be due to the disconnection of a large load or outage of a large power source from the system. In such cases, a specific amount of the load or generated power is curtailed manually or automatically to bring back balanced conditions so that the frequency returns to the nominal value. In modern interconnected power systems, considerable variations in the frequency rarely happen. Frequency variations occur mostly for loads that are fed using a generator disconnected from the rest of the network. In this case, the operation of the governor to regulate frequency and return it back to the acceptable limits may not suffice [115].

Notching might be sometime inaccurately be used instead of the term frequency deviation. Notches can bring the voltage wave close to zero and cause misoperation of devices and control systems that depend on zero crossings to operate properly.

In the range of acceptable frequency deviation, power frequency deviation mostly changes the speed of rotary machines. Therefore, motors produce less or more electrical power. The amount of this variation relies on the speed-torque relation of the load supplied by the motor. Furthermore, frequency variations adversely affect harmonic filter

tuning and the performance of devices operating based on frequency as the synchronizing pulse [115].

4.12 PQ terminology

PQ term covers a broad category of electromagnetic phenomena occurring in power systems. During recent years, the ever-increasing application of electronic devices has raised attention to PQ problems. This makes it necessary to provide a glossary of technical terms for describing the above phenomena. Unfortunately, the available technical terms in different sections of the industry do not match and have different meanings. Thus, this may confuse the utility and customers as they are trying to find the cause of an event. For instance, the term surge describes a broad category of distortions in the power system (those that lead to the failure of the devices or make them mis operate). A surge arrester can prevent some of the phenomena, while being useless for the rest of the events. Under such conditions, a comprehensive glossary is considered among the main objectives of standards. The glossary must be procured in such a way that it includes most of the concepts and terms being used in the area of PQ. Further, it has to prevent any ambiguity of concepts that cause misunderstanding and conflict in recognizing PQ [117]. Therefore, the terminology used in PQ subject are as follows [115]:

- ***Instantaneous:*** When this term describes the duration of a short-duration change, it takes between half to thirty cycles of the system frequency.
- ***Overvoltage:*** When this term describes a kind of long-duration voltage variations it points to a voltage value of 5% above the rated voltage and takes longer than 1 minute.
- ***Distortion:*** Any deviation of an AC quantity from the normal sine waveform.
- ***Harmonic distortion:*** Periodic distortion of a sinusoidal waveform. Refer to the terms "distortion" and "THD".
- ***Voltage distortion:*** Distortion in the AC voltage.
- ***Current distortion:*** Distortion in the AC current.
- ***Waveform distortion:*** A steady change in the ideal waveform of a sinusoidal waveform with the fundamental frequency, which is basically described by its spectral content.
- ***Total demand distortion (TDD):*** This refers to the proportion between the root mean square (RMS) values of the current harmonics to the rated or maximum

demand current with the fundamental frequency. This quantity is given in percentage.

- **THD:** The proportion between the RMS values of the harmonic content to the RMS value of the fundamental frequency component for a given quantity, denoted as a percentage of the fundamental component [123].

- **Ground electrode:** A conductor or group of conductors connected to or in the exposure of the ground to provide a connection with the ground [128].

- **Frequency deviation:** A rise or drop in the fundamental frequency, which may take cycles up to hours.

- **Isolation:** Detachment of one part of the system to prevent the adverse effect of the rest of the system.

- **Sustained:** When used to describe the duration of a group of long-duration voltage variations, it refers to the changes taking longer than 1 minute.

- **Linear load:** An electrical device that, when is powered, shows majorly a fixed load impedance to the power source in steady conditions.

- **Nonlinear load:** An electrical load that draws non-sine current when powered by a sine voltage, or in other words, its impedance changes.

- **Critical load:** Devices whose unsatisfactory operation endangers the safety of the personnel or leads to financial loss or damage to the critical and important asset.

- **Conducting body:** The conducting body or skeleton of electrical equipment that is accessible and can be touched. This part of the equipment is not energized in normal conditions, but it can be energized due to a failure in the device or because of an internal fault.

- **Voltage swell:** A temporary rise in the RMS voltage value above 10% of the rated voltage at the fundamental frequency and takes half cycles to one minute.

- **Voltage magnification:** The increase in the fluctuating transient voltage caused by capacitor switching on the primary side of a transformer due to the presence of capacitors on the secondary side of the transformer.

- **Synchronous closing:** This is usually used for the synchronous closing of all three poles of a breaker in feeders. This action will reduce transient phenomena.

- **Notching:** Distortion in the normal voltage, which takes less than 0.5 cycles. This phenomenon has intrinsically an opposite polarity than the fundamental

waveform. Thus, it is removed from the normal waveform and is stated in terms of the peak value of the distorted voltage. Notching may lead to the complete voltage interruption for up to a half-cycle.

- **Frequency response:** When dealing with PQ problems, this term points to the system impedance variations (or a metering transducer).

- **Pulse:** A sudden short-duration change in a parameter, after which it quickly goes back to its initial value.

- **Harmonic resonance:** Harmonic resonance refers to a case in which the power system resonates close to one of the main harmonic components and produces harmonic distortion. These harmonic components are caused by nonlinear elements of the power system.

- **Voltage variation:** A variation in the peak or RMS value of the voltage happening between two sequential steady-states with an indefinite duration.

- **Short-duration voltage variations:** A change in the RMS value of the voltage taking 0.5 cycles to 1 minute. These variations are often used with one voltage amplitude modifier (sag, swell, interruption) and one duration modifier (momentary, instantaneous, and temporary).

- **Long-duration voltage changes:** A change in the value of the nominal voltage that takes less than one minute. This is normally used along with another term that refers to oscillations in the magnitude of the voltage (e.g. under-voltage, overvoltage, or voltage interruption).

- **Voltage regulation:** This refers to the control and stability level of the load's RMS voltage. This parameter is frequently characterized together with other quantities including the input voltage variations, load variations, and temperature variations.

- **Phase shift:** Time shift of one voltage waveform with respect to other waveforms.

- **Outage:** A state of an element in which the element is unable to perform the demanded request due to some events concerned with that element. An outage can lead to service interruptions for customers, but this does not occur all the time (it depends on the system arrangement).

- **Dropout:** The loss of operation of equipment because of distortion, sag, or interruption.

- **Fault:** Usually points to short-circuits in the power system.
- **Transient fault:** Short-circuit on the system caused by lightning, dropping off a tree on conductors, or animals and is cleared by instantaneous interruption of current.
- **Return time:** The time required for the voltage or current after a step load change to return to the default range. Also, it may refer to the duration required for a system after an interruption to return to the normal operating conditions.
- **Safety ground:** This is formed by using a conductor that connects DE energized bodies of steel pipes, cable trucks, and equipment cabins to the neutral point and the grounding electrode.
- **Grounded:** connected to the ground (ground electrode), in contact with it, or connected to a wide conductor that operates as the earth [123].
- **Electromagnetic compatibility:** Capability of a device, equipment, or a system to show satisfactory performance in its electromagnetic environment without causing electromagnetic interference with other elements in that environment [117-129].
- **Ground grid:** A configuration of bare conductors placed under the ground, the main aim of using which is to save the lives of the personnel. This is done by limiting the potential difference around the person to safety levels. The potential difference can be established due to the flow of high currents from the ground grid [123].
- **Shield:** Shield is a conductive sheath (generally metallic material) around the insulation of a conductor or a series of conductors to provide coupling between the shield conductors. These conductors may be receiving or generating electrostatic or electromagnetic fields.
- **Shielding:** Shielding refers to the application of a conductor or a ferromagnetic barrier between a noise source and a noise-sensitive circuit. The use of shields is in the protection of cables and electronic circuits. Shielding can be metal barriers or be wrapped around the source circuit and receiving circuits.
- **Overhead line shielding:** This means placing one or several ground conductors on overhead lines to prevent lightning strikes to the phase conductors.
- **Impulse:** A pulse that gives an approximation of a unit pulse or a Dirac function (the derivative of the impulse function) for a given application. If this term would

be used in a PQ monitoring subject, it is better to employ the term transient impulse [117].

- **Peak factor:** the relation between the peak values of the measured waveform to its corresponding RMS value. As an instance, the peak factor of a sinusoidal waveform equals $\sqrt{2}$.

- **Power factor:** Power factor of fundamental frequency components of voltage and current waveforms.

- **True power factor:** Active power (W) divided by apparent power (VA).

- **Harmonic number:** The frequency of a harmonic divided by the fundamental frequency. This is an integer [117].

- **Voltage unbalance:** A condition when either the amplitudes of the three phase voltages differ or the phase shifts between the voltages differ from 120 degrees. The above two cases may occur simultaneously. Voltage unbalance is expressed in terms of the ratio of the zero- or negative-sequence voltage to the positive-sequence voltage (in percent).

- **Flicker:** The transient impact of a light source on visual sensation while its spectrum distribution or luminance is changing [117].

- **Sag:** A decrease in RMS value of voltage or current at the fundamental frequency to a range between 0.1 p.u. and 0.9 p.u. that takes half cycles to one minute.

- **Active filter:** A set of power electronics devices used to remove harmonic distortion.

- **Passive filter:** A mixture of capacitors, inductors, and resistors to remove one or several specific harmonic components. The widely-used type of such filters includes one inductor and one capacitor. The capacitor is short circuited against the most annoying harmonic component of the system and absorbs it.

- **Harmonic filter:** Harmonic filter filters one or several harmonic components, especially used in power systems. Mostly a combination of passive elements like inductor, capacitor, and resistor is used in their structure. Today, in most modern systems, active filters are used, which can deliver reactive power besides performing the filtering action.

- **Sustained interruption:** This refers to a long-duration variation. The whole duration of a voltage interruption (less than 0.1 p.u.) in one or several phase conductors during an interval longer than one minute.

- ***Momentary interruption:*** This refers to a short-duration voltage variation and is the whole voltage interruption (less than 0.1 p.u.) in one or several phase conductors during an interval taking thirty cycles to three seconds.
- ***Temporary interruption:*** This is a short-duration variation and refers to the complete interruption of voltage (less than 0.1 p.u.) in one or several phase conductors during an interval that takes three seconds up to one minute.
- ***Voltage interruption:*** This term refers to voltage disappearance on one or several phases and is normally accompanied by a time modifier that refers to the time duration of the interruption period (like momentary, instantaneous, and temporary).
- ***Fast tripping:*** This is the common operation of protective systems where a switch or a recloser of the line operates faster than its fuse. This is very effective in clearing transient faults, but its application causes problems because it leads to temporary or momentary interruption of industrial loads.
- ***Undervoltage:*** When used as a modifier of a kind of long-duration variations, it indicates a voltage variation greater than 10% below the rated voltage for longer than one minute.
- ***Coupling:*** An element or elements of a circuit or a system where energy among them is transferred from one element to another [123].
- ***Transients:*** This refers to an event or a parameter that changes between different steady-state situations of a system during a short duration. The transient phenomenon may appear as an unidirectional surge with specific polarity and/or as a damping oscillatory wave in which its first peak occurs with a positive or negative polarity [117].
- ***Momentary:*** In the case this term is used as a time modifier for a short-duration change, it takes thirty cycles up to three seconds.
- ***Fundamental component:*** The first harmonic component (50 Hz) in the Fourier series of a periodic parameter [117].
- ***Harmonic content:*** This is found from the difference of its fundamental component and its value.
- ***Computer Business Equipment Manufacturers Association (CBEMA) curve:*** Curves that indicate the magnitude and duration of the voltage distortion. These

curves will be used as criteria to measure how various elements of the power system operate [130].

- **Transient impulse:** An abrupt variation in the steady-state conditions of voltage or current with a non-fundamental frequency with unidirectional polarity (positive or negative) [117].

- **LV-side surges:** This describes a current surge injected to the terminals of the secondary side of the transformer when lightning strikes the grounded conductor close to the transformer.

- **Temporary:** When used as the time modifier of a short-duration variation, it takes 3 seconds to 1 minute.

- **Voltage oscillation:** A series of voltage variations or periodic changes in the envelope of the voltage curve that can cause flicker.

- **Noise:** Unwanted electrical signals that cause undesired influence on control system circuits [123].

- **Reclosing:** Reclosing of switches shortly after the fault is cleared. It should be noted that the majority of the faults occurring in overhead lines are of transient or temporary nature.

- **Instantaneous reclosing:** A term used normally for reclosing a switch as fast as possible after clearing a fault current. The typical time duration of this action is 18 to 30 cycles.

- **Differential mode voltage:** The difference between the voltages of two specific energized conductors [115].

4.13 Main indexes of PQ

4.13.1 Voltage sag and interruption

Voltage sag is a short-term drop in the amplitude of the RMS voltage (0.5 cycles to 1 minute) due to faults in the system and/or in large motor drives. Utilities encounter various problems concerning the voltage sag event [119].

There are numerous reasons to study voltage sag. The most important of which is the presence of sensitive loads located at residential, commercial, or industrial customers. The equipment used by the customers, including controllers, adjustable speed drives, computers, etc. are sensitive to voltage sag. Even relay and contactors used for driving motors show sensitivity to this phenomenon. On the other hand, due to any defect in the

network, the memory of computer controllers might be erased. In addition, the processes controlled by computers become even more complicated every day, so it may require a long time to restart them. Therefore, the occurrence of voltage sag or interruption will be more influential compared to the past [119].

Before the comprehensive analysis of the voltage sag it is necessary to discriminate interruption (the complete lack of voltage) and voltage sag. Interruption happens in the case a protective element disconnects the power circuit of a specific customer. Such action appears in power systems when a short circuit has happened before that. On the other hand, during a short circuit, an extensive range of the power system is prone to voltage sag. A short circuit in parallel feeders or in the transmission network causes voltage sag; however, its results are not a voltage interruption and, consequently, the probability of a voltage sag occurrence is higher than that of voltage interruption [131-132].

Amplitude and duration are the two main characteristics of voltage sag. Amplitude is the RMS voltage that is established following an event, which is expressed in percent or per unit. For instance, a 90% sag amplitude means that the voltage has dropped 10% compared to its rated value. The duration of voltage sag depends on the characteristics of the protective device. Short circuits can occur in transmission and distribution systems. When occurred in the transmission system, short circuits can influence many end-users. Even consumers located several hundred kilometers away from the short circuit point may experience the voltage sag [131-132].

Single-phase to ground faults are the most prevalent faults appearing in a network. Three-phase faults have a more intense nature; however, they rarely happen. The main cause of single-phase to ground faults is environmental conditions like lightning, wind, and ice on transmission, sub-transmission, and distribution lines. Animals and activities such as transportation under transmission lines may establish a fault. Although utilities prevent most of the short circuits, they are unable to fully remove them.

Lightning is the origin of the majority of faults occurring in overhead lines of transmission, sub-transmission, and distribution systems. Direct strike of the lightning to the phase conductor or to a grounded object, like the guard wire, and the creation of a returning arc to the phase wire will cause a fault. Such faults are temporary [131-132].

As mentioned earlier, single-phase to ground fault is the most widespread cause of voltage sag for a customer. The faulty phase voltage reaches zero at the fault point. Voltages at the substation and other parallel feeders change in proportion to the distance to the fault.

In transmission systems, the short-circuited phase voltage at a point farther away from it will depend on the general impedance of the system. The voltage sag amplitude at a specific place relies on the system impedance, the fault impedance, the transformer type, and the voltage value before the voltage sag occurrence. Moreover, the level of influence of voltage sag relies on how sensitive is the equipment [131-132].

Most of the sags occurring due to short circuits have similar characteristics. A short circuit commences usually when the voltage magnitude exceeds the insulation withstand level because electric arc starts before physical contact. This phenomenon leads to an abrupt voltage variation and causes voltage unbalance as well. Voltage sag terminates when fault clearance devices interrupt the short circuit current and this happens close to the zero point of the fault point. Thus, voltage sag is terminated with a fast transfer from reduced voltage amplitude to normal amplitude [131-132].

4.13.1.1 Causes of voltage sag

Short circuits are the primary cause of voltage sag. However, starting up motors can cause sags, although the duration of sags in the latter is more than 30 cycles and the voltage sag amplitude is low. Some researchers consider voltage changes due to starting up motors as voltage flicker [115]. Anyhow, this event can also be taken into account as a voltage sag. According to what has been stated, the main cause of voltage sag is the occurrence of short circuit. A short circuit can happen at any point in the system and/or within the internal network of a customer, and the voltage sag may last until a protective device trips and removes the fault. The device is usually is fuse or a switch. The voltage sag phenomenon can happen several times when the reclosing action is carried out [22].

4.13.1.1.1 Voltage sag arising from short circuit

Consider the simple distribution system shown in Fig. 4.21, which includes a 30 MVA sub-transmission substation along with three medium voltage (MV) feeders. Each feeder is equipped with one circuit breaker and the related protective relays to identify and remove the fault if necessary. Point C, located at feeder F₁, is an industrial factory that is supplied via a 400 V distribution transformer [115].

The second diagram in Fig. 4.21 shows the RMS voltage value of points B and C during the fault at point A on feeder F₂. The horizontal axis illustrates the sequence of events. Feeder F₂ is assumed to be equipped with a recloser, which can lead to several voltage sags following a permanent fault. During fault clearance by the breaker, each of the loads

on F₂ (including B) experiences interruption, while loads on feeders F₁ and F₃ face with voltage sag. Voltage sag occurs when the fault current flows on the system impedance and moves toward the fault point. When the breaker located at F₂ removes the fault current, the voltage on feeders F₁ and F₃ returns to the normal operation mode. If the amplitude and duration of voltage sag are out of the capabilities of sensitive loads, loads will be disconnected. Sag also may appear following an Line to Ground (LG) or Line to Line (LL) fault, in which case the amplitude of voltage sag in different phases will differ from each other [115].

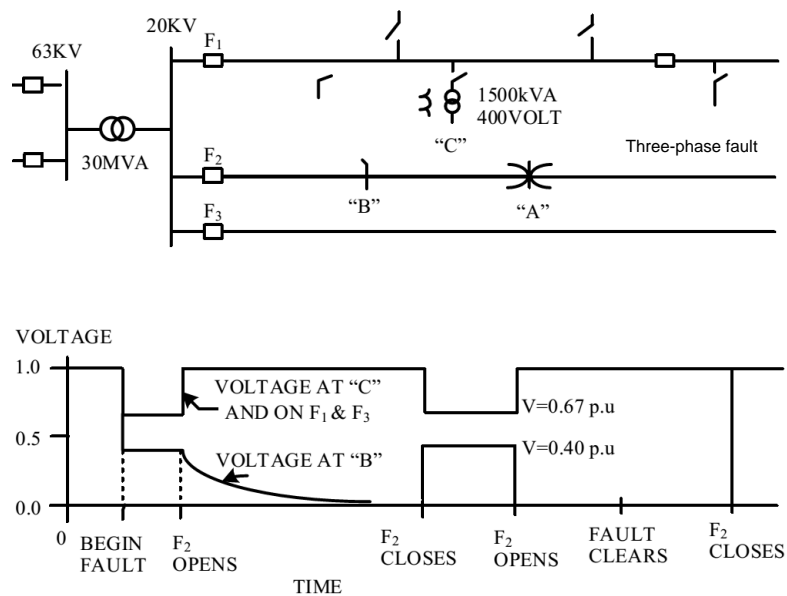


Fig. 4.21. Voltage sag following a fault and when the fault is cleared [115].

The main tools to estimate voltage sag include a software package to calculate unbalanced currents and voltages, the information about reliability, and the characteristics of fault clearing devices. These calculations can be carried out based on a short-circuit analysis computer program. In complicated and interconnected systems, the use of short-circuit analysis programs allows the user to meticulously conduct studies and apply different short circuits along the network to obtain voltage sag magnitude on all buses [115].

4.13.1.1.2 Voltage sag arising from motor starting

One detrimental impact of motors is drawing currents several times the rated current at the starting moment. When the starting current flows from the system impedance, voltage sag occurs and it may reduce the light intensity of lamps, disconnect contactors, and

disrupt sensitive equipment. This situation becomes even more severe due to the low power factor of the starting moment, which is about 0.15 to 0.3. The time required for motor acceleration from the idle moment to reaching the nominal speed is directly a function of the sag amplitude, and large voltage sag can even preclude a successful motor starting. Voltage sag caused by motor starting may last several seconds [115].

4.13.1.2 Estimation of different voltage sag characteristics

4.13.1.2.1 Estimation of the voltage sag amplitude arising from motor starting with a complete voltage

During an induction motor startup, if the startup action is performed with the complete voltage, the voltage sag in per unit will be calculated as follows [115]:

$$V_{min}(pu) = \frac{V(pu).KVA_{SC}}{KVA_{LR}+KVA_{SCmin}} \quad (4.4)$$

where: $V_{min}(pu)$ shows voltage sag amplitude, $V(pu)$ is real voltage (p.u.), KVA_{LR} presents apparent power in the rotor-locked mode and KVA_{SC} demonstrates short-circuit power of the system at the motor place.

If the calculation result concerning the voltage sag during motor startup is higher than the minimum allowable steady-state voltage of sensitive equipment, then motor starting with complete voltage is acceptable. Otherwise, other startup methods should be used [115].

4.13.1.2.2 Estimation of the voltage sag arising from short circuit

The amplitude and duration of voltage sags occurring due to short circuits are predictable. Sag amplitude can be calculated using mathematical relationships and sag duration needs an estimation of the total fault clearance time by protective devices. Voltage sag waveform can be predicted using transient analysis of the system. The prediction method of sag characteristics is simple. First, an accurate electrical model is provided to model the system. Then, by applying short circuits at various points, the amplitude of voltage sag at the considered load place is obtained. After that, using the characteristics of protective devices, the sag duration is estimated [115].

4.13.1.2.2.1 Voltage sag amplitude

To calculate voltage sag amplitude, we need system impedances, fault impedance, and the distance between the fault and the considered load. Moreover, the connection type of

transformers and the voltage before the sag occurrence impact calculations. Fig. 4.22 shows an impedance divider used for calculating the sag amplitude. In this case, V_{sag} can be written [115]:

$$V_{sag} = \frac{Z_s + Z_f}{Z_1 + Z_2 + Z_f} \quad (4.5)$$

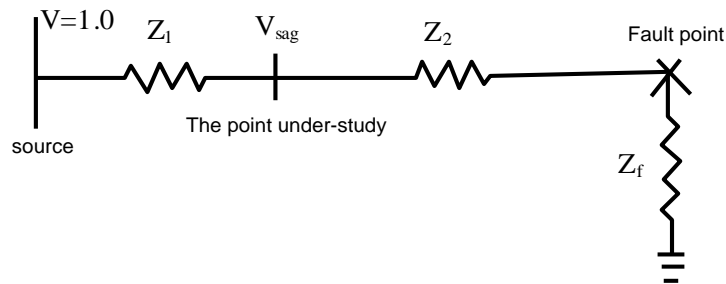


Fig. 4.22. An impedance divider to calculate sag amplitude [115].

Fig. 4.23 and equations (4.6) to (4.8) present calculations related to the amplitude of a voltage sag due to a three-phase fault with an impedance of $Z_f = 0$. If resistances are neglected, the calculations will be simpler. However, in practice, the zero- and negative-sequences and resistances should be used whenever required.

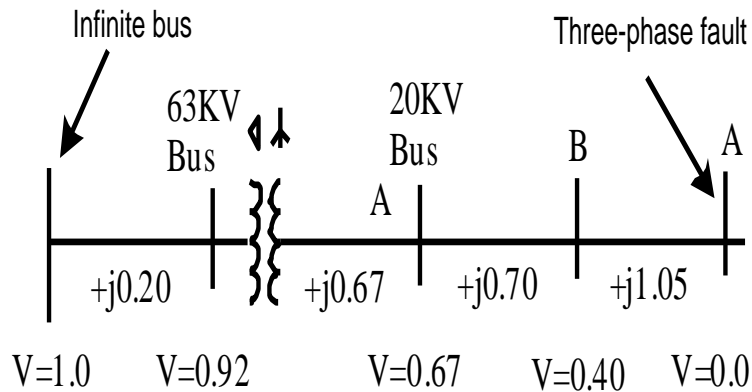


Fig. 4.23. The impedance diagram and voltages of different points [115].

When the fault current flows from the infinite bus towards point A, the voltage at point B is obtained from (4.6) [115]:

$$V_B = \frac{j1.05}{j0.2 + j0.67 + j0.7 + j1.05} = 0.4pu \quad (4.6)$$

The voltage at 20 kV bus is obtained from (4.7) [115]:

$$V_{20kv} = \frac{j0.7+j1.05}{j0.2+j0.67+j0.7+j1.05} = 0.67pu \quad (4.7)$$

and the voltage at 63 kV is obtained from (4.8) [115]:

$$V_{63kv} = \frac{j0.67+j0.7+j1.05}{j0.2+j0.67+j0.7+j1.05} = 0.92pu \quad (4.8)$$

These equations illustrate how a fault at a feeder changes voltages of other feeders.

4.13.1.2.2.2 Duration of voltage sag

The duration of voltage sag depends on the characteristics of the protective device. There are various types of fault clearance devices, but they all have one thing in common and it is the existence of a minimum time needed for complete clearance of the fault.

Additionally, sometimes, a total time delay is also assumed regarding the coordination of series-connected protective devices. Moreover, since the majority of short circuits on transmission lines are temporary, the automatic reclosing operation is utilized in most power systems. Table 4.3 lists the fault clearance time for some equipment used in power systems [133].

4.13.1.2.2.3 Voltage sag occurrence frequency

Prediction of the voltage sag occurrence frequency needs precise modeling of the system impedance besides obtaining the data of reliability for all equipment available. To this end, initially, the equipment on which a short circuit would create considerable voltage sag at the point under study is determined, and then the occurrence probability of each short circuit is calculated. It is, however, easy to identify which part of a line can cause significant voltage sag when a fault occurs [135]. The main reason for a voltage sag in a large industrial customer is lightning striking to lines and equipment or probably to the customer's internal network. Lightning can vary from season to season or year to year depending on weather and environmental conditions. Nonetheless, during a long period, environmental conditions mostly follow a series of patterns. If N_g is assumed as the annual number of lightning strikes to the ground per Km, which is obtained by multiplying the isokeraunic level of the region by a conversion factor, basic impulse insulation level (BIIL) of insulators and the N_g value of joints per kilometer of the line per year (the fault ratio) will be achieved [134-135].

Table 4.3. Sample fault clearance times [133].

The type of fault clearing equipment	Fault clearance time (cycle)		
	Minimum	Time delay	Frequency
Fuse	0.5	0.5 to 60	-
Current limiting fuse	0.25 or less	0.25 to 6	-
Electronic recloser	3	1 to 30	0 to 4
Oil breakers	5	1 to 60	0 to 4
SF ₆ or vacuum breakers	3	1 to 600	0 to 4

4.13.1.2.2.4 Vulnerability zone

In calculating the occurrence probability of voltage sag with a magnitude smaller than a determined value, the "vulnerability zone" term is used. Fig. 4.24 depicts the vulnerability zone of a large industrial customer supplied by the transmission system [115]. Using simulations, the magnitude of the considered voltage sag due to a fault at different areas is found and the voltage of the load bus can be presented as a function of the fault area. The vulnerability zone is calculated for a given level of voltage sag [119].

According to Fig. 4.24, the vulnerability zone depends on the sensitivity of the equipment. Contactors that become defected at 50% of the rated voltage have rather smaller vulnerability zone, while adjustable speed drives that run out of service at 90% of the rated voltage are sensitive to a fault occurring at a wider range of the transmission system and, thus, will have a larger vulnerability zone [119].

4.13.1.2.2.5 Classification of voltage sags

Studies show that four general categories of voltage sags can be defined for three-phase equipment. These four types of sags are provided in Fig. 4.25 in a vector form.

Type A occurs as a result of a three-phase short circuit, while type B corresponds to a single-phase fault. Types C and D are related to two-phase and single-phase faults, respectively [119].

The presence of a transformer in an electrical system transfers voltage sag occurring on its primary side to the secondary side and, in some cases, the voltage sag amplitude changes [119].

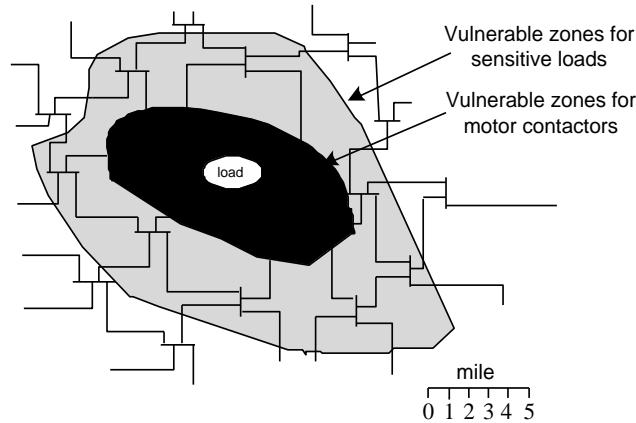


Fig. 4.24. Description of the vulnerability zone of a transmission system [119].

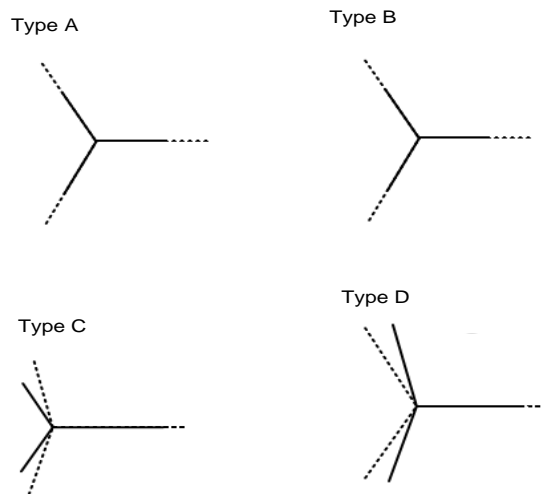


Fig. 4.25. Types of voltage sags [119].

4.13.1.3 The sensitivity of equipment to voltage sag

Electrical energy distribution in industrial factories is often implemented using three-phase 400 V feeders. Loads, depending on their type and how they are connected to the system, are classified as follows [136]:

- Motors with thermal elements and three-phase loads that are connectable to 400 V feeders;
- Adjustable speed drives and other power electronics devices that utilize three-phase power are connected to 400 V feeders directly or via an isolated transformer;
- Lighting loads that are connected to the phase-to-neutral voltage of 200 V; and

- Control equipment such as PCs, contactors, and PLCs that use single-phase 400V/120V transformers.

When voltage sag occurs, the voltage on equipment depends on their connection type. During a single-phase short circuit on the primary side of the transformer, voltage values on each of the phases and line-to-line voltages vary considerably. In this case, even if the sensitivity of loads to voltage sag is identical, some single-phase loads are not impacted, while some others may be interrupted. Voltage unbalance can also be considered as an important issue for motors; however, voltage unbalance duration during fault conditions is not long enough to heat up the motor temperature significantly [136].

Different groups of equipment, even various equipment within the same group (for example, two different models of adjustable speed drives), may show differing sensitivities against voltage sag and this makes it very challenging for the presentation of a general standard containing sensitivity of industrial-related equipment. The CBEMA curve which shows that load sensitivity highly depends on voltage sag duration is very similar to a standard [136-137]. As is observed, the allowable range covers 0% of the rated voltage for 0.5 cycles to 87% of the rated voltage for 30 cycles. This curve can also be used for a frequency of 50 Hz. While the range of the CBEMA curve proposes a standard sensitivity concerning voltage sag, the responses of equipment in factories during voltage sag are different. The following examples are provided in this case:

- *Contactors and electromechanical relays*: some outdated contactors fail in 50% of the rated voltage (if these conditions take more than one cycle) [138]. However, new manufacturers of contactors have presented curves whereby a contactor may fail at 70% or higher percentage of the rated voltage.
- *High-Intensity Discharge (HID) lamps*: Mercury lamps turn off at 80% of the normal voltage and will need a period to return.
- *Adjustable-speed drives (ASD)*: The design of drives is such that they are capable of getting dispose of voltage sag. The dispose time ranges between 0.05 s and 0.5 s (which relies on the manufacturer and the model being used).
- *Programmable logic controllers (PLCs)*: These devices are an important group in industrial processes [119].

4.13.1.4 The relationship between voltage sag and equipment operation

As mentioned earlier, voltage sag is a phenomenon that can highly influence the reliability of industrial customers. Modern controllers, industrial processes, and adjustable-speed

drives are highly impacted by voltage sags. Sag may even lead to the outage of a circuit from an industrial process. Ability to calculate and predict voltage sag provides a golden opportunity to prevent most problems and overcome many challenges. For instance, by reducing the amplitude or duration of a sag or the number of sag occurrence, many problems can be reduced. Furthermore, by small changes in the characteristics of the internal equipment of industrial customers, the number of outages of equipment due to sag may significantly be reduced. As stated earlier, the magnitude and duration of voltage sag are two basic characteristics to calculate the behavior and operation of customers' different equipment. This subsection, initially, depicts the data of voltage sag (amplitude and duration) on a curve, and then the sensitivity curve of equipment is depicted on the former curve. Using this method, the number of outages caused by voltage sag can be directly obtained during a year for the given equipment [115].

4.13.1.4.1 Reporting voltage sags

4.13.1.4.1.1 The number of phases

Voltage sags at individual phases of a three-phase system differ from each other. Due to a short circuit, one, two, or all three phases may encounter sufficiently low voltages called voltage sag. Even if all three phases face voltage sag, their amplitudes will be different. Thus, during a voltage sag, the unknown phase amplitude cannot be immediately considered as the actual voltage sag amplitude. Anyhow, three methods can be presented as follows [115]:

- In the first method, the lowest phase voltage amongst the three phases is reported for any given event. This method can be employed in three-phase loads that are sensitive to the lowest phase voltage or single-phase loads that are distributed in the three-phase system and the disconnection of single one of them will fail the whole production operation. For each fault in this method just one voltage sag event is reported. If voltage sag occurs on one phase but the other remaining two phases have proper voltage values, three-phase equipment may tolerate this phenomenon.
- In the second method, the reports of every single phase are considered separate events. This method is applicable to single-phase loads or at least single-phase controllers. In monitoring the results, the average number of occurrence of sags for individual phases is calculated to estimate the number of sags a single-phase

load encounters (it should be noted that if a load is between two phases, it may experience a higher number of sags compared to a load connected between the line and the neutral). In practice, the probability of fault occurrence on individual phases is equal. This means that a sag occurring following an LG or LL fault is considered 1/3 of the sag on phase A, 1/3 of the sag on phase B, and 1/3 of the sag on phase C [115].

- The third method assumes that three-phase loads are sensitive to the average values of three-phase voltages. Only one voltage sag occurrence for any given event is reported in this method. The reported voltage sag amplitude will be, in fact, the average value of sag amplitudes that occurred in three phases, and this amplitude will not be adaptable with any sag of three phases [115].

4.13.1.4.1.2 Reclosing issue

Automatic reclosing is a common practice in power systems. In the presence of this event, the calculation of the number of voltage sags can be performed using two different methods as follows [115]:

- In the first method, if several sags occur during a short period of time (e.g. 3 minute), only one sag is taken into account. For instance, two sags caused by a single reclosing are considered only one voltage sag. The basis of this method relies on the fact the device will fail following the first sag and the next sags that will happen before reconnection of the equipment to the circuit are neglected because of their negligible impact on the equipment. The problem with this method is that it is difficult to determine the period in which voltage sag has occurred only once. This period may be different for different loads.

- In the second method, all sags, despite the fact that they appear within several seconds, are taken into account. This method precisely determines the number of sags occurring. However, the number of outages from the estimated circuits may be greater than the real value.

In the PQ monitoring subject, both of the aforementioned methods can be applied. Nevertheless, the prediction methods depend on the reported number of outages. Yet, it might be that for any event, these numbers are assumed one number and/or events occurring during a sequence of automatic reclosing actions are considered only one outage. The voltage sag prediction method must exactly consider these changes so that proper results are obtained [115].

4.13.1.4.1.3 Voltage sag duration

Most of the methods that present the duration of voltage sag assume rectangular shapes for sags, where the voltage sag duration is specified. However, sags are not always rectangular. For instance, sometimes during a short circuit, the fault impedance value changes and the voltage sag may have two or several amplitudes in a given event. The presence of high-power motors can also vary the shape of sags [138].

4.13.1.4.2 Coordination curves of the voltage sag

To examine the behavior of different equipment of customers, especially industrial customers, against voltage sag, the coordination curve of voltage sag is utilized. The curve shows the sag characteristics and the response of various equipment of customers to the sag. The horizontal and vertical axes in this curve represent the duration and sag amplitude, where a set of contours illustrate the characteristics of the sag on this curve. Each contour presents the number of sags occurring in a year. The characteristics curve of the device on this plot represents the voltage tolerance of the device. Using this plot, the number of outages arising from voltage sag that occur per unit of time in the device can be predicted. Two information sets will be required for predicting the number of outages. The first set is the information related to the characteristics of voltage sag obtained from network monitoring data or calculation methods. The second set of information concerns the responses of equipment to the established sags that are either obtained from the technical characteristics of the manufacturer or extracted from the behavior of test data [115].

4.13.2 Long-term voltage variations, voltage unbalance and frequency deviations

4.13.2.1 Long-term voltage variations

Voltage amplitude is the main index of balance between the generated reactive power and the required reactive power at the network level. Long-term voltage variations not only can cause damages to the devices and equipment in the system owned by customers but also may lead to significant interruptions and instability in the network level in critical situations. Long-term voltage oscillations are generally put in three major groups: overvoltage, under-voltage, and long-term interruptions [139].

4.13.2.1.1 The roots of long-term voltage variations

The following factors can be stated as the causes of long-term overvoltage [115]:

- Low load or unload situation;
- Presence of capacitor banks;
- Incorrect settings of the transformer tap;
- Lack of a proper voltage control system; and
- Inability to control reactive power from near power plants.

Also, the following are the reasons for the occurrence of long-term under-voltage [115]:

- Overloading;
- The weak setting of voltage;
- Disconnection of large capacitor banks; and
- Meaningless presence of shunt reactors.

Failure in some critical equipment of the network such as breakers is one of the reasons for long-term interruptions.

4.13.2.1.2 Principles of voltage regulation

To explain the issue related to voltage regulation in the network, consider Fig. 4.26. When the load current increases, the voltage drop occurs on the impedance. To compensate for this voltage drop, a change should be applied to the network. The correction methods would include the compensation of impedance Z or, in other words, the compensation of voltage drop, i.e., $(R + jX) I$. The improvement methods are as follows [115]:

- The use of voltage regulators that increase V_1 ;
- Placing a shunt capacitor in the network to reduce current I and reduce the phase angle between current and voltage;
- Placing a series capacitor in the system to compensate voltage drop on the inductive impedance;
- Increasing the cross-section of line conductors to reduce impedance Z ;
- Increasing the apparent power of the transformer to reduce impedance Z ; and
- Adding static var compensators.

4.13.2.1.3 Voltage regulation equipment

Many different kinds of voltage regulation equipment are available. This equipment can be generally divided into four major categories as follows [115]:

- Generator Automatic Voltage Regulator (AVR);
- Transformer tap-changers;
- Isolation equipment with distinct voltage regulators; and

- Impedance compensating equipment, like capacitors and reactors.

Isolation equipment includes UPS systems, Ferro-resonance transformers, the motor-generator sets, etc. This equipment isolates the load from the power supply via energy conversion. Thus, the equipment voltage is regulated on the load side, and despite what occurs on the power supply side, the load voltage is maintained as constant. The disadvantages of this type of equipment are that they cause much more loss and issues such as harmonic problems in the supply network. Shunt capacitor helps stabilize (regulate) the voltage by reducing line currents. Also, by overcompensation of inductive circuits, higher voltage values can be reached. To stabilize and regulate voltage properly, capacitors are switched together with the load. Series capacitors are rarely used in power systems. Most utilities avoid this device due to its complicated installation and operation issues. In any case, they are very effective in some specific conditions of the system, particularly when there are large loads with abrupt changes. The following describes various kinds of voltage regulator devices.

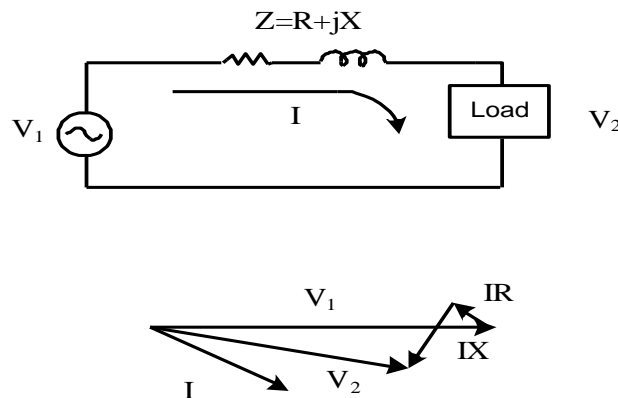


Fig. 4.26. Voltage drop on the system impedance, causing many voltage regulation problems [115].

4.13.2.1.3.1 Step-voltage regulators

Regulators with taps can be manufactured in different ranges (for example, regulators with voltage regulation range between -10% to +10% of the input voltage with 36 steps). Fig. 4.27 shows a sample regulator. These regulators have a rather slower response time [115].

4.13.2.1.3.2 Ferro-resonance transformers

Ferro-resonance transformers can be used for regulating voltage in the range of $\pm 1\%$. Fig. 4.28 depicts the input and output characteristics of a 120 VA Ferro-resonance transformer

with a 15 VA load in the steady state. As is observed, when the input voltage reduces to 30 V, the output voltage is virtually fixed. In the case the input voltage reduces further, the output voltage will not be constant anymore. Among the demerits of this device are its high losses [115].

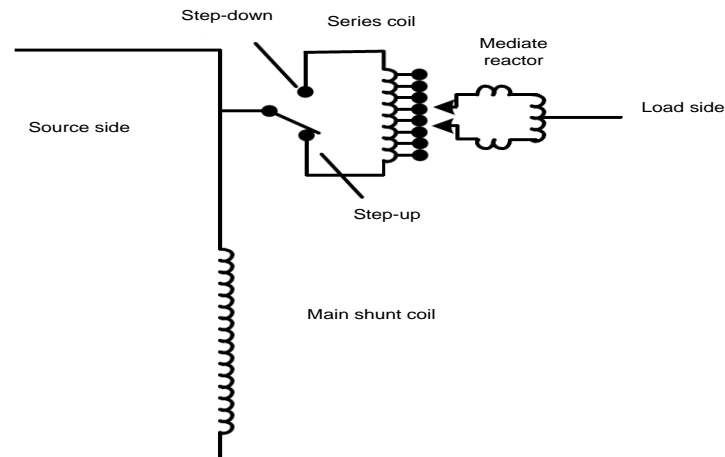


Fig. 4.27. Schematic diagram of a voltage regulator [115].

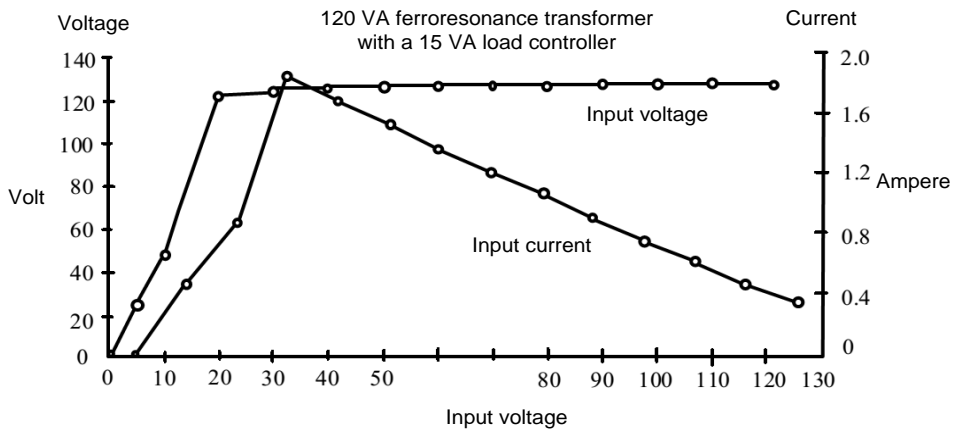


Fig. 4.28. Characteristics of a Ferro-resonance transformer [115].

4.13.2.1.3.3 Electronic regulator

An electronic regulator is illustrated in Fig. 4.29. The efficiency of these devices is higher than that of Ferro-resonance transformers and silicon rectifiers or triacs which are used in them to rapidly change the tap. This type of regulator provides a very fast response and is useful for applications with average power [115].

4.13.2.1.3.4 Motor-generator set

The motor-generator set shown in Fig. 4.30 can be used for a voltage regulator as well. The set fully separates the load from the electric network and protects it against transient problems. Voltage regulation is performed by the control system embedded on the generator. The main problem of the motor-generator set is its long response time to the changes in large loads [115].

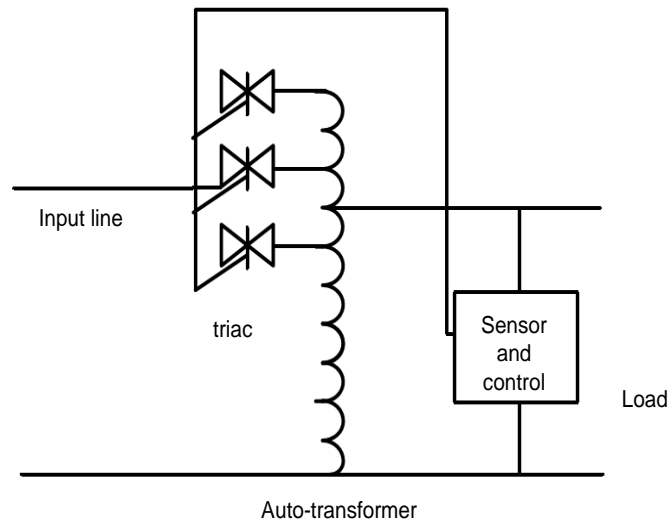


Fig. 4.29. Electronic regulator [115].

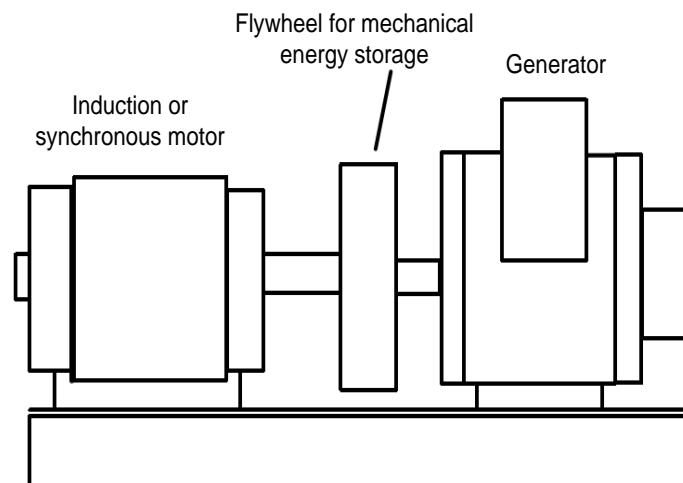


Fig. 4.30. Motor-generator set [115].

4.13.2.1.3.5 Static Var Compensators (SVCs)

SVCs with their rapid response to load changes are suitable devices for voltage regulation. SVCs do this by reactive power consumption or generation. In general, two types of SVCs are used in practice (Fig. 4.31) [115].

4.13.2.1.3.6 Capacitors for voltage regulation

The capacitors used for regulating voltages in an electric network are configured in shunt and series arrangements as follows [115]:

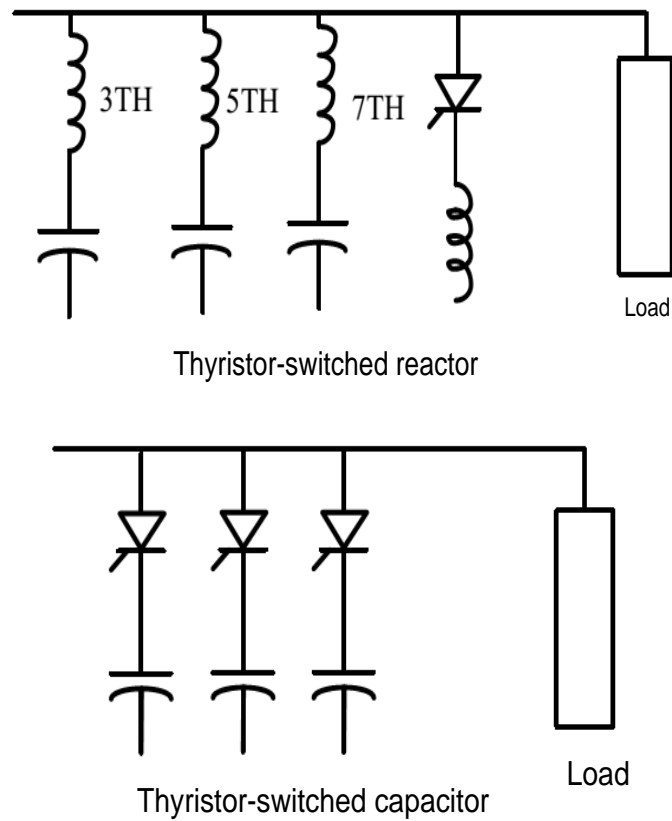


Fig. 4.31. Two types of SVCs [115].

- Shunt capacitors

A shunt capacitor located at one side of a given feeder leads to the gradual variation in the voltage along the feeder. Theoretically, the voltage increase percentage at the capacitor place is found as follows [115]:

$$\% \Delta V = \frac{100(V_{withcap} - V_{nocap})}{V_{withcap}} \quad (4.9)$$

where, V_{nocap} is the load voltage without a capacitor and $V_{withcap}$ shows the load voltage with a capacitor

Capacitors switching is usually carried out automatically so that suitable regulation is established in different loads and over-voltages during low loads are prevented.

- Series capacitors

Unlike shunt capacitors, series capacitors joined with the feeder increase the voltage of the feeder end and its changes will be directly proportional to the load current. During no-load conditions, the voltage increase is zero and it is at maximum during the rated load. Therefore, series capacitors do not have to be switched during load changes. Further, the power of series capacitors will be less than that of shunt capacitors for a similar condition. Series capacitors pose many disadvantages. They lack reactive power compensation and thus cannot effectively reduce system loss. Moreover, series capacitors are unable to balance the short circuit current, leading to over-voltages on series capacitors which makes it essential to use arresters on the capacitors. Resonance and Ferro-resonance issues also may be intensified due to the presence of series capacitors. Considering the above reasons, series capacitors are rarely utilized in power systems [115].

4.13.2.1.4 The allowed range of long-term voltage variations

Concerning the effect of voltage changes on the function and protection of the network, the following voltage ranges are defined [115]:

- Normal voltage: increase up to 2% and/or decrease up to 2% of the rated voltage;
- Abnormal voltage: increase up to 5% and/or decrease up to 10% of the rated voltage; and
- Intolerable: increase over 5% and/or decrease over 10% of the rated voltage.

4.13.2.2 Voltage unbalance

Voltage unbalance refers to conditions where the voltage magnitudes of all three phases differ from each other and/or the phase-shift between the phases is not 120° . These two separate conditions can also occur at the same time. Voltage unbalance is defined using the asymmetric components [115].

4.13.2.2.1 The causes of voltage unbalance

Voltage unbalance appears mainly due to the presence of single-phase loads in the network. This phenomenon may also happen as a result of the outage of one of the phases of a three-phase capacitor bank. Basically, in distribution networks with different kinds of industrial, residential, and commercial loads, most loads are composed of single-phase loads; thus, reaching a balanced condition is difficult or even impossible. It should be noted that it would not suffice to equalize the phase loads or balance it to make the neutral

current zero or reduce it. The power factor of a phase plays a key role in forming neutral current. Further, the unbalanced impedance of the system, particularly in transmission and distribution lines, causes voltage unbalance [115].

4.13.2.2.2 The effects of voltage unbalance

4.13.2.2.2.1 The effects on the normal operation of three-phase motors

In the case the phase currents are unbalanced, negative- and zero-sequence currents will appear. Hence, in most cases, the stator of three-phase motors are connected in delta or ungrounded-star form. So, zero-sequence current cannot pass, and, as a result, only the motor's reaction to negative- and positive-components is studied. In the case of unbalance, negative-sequence current forms a rotating field with a fixed magnitude but in the reverse direction, the speed of which with respect to rotor coil is $(2 - s) \times n_1$ (s is the slip and n_1 denotes the rated speed of the motor) and induces a voltage with a frequency almost twice in the rotor coils. In this case, the total torque is the difference between positive and negative torques. Consequently, in the case of current unbalance, the total torque will decrease. Another disadvantage of load unbalance is that due to the voltage unbalance a complete rotating field will not be formed in the motor and its amplitude will change. Thus, the motor power varies over time, leading to motor vibration. The other demerit is the reduction in the motor's efficiency [139].

4.13.2.2.2.2 The effects on the operation of contactors

As mentioned earlier, one of the effects of load unbalance is phase voltage unbalance and, consequently, a reduction in the phase voltage amplitude. This issue can cause faults on the consumption energy metering device (three-phase contactors). In the case of an unbalanced load, the disk of electricity meter will rotate slowly compared to the rate voltage case and records less energy consumption. The results show that for a 10 V reduction in the voltage at the customer's place, almost 25 kWh less electrical energy is recorded during a month and this is not desirable for power companies [139].

4.13.2.2.2.3 The effect on the safety of customers

When current flows on the neutral line, the line has voltage with respect to the ground. This phenomenon eliminates the safety and protection effect of the neutral line and may cause shock or damage if the person touches the neutral line [139].

4.13.2.2.4 The effect on power loss

Unbalanced currents flowing on coil phases of three-phase transformers change the line and phase voltages and, thus, iron and copper loss and overheating. Moreover, the current unbalance on transmission and distribution lines increases the power loss. Load unbalance not only increases the energy loss but also poses adverse effects on customers in terms of voltage drop [139].

4.13.2.2.3 The allowed range of voltage unbalance on buses

The allowed ranges of voltage unbalance percentages in different buses are recommended based on the Table 4.4 [140].

Table 4.4. The allowed range of voltage unbalance percentages [140].

Network type	LV, sub-transmission and distribution networks	HV and Extra High Voltage (EHV) transmission network
Voltage unbalance percentage	2	1

4.13.2.2.4 Voltage unbalance measurement method and determining its index

Voltage unbalance can be measured using three Voltage Transformers (VTs) with open delta connection on the secondary sides.

4.13.2.3 Frequency deviations

Fundamental frequency deviations are, in fact, the oscillations in the network frequency with respect to the rated frequency (50 Hz). The fundamental frequency is directly proportional to the rotational speed of the generators feeding the network and is reversely in proportion to the number of poles of the generator. In interconnected networks, frequency is one of the main indices of stability and balance between supply and demand. The network frequency oscillation at any moment depends on the balance between the mechanical power input to the exciters of the generators and the electrical power consumption. Following the loss of part of the generation and before automatic load control systems can act to increase the mechanical power, the frequency reduces from its rated limit because of the unbalance condition between the mechanical and electrical

powers. In the case of continuity of this situation, frequency drop may lead to the sequential outage of units and the loss of most part of the generation. This trend can ultimately result in the loss of the system. However, any type of oscillation or deviation from the normal operation frequency, in addition to affecting all electrical devices joined with the network, will impact the percentage of stability of the network directly and in proportion to the amplitude of oscillations. Governors can sense small changes in the speed resultant from gradual load changes and regulate mechanical power so that the frequency is maintained in the normal range. Yet, large and abrupt changes caused by the outage of a power plant unit or a key line will lead to rapid frequency variations, in which case the response of governors may not be sufficient and the system experiences failure. Frequency oscillation can be evaluated from three different aspects as follows [115]:

- Damage to turbo-generators due to the operation under non-rated frequency;
- Selecting proper control systems; and
- Adopting necessary decisions to control the frequency at the network control center under various normal and emergencies.

4.13.2.3.1 Damages to turbo-generators

Turbines are affected by periodic forces. Different parts of a turbine vibrate under such forces and this leads to the establishment of dynamic stress on turbines. This equipment is particularly affected by frequencies equal to or multiples of the natural frequency of the turbine (resonance phenomenon). Therefore, they cannot be utilized under any given frequency. The adverse vibration ultimately determines whether the turbine can be operated under non-rated frequencies [115].

4.13.2.3.2 Frequency control systems

Generally, there are two types of control systems applicable in frequency: frequency control under normal and emergency conditions [115].

4.13.2.3.2.1 Frequency control under normal conditions

In these conditions, frequency controllers (governors) can change the turbine output automatically and proportional to the slope characteristics of the frequency [115].

4.13.2.3.2.2 Frequency control under emergency conditions

Emergency conditions appear when an abrupt interruption of units or lines occurs. If no maneuvers are taken, the situation can sequentially cause the disconnection or more

equipment from the network and turn into a critical situation. Under critical conditions, generators are tripped by frequency relays [115].

4.13.2.3.3 Adopting control decisions

Regarding dynamic characteristics of generators and transmission lines, any supervision or control actions toward balancing the supply and demand and finally frequency control in a network should be implemented in a centralized manner. Concerning the dependency of frequency oscillations amplitude to the intensity of changes in supply and demand, frequency control requires policies and controller tools specific to the occurring situation. Frequency control decisions are taken according to the following steps [115]:

- **Step 1:** In normal conditions, the loads of units are determined based on hourly load prediction and economic power flow in units. Also, some units are used for frequency regulation.
- **Step 2:** When one or several units are disconnected or the network experienced interruption due to line outages, the units should be able to control the system so that it could not lead to an emergency condition. Hence, the maximum frequency deviation in the case the largest unit is interrupted should be analyzed under different loads and the frequency drop characteristics curve should be specified. It is crystal clear that these frequency changes with respect to different loads and characteristics of the units differ. Based on this analysis, the frequency characteristics must be determined in accordance with the units to make frequency compensation possible during about 30 seconds.
- **Step 3:** In the case of losing a major part of the supply and an unbalance between supply and demand, an automatic load curtailment system with accurate and fast function should be employed. In this case, at first, the damaged sections of the interconnected system are separated and then automatic load curtailment will be taken into account. In fact, under such conditions, load curtailment using under-frequency relays will be of high importance for adjusting frequency steps and the level of load removed at different steps. The amount of load curtailed at each step relies on the kind of event and its situation, the kind of consumption load, the performance of speed and excitation controllers, and the effect of under-frequency on the blades of turbo-generators and the unbalanced condition changes with frequency and voltage.

- **Step 4:** The disconnection and supplying the internal consumption is possible in power plants and when a unit is disconnected other units can supply only their internal consumption so that the units can be in parallel again as soon as possible.

4.13.2.3.4 The effect of frequency changes on the equipment available on LV systems

In the acceptable range of deviation, the main effect of frequency changes is the change in the speed of rotary machines. On the other hand, any electronic device using the supply frequency as the time reference will be affected [115].

4.13.2.3.5 Allowed frequency range

In all voltage levels, the change of frequency under normal operation should be in the range of ± 0.3 Hz. Frequency control curve follows Tables 4.5 [115]:

4.13.3 Voltage of flicker

4.13.3.1 Causes of voltage flicker

Events that cause no alteration in the voltage RMS value can be a cause of flicker. Motor starting is one of the common and main reasons for flicker occurring in power systems. The combination of high surge current and low power factor during starting can cause voltage flicker. This general classification includes all types of fans, pumps, compressors, fridges, elevators, etc. Another cause of flicker is electric arc furnaces. With regard to the ever-increasing development of metal melting complexes and the connection of electric arc furnaces to the main grid, the voltage flicker issue caused by these furnaces is of high importance. During the operation of the furnace, the secondary of the furnace transformer undergoes several short circuits and, due to the high turn ratio of the transformer, it causes severe voltage oscillations in low power factor. The melting process may last as long as three to eight hours. During the first half an hour or one and a half an hour, the voltage flicker is at its maximum. However, once the iron is melted in the next stages, the arc length remains rather constant and the flicker will be negligible [115].

4.13.3.2 Methods of determining flicker index

In general, three methods are used for determining the flicker index. The first method uses the Short Circuit Voltage Depression (SCVD) index. The second method makes use of an equivalent 10-Hz flicker-meter and the last method employs the IEC flicker meter. The following introduces these methods [141].

4.13.3.2.1 The SCVD index

The SCVD index is based on the relation between the complaints received from customers located in the neighborhood of an industrial customer due to the flickering issue and voltage reduction at the connection point of the industrial customer. Using this method, mostly the voltage oscillation amount caused by the installation of the induction furnace is obtained. In fact, using the short circuit power of the furnace and the short circuit level of the network at the Point of Common Connection (PCC) of the industrial customer to the network, the voltage oscillation level is estimated. The SCVD index is usually given as the percentage of voltage reduction at the PCC from open-circuit to three-phase short circuit modes. Assuming that the system impedance has a negligible impact on the power absorbed by the furnace in the short circuit mode, the SCVD index can be obtained with high accuracy as follows [141]:

$$SCVD = \frac{St}{Sc} \times 100\% \quad (4.10)$$

Table 4.5. Frequency control methods [115].

The range of frequency changes	Control method
Up to 0.6%	Frequency control in normal operation by the control center
0.6-1%	Frequency control by the power plant-Contact with the control center
1-1.6% Less than 10 minute	Frequency control by power plant
1-1.6% More than 10 minute	Manual load disconnection by substations
1.6-3.2%	Load curtailment program by load curtailment relays
Above 3.2%	Delayed disconnection by frequency relay
Above 4%	Fast disconnection of the power plant by frequency relay

4.13.3.2.2 Equivalent 10-Hz flicker-meter

A 10-Hz flicker-meter calculates the flicker based on the changes of voltage in constant time intervals and specific frequencies between 0.01-30 Hz. Then, it applies specified and

constant coefficients, known as human sensitivity coefficients, to the values of voltage changes. Finally, the squared values of these quantities give the flicker value [141].

4.13.3.2.3 The IEC flicker-meter

Among important and determining factors in the voltage oscillation intensity is the sensitivity of human eyes to the amplitude and frequency of light fluctuations. The flicker measurement method can be based on human senses caused by light oscillations of the lamp. In fact, flicker-meter is a measure of the flicker intensity created by voltage oscillations applied to a lamp. The basis of calculation in the IEC flicker-meter is the amount of flicker in the input waveform can be expressed in terms of a quantity proportional to the flicker intensity. Thereby, the value of considered quantity at any given moment presents the flicker status in the input signal and shows the intensity and weakness of the flicker level. Moreover, the value of this quantity becomes equal to unity when the intensity of flicker is sensible by humans [142].

4.13.3.3 The allowed range of flicker at different voltage levels

The allowed range of voltage flicker for buses with different voltage levels is recommended in Table 4.6 [143-144]:

Table 4.6. The allowed range of flicker in different networks [143-144].

Network type	LV network	MV network	HV and EHV networks
Total short-term index of flicker	1	0.9	0.8
Total long-term index of flicker	0.8	0.7	0.6

4.13.4 Harmonics

4.13.4.1 An introduction to harmonics

One of the PQ problems emerging on transmission and distribution networks is harmonics, which has gained much attention recently and so many books and articles have been published in this area. Harmonic distortion causes specific problems in power

systems, including mis operation of equipment, degradation, and reduced efficiency of devices. In such a case, the study of harmonics and presentation of a set of rules and laws will be inevitable. Limiting harmonic distortion is essential from both utility and customer perspectives. Utilities need to present limitations to prevent the damage to customers' equipment, should it be either residential or industrial customers. On the other hand, since utilities cannot ensure providing a pure sinusoidal waveform, customers should limit distortions produced by their equipment [115].

In the case of harmonics, customers will tolerate even more problems than utilities. Industrial customers that use adjustable-speed motor drives, electric arc furnaces, induction furnaces, and other similar devices, are more prone to harmonic distortion than the rest of customers. Utilities assume that the sinusoidal voltage waveform generated at electrical energy generation centers are free of harmonics. In most cases, the voltage distortion level in transmission systems is less than 1% and close to customer, the amount of harmonic distortion is increased. On the other hand, in some loads, the current waveform deviates from its sinusoidal form and experiences many distortions. Although sometimes the distortion in the system is stochastic, most of the distortions are periodic, meaning that sequential cycles are almost similar and they may change slowly. This concept, in principle, defines the term harmonics [115].

When the use of power electronics converters became common in the early 1970s, it drew the attention of many engineers concerning the acceptance of harmonic distortion in power systems. Disappointing predictions of the fate of the power system in the case of using such devices spread out, even though some of these concerns gained much more attention than needed. Thus, the quality of electricity owes these people for their pursuing the newly emerging problem at the time. Analysis of harmonics problems led to research as the result of which established many comments and views concerning PQ. From some scholars' points of view, harmonic distortion is still the most critical problem of PQ. Harmonic problems oppose most of the common rules of the design of power systems and its operation under the power frequency. In fact, many distortions that are caused by transient events are blamed as harmonics. A distorted waveform with high frequencies is present in the measurement of any phenomenon. While transient distortions also include high-frequency components and transient states, harmonic components have differing natures and are studied in a completely different way. Transient states have higher frequencies and are formed only moments after a sudden interruption. These frequencies

are not undoubtedly harmonic frequencies and might be the natural frequency of the system at the switching moment. They have no relationships with the fundamental frequency of the system. Harmonics appear in the steady state and are integer multiples of the power frequency. Distorted waveforms containing harmonic components appear constantly and/or disappear after several seconds. Transients, in general, disappear after several cycles. A transient state happens when a change occurs, like a capacitor switching, while harmonic content is produced when the load is operating. The case that eliminates this discrimination is transformer energizing. This is assumed as a transient phenomenon but produces a significant distortion waveform for several seconds and can lead to resonance in the system. The study of harmonic distortion in power systems has a long history. Distortion has always been discussed for alternating current systems and has been addressed fully. The search into literature and resources available from the past decades shows that various articles have been published in this regard. The first known sources of harmonics were transformer and the first emerged problem was in telephone systems. The use of many electric arc lamps at the same time also gained attention because of harmonics producing problem. However, the importance of none of the above-mentioned items was equal to the problem of power electronics converters used during recent years. Harmonic distortions produced in power systems originate from an internal cause. For instance, generators, transformers, and thyristor-controlled equipment, such as conversion substations that are used in high-voltage direct current (HVDC) systems, can cause harmonic distortions. During the years, the researchers have noted that if the transmission system is well designed, such that it could easily supply the demand, the probability of harmonic problems for power systems will be very low, although these harmonics can cause problems for telecommunication systems. Often in power systems, problems occur when the capacitors present in the system cause resonance in a harmonic frequency. Under such conditions, distortions and disturbances will be much higher than the usual. These problems can also happen in small consumption centers, but the worst situations emerge in industrial systems due to the high degree of resonance [115].

4.13.4.2. Harmonic distortion

Harmonic distortion in power systems is caused by nonlinear elements. For a nonlinear element, there is no direct relationship between current and voltage. Fig. 4.32 displays a non-sinusoidal current with a nonlinear resistor in case the voltage is not sinusoidal. Increasing the voltage up to some percentage may double the current and the current

waveform takes another form. This case is a simple case showing how distortion is established in the power system [115].

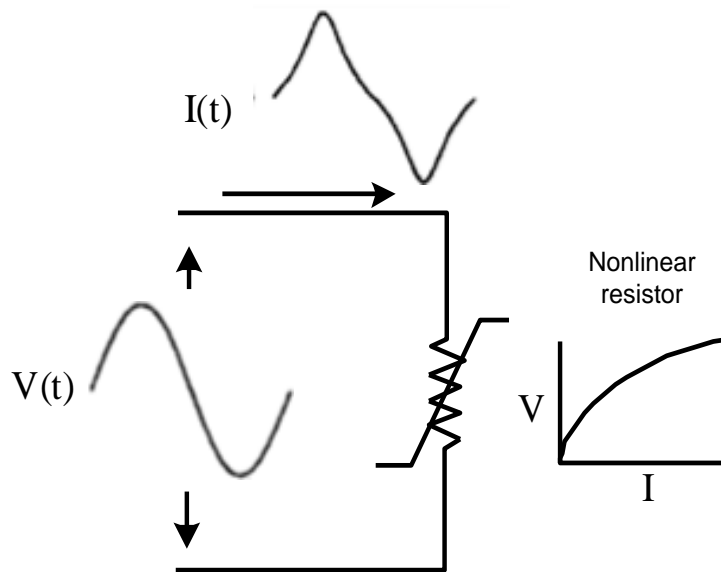


Fig. 4.32. Current distortion caused by a nonlinear resistor [115].

Fig. 4.33 shows that a periodic distorted waveform can be represented by the sum of several sinusoidal waves. It means that when the waveform does not change between cycles, it can be expressed by the sum of pure sinusoidal waveforms where the frequency of waveforms is an integer multiple of the fundamental frequency of the distorted waveform. These sinusoidal waveforms, the frequencies of which are integer multiples of the fundamental frequency, are called fundamental component harmonics. The sum of these sinusoidal waveforms is the so-called Fourier series because this mathematical concept was first noticed by a French mathematician, Fourier. Fourier series used for representing harmonic waveforms can easily obtain the system response to a sinusoidal input. Also, in this case, conventional techniques can also be utilized in the steady state. In this method, the system is studied independently for individual harmonic components and the outputs obtained for different frequencies are combined to find the required response, i.e. the output waveform. When positive and negative half-cycles of a given wave are similar, the Fourier series includes only odd harmonic components. This simplifies the study on power systems because most of the harmonic-producing devices show similar behavior against both positive and negative half-cycles. The presence of even harmonics is an indication of a failure. The failure might be due to a load or a

transducer (used for measurement). Some exceptions in this case include half-wave rectifiers and electric arc furnaces where arcs appear stochastically [115].

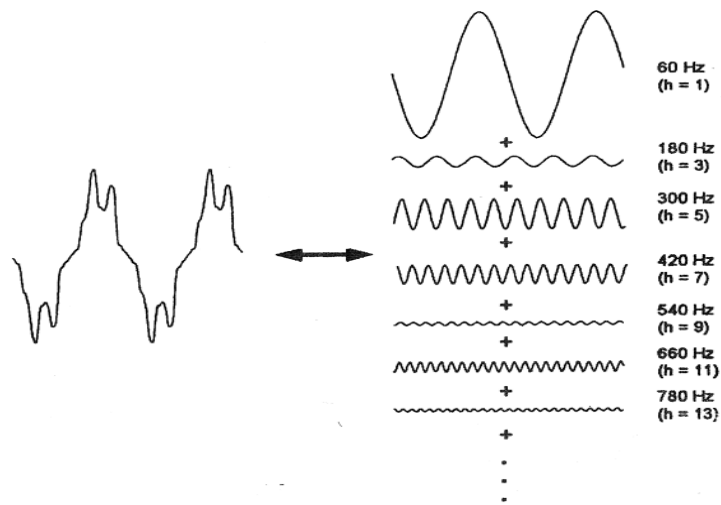


Fig. 4.33. Fourier series representation of a distorted waveform [115].

The amplitude of high-order harmonics (over the 50th order) in power systems is negligible. However, these harmonics can interrupt the operation of low-power electrical devices even though they cannot harm power systems. If a power system is divided into series and shunt elements, the majority of nonlinear elements will be among those shunt elements (loads). Series impedances (the short-circuit impedance between the source and load) are normally linear. The shunt branch (magnetizing impedance) in the transformer equivalent circuit is the harmonic generation source. This sentence does not imply that all customers experiencing harmonics are the main sources of harmonic generation. But it should be said the harmonic distortion of some loads of customers or a combination of them can be the reason for a harmonic generation [115].

4.13.4.3 Current and voltage distortion

The term "harmonics" is mostly employed individually with no use of other descriptor terms or words beside it. For instance, it is believed that an adjustable-speed motor drive or an induction furnace cannot work appropriately due to the presence of harmonic components. Why this is true? The answer could be one of the three following answers [115]:

- The voltage harmonic level is so much high that the firing angle control system cannot operate properly;

- The current harmonic level is higher than the capacity of some equipment in the supply network (such as transformers and motors), which should operate under their rated power; and
- The voltage harmonic is high because the resultant current harmonic is large.

As these show, various parameters impact harmonic content and the relationships between them. Therefore, the term harmonic solely is ambiguous, without which it is difficult to report an issue accurately. Further, nonlinear loads produce current harmonics and inject them into the power system. For further studies it would suffice to model the harmonic producing loads in the system as current sources. However, there are some exceptions, which are explained in the following. As shown in Fig. 4.34, voltage distortion appears owing to the flow of distorted current from the series and linear impedance. While it is assumed here that the source includes only the voltage with fundamental frequency, harmonic currents passing through the system impedance lead to voltage drop in harmonic components and, as a result, creates a harmonic voltage across the load. The magnitude of voltage distortion relies on the values of impedance and current. Supposing that the distortion on the bus is maintained within an acceptable range (generally smaller than 5%), the magnitude of harmonic current established by the load is almost invariable for every load level [115].

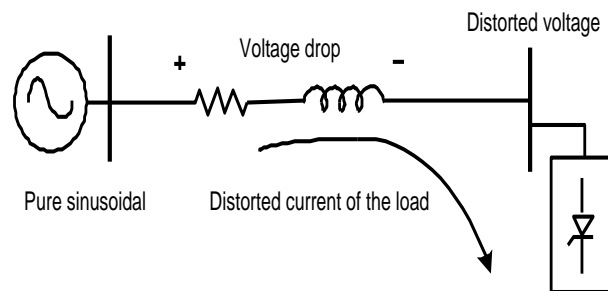


Fig. 4.34. Harmonic currents flowing from the system impedance and produce voltage harmonic on the load [115].

While current harmonics produced by the load finally lead to voltage distortion, it is worth noting that voltage distortion is not controlled by the load. A given load produces two values for voltage distortion if it is located at different points of the system. Understanding this fact is the basis for sharing responsibilities in harmonics control as follows [115]:

- The current harmonic value injected into the system should be controlled at the common connection point.

- If the injected current harmonic varies in the allowable range, the voltage distortion can be maintained in the allowed range by controlling the system impedance.

4.13.4.4 RMS values and the THD

There are several numerical criteria for showing harmonic magnitudes of a waveform. Among the most popular ones is the THD, which can be calculated for current and voltage waveforms as follows [145]:

$$THD = \frac{\sqrt{\sum_{h=2}^{h_{max}} M_h^2}}{M_1} \quad (4.11)$$

where, M_h is the RMS value of the h th harmonic component of M . THD is the measurement criterion of the RMS value of a harmonic component of a distorted waveform.

The RMS value of a waveform differs from the sum of its components. However, it is obtained from the sum of the squared root of the sum of squared values of all components of the waveform. The following equation relates the THD to the RMS value [145]:

$$RMS = \frac{1}{\sqrt{1+(THD)^2}} \sqrt{\sum_{h=1}^{h_{max}} M_h^2} \quad (4.12)$$

THD has widespread usage in various applications and, thus, its restrictions should also be considered. This quantity helps to have a sense of overheat in a resistive load when imposed on a distorted voltage. Moreover, it indicates the excess loss created due to the flow of current through a conductor. Nonetheless, it cannot represent the voltage stress on a capacitor on the account that the stress is concerned with the peak value of a voltage signal. According to (4.11), the THD index indicates the proportion of harmonics and the fundamental component values. If there is no fundamental frequency, then the value of THD will be infinite as is the case for the signal $i(t) = \cos(3\omega t) + \cos(5\omega t)$. These conditions will occur when the current or voltage is modulated with the rated frequency of the network either electronically or using subsynchronous switching or via the distortion caused by controlling signals employed for improving the switching strategy. If in a 50 Hz system, a Pulse Width Modulation (PWM) system is used for speed control of an induction motor, the stator voltage of the motor will have $50 \pm f_m$ components, where f_m is a low frequency equal to 0.2 Hz. Thus, 50 Hz frequency is no longer available

in the voltage waveform. To avoid such issue, another index is employed, called distortion index (DIN) [145]:

$$DIN = \left[\frac{\sqrt{\sum_{i=2}^{\infty} I_i^2}}{\sqrt{\sum_{i=1}^{\infty} I_i^2}} \right] \quad (4.13)$$

THD and DIN are related to each other as follows [145]:

$$DIN = \frac{THD}{\sqrt{1+(THD)^2}} \quad (4.14)$$

$$THD = \frac{DIN}{\sqrt{11(DIN)^2}} \quad (4.15)$$

In the case the value of harmonic distortion is low, Taylor expansion series $\frac{1}{1+x}$ and $\sqrt{1+x}$ can be used and the following approximate equations are obtained [145]:

$$DIN \cong THD \left(1 - \frac{1}{2} (THD)^2 \right) \quad (4.16)$$

$$THD \cong DIN \left(1 + \frac{1}{2} (DIN)^2 \right) \quad (4.17)$$

If the distortion is low, the THD and DIN values will be equal.

Voltage harmonics during the sampling process are referred to as the fundamental values of the waveform. Since voltage changes only a small percentage, the THD value of voltage has an engineering meaning. Yet, it cannot rule on current. A minor value of current can cause large THD, yet having no significant impact on the system. As most of the monitoring devices calculate the THD value in terms of the available samples, the users are more probable to get misled by whether the current is unfavorable to the system or not. Some system analyzers avoid this issue by referring to the peak value of the current demand instead of the fundamental component of available samples. This quantity is named the total demand distortion (TDD) [145].

4.13.4.5 Power and power factor

Harmonic distortion makes it difficult to calculate power and power factor as most of the simplifications used in the system frequency analysis cannot be adopted in this case.

Three standard quantities are used in association with power as follows [115]:

- Apparent power (S): The multiplication of the RMS values of current and voltage.
- Active power (P): The average amount of delivered power.
- Reactive power (Q): Part of the apparent power with 90° phase shift with respect to active power.

In fundamental frequency, these quantities are interrelated as follows [115]:

$$P = S \cos \theta \quad (4.18)$$

$$Q = S \sin \theta \quad (4.19)$$

Where, θ is the phase shift between current and voltage.

The parameter $\cos\theta$ is known as the power factor. However, its more accurate definition is [115]:

$$PF = \frac{P}{S} \quad (4.20)$$

P and S can be defined without ambiguity even in the case of distorted current and voltage. Yet, there is no clear definition of the phase shift when there are several frequencies [115].

$$S = V_{rms} \times I_{rms} \quad (4.21)$$

$$P = \frac{1}{T} \int_0^T v(t)i(t)dt \quad (4.22)$$

If the voltage has the fundamental frequency, real power appears as its familiar form [115].

$$P = \frac{V_1 I_1}{2} \cos \theta_1 = V_{1rms} I_{1rms} \cos \theta_1 \quad (4.23)$$

This equation shows that the average active power depends on only quantities with the fundamental frequency. Since voltage distortion in power systems is very small (usually less than 5%), the above equation is a good estimation of reactive power regardless of current distortion. Also, the terms apparent power and reactive power are influenced by distortion. Apparent power (S) becomes distorted depending on the RMS value of the current distortion; thus, its calculation is easy to handle, while it is somehow more complex in comparison to the sinusoidal case. Furthermore, currently, most measurement

devices can directly measure the RMS value of distorted waveforms. Researchers have no consensus about the definition of Q when harmonics are present. As most utilities measure Q and calculated power factor based on it, this can be discussed more in details. Determining the values of P and S is very important because P specifies the amount of energy consumed and S gives the necessary capacity of the power system for power (P) transfer. As a result, Q solely will not be advantageous. From the perspective of engineers, the amount of reactive power when there is distortion is an interesting issue to discuss. The concept of reactive power flow in power systems involves the curiosity of most electrical engineers. When there is distortion, a component of S resultant from distracting P is not a conservative quantity, meaning that its sum is not zero at a given node. In a power system it is assumed that all power quantities are conservative. Some scholars have suggested that Q refers to conservative reactive components and a new quantity is defined for non-conservative components. This new component (D) is distorted power or, simply, distorted volt-ampere. The dimension of this quantity is Volt-Amp (VA). However, it cannot be assumed as a power quantity because it does not flow in the system unlike active power flow. Given this concept, Q is the sum of values of reactive power at any given frequency and D is obtained from the cross product of current and voltage values in different frequencies and has no average value. Parameters P, Q, D, and S are interrelated [115]:

$$S = \sqrt{P^2 + Q^2 + D^2} \quad (4.24)$$

$$Q = \sum_k V_k I_k \sin \theta_k \quad (4.25)$$

Therefore, D can be calculated after that P, Q, and S are determined [115]:

$$D = \sqrt{S^2 - P^2 - Q^2} \quad (4.26)$$

A 3D vector can also be used to show the interrelations between these quantities (Fig. 4.35).

The fundamental frequency component of reactive power (Q_1) will be advantageous when determining the capacitor size required for correcting the power factor. Capacitors correct only Q_1 [115].

The term "displacement power factor" can be utilized for describing the power factor that is obtained from only fundamental frequency components. Devices that monitor PQ can

measure this quantity. Also, these devices can calculate the real power factor, which was already introduced as PF (Eq. (4.20)). Most equipment such as adjustable-speed motor drives has a displacement power factor of unity.

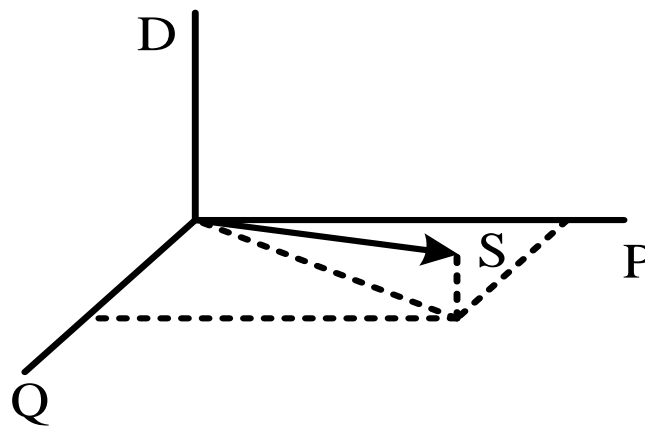


Fig. 4.35. The relationship between different components of apparent power [115].

However, their real power factor is between 0.5 and 0.6. In this case, the capacitor installed on the AC side will have a negligible impact on real power factor correction. In fact, if the capacitor experiences resonance, the distortion will increase and, thus, the power factor becomes even worse. The real power factor determines the capacity of the transmission system that should be structured for load supply. Most of the demand measurement devices calculate only Q_1 . Fortunately, in most cases, harmonic current at the measurement point is not as large as the currents of other loads and, thus, the error is minor (to the benefit of customers). Energy measurements in the presence of low voltage distortion are sufficiently accurate, although demand measurement devices may suffer from high errors. In the end, it can be said that distortion causes additional current components in the system, resulting in energy loss in elements from which these current flow. Consequently, it is essential for the system to have a larger capacity for power transmission [115].

4.13.4.6 Third-order harmonics

Third-order harmonics are odd multiples of the third-order harmonic ($h = 3, 9, 15, 21 \dots$). These harmonics need distinctive analyses since the system response to them differs from those of other harmonics. Third-order harmonics are among the most important subjects in grounded-star connection systems with a current that passes through the neutral wire. Neutral overloading and telephone interferences are two major challenges in this area. Moreover, some equipment does not work properly because their phase to neutral voltage

has become distorted (due to voltage drop of the third-order harmonic in the neutral conductor). For a fully balanced system consisting of single-phase loads (Fig. 4.36) it is assumed that both third-order harmonic and fundamental components are available. By summing currents at the neutral node (node N), the fundamental component current becomes zero. However, as phase components of the third-order harmonics are in-phase, the value of these components will be three times the third-order harmonic phase current [115].

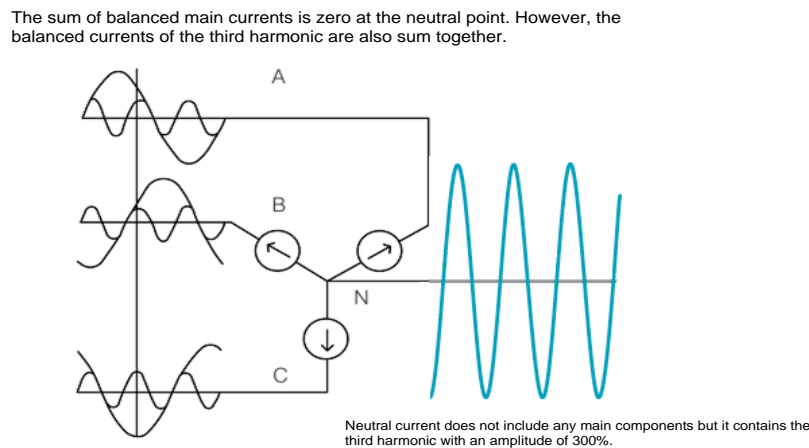


Fig. 4.36. High neutral current in supply circuits of single-phase nonlinear loads [115].

The connection type of transformer windings has a huge influence on the flow of third-order harmonic currents produced by single-phase nonlinear loads. Fig. 4.37 depicts two cases. In a transformer with a star-delta connection, third-order harmonic currents enter the star side. As they are in-phase they are summed at the neutral point. Because of ampere-turns balance law, a third-order harmonic current is generated in delta-side windings. But these currents are confined within the delta and line currents are free of them. In the presence of a balanced current, third-order harmonic currents treat precisely like zero-sequence currents. This type of connection is present in the majority of distribution transformers, where their delta side is connected to the supply feeder. On the other hand, using the grounded-star winding at both sides of the transformer the third-order harmonic is allowed to be transferred to the high-voltage (HV) side with no obstacle.

These harmonics on both sides are available with equal ration. Some important points regarding the PQ problem are provided as follows [115]:

- Transformers and their neutral connections in particular will experience overheating provided that they feed single-phase loads on the star side (because of the presence of a high amount of the third-order harmonic);
- The third-order harmonic components cannot be obtained by current measurement on the delta side of the transformer. As a result, there will be no estimation of the amount of heat the transformer is exposed to; and
- The proper selection of the connection type in transformers can prevent the flow of third-order harmonic currents (via cutting the neutral connection on one or both sides of the star windings or using delta wiring).

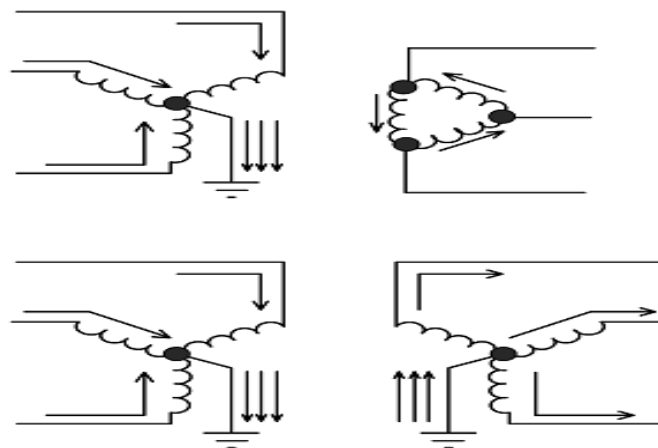


Fig. 4.37. Flow of third-harmonic current in a three-phase transformer [115].

The principles associated with the flow of the third-order harmonic currents in transformers can be applied only under balanced conditions. When phases are unbalanced, the third-order harmonics appear even when they are unexpected. The normal condition for third-order harmonics is the zero sequence. During unbalanced conditions, third-order harmonics may contain positive and negative sequence components as well. One notable point in this case is the three-phase electric arc furnace. Even though these furnaces are supplied with a delta connection, they produce huge third-order harmonics on the line current when operating in unbalanced conditions [115].

4.13.4.7 Harmonic sources

The following provides several harmonic sources [115]:

- Generation of non-sinusoidal waves by synchronous machines due to slots and non-uniform distribution of stator windings;

- Non-uniformity in the reluctance of synchronous machines;
- Non-sinusoidal distribution of magnetic flux in synchronous machines;
- The magnetizing current of transformers;
- Nonlinear loads such as welding machines; and
- Electric arc and induction furnaces.

Moreover, the emergence of semi-conductor elements and their widespread application are other reasons for harmonics in power system. These elements are mostly seen in the following devices and the power systems [115]:

- HVDC systems;
- Equipment used in speed controllers of electrical machines;
- Equipment used in electrical transportation such as electric buses and metros;
- The connection of solar and wind power plants to distribution systems;
- The application of SVC as an important tool in reactive power control;
- The widespread use of rectifiers used in battery chargers; and
- Industries including chemical and petrochemical complexes and aluminium melting industries that employ high-power rectifiers for DC electricity generation required for chemical processes and aluminium melting.

4.13.4.7.1 Arcing equipment

This category includes electric arc furnaces, welding machines, lighting lamps (e.g. fluorescent, sodium-vapor lamp, mercury-vapor lamp) with magnetic ballasts (instead of electronic ballasts). As is seen in Fig. 4.38, the arc can be represented using a voltage source series with a reactance that restricts the current in an acceptable range.

The voltage-current characteristic of electric arcs is nonlinear. Once the arc occurred, the arc current increases and, as a result, its voltage decreases. The current value is limited by the system impedance. In this case, the arc appears as a negative resistance during part of its operating cycle. In the case of fluorescent lamps, ballast impedance is essential for limiting the current in an acceptable and stable value. Thus, this type of lighting system will have external impedance known as ballast [115].

Magnetic ballasts usually produce fewer harmonics, but the main harmonic distortion is created by the behavior of arc. In any case, some of the electronic ballasts that are used for correcting the energy efficiency in switching power supplies may double or triple the number of harmonics.

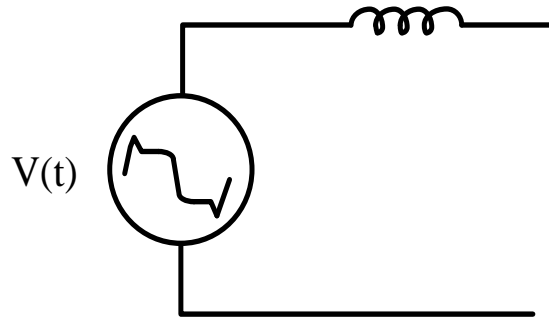


Fig. 4.38. The equivalent circuit of an arcing device [115].

Other types of electronic ballasts are designed in a way that they reduce the amount of harmonic content and, in fact, produce fewer harmonics than magnetic ballasts. In electric arc furnaces, the limiting impedance includes a cable, furnace connecting wires, the system impedance, and the furnace transformer. Currents with magnitudes greater than 60 kA are very common in these furnaces.

Electric arc furnaces are better to be represented as voltage harmonic sources. If the voltage across the arc is analyzed, its waveform is almost trapezoidal and its value is a function of the arc length. In any case, the ballast impedance behaves like a buffer such that the source voltage is less distorted. Therefore, arcing loads appear as rather stable current harmonic sources, a necessity for the majority of modeling. The exception case happens when the system is close to the resonance state where the Thevenin equivalent circuit by employing the voltage waveform of the arc provides more realistic responses [115].

4.13.4.7.2 Saturable elements

Transformers and other electromechanical devices with steel cores, such as motors are among saturable elements. Harmonic content is the result of the nonlinear magnetizing characteristic of iron (Fig. 4.39). When the voltage of a motor increases, its current becomes distorted. Although this has several consequences, the current waveform of some low-power single-phase motors is triangular and includes huge third-order harmonics. Power transformers are designed such that they operate in the linear region of the magnetizing characteristic. The maximum flux density of a transformer is chosen according to optimizing the price of iron, non-load loss, noise, and some differing factors. Manufacturers try to design transformers with the least possible design cost. To reduce non-load loss and noise, more iron has to be used in the core [115].

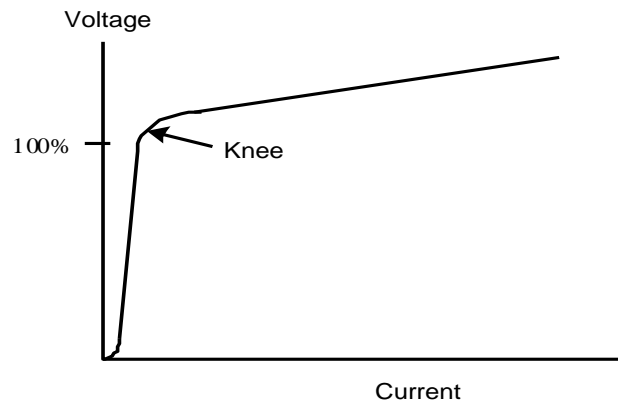


Fig. 4.39. Magnetic characteristic of an iron core [115].

Although the excitation current of the transformer contains many harmonics at its operating voltage levels, the value of this current is about 1% of the full-load current and, as a result, the impact of the transformer will not be similar to that of power electronics converters and arcing equipment that produce current harmonic of about 20% of the rated value. However, its effect especially on distribution networks with many transformers is considerable. It is worth noting that the third-order harmonics during low load increase dramatically due to the increase in the voltage. In this case, the excitation current of the transformer will be comparable to its load current. Voltage harmonic distortion caused by excitation current appears only under low load conditions of the system. Some transformers often operate in the saturation region. A type of such transformers is those that are used for generating a frequency of 150 Hz in induction furnaces [115].

4.13.4.8 The effect of harmonic distortion on the operation of equipment and power system

Some detrimental impacts harmonics impose on the power system and its elements include as follows [115]:

- Insulation breakdown of capacitor banks and an increase in the current and reactive power of capacitor banks;
- Interference with ripple control systems and affecting the remote control of switching and measurement systems;
- Additional ohmic and core loss and overheating electrical machines;
- Insulation breakdown of cables;
- Interference with telecommunication systems and PLC;
- Causing errors in measurement devices;
- Mis operation of control systems;

- Mis operation and wrong response of relays; and
- Mis operation of firing circuits in power electronics systems, specifically in firing circuits operating based on the voltage zero-crossing detection.

4.13.4.8.1 The effects on capacitors

Allowed steady state values for capacitors have been specified as follows [115]:

- 135% of the rated kVAr
- 110% of the rated RMS voltage (including harmonics except for the transient state)
- 130% of the rated current (including harmonics and the fundamental component)
- 120% of the peak voltage (involving harmonics)

Table 4.7 exemplifies a voltage assessment. In this example, the capacitor experiences a harmonic voltage. The goal is to compare the values calculated for this capacitor with the acceptable ranges given above. The fundamental component current of the load for a 1200 kVAr capacitor in a system with a line voltage of 20 kV is given by [115]:

$$I_c = \frac{Kvar_{3\phi}}{\sqrt{3}KV_{\phi\phi}} = \frac{1200}{\sqrt{3} \times 20} = 34.6A \quad (4.27)$$

Basically, capacitors are exposed to fifth- and seventh- order harmonics. Voltage disturbances of 4% in the fifth-order harmonic and 3% in the seventh-order harmonic causes 20% fifth order harmonic and 21% seventh order harmonics in the current. The values obtained in this case, are all standard. Harmonics, in general, increase insulation loss in capacitors.

4.13.4.8.2 The effects on transformers

Transformers are designed such that they transfer power to the load in the fundamental frequency and with the least possible loss. Harmonic content available in current leads to significant overheating, in addition to causing voltage harmonics. The design of transformers so that it could tolerate higher-order harmonics including the use of a transposed conductor rather than solid conductor and inserting more cooling channels. It is accepted that a transformer with higher than 5% current distortion will have smaller rated power [146-147]. Different cases of load current harmonic components that lead to a temperature increase in the transformer include [146-147]:

- **RMS current:** In the case the transformer capacity is selected equal to the load KVA, the current harmonics will cause the transformer's RMS current greater than

the allowed capacity. This increase in the current causes increased loss in the conductors.

Table 4.7. Evaluation of capacitors [115].

Calculations associated with capacitors when supplied with non-sinusoidal voltages				
Data of the capacitor bank				
Rated power	1200 kVAr	Frequency of the fundamental Component		50 Hz
Rated voltage	20000 V	Rated current of the fundamental Component		34.64 A
Operating voltage	20000 V	Capacitor reactance		333.3 Ω
Harmonics distribution in the bus voltage:				
Harmonic order	Frequency (Hz)	Voltage amplitude (% of the fundamental component)	Voltage amplitude (V)	Line current (% of the fundamental component)
1	50	100	11547	100
3	150	0	0	0
5	250	4	461.8	20
7	350	3	364.4	21
11	550	0	0	0
13	650	0	0	0
17	850	0	0	0
19	950	0	0	0
21	1050	0	0	0
23	1150	0	0	0
25	1250	0	0	0
THD of the voltage: 5%			THD of the capacitor current: 29%	
RMS voltage of the capacitor: 11561.48 V			RMS current of the capacitor: 36.05 A	
Ranges of the capacitor bank:				
	Calculation (%)		Acceptable range (%)	
Voltage peak	107		120	
RMS voltage	100.1		110	
RMS current	104.1		130	
Rated power	104.3		135	

- **Eddy current loss:** Eddy currents, as induced currents, appear in the transformer owing to magnetic fluxes and are present in wirings, core, and parts of the conductor exposed to the field flux, leading to additional heat loss. Eddy current loss increases as a function of the squared frequency of the eddy current and contributes to a large part of the transformer loss.

- **Core loss:** Core loss increase caused by harmonics depends on the influence of the harmonics on the voltage and the configuration of the transformer core. Increased voltage distortion can increase eddy current in the core layers. The total effect relies on the thickness of the core layers and the quality of the core iron. Increased core loss due to harmonics is not as much as the previous two items [146-147].

Table 4.8 depicts a simple way to obtain the reduced rated power of a transformer due to the presence of harmonics [115-146].

Table 4.8. Calculation of K factor for transformers [115-146].

Load current harmonic distribution in a transformer					
Harmonic order	Current (%)	Frequency (Hz)	Current (p.u.)	I^2	$I^2 \times h^2$
1	100	50	1	1.000	1.000
3	1.6	150	0.016	0.000	0.002
5	26.1	250	0.261	0.068	1.703
7	5.0	350	0.050	0.003	0.123
9	0.3	450	0.003	0.000	0.001
11	8.9	550	0.089	0.008	0.958
13	3.1	650	0.031	0.001	0.162
17	4.8	850	0.048	0.002	0.666
19	2.6	950	0.0026	0.001	0.244
21	0.1	1050	0.001	0.000	0.000
23	3.3	1150	0.033	0.001	0.576
25	2.1	1250	0.021	0.000	0.276
			Total	1.084	5.712
K factor: 5.3					
Reduced rated power with respect to the standard value: 0.87 p.u.					
Loss coefficient of the assumed eddy current (P_{EC-R}): 8%					

The loading loss P_{LL} has two parts, namely, ohmic loss (I^2R) and eddy current loss (P_{EC}) [115]:

$$P_{LL} = I^2R + P_{EC} \quad (W) \quad (4.28)$$

Component I^2R is directly corresponding to the RMS current value, while eddy current depends on the square of the current and frequency [115]:

$$P_{EC} = K_{EC} \times I^2 \times h^2 \quad (4.29)$$

where, K_{EC} is the proportionality constant

The full-load loss in p.u. when current harmonic conditions are present will be [115]:

$$P_{LL} = \sum I_h^2 + (\sum I_h^2 \times h^2) P_{EC-R} \quad (4.30)$$

where, P_{EC-R} denotes the eddy current loss factor under nominal conditions.

The coefficient K that is used in PQ references regarding the transformer capacity reduction is given in terms of current harmonics [115]:

$$K = \frac{\sum(I_h^2 \times h^2)}{\sum I_h^2} \quad (4.31)$$

Therefore, the RMS value of the distorted current is found [115]:

$$\sqrt{\sum I_h^2} = \sqrt{\frac{1+P_{EC-R}}{1+K \times P_{EC-R}}} \quad (PU) \quad (4.32)$$

where, P_{EC-R} shows Eddy current loss coefficient, h is harmonic order and I_h demonstrates current harmonic. Consequently, transformer capacity reduction in p.u. will be provided by having the eddy current loss coefficient which is calculated as follows [115-147]:

- Collecting the coefficient data from the transformer designer (manufacturer).
- Utilizing the test data and the method mentioned in standards.
- Using the sample values according to the type and size of the transformer (Table 4.9) given in [115].

4.13.4.8.3 The effects on motors

Motors are susceptible to voltage harmonic distortion. Voltage harmonic distortion at output terminals of the motor leads into harmonic flux inside the motor. Harmonic fluxes

do not participate in the establishment of torque but rotate with a different speed from the fundamental frequency. As a result, they produce high-frequency currents in the rotor. The effect of harmonics on motors is similar to the effect of negative-sequence current in the fundamental frequency. Thus, fluxes pose other problems in addition to increasing the loss. Efficiency reduction along with overheating, vibration, and noise are other adverse effects of voltage harmonic distortions in motors [115].

Table 4.9. Sample values of P_{EC-R} [115].

Type	Rated power (MVA)	Voltage	% P_{EC}
Dry Oil	≤ 1	400 V in LV	3-8
	≤ 2.5	400 V in LV	1
	205-5	400 V in LV	1-5
	> 5	400 V in LV	9-15

In harmonic frequencies, motors are represented by locked-rotor reactive connected to the line. The low-order harmonic components of voltage that have high amplitudes with small impedance are more important for motors. When the voltage distortion is between 5-10% or more, an additional thermal loss is produced. To increase the lifelong of the motor, such distortion should be corrected and reduced. Motors are exposed to harmonic current flow parallel to the power system impedance. Consequently, they increase the resonance frequency due to a reduction in the system inductance. This problem will not be a problem to the system and its severity is corresponding to the resonance frequency of the system before starting the motor. Motors play a role in the damping of harmonic components and its value depends on the X/R ratio in the locked-rotor circuit of the motor. Systems that include many low-power motors with small X/R ratios largely weaken the harmonic resonance. It should be noted that this is not expected from large motors [115].

4.13.4.8.4 Telecommunication interferences

Harmonic currents in distribution systems or on its path to customers cause interferences in telecommunication circuits that have a common path with them. In conductors parallel to the harmonic current paths, the induced voltage is mostly established in the range of bandwidth of audio communications [115].

Harmonics in the range of 540-1200 Hz usually pose more catastrophic effects. The induced voltage per current ampere increases with the frequency. In four-wire systems, these harmonics are not problematic because the third-order harmonics are in-phase. In this case, the third-order currents are summed in the neutral conductor and cause an improper effect on the telecommunication systems. Harmonic components are transferred to telephone systems via induction or direct conduction [148].

4.13.4.9 Identifying the locations of harmonic sources

In radial distribution feeders and industrial factories, the produced harmonics flow from their origin (harmonizing loads) toward the power source in the power system. Fig. 4.40 illustrates such a case. The system impedance is usually the minimum impedance the harmonic current encounter. Thus, the major part of the current flows toward the power source and this can be exploited to locate harmonic producing sources [115].

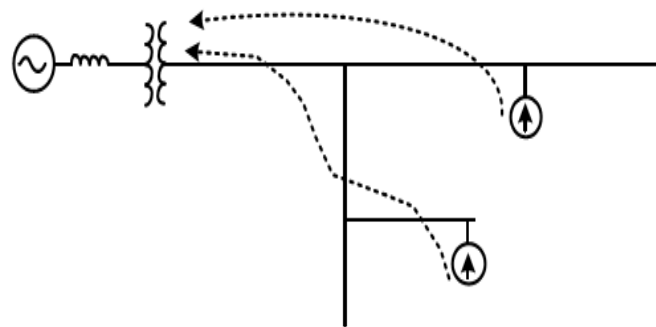


Fig. 4.40. The general path of harmonic currents in radial networks [115].

Using a PQ monitoring device to show current harmonic components, current harmonics on each branch can be easily measured. This should be commenced from the beginning of each circuit to find harmonic sources. Capacitors used for power factor correction are capable of changing the pattern of the current path at least in one harmonic component. Including a capacitor to the previous circuit, for instance in Fig. 4.41, draws a major part of the harmonic current toward this circuit. If the mentioned method above is used in this case, it may wrongly follow the path ended in the capacitor bank instead of tracking the main path that ends in harmonic generation sources. Hence, it is necessary to switch off all capacitor temporarily to determine the locations of harmonic sources accurately [115]. The harmonic current originating from real harmonic sources and the harmonic current resulting from resonance with a capacitor bank can be easily discriminated. Resonance-

produced currents include one ruling harmonic component carried on the original sine waveform.

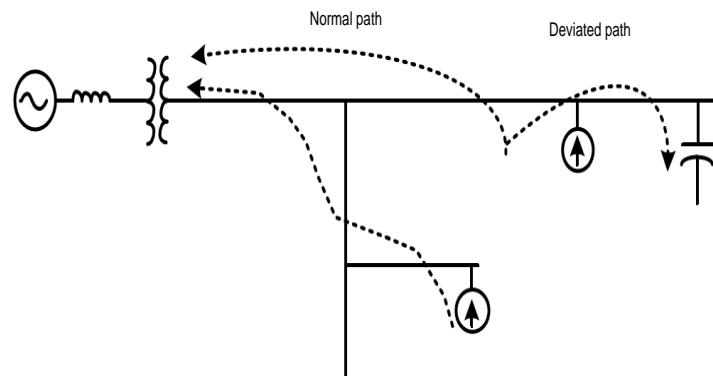


Fig. 4.41. Power factor correction capacitors are able to change the path of one of the current harmonic components [115].

Harmonic current waveforms will not have only one component (in addition to the fundamental component). These waveforms have different forms depending on the harmonizing phenomenon. However, they will have several harmonic components with different amplitudes. A high-amplitude harmonic almost always shows resonance conditions. The following fact can be used for determining the resonance conditions and their presence in the system. To this end, initially, the input current to capacitors is measured. If the current comprises of a large value of one harmonic plus the fundamental component, one can conclude that the capacitor is resonating with the rest of the system. Always in the first step inspect and measure capacitor currents [115].

4.13.4.10 Harmonic study methods

The ideal method to conduct a study on the system harmonic is described as follows [115]:

- First, the study objective should be determined. It is crucial to guide the study to the proper track. For instance, the objective may be the determination of factors and problems along with solutions. The other objective may be specifying whether modern equipment such as motor drives with adjustable-speed capability and capacitors cause problems or not.
- Implementing a computer simulation based on the data available. Measurements can impose an additional cost in terms of duration, the use of equipment, and making interruptions in the system. In other words, it will be very economical if there is proper idea and place to search.

- Performing measurements on the available equipment and determining harmonic sources and distortion on buses.
- Calibrating the computer model using measurements.
- Studying new conditions of the circuits and/or the problems regardless of the type of problem-causing factor.
- Finding solutions (filter, etc.) and analyzing the possibility of their interference with the system. Also, revising the sensitivity of results with respect to important variables
- Once the proposed methods are implemented, system monitoring should be used for confirming the system correct operation.

It should be noted that this study trend is based on the assumption that we have sufficient access to computer analysis tools and monitoring devices. All the above-mentioned steps cannot be always implemented accurately. An experienced analyzer can solve the problem without relying on the tests. However, it is highly recommended to conduct the initial measurements because it is possible that some problems in the study of harmonics be neglected from the system analyzer's perspective [115].

4.13.4.10.1 Symmetric components

Power engineers traditionally use symmetric components to better understand the behavior of three-phase systems. Using these components, the three-phase system turns into three single-phase systems, which is easy to analyze. The symmetric components method can also be employed in analyzing the system response to harmonic currents provided that the necessary precision in using the method and its basic assumptions are taken into account. Using this method, any given set of unbalanced currents and voltages can be converted into three balanced sets. The positive-sequence set includes three sinusoidal waves with a 120° phase-shift with respect to each other (A-B-C).

Also, negative-sequence sinusoidal waves have 120° phase-shift with respect to each other but with reverse direction compared to the positive sequence, i.e., A-C-B. Zero-sequence sinusoidal waves are in-phase. In a fully balanced system, there are following states [115]:

- Harmonic orders $h = 1, 7, 13, \dots$ are in positive sequence;
- Harmonic orders $h = 5, 11, 17, \dots$ are in negative sequence; and
- Third-order harmonics $h = 3, 9, 15 \dots$ are in zero sequence.

In a balanced system, the terms third-order harmonic and zero-sequence are synonyms. In the case these conditions are not met, each of the harmonics will be part of the sequences. The system's response to positive sequence harmonics is clear. In the case only the positive sequence needs to be analyzed, the problem will be very simple. Power engineers use positive sequence components for power flow and voltage drop calculations. Fortunately, such studies can be done for most of the three-phase industrial load. In simple words, when the delta wiring of a transformer is in series with harmonic sources and the network, only the positive-sequence circuit would suffice for determining the system's response. Zero-sequence harmonics are not available in such systems and their path of flow is prevented. Fig. 4.42 depicts this principle. The figures show what model can be used for different applications [115].

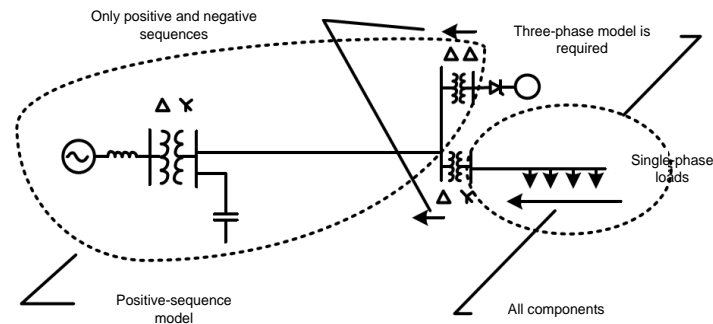


Fig. 4.42. The effect of transformer connection type on modeling requirements for network harmonic analysis [115].

Both positive and negative sequence networks usually have identical responses against harmonics and one single circuit model can be used for both of them. If the third-order harmonics present during the measurement process, they are not zero-sequence harmonics in the case of the presence of unbalanced harmonics and they can be modeled using the same model. The symmetric components method to analyze four-wire distribution systems with many single-phase loads will not be useful because both zero and positive sequence networks are involved in calculations. Generally, to analyze such problems, handy calculations are not practical and computer programs capable of accurate modeling of these systems and solving them should be employed. The use of symmetric components increases the probability of error because the system analyzer's error is also possible. Therefore, it is recommended to avoid the use of symmetric components methods by individuals who are unfamiliar with the unbalanced system's behavior.

In summary, most harmonic studies can be conducted using symmetric components modeling techniques. In the case of studying industrial loads, in most cases, such loads can be solved using the positive-sequence impedance model. One exception is the study of the harmonics caused by single-phase loads in distribution feeders of commercial and industrial buildings [115].

4.13.4.10.2 Modeling of harmonic sources

Most of harmonic analyses are carried out using linear circuits solving technique in the steady state. Harmonic sources that are nonlinear elements are modeled as sources injected into the linear network. For most of harmonic power flow studies, harmonic sources can be modeled using uncomplicated sources of harmonic currents. This model can be applied when the voltage distortion in the main bus is less than 5%. Fig. 4.43 illustrates a power electronics converter plus a current source in the equivalent circuit.

The value of the injected current has to be measured. If this value or other information is unavailable, it is assumed that the value of harmonics is proportional reversely with the harmonic order, meaning that the fifth harmonic current is equal to 20% of the fundamental component, and the rest is similar. This is resultant from the Fourier series of the square wave. Most nonlinear loads may draw square current. However, this principle cannot be employed in the case of drivers that use an advanced PWM technique and switching power sources that contain larger harmonic components. When the system is close to resonance, the use of a simple current source will not provide a good estimation of the distorted voltage. In this case, a simple current source model means injecting constant current to a large impedance, which does not represent real system conditions. Often, the most important problem is to determine the resonance frequency and this can be obtained straightforwardly using the simple model. When resonance conditions are eliminated by adding a filter, the response found from the simple model will be more realistic. For the cases that a more accurate response is needed under resonance conditions, more complicated models should be utilized [115].

For most of the equipment in the power system, Thevenin or Norton equivalent circuits would suffice (Fig. 4.44). In this case, the additional impedance will correct the response of the shunt resonance circuit. The Thevenin equivalent circuit can be easily obtained for most nonlinear loads. An electric arc furnace, as an example, can be shown using a square wave voltage with a peak of almost half of the rated AC voltage of the system. Its series

impedance is the short circuit impedance of the furnace's transformer and connecting wires [115].

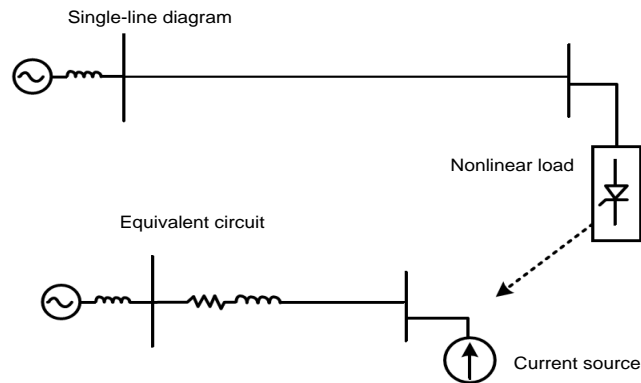


Fig. 4.43. Representation of a nonlinear load using a harmonic current source to analyze the system [115].

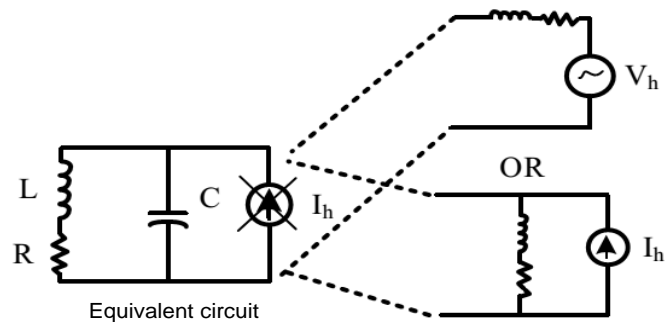


Fig. 4.44. Replacement of a simple model of the current source with a Thevenin or Norton equivalent circuit to improve and model the system under resonance conditions [115].

Obtaining a specific equivalent impedance for most nonlinear loads is difficult. In these cases, the accurate simulation of harmonic-producing loads will be essential. This can be done using computer programs that use iterative methods or programs that use the accurate analysis method in the time domain [115].

4.13.4.10.3 Computer programs for harmonic calculations

It has become evident from the previous sections that each system, even the simplest one, requires a computer program. Characteristic of such a program is given below.

First, it should be noted that a simple circuit is an appropriate model for the analysis of small industrial systems and its analysis is based on handy calculations (Fig. 4.45). This

system is basically a single-bus circuit plus a capacitor. The two cases can be easily performed as follows [115]:

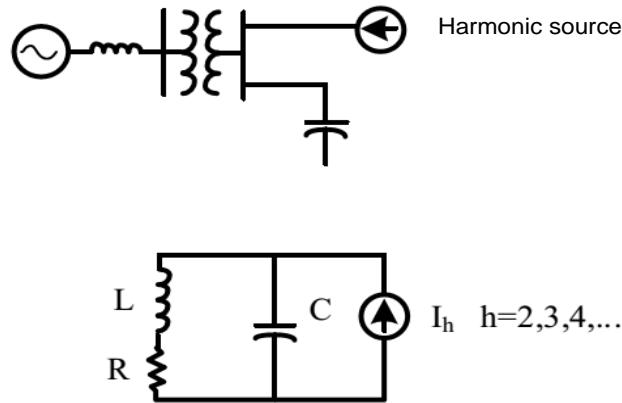


Fig. 4.45. A simple circuit that can be solved by hand [115].

- Determining the resonance frequency. In the case the resonance frequency is close to a harmful harmonic for the system, the value of the capacitor should be changed or a filter has to be considered for it.
- An estimation of voltage distortion caused by current I_h . Voltage V_h is calculated as follows [115]:

$$V_h = \left(\frac{R + j\omega L}{1 - \omega^2 LC + j\omega RC} \right) I_h \quad h = 2, 3, \dots \quad (4.33)$$

If the resonance frequency close to a harmonic is not important and voltage distortion is low, it can be said that the system is probably successful. To use computer programs, the system under-study, loads, and sources should be determined. The data can include the following items [115]:

- Transformer and line impedances;
- Type of connection of transformers;
- The values and the places of capacitors;
- Harmonic spectrum caused by nonlinear loads; and
- Power source voltages.

The above values are fed to the software as inputs. The program has to determine the impedances in the considered harmonic automatically and solve the program.

4.13.4.10.4 Capabilities of harmonic analysis programs

Computer programs accepted for harmonic analyses in power systems need to meet the following requirements [115]:

- They should be able to solve large systems with numerous nodes.
- They should solve multi-phase systems with any combination. Distribution networks can be solved using positive-sequence components in balanced networks. However, this cannot be generalized.
- The program needs to be able to model systems with positive sequence models. In the case no zero-sequence harmonic is available, using three-phase modeling will not be necessary.
- The program has to be able to obtain the system impedance for different frequencies (with variations about 10 Hz, for instance). In this case, the frequency response characteristic can be found for determining resonance conditions.
- The program must be able to solve several harmonic sources simultaneously so that the real distortion values of current and voltage are obtained.
- The program should include prebuilt common harmonic source models.
- The program should be able to model the harmonic current source and harmonic voltage source at the same time.
- These programs should adjust the phase angle of sources automatically based on phase angles of the fundamental frequency component.
- These programs should be able to model any type of transformer connections.
- These programs should represent the results in a meaningful way so that the user could work with it easily.

4.13.4.11 General principles and requirements for harmonics

This subsection deals with the basic principles required for connecting distorted large loads to the network and the allowed amount of harmonic level in power systems. Some electrical equipment, particularly modern ones, disrupts the power system and lower the PQ such that it leads to changes in operating conditions of other devices. Therefore, it is essential to study how such equipment, which is extensively manufactured and used, is connected so that the electrical network can be utilized appropriately and safely for equipment sensitive to disturbances. Further, concerning a harmonic distortion event, it should be stated that the greatest effect is caused by voltage harmonic, while current harmonics can also have direct impacts, such as telephone interferences. The effect of

current and voltage harmonics can be observed in long distances from the harmonic producing source. In fact, the allowed range of these harmonics will be set such that they do not establish adverse effects on the equipment under operation. As voltage harmonic is caused by current and impedance harmonics of the system at that frequency, some limitations should be applied to the level of current harmonics. The following technical and economic issues should be considered when solving harmonic problems [149-150]:

- All power systems contain voltage harmonics, whether with a specific frequency or a continuous spectrum of frequencies where frequency, amplitude, and phase angle change with no specific pattern.
- All equipment must be able to tolerate voltage harmonic up to a specific range determined reasonably and continue their operation under such conditions.
- It could be possible to connect harmonic producing equipment subject to accepting some conditions.

Nonetheless, these conditions are not solely concerned with the equipment users and they should include the equipment manufacturers as well, such that the manufacturer is prevented from manufacturing equipment that produces excess harmonic and interrupts the system operation. According to the above complex conditions, the problem of harmonic limitation can be realized only when very simple and coordinated conditions and principles are observed. To determine the immunity limit or allowed level of harmonics in the systems, the probabilistic nature of harmonics should be considered. In a given device, the interruption limit and the immunity limit change with respect to time and each other and usually the real conditions will not be the same as test time. To this end, the adaptation limit or the minimum allowance is used. Using this parameter, the joint operation of harmonic producing equipment and sensitive equipment against harmonics can be analyzed.

Adaptation limit for a given harmonic means the level of harmonic that the probability of producing more harmonic than that is very small and only in 5% of the cases the produced harmonic can be greater than the adaptation limit. In addition, the adaptation level has to be determined such that the major part or almost all of the equipment could tolerate it with higher probability and continue their operation. Table 4.10 shows an example of the adaptation limit of harmonics in LV and MV networks [149-150]. The adaptation limit values in different countries may differ from the above values. This difference depends on the power system, the system design and type of equipment, the size and adaptation

limit of equipment against harmonics, and the evaluation and analysis of interference probability and irritation caused by harmonics. The immunity limit test (design levels) can be conducted for different equipment based on the determined adaptation limit. Immunity limits are specified considering the required reliability factor and the values are generally greater than the adaptation limit or are equal to the adaptation level in less important cases. Table 4.11 lists sample values of the immunity limit for different voltage levels [150].

Table 4.10. Adaptation limit of voltage harmonics in LV and MV networks in percentage [150].

Odd harmonics that are not multiples of 3		Odd harmonics that are multiples of 3		Even harmonics	
Order (h)	LV and MV	Order (h)	LV and MV	Order (h)	LV and MV
5	6	3	5	2	2
7	5	9	1.5	4	1
11	3.5	15	0.3	6	0.5
13	3	21	0.2	8	0.5
17	2	> 21	0.2	10	0.5
19	1.5			12	0.2
23	1.5			> 12	0.2
25	1.5				
> 25	$0.2 + \frac{1.3 \times 25}{h}$	The THD of voltage for LV and MV systems: 8%			

To determine the allowed limit of harmonic generation for a given device, the adaptation limit of the system and the point that other equipment operate simultaneously should be taken into account [150].

4.13.4.11.1 The accumulate effect of harmonics

When studying harmonics, it is essential to calculate the real values of current and voltage harmonics at each node of the network caused by different loads.

Table 4.11. Design levels of voltage harmonics in different networks in percentage [151].

Odd harmonics that are not multiples of 3			Odd harmonics that are multiples of 3			Even harmonics		
Order (h)	LV and MV	HV	Order (h)	LV and MV	HV	Order (h)	LV and MV	HV
5	5	2	3	4	2	2	1.6	1.5
7	4	2	9	1.2	1	4	1	1
11	3	1.5	15	0.3	0.3	6	0.5	0.5
13	2.5	1.5	21	0.2	0.2	8	0.4	0.4
17	1.6	1	> 21	0.2	0.2	10	0.4	0.4
19	1.2	1				1	0.2	0.2
23	1.2	0.7				> 12	0.2	0.2
25								
> 25	$0.2 + \frac{0.52 \times 5}{h}$	$0.2 + \frac{0.5 \times 25}{h}$	The THD of voltage for LV and MV networks: 6.5% The THD of voltage for HV network: 3%					

Two methods are generally employed for these calculations as follows [151]:

- **First method:** The first method can be used for calculating voltage harmonic as follows [151]:

$$U_h = U_{ho} + \sum_j K_{hj} U_{hj} \quad (4.34)$$

where, U_{ho} is the voltage harmonic of the bus in the absence of all loads. The value of K_{hj} depends on the following factors [151]:

- The type of the considered equipment;
- Harmonic order; and
- The ratio between the rated power of the considered equipment (S_{rj}) and the short circuit level at the common connection point S_{sc} .

- **The second method:** Voltage harmonic at any point of the system is the vector sum of voltage harmonics caused by different sources of that type of harmonic. Analysis and study concerning the superposition of harmonics give the following equation [151]:

$$U_{hr} = [(U_{h1})^a + (U_{h2})^2 + (U_{h3})^a + \dots]^{1/a} = (\sum U_{hi}^a)^{1/a} \quad (4.35)$$

where, U_{hr} is the h th order voltage harmonic at point r , a is a constant factor, and U_{hi} is the h th harmonic voltage resultant from the i th source. Constant a depends on three parameters as follows [151]:

- The probability limit that voltage harmonics are less than a specified value.
- The range of probabilistic and stochastic changes of the amplitude of voltage harmonics of each source; and
- The range of probabilistic and stochastic changes of the angle (phase) of voltage harmonics of each source.

It is evident that low-order odd harmonics have the following characteristics:

- These harmonics are present in most points of the network and have significant values.

- The phase angle of voltage harmonics has rather small changes and this can be the opposite in the case of higher-order harmonics. Considering the value of 0.95% for the probability limit that voltage harmonics are less than a specified value, the following values are obtained for a [151]:

- For harmonic orders less than 5: $a = 1$ (these values are valid for voltage harmonics with constant amplitude where the phase angle may probabilistically and stochastically vary between zero to 90°);
- For harmonic orders between 5 to 10: $a = 1.4$ (These values are valid for voltage harmonics where their amplitude may probabilistically and stochastically change between the half of the maximum value and the minimum value and their phase angle probabilistically and stochastically varies between zero and 270°); and
- For harmonic orders above 10: $a = 2$ (These values are valid for voltage harmonics where their amplitude may probabilistically and stochastically change between zero and the maximum value and their phase angle probabilistically and stochastically varies between zero and 360°).

When harmonics are in the same phases, $a = 1$ can be used for harmonic orders above five [151].

4.13.4.11.2 Acceptable harmonic production level for customers

Only part of the acceptable harmonic production level at the bus can be assigned for each customer. A reasonable suggestion is to determine the acceptable harmonic production level of each customer according to the power ratio between the customer's consumption (S_i) and the total output power of the bus (S_t) (note that S_t is the total power of different customers supplied by this bus) [115]. If E_{hi} is the h th acceptable voltage harmonic production level of the i th customer, by using (4.35) [115]:

$$(E_{h1}^a + E_{h2}^a + E_{h3}^a + \dots)^{1/a} = G_{hs} \quad (4.36)$$

or

$$E_{h1}^a + E_{h2}^a + \dots = G_{hs}^a \quad (4.37)$$

If the acceptable harmonic production level for each customer is proportional to its consumption power, (4.38) will be obtained for the h th acceptable voltage harmonic production level of each customer i [115]:

$$E_{hi}^a = G_{hs}^a \times (S_i/S_t) \quad \text{Or} \quad E_{hi} = G_{hs} \times (S_i/S_t)^{1/a} \quad (4.38)$$

(4.38) is based on the assumption that the minimum value of S_t is equal to the sum of S_i values and parameter a is equal to 1 for harmonic orders 3, 5, and 7, is 1.4 for harmonic orders 11 and 13, and is 2 for harmonic orders higher than 13. If the input impedance of the network in different frequencies and at the common connection point is Z_n , the acceptable limit value of current harmonics for each customer will be as follows [115]:

$$I_{hi} = E_{hi}/Z_i \quad (4.39)$$

(4.39) may impose greater restrictions for low-load customers. To avoid this problem, it has been suggested to choose the value of 0.1% as the acceptable harmonic production limit for the customer if the limit is less than 0.1.

4.13.4.12 Regulations of some countries on accepting harmonic producing customers

To get familiar with harmonic production restrictions and regulations on harmonic producing customers in a power system, the methods used in Germany, Australia, and England are presented in this subsection [115].

4.13.4.12.1 Germany

In the first stage of regulations in this country, only those equipment can be connected to the network that the ratio between their rated power (P) and the short-circuit level (S_{sc}) of the bus at the supply point is less than 0.1. In other words, if the following equation is met for a device, there is no need to analyze harmonics or conduct thorough studies and it can be automatically accepted [115].

$$P/S_{sc} < \frac{0.1}{100} \% \quad (4.40)$$

In the second stage of this country's regulations, instead of determining the acceptable limit of harmonics, the ratio between the capacity of nonlinear load and the whole load is determined. The ratio can change from 3% to 30% depending on the operating conditions of customers.

In the third stage of regulations, the allowed voltage harmonics value at the common bus is applied, which should be less than 5% for fifth and seventh order harmonics and less than 3% for eleventh and thirteenth order harmonics [115].

4.13.4.12.2 Australia

In Australia, the maximum capacity of a three-phase converter connectable to the distribution system and the utility does not conduct any study on that (the first stage of regulations) is 0.3% of the short-circuit power of the connection bus.

Moreover, regulations of the second and third stages have to be applied if the following conditions are presented [115]:

- The minimum short-circuit levels of LV and MV networks are less than 5 MVA and 50 MVA, respectively.
- The capacity of the device in LV and MV networks has to be greater than 75 kVA and 500 kVA, respectively.
- The amount of harmonics produced by several customers that are controlled together has to be greater than the previous item.

In the second and third stages of the standard in Australia, a specific allowed limit is not determined for a given harmonic producing customer and the customer acceptance is realized based on the allowed harmonic limit at the common connection point. It means that the first customer can produce harmonics equal to the allowed value of the network harmonics and occupy the whole capacity. The allowed voltage harmonic limit at the bus for different voltage levels in Australia is given in Table 4.12. Regulations in Australia determine the allowed limits of the single voltage distortion and the total voltage distortion.

4.13.4.12.3 England

For the regulations of stage one in this country, the equipment is divided into two categories: three-phase and single-phase. Concerning three-phase equipment, regulations of stage one are as follows: the maximum capacity of the converter or a regulator that can be connected to LV or MV network with no detailed analysis is given as Table 4.13 [115].

Table 4.12. The allowed limit of voltage harmonics in Australia

Network type	Voltage of the supply network	Total voltage distortion (THD)	Single voltage distortion in percent	
			Odd harmonic	Even harmonic
Distribution network	Up to 33 kV	5	4	2
Transmission network	22, 33, and 66 kV	3	2	1
	110 kV and above	1.5	1	0.5

Table 4.13. Maximum capacity of converters for automatic acceptance in England [115].

Type of the distribution system	Maximum capacity of converters of three-phase regulators (KVA)			Maximum capacity (KVA)	
	3-pulse	6-pulse	12-pulse	6-thyristor	3-thyristor/3-diode
LV	8	12	-	14	10
MV	85	130	250	150	100

The maximum capacity of single-phase rectifiers and regulators that do not produce even harmonics theoretically and are used in industrial equipment or chargers can be 5 kVA for a voltage of 240 V and 7.5 KVA for voltages 415 V or 480 V. Additionally, equipment that produces both odd and even harmonics is not considered appropriate for connection to the network. In the case several single-phase harmonic producing devices are connected from one side to the system, it is recommended to connect them to a different phase to provide a balanced situation for linear loads. Regulations of this stage do not allow the connection of two rectifiers or regulators to one phase and regulations of the second stage must be applied in such cases.

Regulations of the first stage in England do not allow the connection of equipment that injects DC current into the AC system. Regulations of the second and third stages in England are almost identical to those of Australia.

The acceptable voltage harmonics limit in the power system in England and the allowed total voltage distortion limit for different voltage levels are tabulated in Table 4.14 [115].

Table 4.14. The allowed limit of voltage harmonics in England [115].

Network voltage	Total voltage distortion (THD) in percent	Single voltage distortion in percent	
		Odd harmonic	Even harmonic
415 V	5	4	2
6.6 kV and 11 kV	4	3	1.75
33 kV and 66 kV	3	2	1
132 kV	1.5	1	0.5

4.14 Conclusion

In this chapter, general classification of PQ issues, long-duration and short-duration voltage oscillations, their problems in the electrical network and their direct and indirect impact on network equipment and consumers, as well as traditional solutions to reduce their impact in different situations are examined. Also, all PQ indices, the problems caused by the continuity of these indexes, and their negative effects in the long and short term are comprehensively examined. Then, the main and important indexes of PQ such as voltage sag, voltage swell, under voltage, and harmonics are investigated that shows these indexes are the greatest destructive effect on power grids and therefore, they are considered as the main basis of the objective function in this research, which are discussed in chapters 5 and 6.

Chapter 5. Problem Formulation

5.1 Introduction

In this chapter, formulation of optimal designing and placement of a battery storage-based photovoltaic-wind turbine HDG (PVWTBAHDG) system is presented to enhance power quality (PQ) indices of distribution systems. At first, design of PVWTHDG with PV, WT and storage models is described. Then objective function of the problem with the constraints is described. The structure optimization algorithm and its implementation steps used in solving the problem are presented.

5.2 Problem Formulation

5.2.1 HDG System Modeling

In this study, the HDG system including solar panels and wind turbines with battery storage and an inverter disconnected from the grid is shown in Fig.5.1. Designing a HDG system means determining the size of solar panels, wind turbines, and battery banks to minimize the cost of energy generation and fully supply the HDG system load [16].

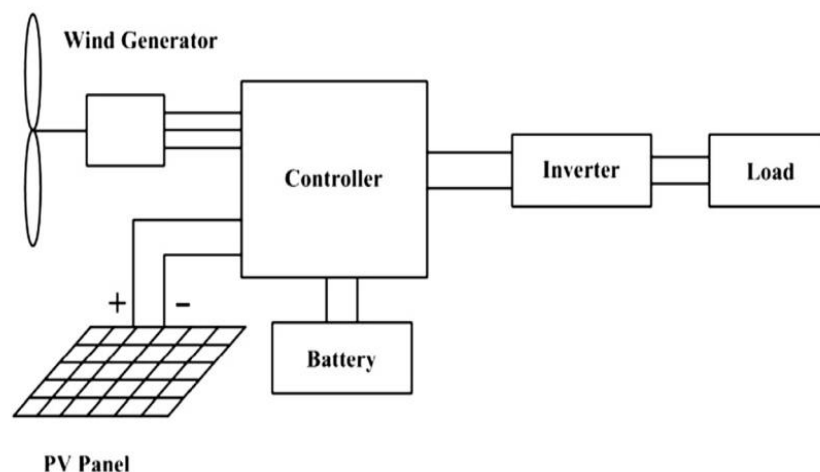


Fig. 5.1. The off-grid HDG system under study [16].

The following scenarios describe how to use the HDG system connected to the distribution network:

- The supply (overall energy generation) and demand (load) are equal. In this case, the whole power output of RESs meets the load through the inverter.
- The supply is greater than the demand. In this case, the excess output power of wind and PV units is stored in battery storage systems. When the injected power exceeds the maximum battery level, power output of HDG supplies the distribution network.

- The overall energy produced by RES is less than the demand. Under these conditions, the shortage of load demand is supplied by the battery. If the nominal capacity of the battery is less than the shortage, the load should be curtailed, leading to the load outage.

The output power of each PV panel according to the irradiation is calculated in (5.1) [90]:

$$P_{PV} = P_{PV,Rated} \left(\frac{G}{1000} \right) * [1 - k (T_C - T_{Rated})] \quad (5.1)$$

where, G represents the irradiation (W/m^2), $P_{PV-rated}$ shows the nominal power of individual PV arrays assuming $G = 1000 \text{ W/m}^2$. T_C And T_{Rated} refer to PV temperature and rated temperature. The Maximum Power Point Tracking (MPPT) is generally employed in solar systems so to extract the maximum output power.

Wind energy is one of the most important RESs. The primary positive points about it are the lack of greenhouse gas emission and being cost-effective. Considering a wind turbine, its generator starts up when the speed of wind exceeds V_{cut-in} . In the case wind speed is greater than the nominal speed of the wind turbine, the output power is constant, and if the wind speed exceeds $V_{cut-off}$, then the wind turbine generator is stopped for protection reasons. The output power of a wind generator is determined based on V_{cut-in} and $V_{cut-off}$, and its rated power (P_{Rated}) is calculated according to the wind speed [90]:

$$P_{WT} = \begin{cases} 0 & v \leq V_{ci} \text{ or } v \geq V_{co} \\ P_{Rated} \times \frac{v - V_{ci}}{V_r - V_{ci}} & V_{ci} \leq v \leq V_r \\ P_{Rated} & V_r \leq v \leq V_{co} \\ 0 & v \geq V_{co} \end{cases} \quad (5.2)$$

where, v is the wind speed. V_{ci} , V_{co} and V_r indicate the cut-in, cut-off and rated speeds of the wind turbine. P_{Rated} represents the rated power of the wind turbine generator.

Hybrid power systems utilize battery banks to store or supply electricity in the event of a shortage of power produced by wind turbines and/or PV panels. Because of the stochastic nature of PV arrays and wind turbines, capacity of the battery bank varies continuously in the hybrid system, and the State of Charge (SOC) of the battery can be stated as [90]:

- If the sum of output powers of solar cells and wind turbines exceeds the demand, the battery bank operates in the charging mode. The amount of charge of the battery bank at time t will be:

$$SOC(t) = SOC(t-1) + \left(\frac{P_{Bat}(t)}{V_{bus}}\right) * \Delta t \quad (5.3)$$

$$P_{Bat}(t) = P_{PV}(t) + P_{WT}(t) - P_{Load,HDG}(t)/\eta_{Inv} \quad (5.4)$$

where, $P_{Bat}(t)$ is the input / output power of the battery (positive for charging states, and negative for discharging states), V_{bus} is the DC bus voltage (V) and Δt shows the simulation time step and is set to 1 hour [168]. η_{Inv} indicates the efficiency of the inverter. Also, in this study, SOC_{min} is 20% of battery maximum size and SOC_{max} is set on 100% [90].

- If the output powers of solar cells and wind turbines are smaller than the load, the battery is in the discharging mode. Therefore, the amount of battery charge at time t will be as follows:

$$SOC(t) = SOC(t-1) + \left(\frac{P_{Bat}(t)}{V_{bus}}\right) * \Delta t \quad (5.5)$$

$$P_{Bat}(t) = P_{Load,HDG}(t)/\eta_{Inv} - P_{PV}(t) - P_{WT}(t) \quad (5.6)$$

5.2.2 Objective Function

In the PVWTBAHDG system, battery storage is used for continuous generating and supplying the load demands of the distribution system. The present study aims at determining the optimal decision making factors of the problem, including the optimal size and location of the PVWTBAHDG system, such as the optimal capacity of solar panels production, wind turbines and battery storage capacity, so that it improves PQ indices with respect to network operation constraints and PQ constraints. Furthermore, the reduction in network loss and the cost of using the PVWTBAHDG system, including initial investment costs and maintenance costs, should be considered in the problem-solving process for system design. Therefore, the main goal of the problem is to enhance PQ of the distribution network by minimizing network losses and the cost of using the PVWTBAHDG system. The PVWTBAHDG system is seen from the distribution network as a power source, so it is appropriate to determine its desired location to make its benefits maximized. So, two problems are solved simultaneously. The first problem is the design of the PVWTBAHDG system, whose function is to minimize energy costs, which is considered in this constraint process for each PVWTBAHDG system. The second problem is the improvement of PQ indices and reduction of distribution network

losses by taking into account network operation constraints. Hence, two problems were solved simultaneously by the HCSADE method. In other words, the optimal location and size of the PVWTBAHDG are determined to minimize energy costs and improve PQ indices in the radial network. The suggested approach has been tested on an unbalanced 33-bus system. The problem is carried out in the form of a multi-objective optimization problem. Also, the obtained findings are evaluated before and after optimizing the HDG system in the network. Additionally, a comparison has been made between the performance of HCSADE method in problem solving with conventional CAS and particle swarm optimization (PSO) methods. To validate the suggested method, its results and those of previous studies were compared.

The general objective function of the problem is defined as follows:

$$OF = W_1 \left(\frac{C_{HDG}}{C_{HDG,max}} \right) + W_2 \left(\frac{P_{loss}}{P_{loss,max}} \right) + W_3 \left(\frac{V_{sag}}{V_{sag,max}} \right) + W_4 \left(\frac{V_{swell}}{V_{swell,max}} \right) + W_5 \left(\frac{V_{THD}}{V_{THD,max}} \right) + W_6 \left(\frac{V_{unb}}{V_{unb,max}} \right) \quad (5.7)$$

In (5.7), C_{HDG} and P_{loss} show the energy generation costs of the HDG system and the power losses of the network. V_{sag} , V_{swell} , V_{THD} and V_{unb} denote the voltage sag, voltage swell, THD of bus voltages and voltage unbalance of the network. Moreover, $C_{HDG,max}$, $P_{loss,max}$, $V_{sag,max}$, $V_{THD,max}$, $V_{unb,max}$ are the maximum values of the above-mentioned parameters. W_1 , W_2 , W_3 , W_4 , W_5 and W_6 are the weighting coefficients of the functions corresponding to power losses, energy generation cost, voltage sage, voltage swell, THD of bus voltages and voltage unbalance of the network, respectively.

In this subsection, the formulation of the energy generation cost (C_{HDG}) is presented. The design objective function of the HDG is formulated in the form of the sum of investment cost and maintenance and operation costs of the component, including solar panels (C_{PV}), wind turbines (C_{WT}) and batteries (C_{Bat}) as follows:

$$C_{HDG} = C_{PV} + C_{WT} + C_{Bat} \quad (5.8)$$

$$C_{PV} = C_{PV-inv} + C_{PV-O\&M} \quad (5.9)$$

$$C_{WT} = C_{WT-inv} + C_{WT-O\&M} \quad (5.10)$$

$$C_{Bat} = C_{Bat-inv} + C_{Bat-O\&M} \quad (5.11)$$

where, C_{PV} , C_{WT} , and C_{Bat} represent the energy generation cost of the HDG caused by solar panels, wind turbines, and batteries, respectively. Also, C_{PV-inv} , C_{WT-inv} , and

$C_{Bat-inv}$ are the initial investment costs due to purchase of solar panels, wind turbines, and batteries, respectively. Additionally, $C_{PV-O\&M}$, $C_{WT-O\&M}$ and $C_{Bat-O\&M}$ denote the maintenance and operation costs per kW/kAh of capacity of solar panels, wind turbines and batteries, respectively.

Power losses consist of the power lost in the resistance of the network lines due to the current flow and can be shown using equations (5.12) – (5.14) [14-15]:

$$P_{LOSS} = RI^2 \quad (5.12)$$

$$I_K = (V_i - V_j) / (R_K + j X_K) \quad (5.13)$$

$$P_{LOSS} = \sum_{K=1}^{N_b} I_K^2 \quad (5.14)$$

where, R is the resistance of the considered lines and I is the flowing current. Also, R_k and X_k are the resistance and reactance of the k -th line, and N_b shows the number of lines. The line k is between buses i and j .

This ate the average voltage drop on all buses and thus reduce voltage drop in the whole system. Voltage sag is determined through sensing the residual voltage of a given bus when voltage drop occurs according to (5.15) [6]:

$$V_{sag,av} = 1/m \sum_{j=1}^m (1/n \sum_{i=1}^n V_i^j) \quad (5.15)$$

In (5.15), V_i^j shows the voltage of bus i when a fault occurs at bus j . Also, i denotes the bus number and j indicates the number of faults that are likely to happen, and $V_{sag,av}$ shows the average bus voltages under voltage drop situations.

The voltage swell is determined by measuring the residual voltage ((5.15)) and increase in RMS Voltage.

The harmonic distortion is calculated using the THD of bus voltages according to (5.16) [6]:

$$\%V_{THD,i} = \frac{V_{d,i}}{V_{rms,i}} * 100 \quad (5.16)$$

where,

$$V_{rms,i} = \sqrt{V_{1,i}^2 + V_{d,i}^2} \quad (5.17)$$

where, $V_{d,i}$ is the distortion component of the bus voltage and is obtained from (5.18) [6]:

$$V_{d,i} = \sqrt{\sum_{h=1}^m V_{h,i}^2} \quad (5.18)$$

Network unbalanced conditions is due to unbalanced loads. In this study, the unbalanced level of the network is calculated by measuring the unbalanced bus voltages [6]:

$$V_{unb,av} = 1/n \sum_{i=1}^n (\sum_{j=a}^c (100 | \frac{V_{neg,i}}{V_{pos,i}} |)) \quad (5.19)$$

where,

$$V_{pos,i} = \frac{1}{3} (V_i^a + \alpha_1 V_i^b + \alpha_2 V_i^c)$$

$$V_{neg,i} = \frac{1}{3} (V_i^a + \alpha_2 V_i^b + \alpha_1 V_i^c) \quad (5.20)$$

$$\alpha_1 = \text{complex} (-0.5, 0.866)$$

$$\alpha_2 = \text{complex} (-0.5, -0.866)$$

$V_{pos,i}$ gives the positive sequence voltage at bus i , $V_{neg,i}$ denotes the negative sequence voltage at bus i , and V_i^j shows the j -th phase voltage of the i -th bus.

5.2.3 Constraints

Solving the optimization problem is accompanied by a series of technical constraints that should be followed in the implementation of the optimization process. These constraints can be described as follows:

- Power balance during the day [11]:

$$\sum_{t=1}^{24} P_{slack}^h + P_{PV}^t + P_{WT}^t + P_{Bat}^t - P_{D-HDG}^t - P_{loss}^h - P_{D-DN}^h = 0 \quad (5.21)$$

- Satisfying the constraints of the solar panel and the wind turbine:

$$0 < P_{PV} < P_{PV}^{max} \quad (5.22)$$

$$0 < P_{WT} < P_{WT}^{max} \quad (5.23)$$

- Satisfying the charging and discharging conditions:

$$SOC_{min} < SOC_t < SOC_{max} \quad (5.24)$$

- Satisfying the bus voltages:

$$V_{min} < V < V_{max} \quad (5.25)$$

- Satisfying the line powers:

$$F_b < Limit_b \quad (5.26)$$

where, $P_{PV}^t, P_{WT}^t, P_{Bat}^t, P_{D-HDG}^t, P_{slack}^h$ and P_{D-DN}^h show the generated power by solar panel, wind turbine, battery, power consumption of the HDG, power supplied from the main substation and distribution system load at hour t, respectively. Furthermore, $P_{PV}^{max}, P_{WT}^{max}, SOC_t, SOC_{min}, SOC_{max}, V, V_{min}, V_{max}, Limit_b,$ and F_b are the maximum generated power by solar panel, maximum generated power by wind turbine, battery charging conditions, maximum and minimum battery charging conditions, bus voltage, minimum and maximum bus voltages, the power flowing for line b, and the thermal limit of line b respectively.

5.3 Suggested Optimization Technique

The current chapter presents the optimal sizing and allocation of distribution network battery storage based- PVWTHDG system to enhance PQ by using the HCSADE algorithm [18-21]. The emergence of hybrid meta-heuristic Crow Search Algorithm (CSA) dates back to 2016. Proposed by Asgharzadeh, the CSA was inspired by social and intelligent behavior of crows [165]. The CSA algorithm is formulated based on the intelligent behavior of crows, particularly during foraging and searching for food sources. To prevent the CSA from trapping in local optima and to increase the convergence speed of the algorithm when dimension of the problem is increased, crossover and mutation operators of the DE method are utilized so that the performance of the proposed method in problem solving is improved.

5.3.1 Overview of Proposed Hybrid Crow Search Algorithm Differential Evolution (HCSADE)

CSA as a novel meta-heuristic algorithm which imitates the smart social behavior of crows was proposed by Askarzadeh [18]. Crows are assumed as the most brilliant birds and they owe this to their large brain with respect to the size of their body. Crows' brains

are slightly smaller than human brains and this helps them to be smart and remember shapes and figures and alert the rest of crows in the face of a threat. Additionally, crows have the ability to remember where they collected some piece of food source several weeks or even months before. They conceal food from other birds and animals and reach that in the case of emergency when they desire to feed. As crows are voracious, they track other crows hoping to discover new sources of food, although it is not a simple task. Two cases can appear when one crow furtively follows another crow: a) the crow is unaware of being tracked by another crow, and b) it is aware of it. In the first case, the follower ultimately will discover the food place. Hence, the search action starts in a local site. In the second case, a random place will be produced, and the search space appears in a general area [18]. The structure of the CSA is illustrated in Fig. 5.2.

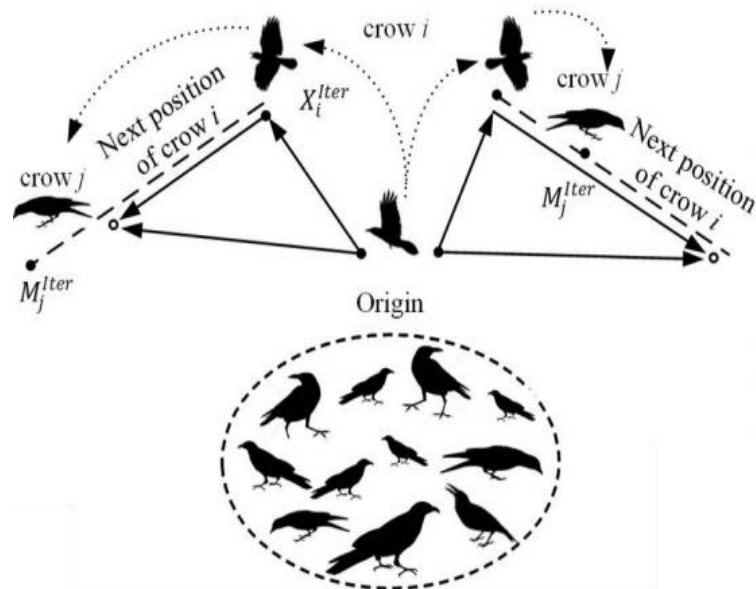


Fig. 5.2. Structure of CSA [18].

If N denotes the number of crows, the position of crow i in iteration $iter$ can be calculated [18]:

$$X^{i,iter} = (i=1, 2, \dots, N; iter= 1,2,\dots, iter_{max}) \quad (5.27)$$

In (5.27), $X^{i,iter} = [x_1^{i,iter}, x_2^{i,iter}, \dots, x_d^{i,iter}]$, $iter_{max}$ gives the maximum number of iterations needed and d denotes a ruling variable. The memory of one given crow will store one of the best experiences the crow has faced with. In iteration $iter$,

$m^{i,iter}$ represents the position the crow remembers. As mentioned before, any given crow attempts to track and follow other crows, hoping to discover new food caches.

The position of crow i is updated through choosing a crow (crow j) in a random manner at each iteration. By doing so, $m^{j,iter}$ shows the memory of crow j when followed by crow i .

The CSA commences using a set of random solutions. Next, the optimal solution in the search space is found via updating the memory. Also, if the awareness probability (AP) is known, the new position of the crow will be obtained. Parameters employed in the CSA include the flight length (FL) and AP. Fig. 5.3 illustrates the flowchart of the CSA.

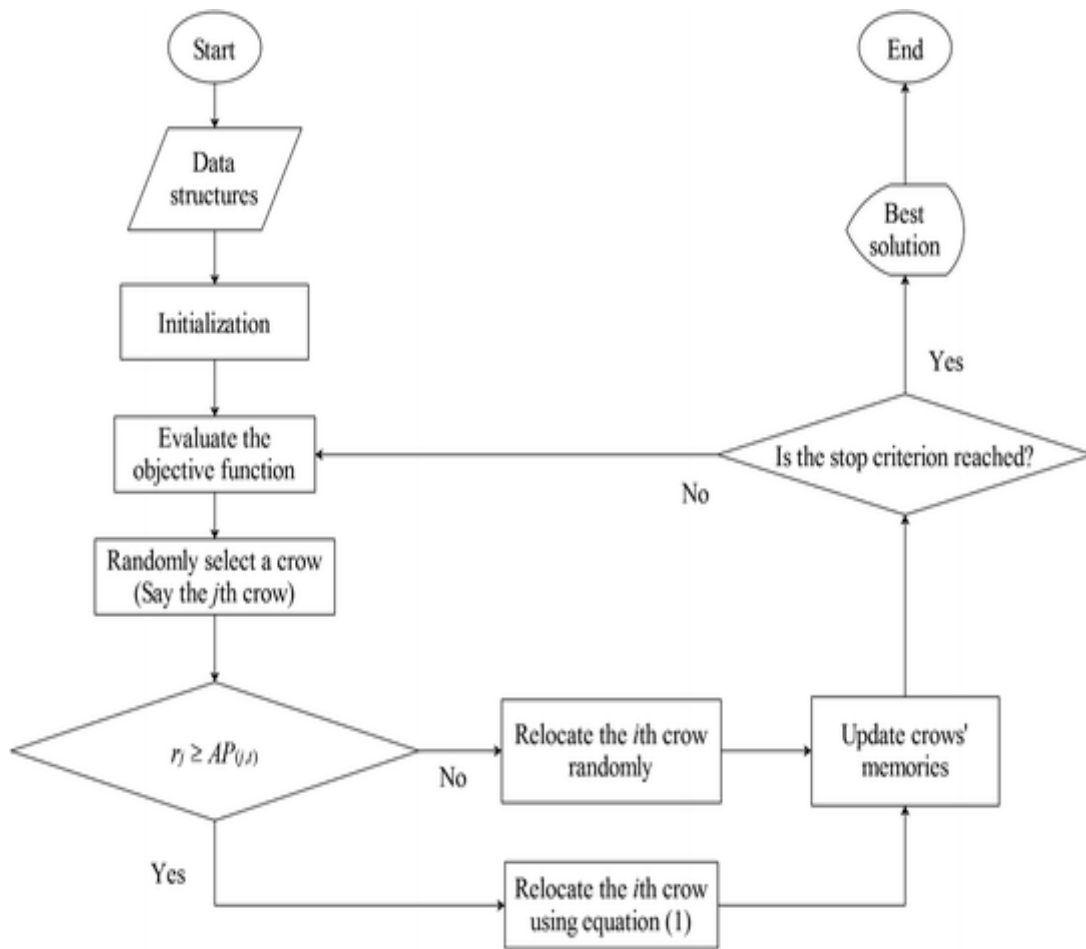


Fig. 5.3. The flowchart of CSA

Two steps observed in the CSA are described as follows:

- **Step 1:** Crow i tracks crow j while the latter is unaware of being tracked. The position of the former crow is updated by (5.28) [18]:

$$x^{i,iter+1} = x^{i,iter} + r_i \times FL^{i,iter} \times (m^{j,iter} - x^{i,iter}) \quad (5.28)$$

- **Step 2:** Crow i tracks crow j while the latter is aware of the situation. Crow j tries to mislead crow i using random moves within the search space.

Regarding steps 1 and 2, the positions of the crows are updated using (5.29) [18]:

$$x^{i,iter+1} = \begin{cases} x^{i,iter+1} + r_i \times FL^{i,iter+1} \times (m^{j,iter+1} - x^{i,iter}) & r_j \geq AP^{i,iter+1} \\ a \text{ random position} & \text{otherwise} \end{cases} \quad (5.29)$$

where, $x^{i,iter+1}$ shows the present position of a crow, r_i and r_j denote random numbers in a uniform distribution range of zero to one. Also, FL represents the flight length, $m^{j,iter+1}$ gives the hiding place, and AP provides the awareness probability [18]. The HCSADE method makes it possible to explore the search space and exploit allowed areas containing the optimal solution. However, the CSA method is less likely to quickly converge in larger scale optimization problems and it might get trapped in local optima. The suggested approach solves the challenges the optimization method encounters as the dimension of the problem is increased. Achieving coverage within the search space and reaching the global optimal point are among the objectives of the problem. The proposed algorithm starts randomly with the generation of primary population randomly and the CSA is used which has a good potential to balance between the exploration and exploitation. The CSA helps to the proposed algorithm to explore the search space and exploit the promising area, which has an appropriate answer. However, in large-scale optimization issues, early convergence and localized trapping of the CSA approach is an important challenge. This can be solved by dividing the population into sub-populations. Therefore, the goal is to ensure appropriate convergence in achieving global optimization. As stated, the population of the algorithm is divided into sub-populations or groups. Each group includes a certain number of populations related to the search process. The population of the algorithm is classified according to $P_{i,j}$ ($i = 1, \dots, v; j = 1, \dots, \eta$) to different groups. Here, operators of the differential evolution (DE) method are used for each population group to increase the search diversity and avoid the unpredictable convergence of the CSA method. The DE method uses a crossover operator for pairing (individuals) and mutation operator that randomly modify the content of individuals to promote diversity for the generation of new individuals. The crossover operator mimics mating in bio-communities. This operator passes the characteristics of good survival plans from the current population to the future population, which, on average, has a better fit.

The mutation operator also improves diversity in demographic characteristics. The mutation operator allows searching the entire space and preventing the trapping of the algorithm at the local minimum. Thus, with increasing population diversity based on the crossover and mutation operators, the challenges of untimely convergence and localized trapping of the traditional CSA method have been solved.

5.3.2 Using HCSADE for Problem Solution

Fig. 5.4 illustrates the flowchart of the HCSADE.

The steps of the HCSADE for problem solving can be summarized as follows:

Step 1) Initiate parameters of flock size, iteration maximum number, FL and AP and crossover mutation probability Pc and Pm

Step 2) Evaluate the crow memory at the first iteration by evaluating the first positions of crows.

Step 3) Calculate objective function values for individual crows.

Step 4) Employ Eq. (5.29) to find new positions of individual crows.

Step 5) Update positions of crows if the new positions are located inside the search area.

Step 6) Calculate objective function values for new updated positions.

Step 7) Utilize crossover and mutation operators to update population groups and improve the solution. Substitute the old solution with the new solution provided that the new solution (fitness) is better.

Step 8) Update the HCSADE memory. (5.29) represents an updated memory of the crows provided that crows discover a better position than that recorded in their memories [18]:

$$m^{i,iter+1} = \begin{cases} x^{i,iter+1} & f(x^{i,iter+1}) \text{ is better than } f(m^{i,iter}) \\ m^{i,iter} & \text{otherwise} \end{cases} \quad (5.30)$$

where, $f(x, y)$ is the value of objective function.

Step 9) Establishment of new positions by crows is not terminated until the maximum value of $iter_{max}$ is reached. If the best obtained solution is selected as an optimal solution go to *step 10*; otherwise, steps 4 to 8 are repeated.

Step 10) Stop the HCSADE and print the optimal results.

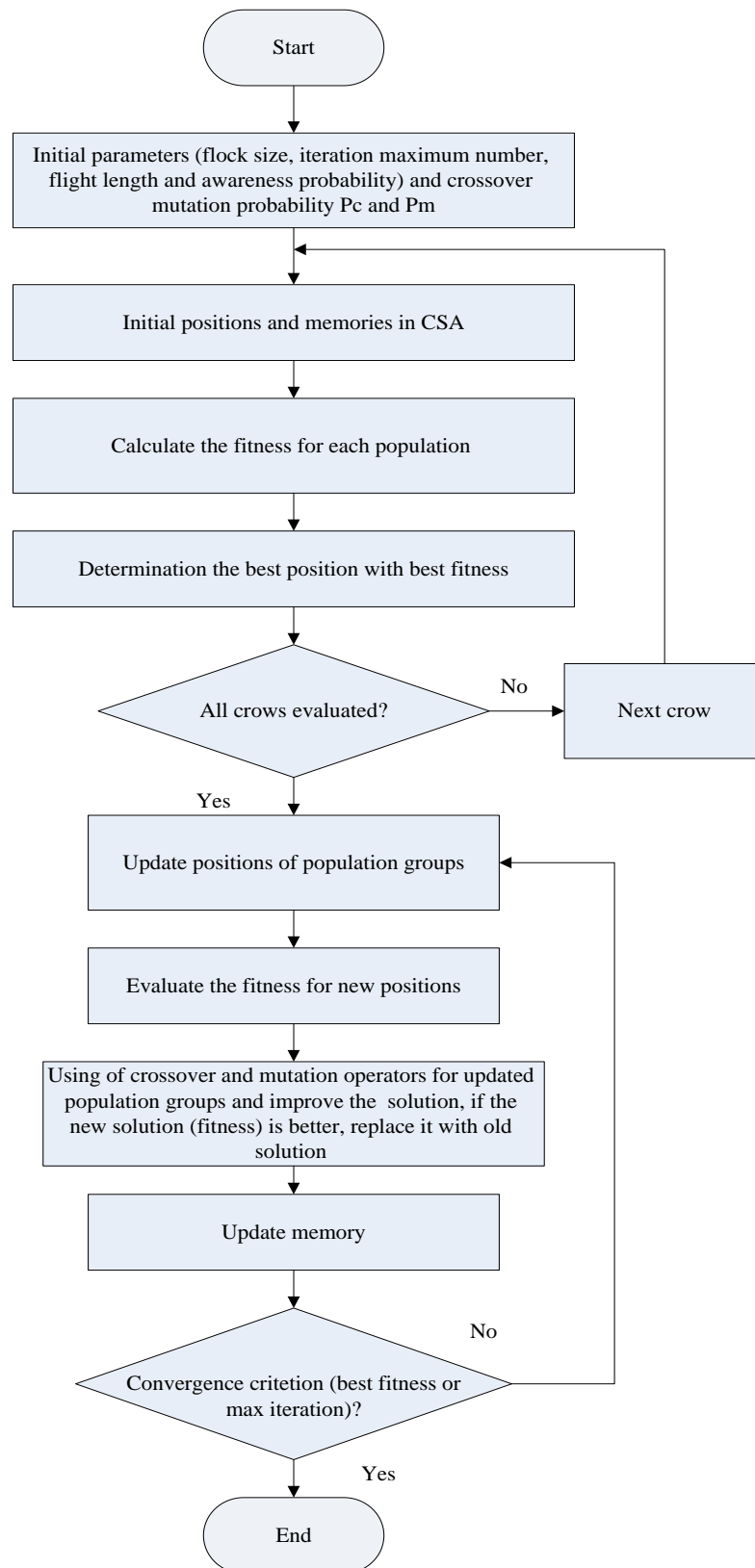


Fig. 5.4. The flowchart of HCSADE

5.4 Conclusion

In this chapter, problem formulation of PVWTBAHDG placement is described in distribution system to improve power quality. Also, this chapter provides the objective function and constraints of the problem. The overview of the proposed optimization algorithm and its implementation procedure for problem solving is presented as well.

Chapter6. Simulation Results and Discussions

6.1 Introduction

In this chapter, simulation results of optimal placement of a photovoltaic-wind-battery hybrid distributed generation (PVWTBAHDG) system in unbalanced 33-bus distribution system is presented with the aim of power quality (PQ) improvement by using HCSADE algorithm. The simulation results are presented in different single and multi-objective scenarios. The effect of the optimally placed HDG system to improve network power quality has been evaluated. The capability of the proposed optimization method is also compared to other methods. The effect of the optimally placed HDG in the network with network load changes has also been studied.

6.2 Simulation Results

6.2.1 The Proposed Distribution System

In this subsection, the simulation results of the design and placement of a HDG system based on solar panels and wind turbines with battery storage are proposed to improve the PQ indices in an unbalanced 33-bus radial distribution network. In the 33-bus system, the total active power consumption of the network is 3.72 MW and the reactive power is 2.3 MVar. The system consists of 33-bus and 37 branches supplied by a 12.6 kV transmission system. The 33-bus IEEE standard single-line diagram is shown in Fig. 6.1 [153].

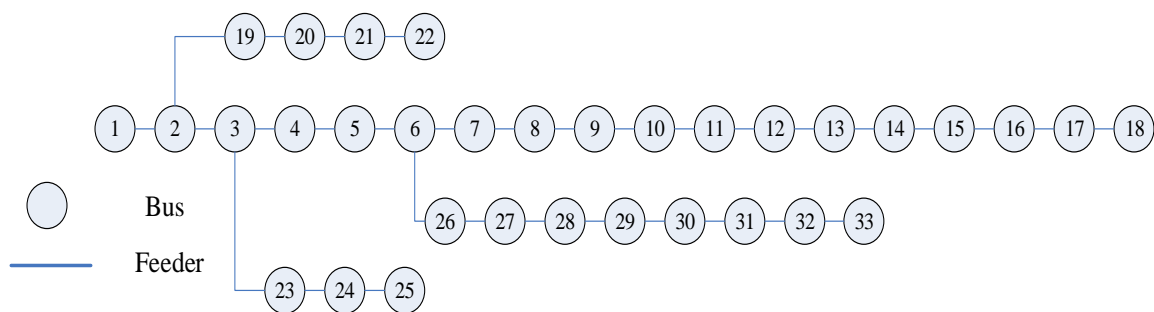


Fig. 6.1. 33-bus IEEE standard (unbalanced) distribution network [153].

6.2.2 Load, Solar and Wind Profile

In the 33-bus network, the total active and reactive power consumption is 3720 kW and 2300 kVAr, respectively. The 33-bus network has 37 branches. The 33-bus network has

a main branch and 3 sub-branches [153]. The variations in solar radiation, ambient temperature and wind speed are presented in Figs. (6.2) - (6.4). The PVWTBAHDG load curve with a 100 kW peak and normalized load of network are also shown in Figs. (6.5) - (6.6).

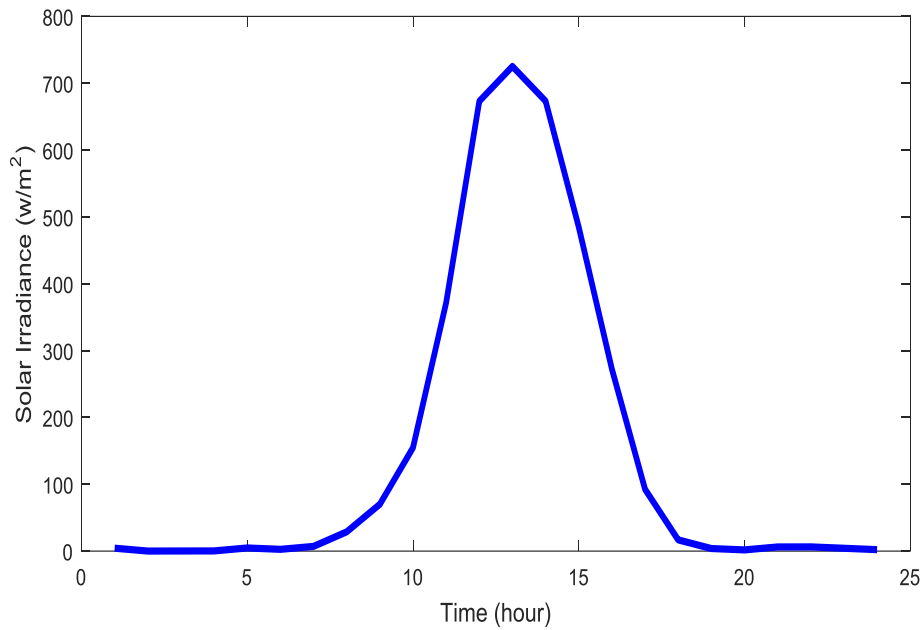


Fig. 6.2. Solar radiation curve for 24 hours

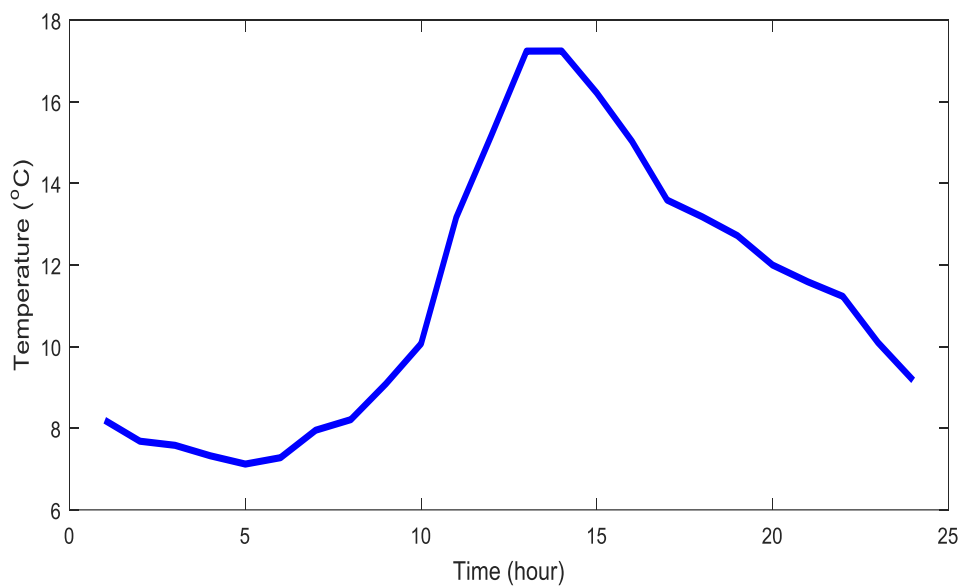


Fig. 6.3. Ambient temperature curve for 24 hours

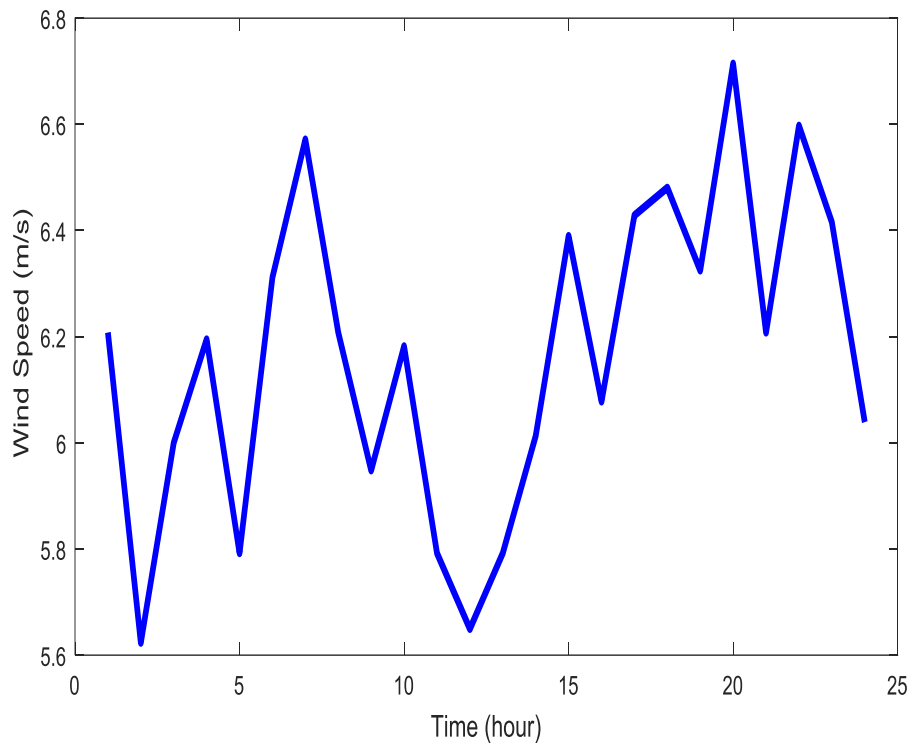


Fig. 6.4. Wind speed curve for 24 hours

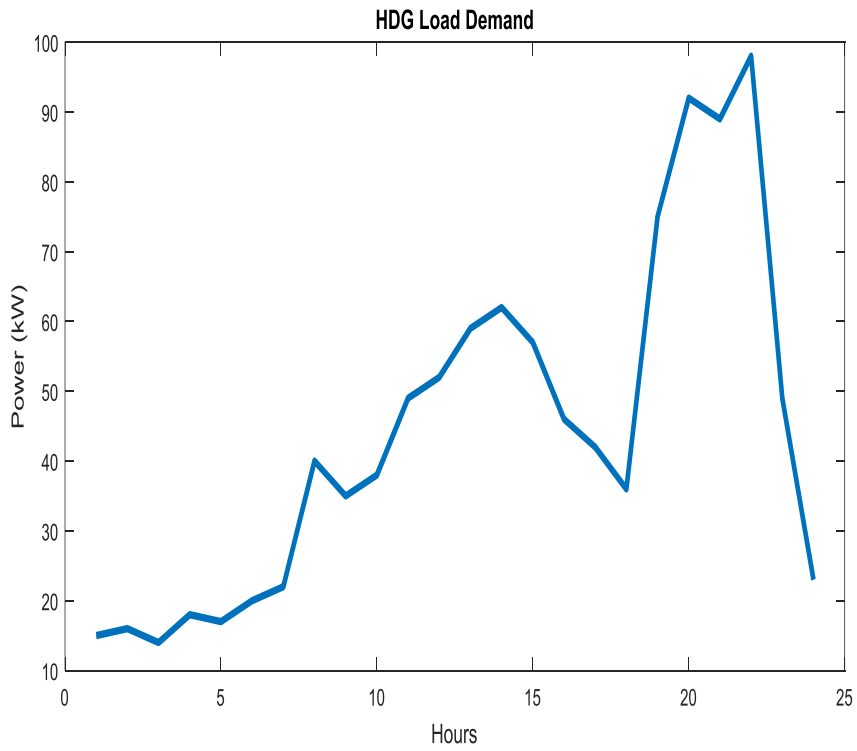


Fig. 6.5. Load demand of HDG for 24 hours

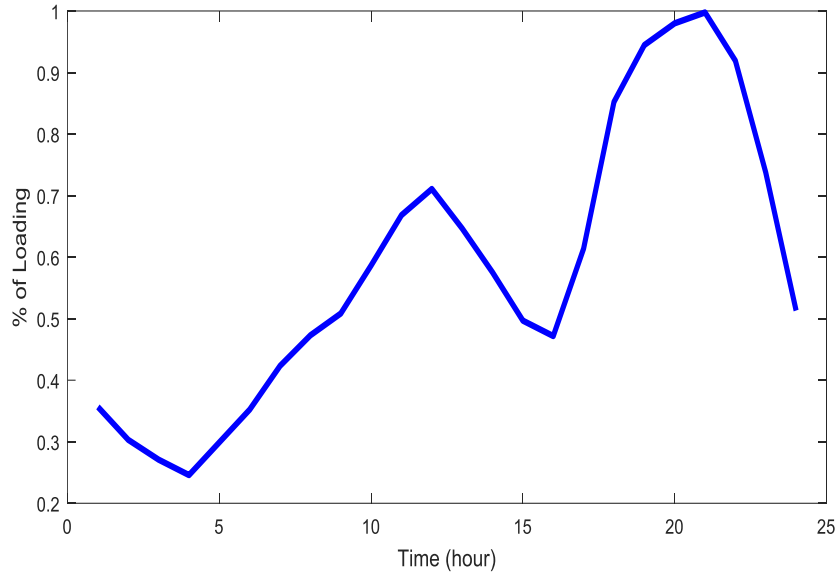


Fig. 6.6. Normalized load curve of 33- bus unbalanced network for 24 hours

6.2.3 Technical and Economic Data of HDG

The technical data for the PV panel, wind turbine and batteries are presented in the following tables, respectively. The technical and economic data of the components of the HDG system are also presented in Tables (6.1) - (6.4).

Table 6.1. PV panel data [90, 152]

Parameter	Value
Standard temperature (T_{STC})	25 ^{oc}
Standard radiation (G_{STC})	1000 w/m ²
Rated power ($P_{rated-PV}$)	1 kW
Temperature coefficient of PV (k)	-0.0037

Table 6.2. WT data [90, 152]

Parameter	Value
Rated power ($P_{rated-PV}$)	1 kW
Rated wind speed (V_{rated})	13
Cut in wind speed (V_{cutin})	4 m/s
Cut out wind speed (V_{cutout})	25 m/s

Table 6.3. Battery data [90, 152]

Parameter	Value
Rated capacity of battery ($P_{rated-Bat}$)	1 kAh
Battery voltage (V_{Bat})	12 V
Battery minimum capacity (SOC_{min})	0.2 kAh
DOD	80 %

Table 6.4. Economic data of system design [90, 152]

Parameter	PV	WT	Battery
Life time	20	20	5
Investment Cost (\$)	2000	3200	100
Operation and maintenance cost (\$)	33	100	5

6.2.4 Simulation Scenarios

The simulation strategies for designing and placement of HDGs in unbalanced 33-bus distribution network are presented as follows:

- **Scenario 1)** Single objective designing and placement of one HDG in unbalanced 33- bus distribution network
- **Scenario 2)** Multi objective designing and placement of one HDG in unbalanced 33- bus distribution network
- **Scenario 3)** Comparison of the single and multi- objective designing and placement of one HDG
- **Scenario 4)** Multi objective designing and placement of two HDG in unbalanced 33- bus distribution network
- **Scenario 5)** Comparison of the designing and placement of one and two HDG in unbalanced 33-bus distribution network
- **Scenario 6)** Performance evaluation of the proposed method (HCSADE) compared to CSA and DE methods
- **Scenario 7)** Impact of HDG load increasing on Multi objective designing and placement of one HDG

- **Scenario 8)** Impact of network load increasing on Multi objective designing and placement of one HDG
- **Scenario 9)** Multi objective designing and placement of one HDG combinations
- **Scenario 10)** Impact of battery cost variations on Multi objective designing and placement of one HDG
- **Scenario 11)** Impact of battery cost variations on Multi objective designing and placement of two HDG
- **Scenario 12)** Performance evaluation of the proposed method (HCSADE) compared to past research

6.2.4.1 Results of Scenario 1 (Single objective-one HDG)

In this subsection, the design and placement of HDG in an unbalanced 33- bus distribution network is presented as a single objective by using the HCSADE method for one HDG. Also, in each of the single-objective optimizations, the convergence curve of the HCSADE method and the design and placement results are presented.

- Results of minimum loss (min Ploss)

In this part, active power loss minimization is considered as the objective function of the HDG placement in unbalanced 33-bus distribution system. In Fig. 6.7, the convergence curve of the HCSADE method for optimal placement of one HDG in the unbalanced 33-bus network is presented. As can be seen, the proposed method has a loss of 322.647 kW. Numerical results of the HDG placement in the network are presented in Tables (6.5) - (6.6). The results show that with the optimal placement of the HDG system, power loss is decreased from 1655.28 kW for single phase (551.76 kW for single phase) in base network to 967.941 kW for single phase (322.647 kW for single phase). In addition, the results show that the voltage sag is decreased from 7.10 to 4.409, the voltage swell is decreased from 165.50 to 83.609, THD is decreased from 8.26 to 8.237 and the voltage unbalance is decreased from 34.98 to 34.327. The optimization program also determines that the optimum location for installing the HDG is selected as at bus 30 with 254 solar panels, 479 wind turbines and 603 batteries. Therefore, the results show a reduction in network losses and an improvement in PQ based on optimal HDG placement. Also, active power loss of unbalanced 33-bus network by considering the minimum (min) Ploss as objective function for three phases is illustrated in

Fig. 6.8 with and without HDG. According to Fig. 6.8, the power loss is decreased with optimal application of one HDG in the network.

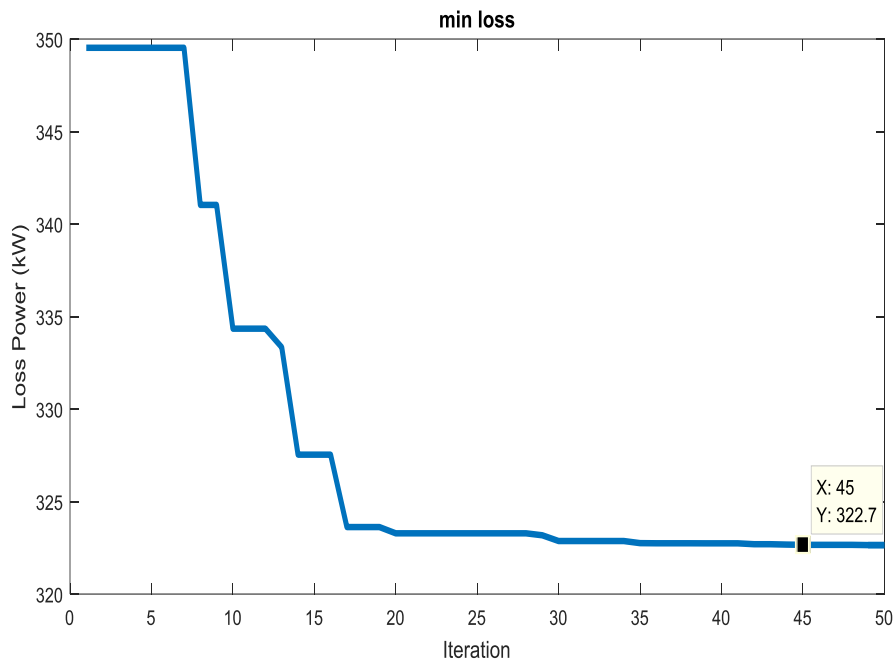


Fig. 6.7. Convergence curve of HCSADE by considering min Ploss objective function (one HDG)

Table. 6.5. Results of one HDG placement in unbalanced 33- bus network by considering min Ploss as objective function

Objective function	Ploss (kW)	$\sum V_{sag}$	$\sum V_{swell}$	$\sum THD$	$\sum Un$
Base Net	1655.28	7.10	165.50	8.26	34.98
min Ploss	967.941	4.409	83.609	8.237	34.327

Table 6.6. Optimal sizing and siting of one HDG in unbalanced 33- bus network by considering min Ploss as objective function

Objective function	PV Number	WT Number	Batt Number	Optimal Location (Bus)	Cost (M\$)
min Ploss	254	479	603	30	10.336

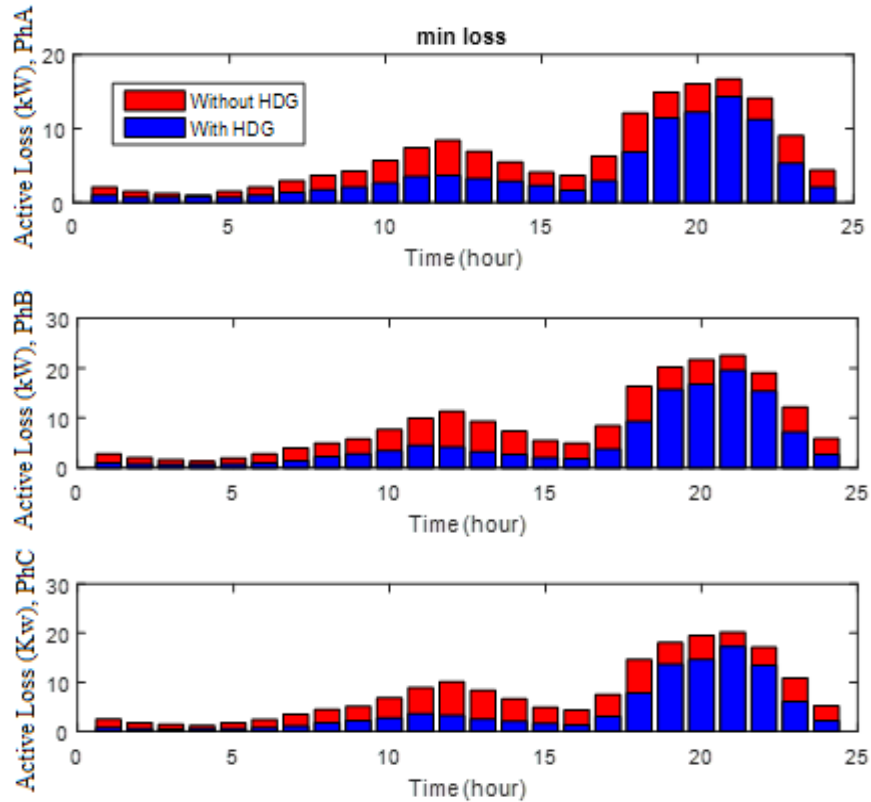


Fig. 6.8. Active loss of unbalanced 33- bus network by considering min Ploss as objective function (one HDG)

- Results of minimum voltage sag ($\min V_{sag}$)

In this part, the objective function of the HDG placement problem in unbalanced 33-bus network is considered as minimum voltage sag ($\min V_{sag}$). In Fig. 6.9, the convergence curve of the HCSADE method for optimal placement of the HDG system in the network is presented. As can be seen, the proposed method has a voltage sag value of 2.949. The numerical results of the HDG system application in the network are presented in Tables (6.7) - (6.8). The results show that with the optimal placement of the HDG system in the network the voltage sag decreased from 7.10 to 2.949 in the base network. In addition, the results show that the amount of power loss is increased from 551.76 to 978.837. The voltage swell index is decreased from 165.50 to 81.049, THD is decreased from 8.26 to 8.207 and voltage unbalance is decreased from 34.98 to 33.464. The HDG installation location is determined at bus 32 with 178 solar panels, 482 wind turbines and 545 batteries. Therefore, the results show an increase in network losses and improvement in PQ based on optimal HDG placement. The voltage sag curve is

also plotted in this simulation in Fig. 6.10, which results in a reduction of the voltage sag with the optimal placement of the HDG system.

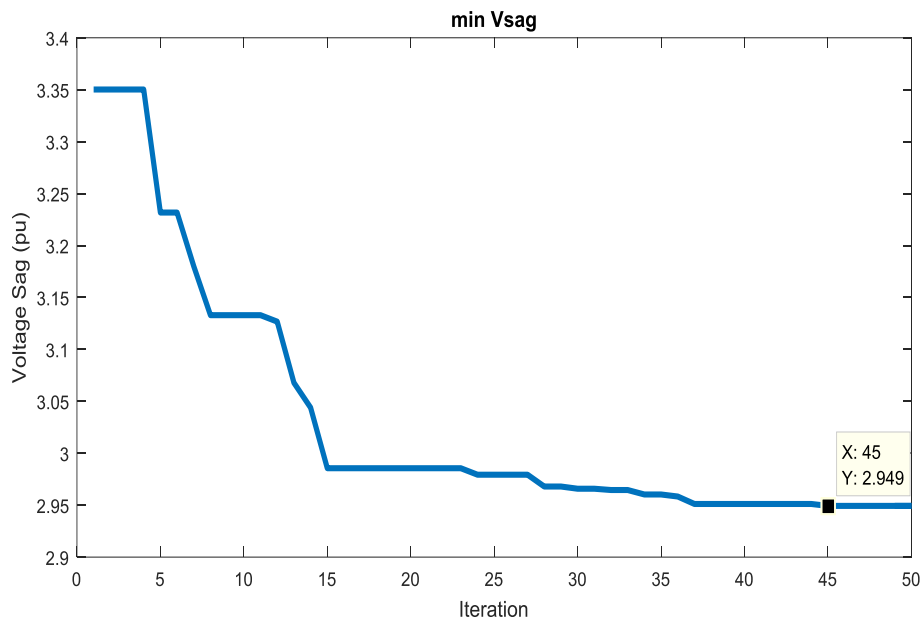


Fig. 6.9. Convergence curve of HCSADE by considering $\min V_{sag}$ as objective function (one HDG)

Table. 6.7. Results of one HDG placement in unbalanced 33- bus network by considering $\min V_{sag}$ as objective function

Objective function	Ploss (kW)	$\sum V_{sag}$	$\sum V_{swell}$	$\sum THD$	$\sum Un$
Base Net	1655.28	7.10	165.50	8.26	34.98
$\min V_{sag}$	2936.511	2.949	81.049	8.207	33.464

Table 6.8. Optimal sizing and siting of one HDG in unbalanced 33- bus network by considering $\min V_{sag}$ as objective function

Objective function	PV Number	WT Number	Batt Number	Optimal Location (Bus)	Cost (M\$)
$\min V_{sag}$	178	482	545	32	9.975

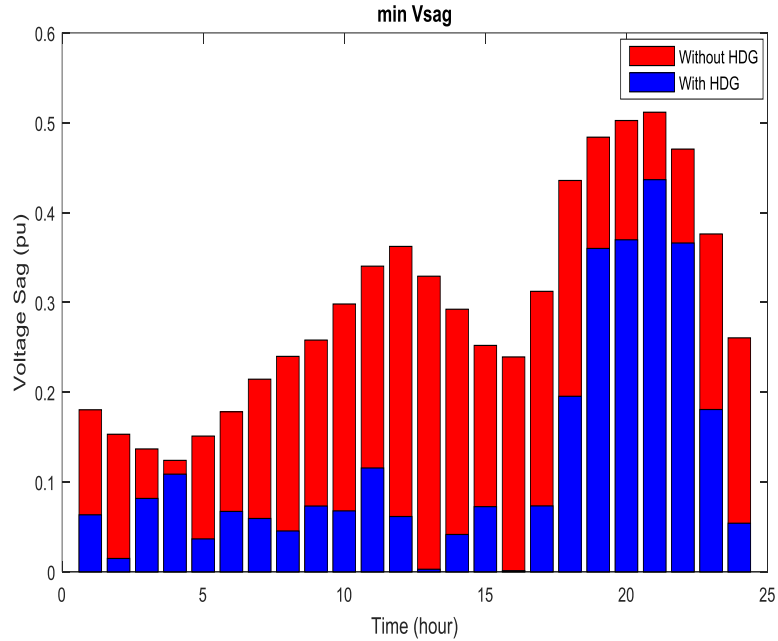


Fig. 6.10. Voltage sag of unbalanced 33-bus network considering $\min V_{sag}$ as objective function (one HDG)

- Results of minimum voltage swell ($\min V_{swell}$)

The objective function of the HDG placement problem in unbalanced 33-bus network is considered as voltage swell minimization in this subsection. In Fig. 6.11, the convergence curve of the HCSADE method for optimal placement of the HDG system in the network is presented. As can be seen, the proposed method has a voltage swell value of 70.545. The numerical results of the HDG system application in the network are presented in Tables (6.9) – (6.10). The results show that with the optimal placement of the HDG system in the network the voltage swell is decreased from 165.50 to 70.545 in the base network. In addition, the results show that the amount of power loss is increased from 551.76 to 5961 kW and voltage sag index also is increased from 7.10 to 10.232. THD is decreased from 8.26 to 7.918 and the voltage unbalance is decreased from 34.98 to 33.099. The HDG installation location is determined at bus 15 with 304 solar panels, 481 wind turbines and 233 batteries. Therefore, the results show an increase in network losses and voltage sag and an improvement in voltage swell, THD and voltage unbalance based on optimal HDG placement. The voltage swell curve is also plotted in this simulation in Fig. 6.12, which results in a reduction of the voltage swell with the optimal placement of the HDG system.

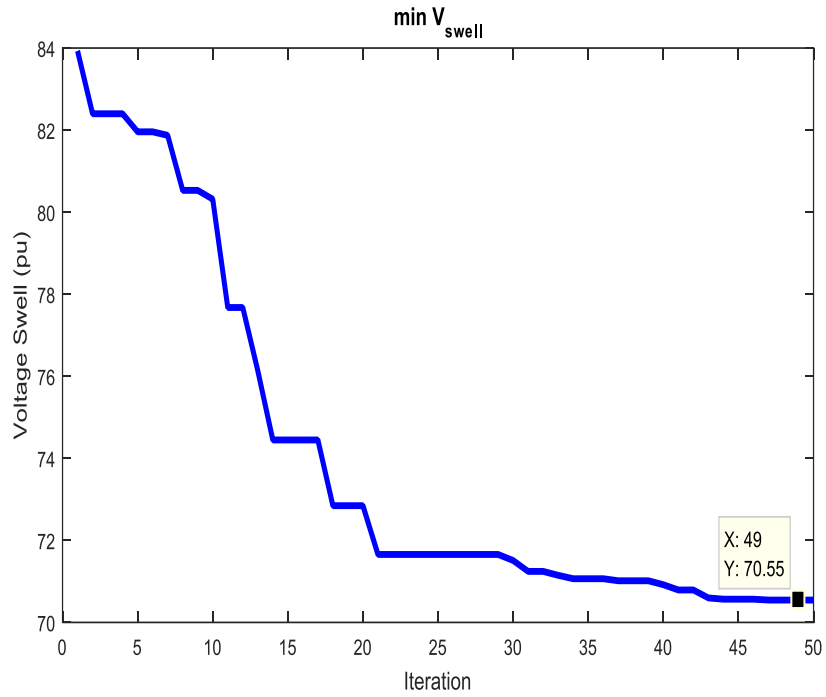


Fig. 6.11. Convergence curve of HCSADE by considering $\min V_{swell}$ as objective function (one HDG)

Table. 6.9. Results of one HDG placement in unbalanced 33-bus network by considering $\min V_{swell}$ as objective function

Objective function	Ploss (kW)	$\sum V_{sag}$	$\sum V_{swell}$	$\sum THD$	$\sum Un$
Base Net	1655.28	7.10	165.50	8.26	34.98
$\min V_{swell}$	5961	10.232	70.545	7.918	33.099

Table 6.10. Optimal sizing and siting of one HDG in unbalanced 33-bus network by considering $\min V_{swell}$ as objective function

Objective function	PV Number	WT Number	Batt Number	Optimal Location (Bus)	Cost (M\$)
$\min V_{swell}$	304	481	233	15	10.648

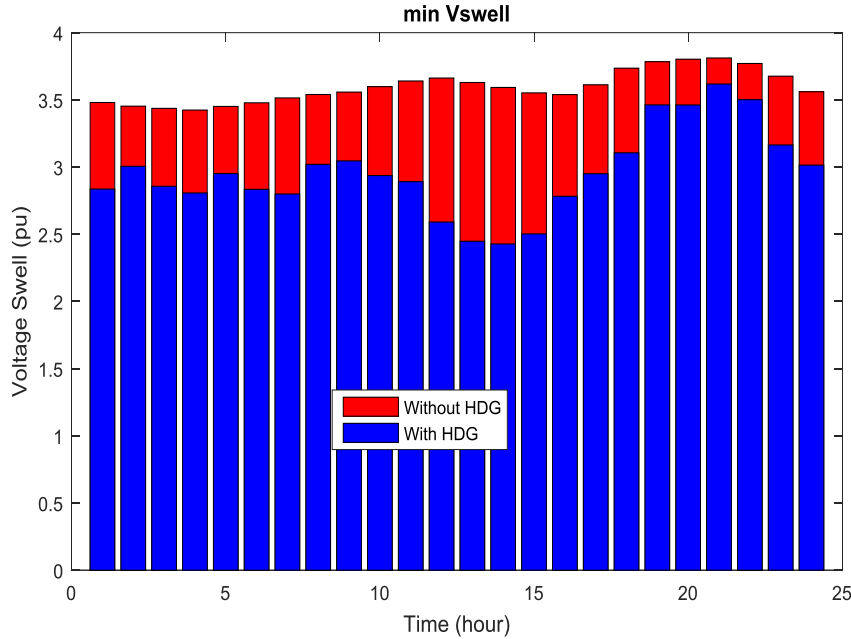


Fig. 6.12. Voltage swell of unbalanced 33-bus network considering $\min V_{\text{swell}}$ as objective function (one HDG)

- Results of minimum THD (min THD)

The THD minimization is considered as objective function of the HDG placement in unbalanced 33-bus network in this subsection. In Fig. 6.13, the convergence curve of the HCSADE method for optimal placement of the HDG system in the network is presented. As can be seen, the proposed method has a THD value of 7.907. The numerical results of the HDG system application in the network are presented in Tables (6.11) – (6.12). The results show that with the optimal placement of the HDG system in the network, the THD is decreased from 8.26 to 7.907 in the base network. In addition, the results show that the amount of power loss is increased from 1655.28? To 5889 kW and voltage sag index is also increased from 7.10 to 10.171. Voltage swell is decreased from 165.50 to 70.660 and voltage unbalance is decreased from 34.98 to 33.114. The HDG installation location is determined at bus 15 with 303 solar panels, 477 wind turbines and 444 batteries. Therefore, the results show an increase in network losses and voltage sag and improvement in voltage swell, THD and voltage unbalance based on optimal HDG placement. The THD curve for three phases is also plotted in this simulation in Fig. 6.14, which results in a reduction of the THD with the optimal placement of the HDG system.

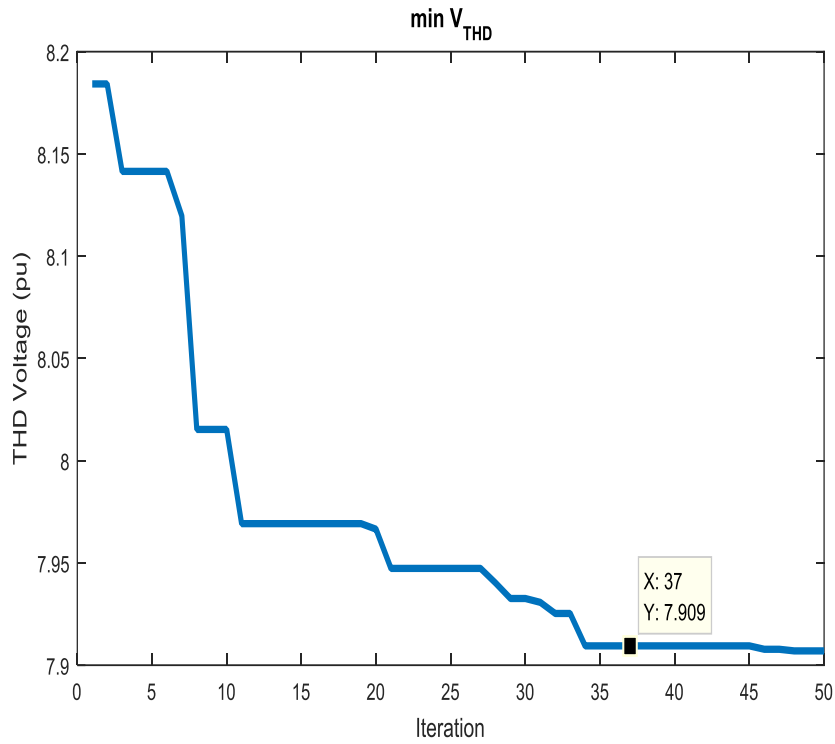


Fig. 6.13. Convergence curve of HCSADE by considering min THD as objective function (one HDG)

Table. 6.11. Results of one HDG placement in unbalanced 33- bus network by considering min THD as objective function

Objective function	Ploss (kW)	$\sum V_{sag}$	$\sum V_{swell}$	$\sum THD$	$\sum Un$
Base Net	1655.28	7.10	165.50	8.26	34.98
min V_{THD}	5889	10.171	70.660	7.907	33.114

Table 6.12. Optimal sizing and siting of one HDG in unbalanced 33- bus network by considering min THD as objective function

Objective function	PV Number	WT Number	Batt Number	Optimal Location (Bus)	Cost (M\$)
min V_{THD}	303	477	444	15	10.579

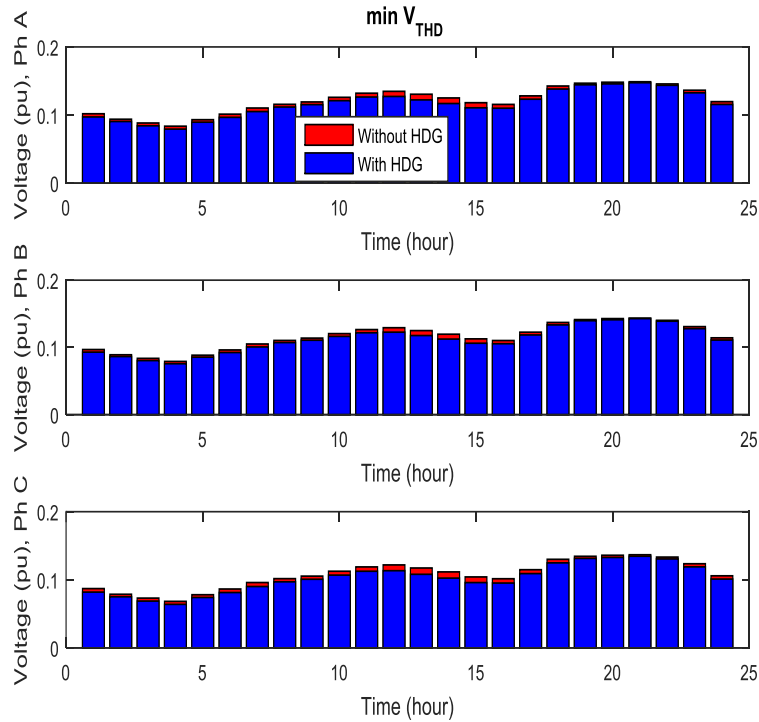


Fig. 6.14. Voltage THD of unbalanced 33-bus network by considering min THD as objective function (one HDG)

- Results of minimum voltage unbalance (min Un)

The voltage unbalance minimization is considered as objective function of the HDG placement in unbalanced 33-bus network in this subsection. In Fig. 6.15, the convergence curve of the HCSADE method for optimal placement of the HDG system in the network is presented. As can be seen, the proposed method has a voltage unbalance value of 31.672. The numerical results of the HDG system application in the network are presented in Tables (6.13) – (6.14). The results show that with the optimal placement of the HDG system in the network, the voltage unbalance is decreased from 34.98 to 31.672 in the base network. In addition, the results show that the amount of power loss is increased from 1655.28? To 6333 kW and voltage sag is decreased from 7.10 to 6.450. Voltage swell is decreased from 165.50 to 75.451. The HDG installation location is determined at bus 33 with 357 solar panels, 448 wind turbines and 692 batteries. Therefore, the results show an increase in network losses and improvement in voltage sag, voltage swell, THD and voltage unbalance based on optimal HDG placement. The THD curve is also plotted in this simulation in Fig. 6.16, which

results in a reduction of the voltage unbalance with the optimal placement of the HDG system.

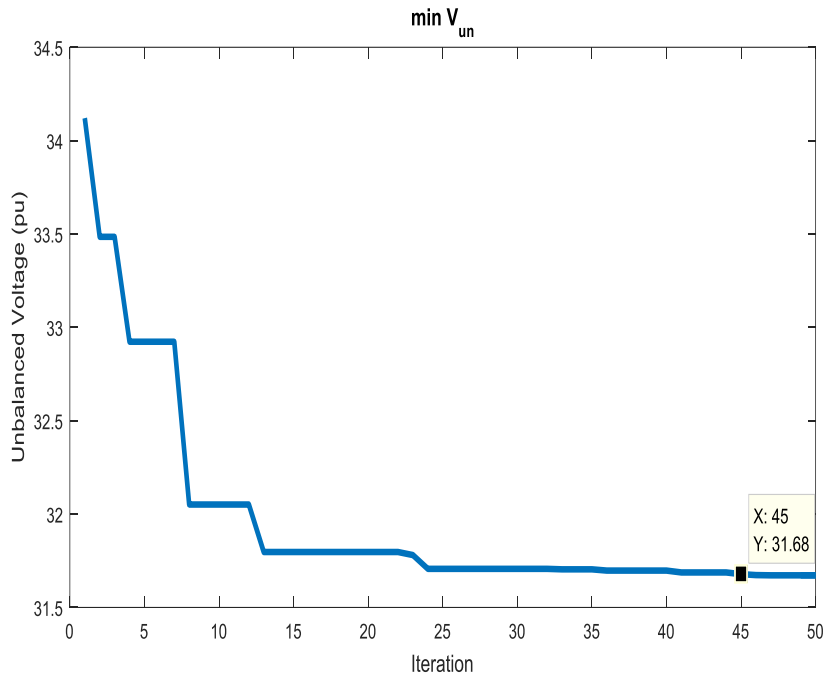


Fig. 6.15. Convergence curve of HCSADE by considering min U_n as objective function (one HDG)

Table. 6.13. Results of one HDG placement in unbalanced 33- bus network by considering min U_n as objective function

Objective function	Ploss (kW)	$\sum V_{sag}$	$\sum V_{swell}$	$\sum THD$	$\sum U_n$
Base Net	1655.28	7.10	165.50	8.26	34.98
min U_n	6333	6.450	75.451	8.145	31.672

Table 6.14. Optimal sizing and siting of one HDG in unbalanced 33- bus network by considering min U_n as objective function

Objective function	PV Number	WT Number	Batt Number	Optimal Location (Bus)	Cost (M\$)
min U_n	357	448	692	33	10.345

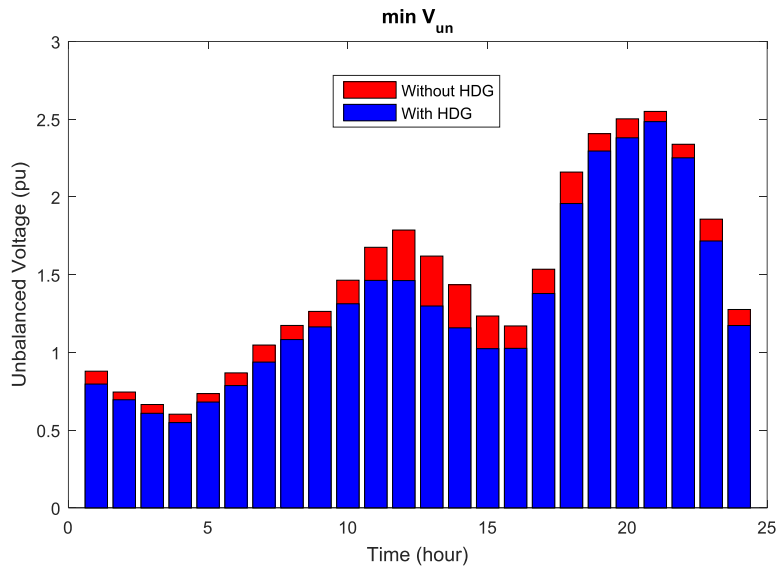


Fig. 6.16. Unbalance voltage of unbalanced 33- bus network by considering $\min V_{un}$ as objective function (one HDG)

6.2.4.2 Results of Scenario 2 (Multi objective-one HDG)

In this section, multi-objective optimization results are presented with and without the C_{HDG} for one HDG and using the HCSADE method. According to Fig. 6.17, it can be seen that in multi objective optimization, without considering the C_{HDG} , the value of the objective function is improved that means a further improvement in the indices of PQ.

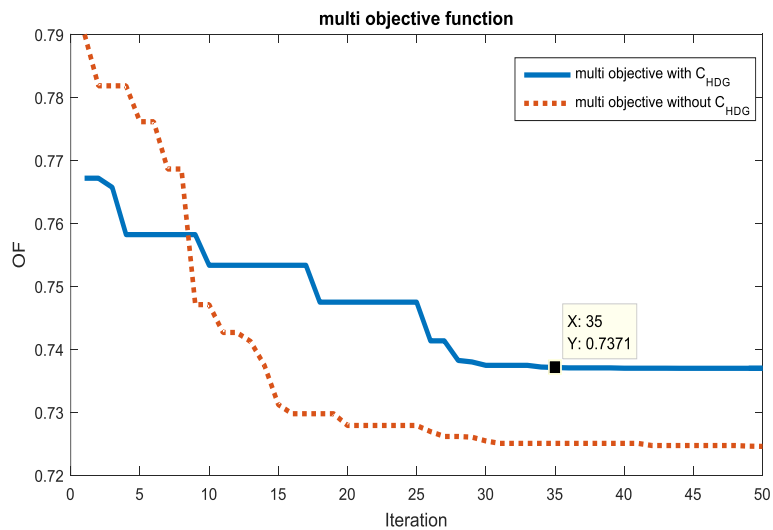


Fig. 6.17. Convergence curve of HCSADE by considering multi objective function with and without C_{HDG} (one HDG)

According to Tables (6.15) - (6.16), it can be seen that without considering C_{HDG} , the generation units generate more power and result in more improvements in the PQ indices.

Table. 6.15. Results of one HDG placement in unbalanced 33- bus network considering multi objective function

Objective function	Ploss (kw)	$\sum V_{sag}$	$\sum V_{swell}$	$\sum THD$	$\sum Un$
Base Net	1655.28	7.10	165.50	8.26	34.98
Multi-Objective without C_{HDG}	354.220	3.663	82.836	8.227	34.058
Multi-Objective with C_{HDG}	364.712	4.453	83.653	8.234	34.204

Table 6.16. Optimal sizing and siting of one HDG in unbalanced 33-bus network considering multi objective function

Objective function	PV Size (kW)	WT Size (kW)	BA Size (kW)	Optimal Location (Bus)	Cost (M\$)
Multi-Objective without C_{HDG}	273	482	290	30	10.505
Multi-Objective with C_{HDG}	125	360	109	30	7.420

The active power loss, voltage sag, voltage swell, THD voltage and voltage unbalance of unbalanced 33-bus network considering multi objective function (with C_{HDG}) are illustrated as in Figs. (6.18) - (6.22).

The results for state of charge (SoC) of battery by considering multi objective function (one HDG) and energy contribution of units for multi objective function with and without CHDG are illustrated in Figs. (6.23) - (6.24), respectively.

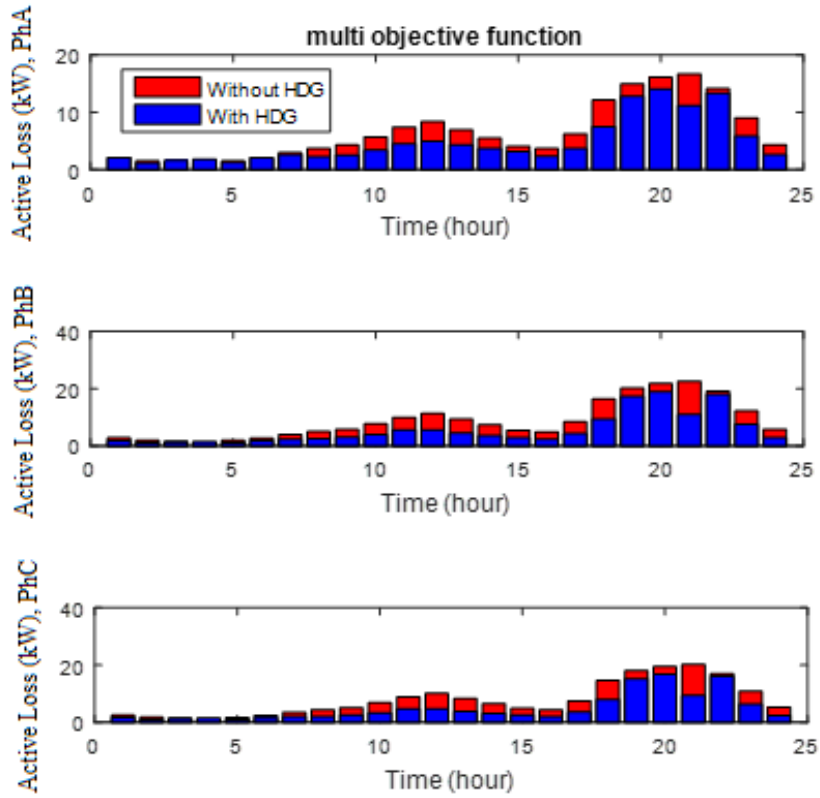


Fig. 6.18. Active loss of unbalanced 33-bus network by considering multi objective function, one HDG (with C_{HDG})

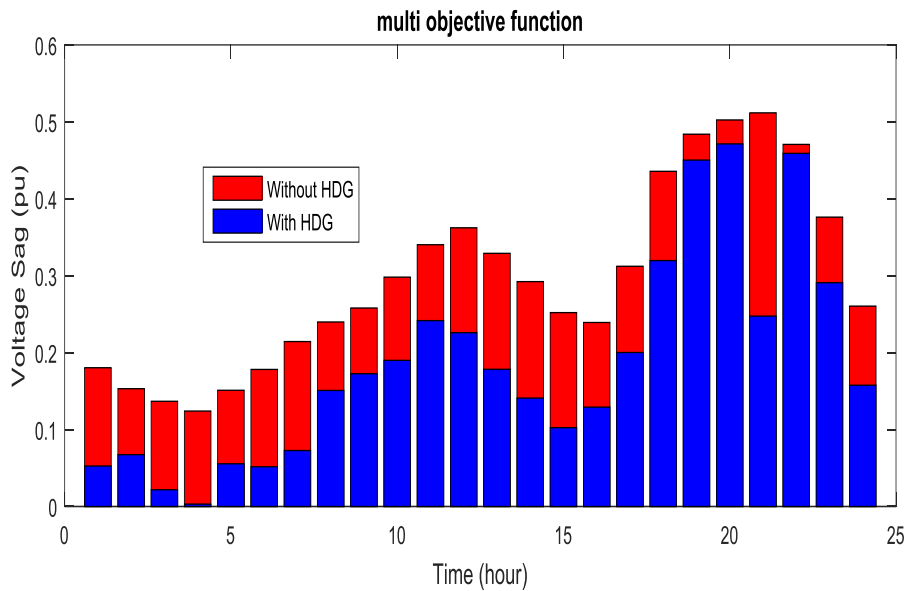


Fig. 6.19. Voltage sag of unbalanced 33- bus network by considering multi objective function, one HDG (with C_{HDG})

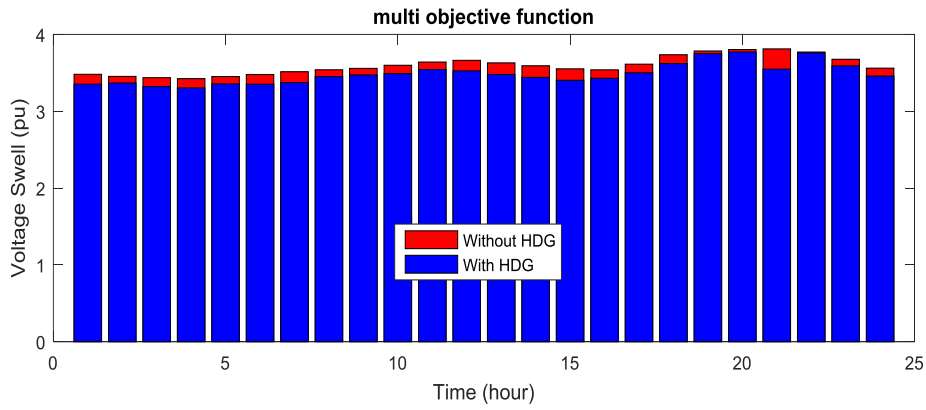


Fig. 6.20. Voltage swell of unbalanced 33- bus network considering multi objective function, one HDG (with C_{HDG})

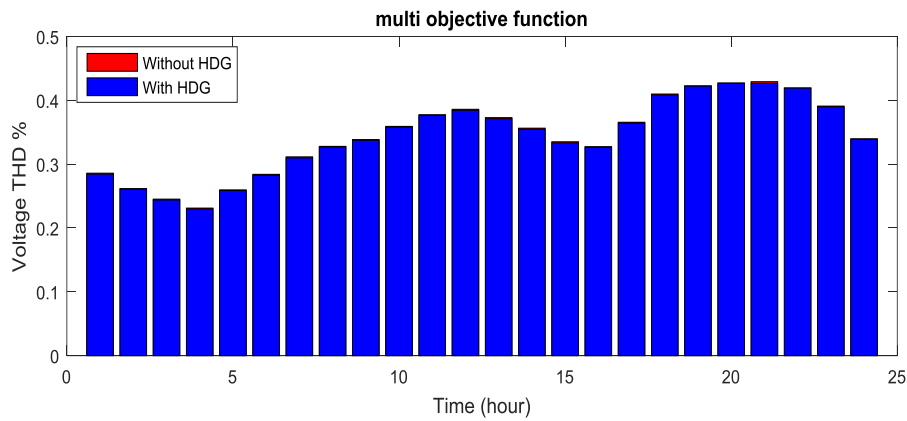


Fig. 6.21. Voltage THD of unbalanced 33- bus network considering multi objective function, one HDG (with C_{HDG})

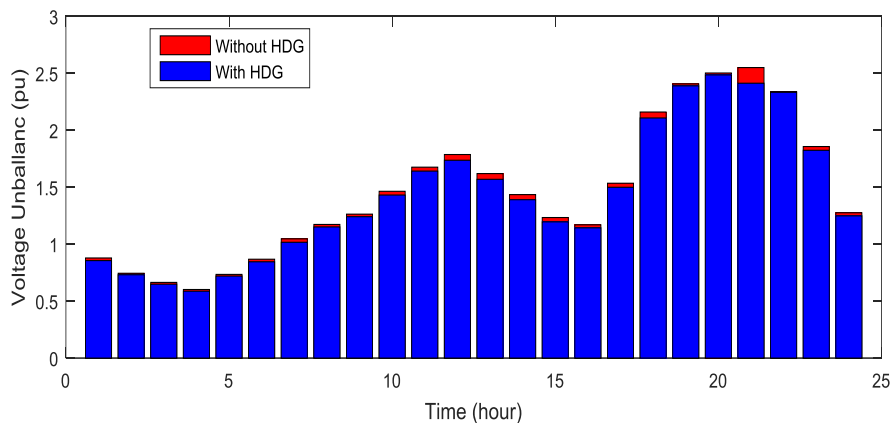


Fig. 6.22. Voltage unbalance of unbalanced 33- bus network considering multi objective function, one HDG (with C_{HDG})

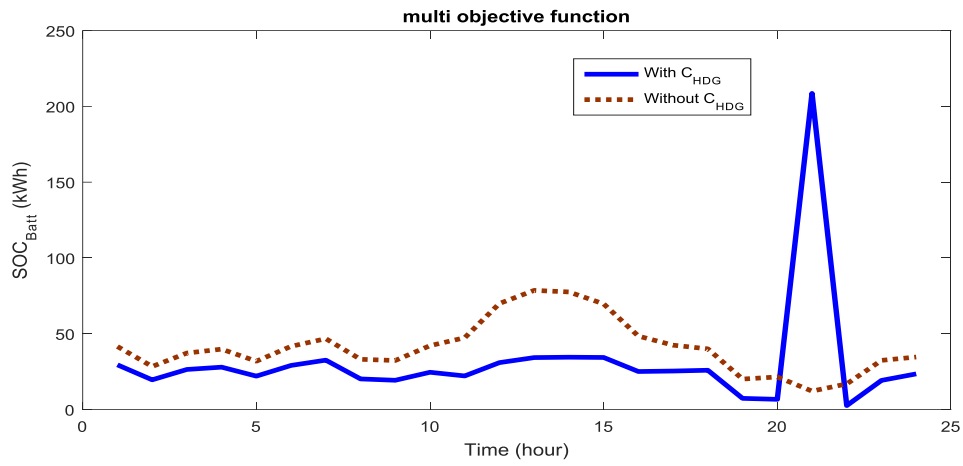
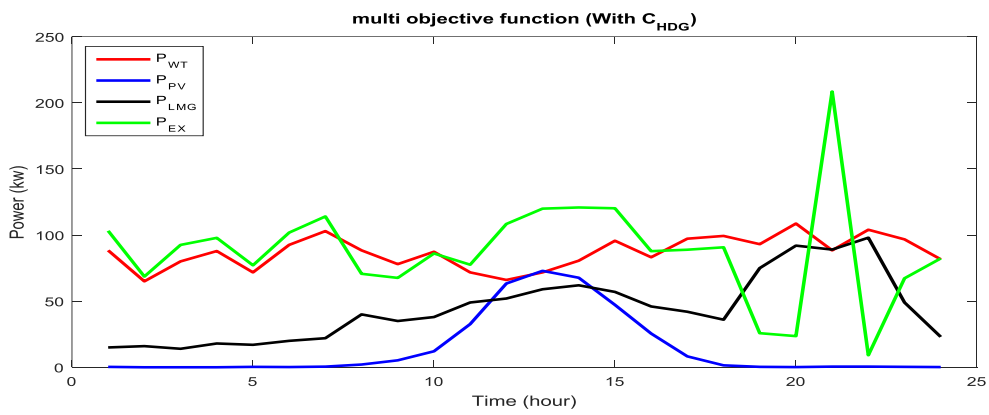
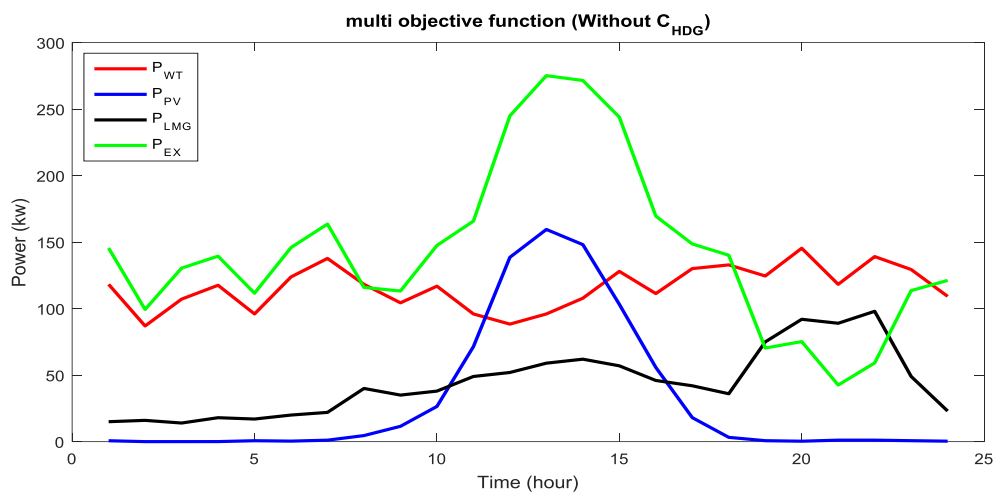


Fig. 6.23. SOC of battery by considering multi objective function (one HDG)



(a)



(b)

Fig. 6.24. Energy contribution of units for multi objective function a) with and b) without C_{HDG} (one HDG)

6.2.4.3 Results of Scenario 3 (Comparison the single and multi- objective results-one HDG)

In this subsection, results of single and multi-objective optimization of one PVWTBAHDG by using the HCSADE method and considering the C_{HDG} are presented in Tables (6.17) - (6.18).

Table. 6.17. Results of one HDG placement in unbalanced 33- bus network by considering multi objective function

Objective function	Ploss (kw)	$\sum V_{sag}$	$\sum V_{swell}$	$\sum THD$	$\sum Un$
Base Net	1655.28	7.10	165.50	8.26	34.98
min Ploss	967.941	4.409	83.609	8.237	34.327
$\min \sum V_{sag}$	2936.511	2.949	81.049	8.207	33.464
$\min \sum V_{swell}$	17883	10.232	70.545	7.918	33.099
$\min \sum THD$	17667	10.171	70.660	7.907	33.114
$\min \sum Un$	18999	6.450	75.451	8.145	31.672
(Multi-Objective)	1094.136	4.453	83.653	8.234	34.204

Table 6.18. Optimal sizing and siting of one HDG in unbalanced 33- bus network by considering multi objective function

Objective function	PV Size (kW)	WT Size (kW)	BA Size (kW)	Optimal Location (Bus)	Cost (M\$)
min Ploss	254	479	603	30	10.336
$\min \sum V_{sag}$	178	482	545	32	9.99
$\min \sum V_{swell}$	304	481	233	15	10.648
$\min \sum THD$	303	477	444	15	10.579
$\min \sum Un$	357	448	692	33	10.345
(Multi-Objective)	125	360	109	30	7.420

According to Tables (6.17)- (6.18), the results of single and multi-objective optimization of one HDG by using the HCSADE method including size and site of one HDG and also values of power loss, PVWTBAHDG system cost, voltage sag, voltage swell, THD and voltage unbalance are as follows:

- More contribution of wind turbines in PVWTBAHDG and an optimal location for PVWTBAHDG installation is at bus 30. Also, the lowest cost of PVWTBAHDG is obtained 7.420 M\$ when a multi-objective optimization is used in the process of problem solution;
- The lowest loss is achieved when the objective function is selected as min Ploss as single objective. Also, the best amount of voltage sag, voltage swell, THD and voltage unbalance are achieved when the objective functions are selected as: $\min \sum V_{sag}$, $\min \sum V_{swell}$, $\min \sum THD$ and $\min \sum Un$ as single objective respectively that means it has positive effect on the improvement of all PQ indices;
- Considering single objective optimization for PQ indices has a negative effect on the power losses reduction. In voltage swell and THD objective optimization, voltage sag is weakened. The lowest value of voltage sag is achieved under the voltage sag objective function. It is observed that the objective function of voltage sag has a positive effect on other PQ indices but, it increases the network losses in comparison with base value;
- By considering the voltage swell as a single objective function, the lowest amount of voltage is obtained in this case. However, it is observed that only the objective function of voltage swell has a positive effect on THD and voltage unbalance and reduce them in comparison with base value but, it has a negative effect on voltage sag as well as cost and loss;
- In objective function of THD optimization, the lowest amount of THD is obtained. THD objective function has a positive effect on voltage swell and voltage unbalance and has negative effect on other indices. The objective function of voltage unbalance improves all PQ indices but, it increases power loss value. Also, the best value of voltage unbalance is obtained in this case; and
- In multi-objective optimization, all objective functions are integrated and normalized.

The results show that in multi-objective optimization of one PVWTBAHDG in the 33-bus distribution network, the power loss is reduced, all indices of PQ are improved and

the minimum PVWTBAHDG cost is obtained. So, by considering multi-objective problem, PQ is improved. Therefore, multi-objective optimization is a more realistic and precise viewpoint to solve a problem that can meet all the objectives.

6.2.4.4 Results of Scenario 4 (Multi objective designing-two HDGs)

In this subsection, the design and placement of two HDGs based on multi-objective optimization using the HCSADE method and considering the C_{HDG} is presented. In this subsection convergence curve of HCSADE method in optimization process, results of designing and placement of HDGs and also energy contribution curve of units are presented. As shown in Fig. 6.25, without considering the C_{HDG} in the objective function, the value of the objective function is reduced, which is to further improve the indices of PQ and loss.

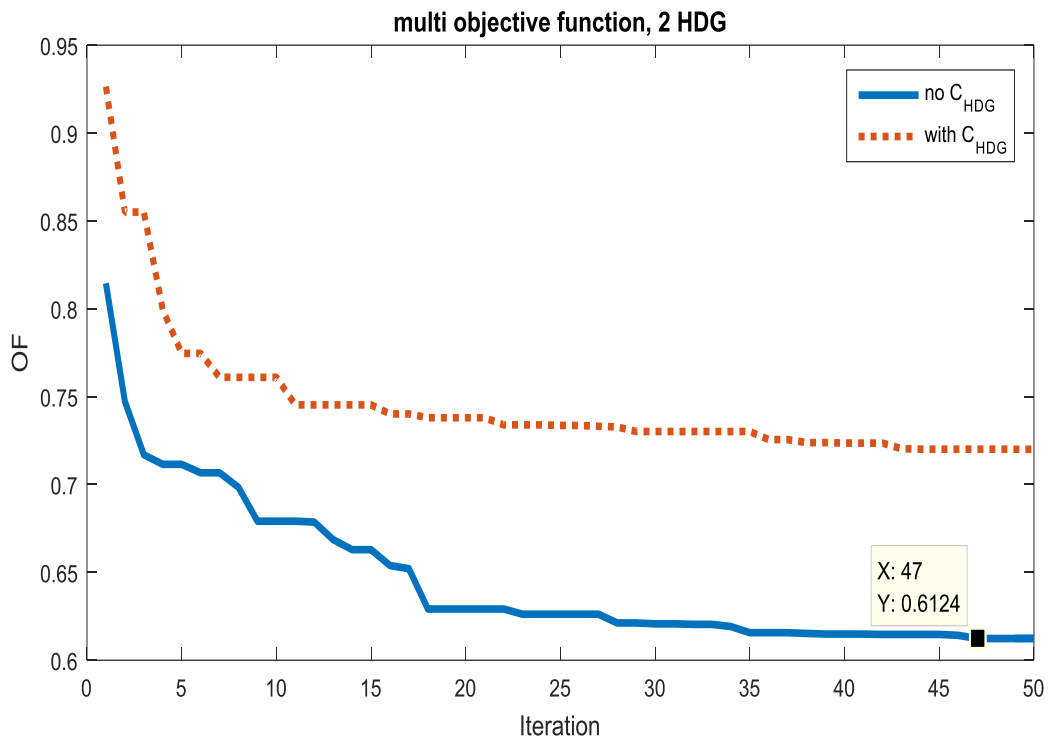


Fig. 6.25. Convergence curve of HCSADE considering multi objective function (two HDG)

As shown as in Tables (6.19) - (6.20), if C_{HDG} is not considered in the optimization process, the renewable energy units generate more energy and it leads to more loss reduction and more improvement of PQ indices in comparison with considering the C_{HDG} . Also, the results show that the system cost including two HDGs is decreased when C_{HDG} is considered in multi-objective function.

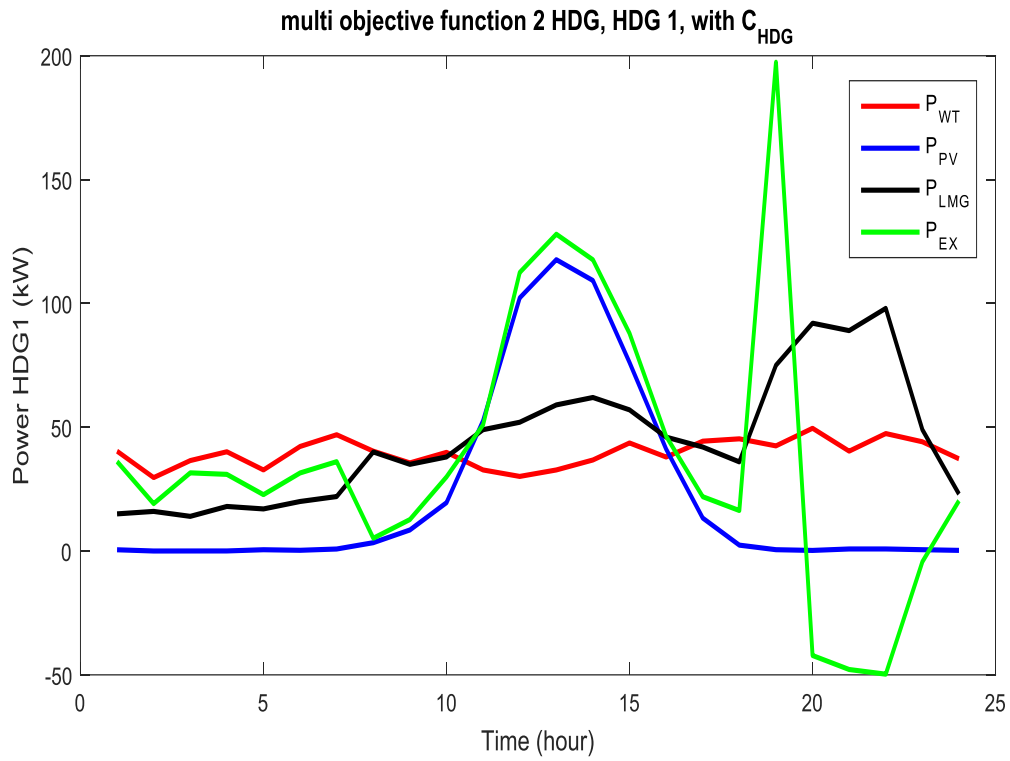
Energy contribution of units for multi objective function in one and two HDGs designing and placement in the 33-bus network with and without C_{HDG} is shown in Figs. (6.26) – (6.27), respectively.

Table. 6.19. Results of two HDG placement in unbalanced 33-bus network by considering multi objective function

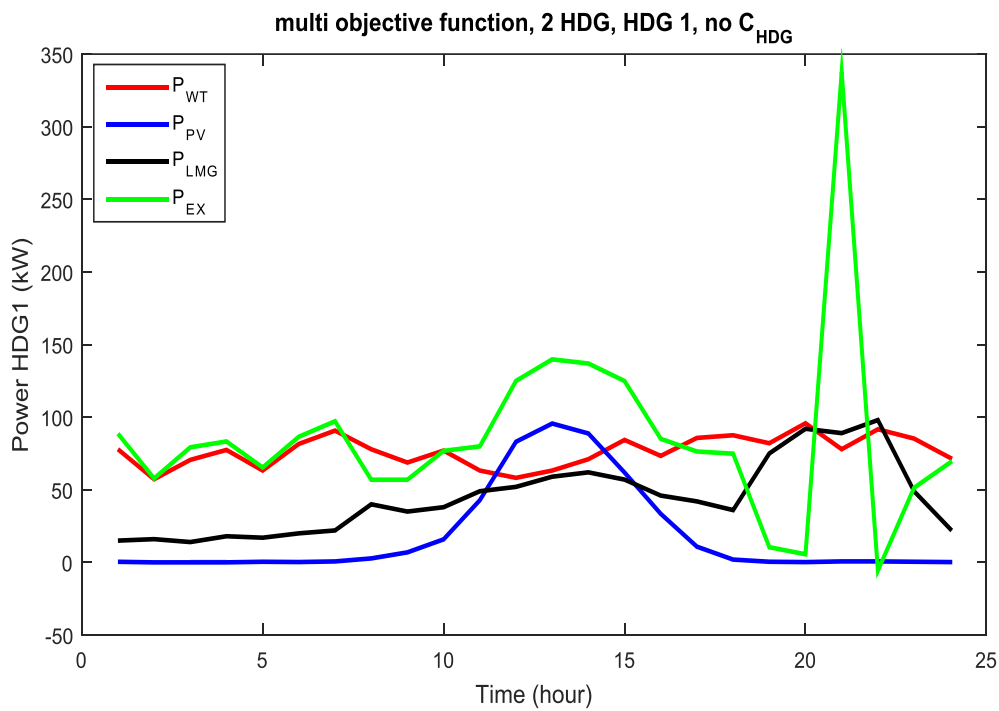
Objective function	Ploss (kw)	$\sum V_{sag}$	$\sum V_{swell}$	$\sum THD$	$\sum Un$
Base Net	1655.28	7.10	165.50	8.26	34.98
Multi-Objective without C_{HDG}	984.825	3.272	82.355	8.221	34.124
Multi-Objective with C_{HDG}	1132.617	4.016	83.205	8.224	34.479

Table 6.20. Optimal sizing and siting of two HDG in unbalanced 33-bus network by considering multi objective function

Objective function	PV Size (kW)	WT Size (kW)	BA Size (kW)	Optimal Location (Bus)	Cost (M\$)
Multi-Objective without C_{HDG}	PV1 (164)	WT1 (318)	Batt1 (42)	Bus (30)	12.617
	PV2 (232)	WT2 (239)	Batt (18)	Bus (12)	
Multi-Objective with C_{HDG}	PV1 (201)	WT1 (164)	Batt1 (4)	Bus (30)	10.642
	PV2 (111)	WT2 (312)	Batt (15)	Bus (11)	



(a)



(b)

Fig. 6.26. Energy contribution of units for multi objective function, HDG 1, a) with and b) without C_{HDG} , (two HDG)

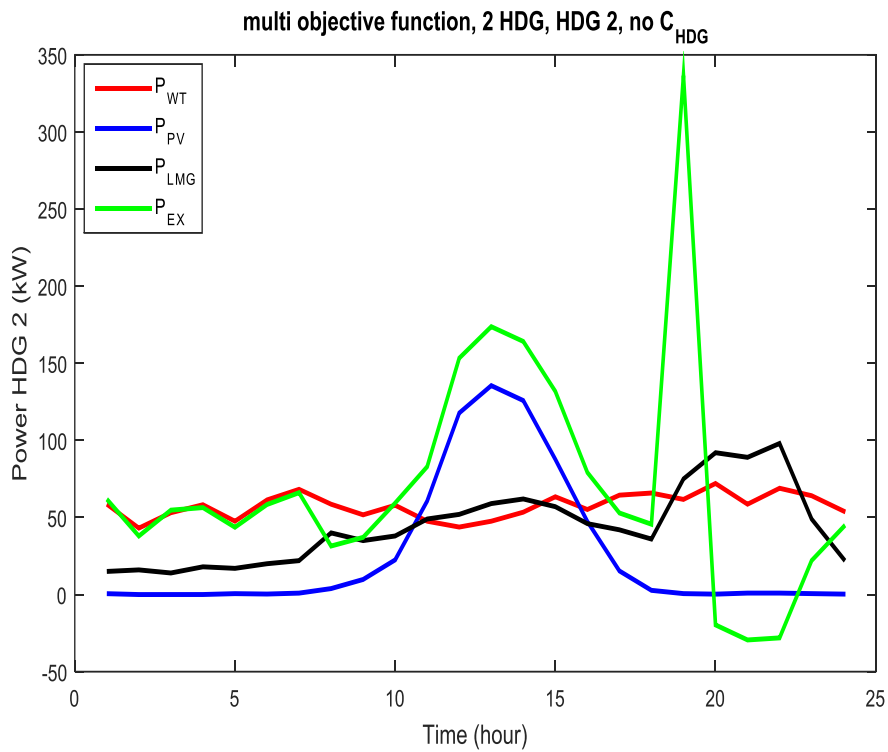
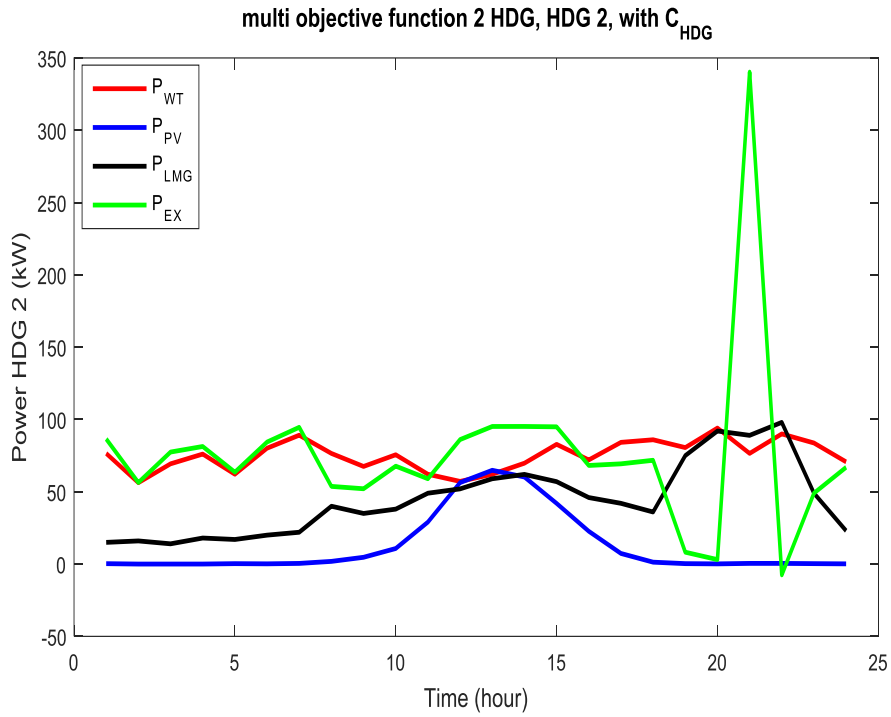


Fig. 6.27. Energy contribution of units for multi objective function, HDG 2, a) with and b) without C_{HDG} , (two HDGs)

6.2.4.5 Results of Scenario 5 (Comparison of the results-one and two HDGs)

In this subsection, the designing and placement results of one and two HDGs are investigated in Tables (6.21) - (6.22). As can be seen, the cost of using the two HDGs is higher than one HDG optimal application. It can also be seen that the amount of power loss, voltage sag, voltage swell and THD is improved while, the amount of voltage unbalance is increased.

Table. 6.21. Results of two HDG placement in unbalanced 33-bus network by considering multi objective function

Objective function	Ploss (kw)	$\sum V_{sag}$	$\sum V_{swell}$	$\sum THD$	$\sum Un$
One HDG	1094.136	4.453	83.653	8.234	34.204
Two HDG	1072.617	4.016	83.205	8.224	34.479

Table. 6.22. Optimal sizing and siting of two HDG in unbalanced 33- bus network by considering multi objective function

Objective function	PV Size (kW)	WT Size (kW)	BA Size (kW)	Optimal Location (Bus)	Cost (M\$)
One HDG	125	360	109	30	7.420
Two HDG	PV1 (201)	WT1 (164)	Batt1 (4)	Bus (30)	10.642
	PV2 (111)	WT2 (312)	Batt (15)	Bus (11)	

6.2.4.6 Results of Scenario 6 (Performance evaluation of HCSADE)

In this subsection, the HCSADE method for multi objective optimization by considering the C_{HDG} is compared with CSA and DE methods. The convergence curve of the optimization methods and the numerical results of designing and the placement of one and two HDGs and the value of PQ indices are presented. According to Figs. (6.28) - (6.29), as can be seen, the HCSADE method has achieved a better objective function value than the other two methods.

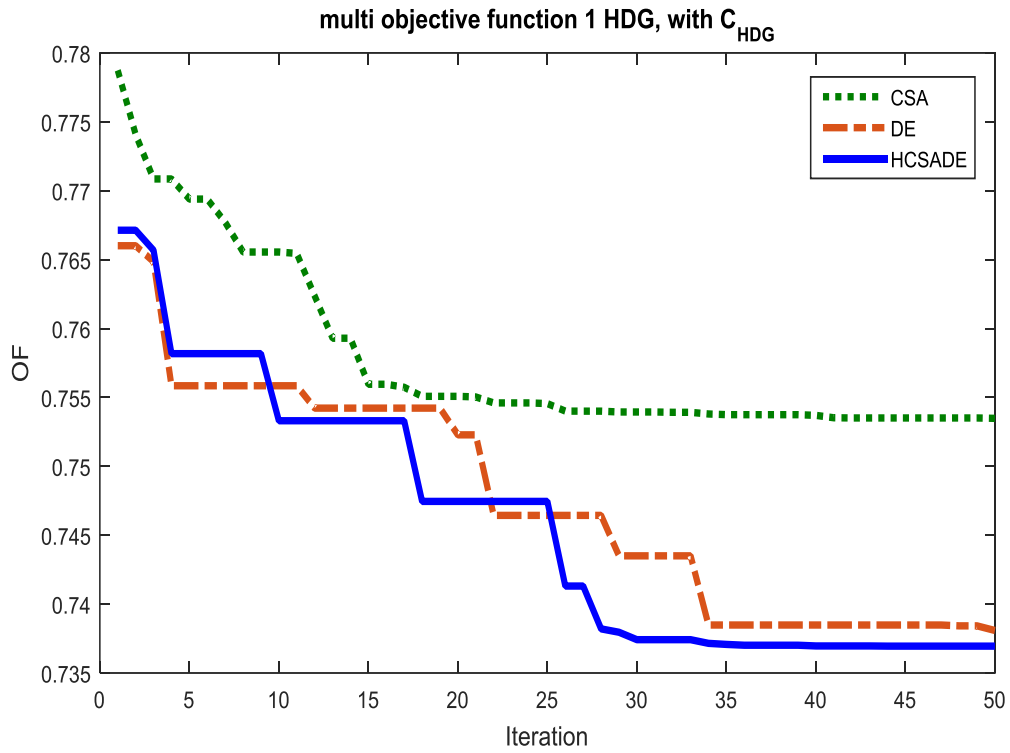


Fig. 6.28. Convergence curve of optimization method by considering multi objective function (one HDG)

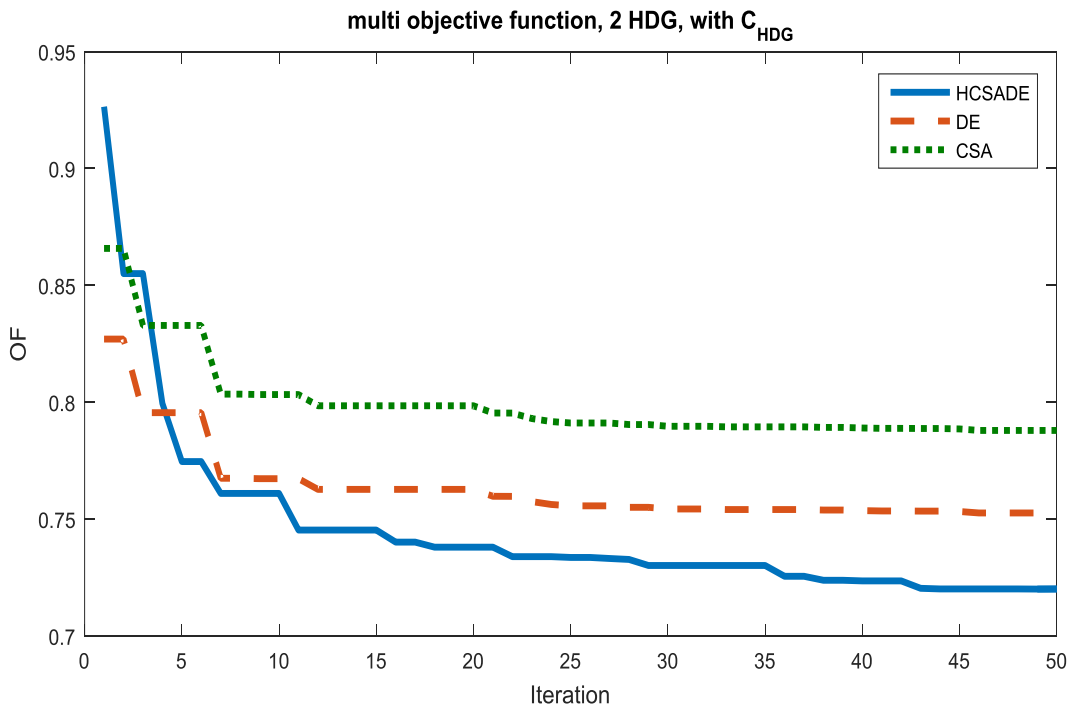


Fig. 6.29. Convergence curve of optimization method by considering multi objective function (two HDGs)

According to the obtained results in Tables (6.23) – (6.26), the simulation results show that the HCSADE method provides lower losses and better PQ indices than CSA and DE methods. Also, in one HDG designing and placement mode, all the optimization methods select bus 30 for installing the HDG. Moreover, in two HDG designing and placement mode, the buses 30 and 11 are determined for installing two HDGs by using HCSADE.

Table. 6.23. Results of one HDG placement in unbalanced 33-bus network by considering multi objective function with C_{HDG}

Objective function	Ploss (kW)	$\sum V_{sag}$	$\sum V_{swell}$	$\sum THD$	$\sum Un$
HCSADE	1094.136	4.453	83.653	8.234	34.204
CSA	1133.520	4.583	83.48	8.235	34.301
DE	1108.950	4.65	83.85	8.236	34.26

Table 6.24. Optimal sizing and siting of one HDG in unbalanced 33- bus network by considering multi objective function with C_{HDG}

Objective function	PV Size (kW)	WT Size (kW)	BA Size (kW)	Optimal Location (Bus)	Cost (M\$)
HCSADE	125	360	109	30	7.420
CSA	114	389	380	30	7.871
DE	87	356	83	30	7.134

Table. 6.25. Results of two HDG placement in unbalanced 33-bus network by considering multi objective function with C_{HDG}

Objective function	Ploss (kw)	$\sum V_{sag}$	$\sum V_{swell}$	$\sum THD$	$\sum Un$
HCSADE	1072.617	4.016	83.205	8.224	34.179
CSA	1205.868	5.371	83.541	8.258	34.607
DE	1077.78	5.438	84.638	8.261	34.649

Table 6.26. Optimal sizing and siting of two HDG in unbalanced 33-bus network by considering multi objective function with C_{HDG}

Objective function	PV Size (kW)	WT Size (kW)	BA Size (kW)	Optimal Location (Bus)	Cost (M\$)
HCSADE	PV1 (201)	WT1 (164)	Batt1 (4)	Bus (30)	10.642
	PV2 (111)	WT2 (312)	Batt (15)	Bus (11)	
CSA	PV1 (205)	WT1 (308)	Batt1 (58)	Bus (32)	10.378
	PV2 (135)	WT2 (147)	Batt (7)	Bus (28)	
DE	PV1 (269)	WT1 (233)	Batt1 (64)	Bus (31)	6.765
	PV2 (79)	WT2 (26)	Batt (0)	Bus (2)	

6.2.4.7 Results of Scenario 7 (Impact of HDG load decreasing-one HDG)

In this subsection, impact of HDG load decreasing on multi objective designing and placement of one HDG is presented. According to Tables (6.27) - (6.28), it is observed that the reduction of HDG load demand can cause a reduction in HDG system cost. Also, the results show that the values of PQ indicators do not change much and are almost constant. Therefore, reducing the HDG load demand has more effect on reducing HDG design costs.

Table 6.27. Results of one HDG placement in unbalanced 33-bus network by considering multi objective function with C_{HDG} using HCSADE

Objective function	Ploss (kW)	$\sum V_{sag}$	$\sum V_{swell}$	$\sum THD$	$\sum Un$
Rated HDG load	1094.136	4.453	83.653	8.234	34.204
20% Decreasing	1143.669	4.464	83.664	8.220	34.219

Table 6.28. Optimal sizing and siting of one HDG in unbalanced 33-bus network by considering multi objective function with C_{HDG} using HCSADE

Objective function	PV Size (kW)	WT Size (kW)	BA Size (kW)	Optimal Location (Bus)	Cost (M\$)
Rated HDG load	125	360	109	30	7.420
20% Decreasing	102	310	559	30	6.341

6.2.4.8 Results of Scenario 8 (Impact of network load increasing-one HDG)

In this subsection, the impact of network load increase on multi objective design and placement of one HDG is studied. According to Tables (6.29) – (6.30), the increase of the network load has led to an increase in PVWTBAHDG size and also in losses value. The amount of PQ indices is also reduced.

Table 6.29. Results of one HDG placement in unbalanced 33-bus network by considering multi objective function with C_{HDG} using HCSADE

Objective function	Ploss (kW)	$\sum V_{sag}$	$\sum V_{swell}$	$\sum THD$	$\sum Un$
Rated network load	1094.136	4.453	83.653	8.234	34.204
20% Increasing	1538.310	5.153	84.321	8.827	34.242

Table 6.30. Optimal sizing and siting of one HDG in unbalanced 33-bus network by considering multi objective function with C_{HDG} using HCSADE

Objective function	PV Size (kW)	WT Size (kW)	BA Size (kW)	Optimal Location (Bus)	Cost (M\$)
Rated network load	125	360	109	30	7.420
20% Increasing	121	441	722	30	8.882

6.2.4.9 Results of Scenario 9 (Multi objective designing-HDG combinations)

In this subsection, the design and placement of various HDG combinations in 33-bus unbalanced distribution network is investigated. Size and optimization results are presented in Tables (6.31) - (6.32). The results show that the combination of PVWTBA with both renewable units based on HDG has lower cost and losses with better values of PQ indices.

Table 6.31. Results of one HDG placement in unbalanced 33- bus network by considering multi objective function with C_{HDG} using HCSADE

Objective function	Ploss (kW)	$\sum V_{sag}$	$\sum V_{swell}$	$\sum THD$	$\sum Un$
PVWTBAHDG	1094.136	4.453	83.653	8.234	34.204
WTBAHDG	1205.595	4.782	83.936	8.223	34.346
PVBAHDG	1269.570	4.794	84.105	8.224	34.472

Table 6.32. Optimal sizing and siting of one HDG in unbalanced 33- bus network by considering multi objective function with C_{HDG} using HCSADE

Objective function	PV Size (kW)	WT Size (kW)	BA Size (kW)	Optimal Location (Bus)	Cost (M\$)
PVWTBAHDG	125	360	109	30	7.420
WTBAHDG	-----	408	1390	30	7.594
PVBAHDG	612	-----	1584	30	7.877

6.2.4.10 Results of Scenario 10 (Impact of battery cost variations-one HDG)

The storage system plays an important role to supply the HDG load and inject the power to the network. In this subsection, results of multi-objective optimization by considering the impact of battery cost variations for one HDG are presented. According to the information in Table 6.4, the capital cost and operation and maintenance cost of each battery unit are considered 100 \$ and 5\$ respectively. The results of Tables (6.33) - (6.34)

show that HDG system cost and PVWTBAHDG size are reduced and power loss and PQ indexes are increased when battery costs are halved. Also, the results show that HDG system cost, power loss and PVWTBAHDG size are reduced and PQ indexes are increased when battery costs are doubled.

Table. 6.33. Results of one HDG placement in unbalanced 33-bus network by considering battery cost variations

Battery Capital Cost	Ploss (kw)	$\sum V_{sag}$	$\sum V_{swell}$	$\sum THD$	$\sum Un$
50 \$	366.833	4.470	83.670	8.235	34.210
100 \$	364.712	4.453	83.653	8.234	34.204
200 \$	364.352	4.740	83.940	8.237	34.300

Table 6.34. Optimal sizing and siting of one HDG in unbalanced 33-bus network by considering battery cost variations

Battery Capital Cost	PV Size (kW)	WT Size (kW)	BA Size (kW)	Optimal Location (Bus)	Cost (M\$)
50 \$	116	360	110	30	7.363
100 \$	125	360	109	30	7.420
200 \$	115	348	98	30	7.396

Active loss, voltage sag, voltage swell, THD voltage, voltage unbalance and energy contribution of unbalanced 33-bus network by considering battery cost variations for one HDG are illustrated as Figs. (6.30) - (6.35).

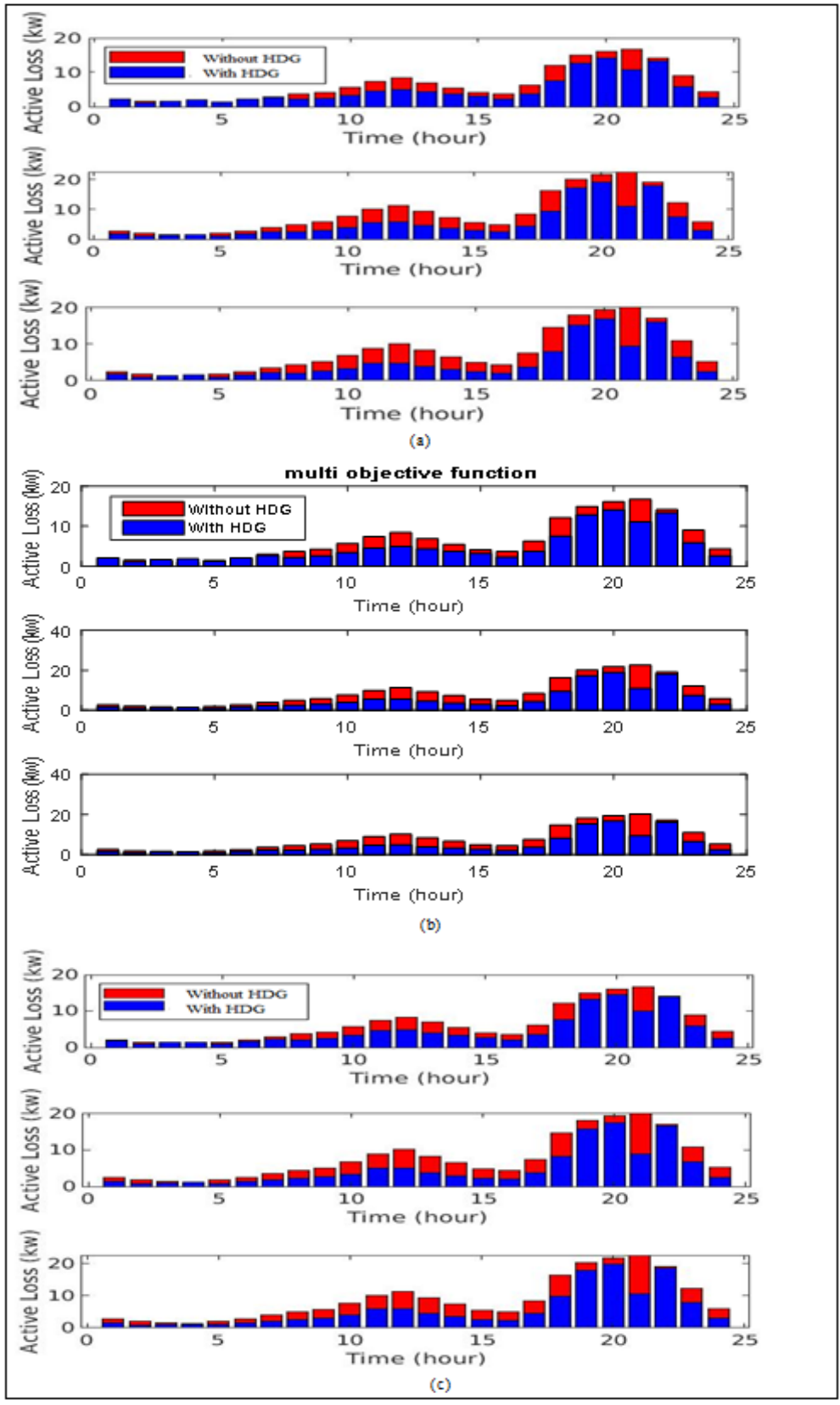


Fig. 6.30. Active loss of unbalanced 33-bus network by considering battery cost variations
 a) 50\$, b) 100\$ (base study) and c) 200\$ [One HDG]

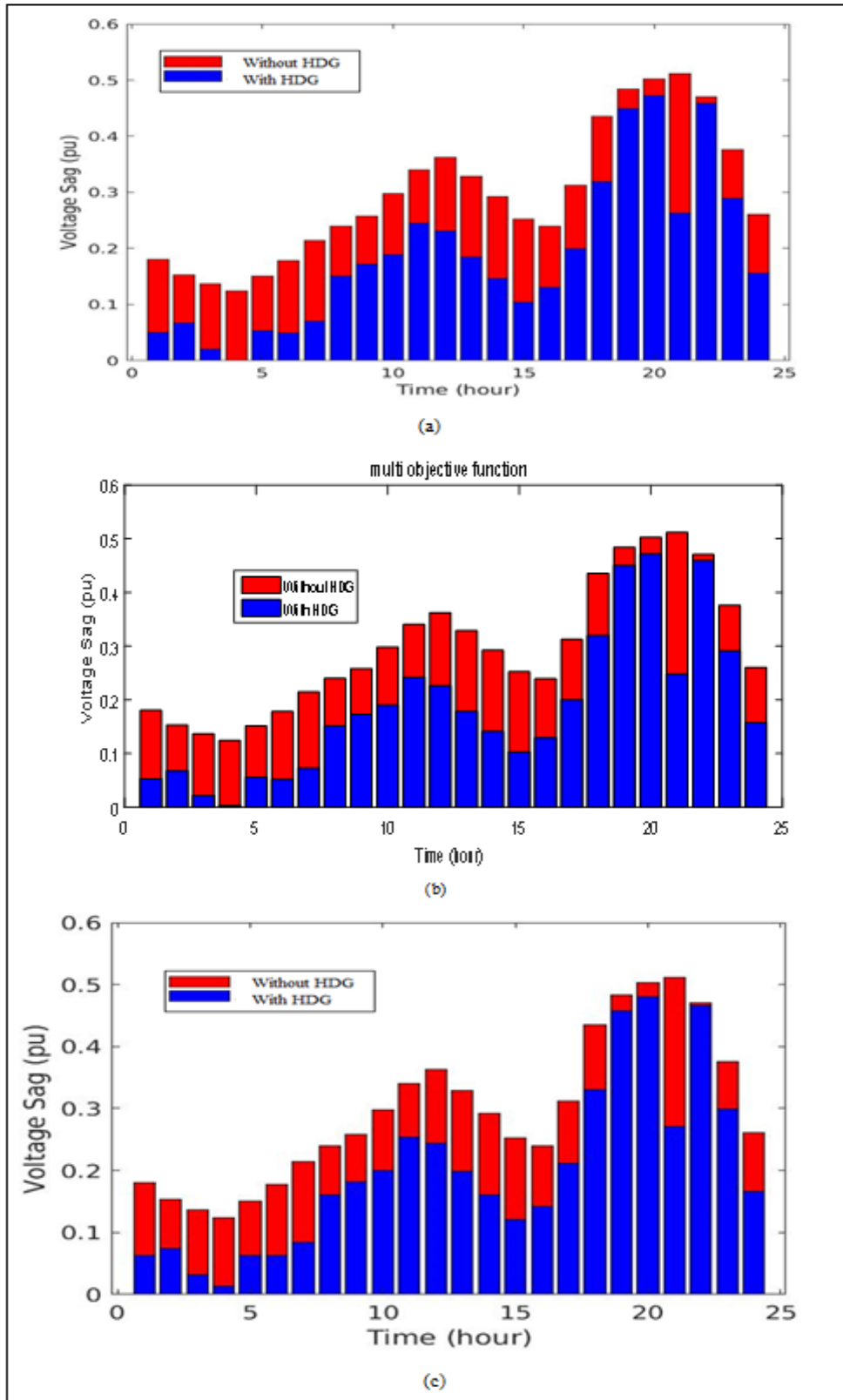


Fig. 6.31. Voltage sag of unbalanced 33-bus network by considering battery cost variations a) 50\$, b) 100\$ (base study) and c) 200\$ [One HDG]

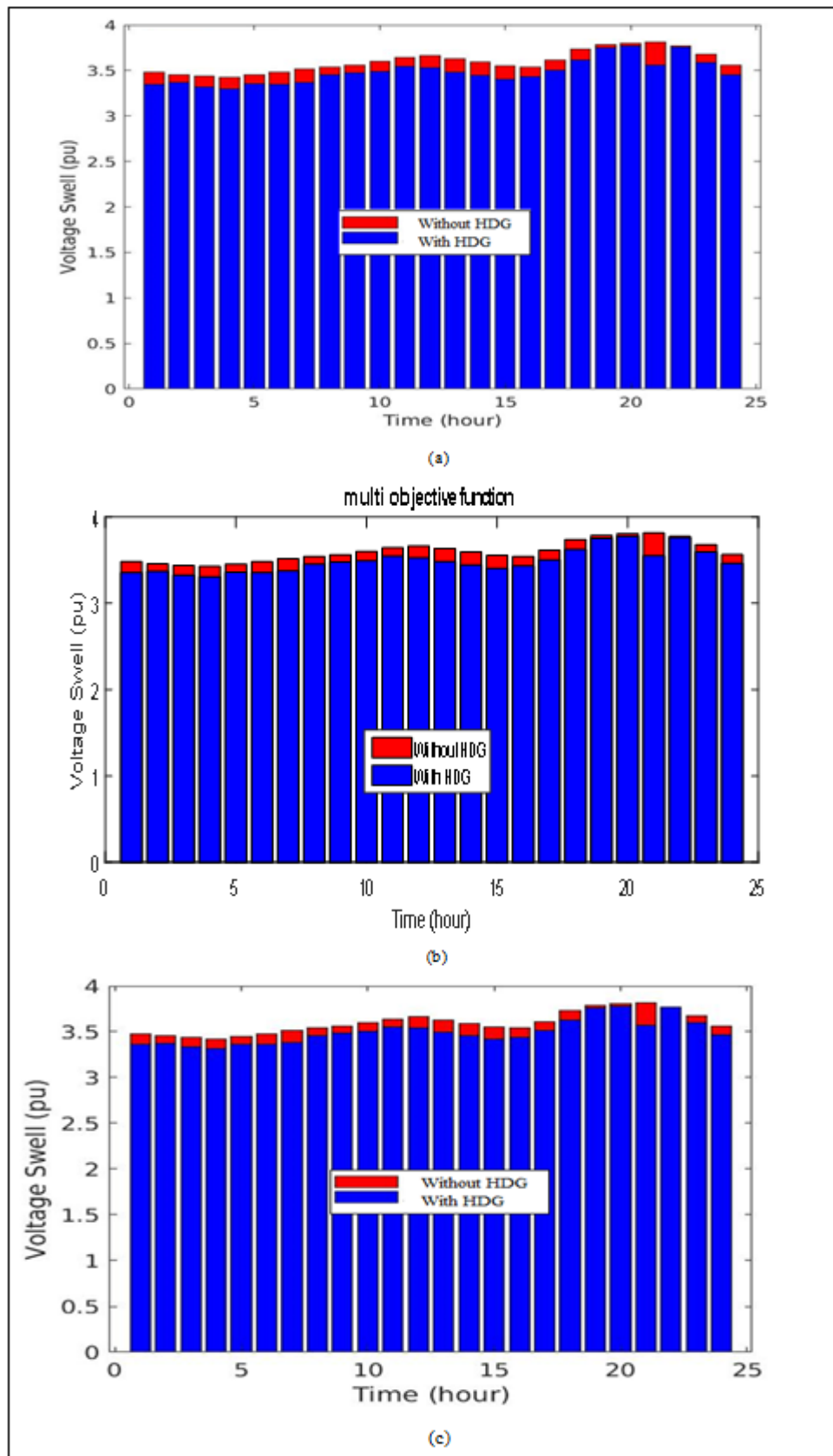


Fig. 6.32. Voltage swell of unbalanced 33-bus network by considering battery cost variations
a) 50\$, b) 100 \$ (base study) and c) 200 \$ [One HDG]

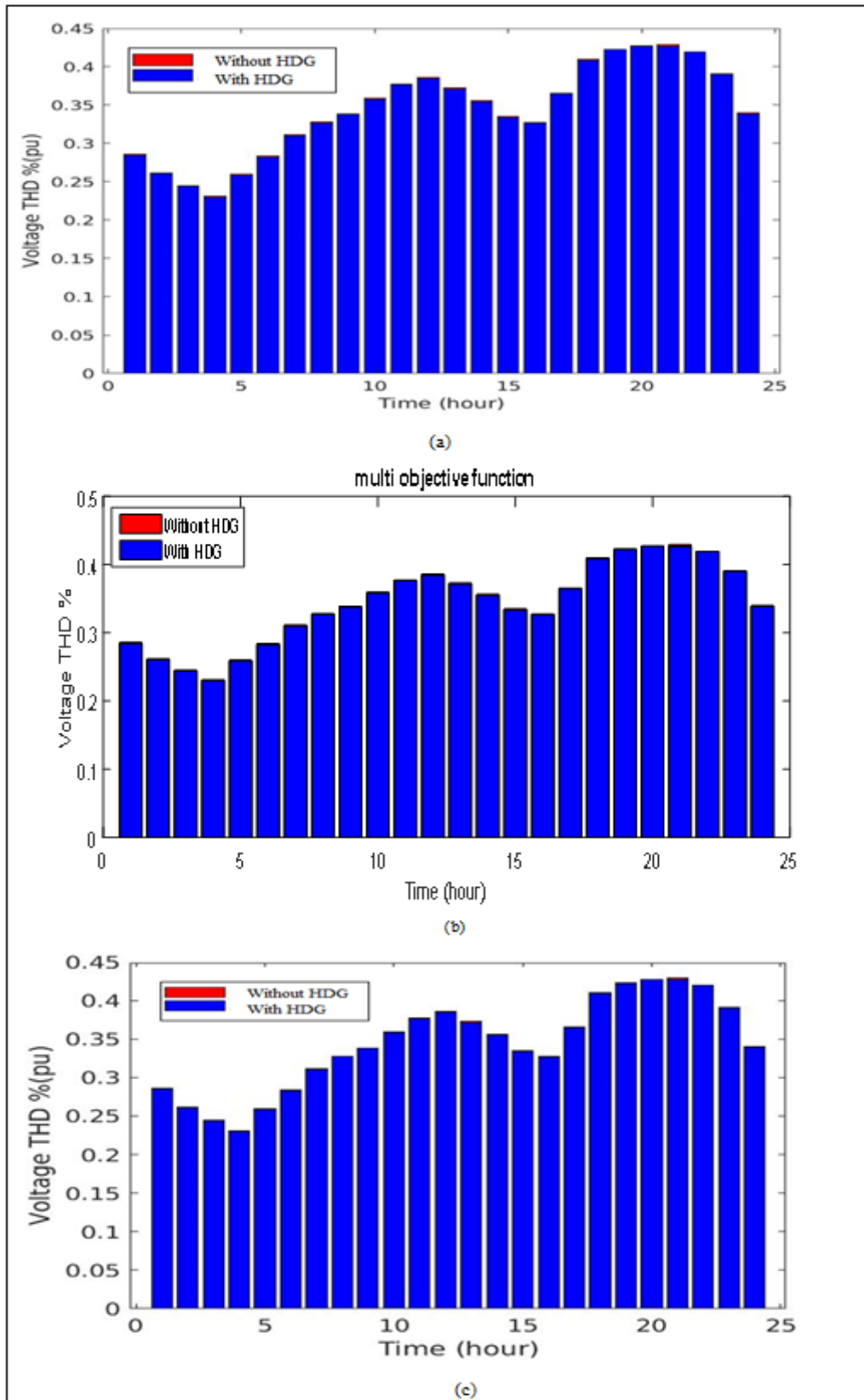


Fig. 6.33. Voltage THD of unbalanced 33-bus network by considering battery cost variations
a) 50\$, b) 100 \$ (base study) and c) 200 \$ [One HDG]

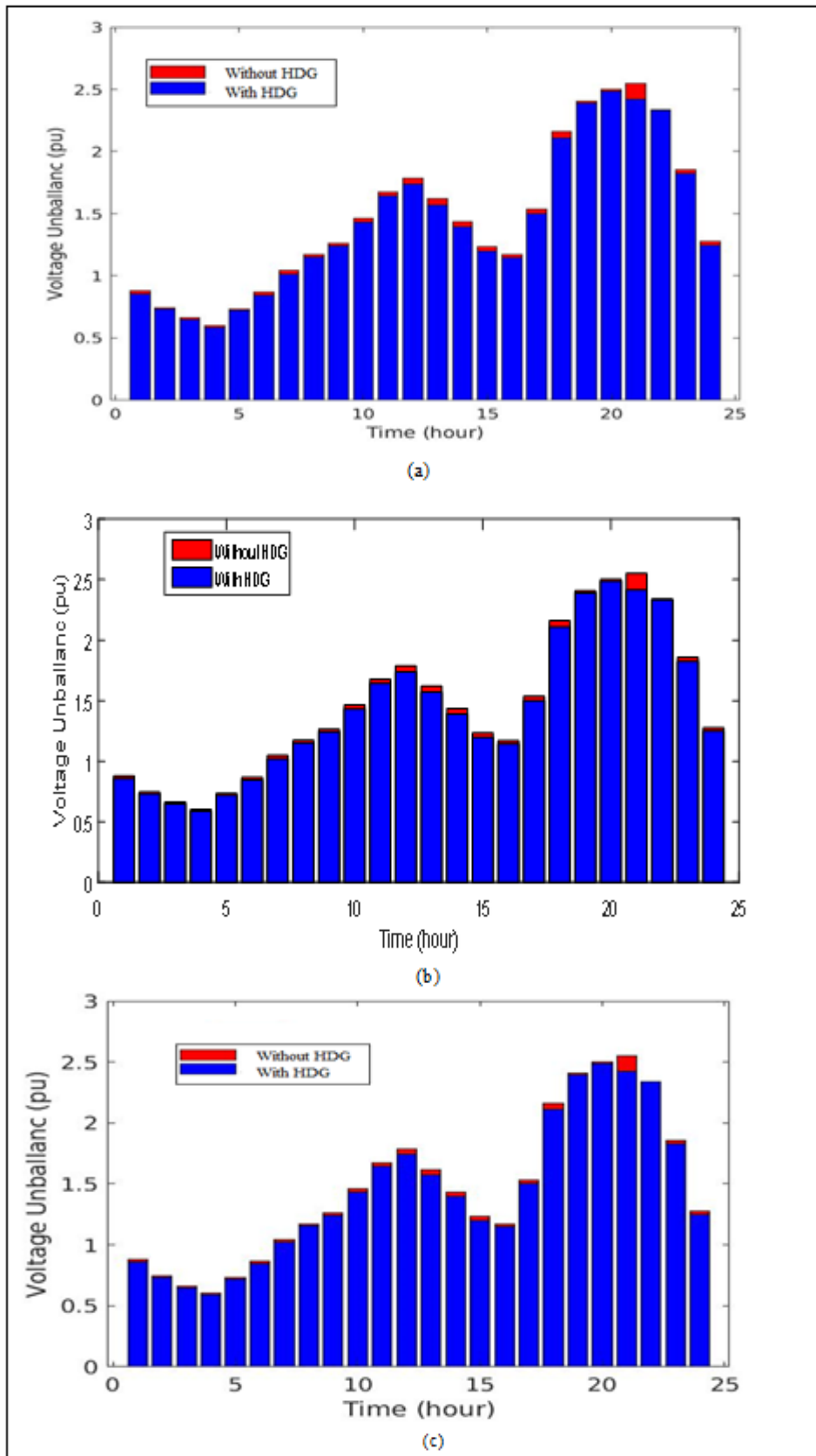


Fig. 6.34. Voltage unbalance of unbalanced 33-bus network by considering battery cost variations a) 50\$, b) 100 \$ (base study) and c) 200 \$ [One HDG]

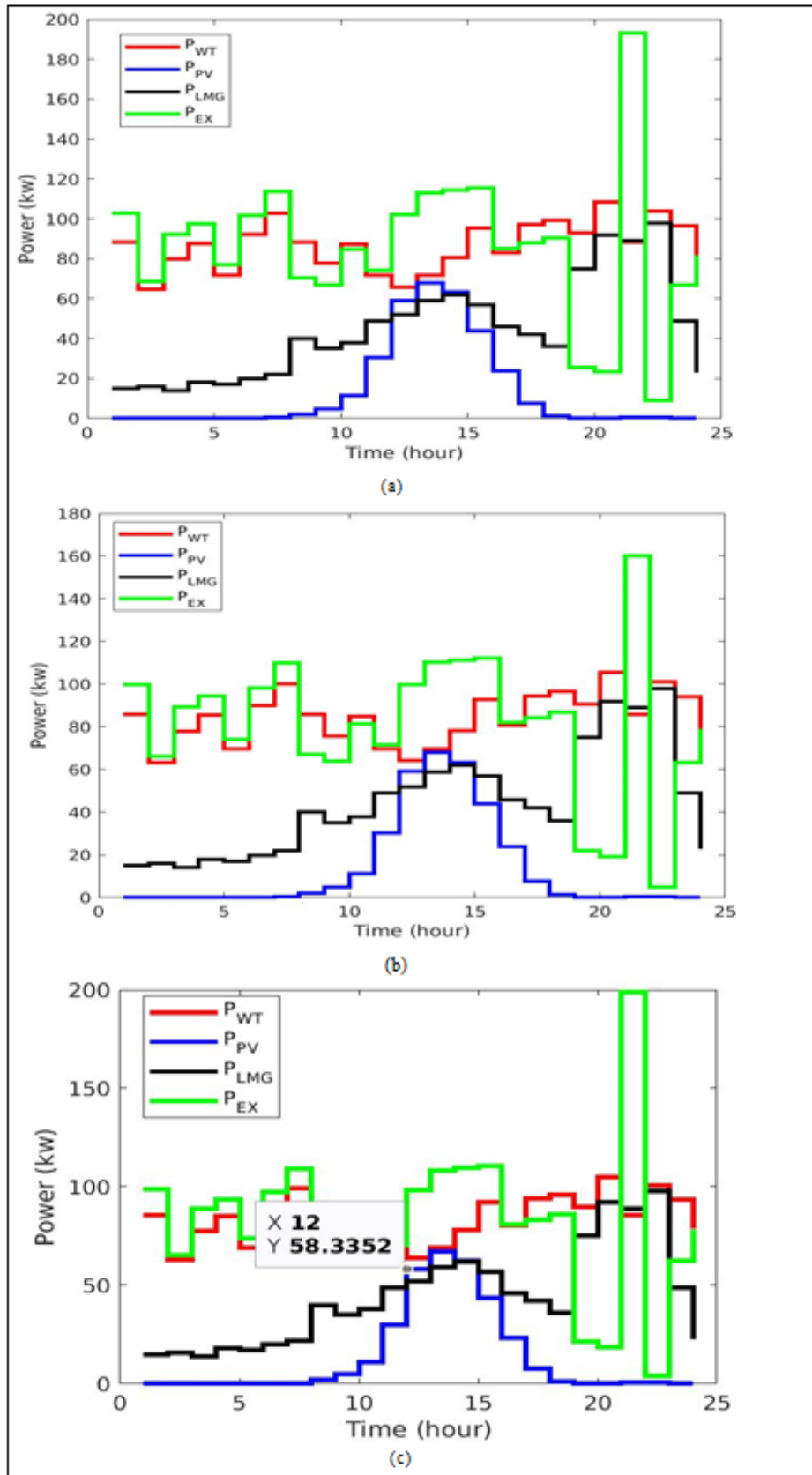


Fig. 6.35. Energy contribution of units by considering battery cost variations
a) 50\$, b) 100\$ (base study) c) 200\$ [One HDG]

6.2.4.11 Results of Scenario 11 (Impact of battery cost variations-two HDG)

In this subsection, results of multi-objective optimization by considering the impact of battery cost variations for two HDG are presented. According to the information in Table 6.4, the capital cost and operation and maintenance cost of each battery unit are considered 100 \$ and 5\$ respectively. The results of Tables (6.35) - (6.36) show that voltage unbalance, power loss, HDG system cost and PVWTBAHDG size are reduced and other PQ indexes including voltage sage, voltage swell and THD are increased when battery costs are halved. Also, the results show that HDG system cost and PVWTBAHDG size are reduced and power loss and PQ indexes are increased when battery costs are doubled.

Table. 6.35. Results of two HDG placement in unbalanced 33-bus network by considering battery cost variations

Battery Capital Cost	Ploss (kw)	$\sum V_{sag}$	$\sum V_{swell}$	$\sum THD$	$\sum Un$
50 \$	369.651	5.047	84.247	8.253	34.429
100 \$	377.539	4.016	83.205	8.224	34.479
200 \$	458.542	5.608	84.808	8.249	34.790

Table 6.36. Optimal sizing and siting of two HDG in unbalanced 33-bus network by considering battery cost variations

Battery Capital Cost	PV Size (kW)	WT Size (kW)	BA Size (kW)	Optimal Location (Bus)	Cost (M\$)
50 \$	PV1 (36)	WT1 (50)	Batt1 (4)	Bus (22)	6.989
	PV2 (127)	WT2 (357)	Batt (102)	Bus (29)	
100 \$	PV1 (201)	WT1 (164)	Batt1 (4)	Bus (30)	10.642
	PV2 (111)	WT2 (312)	Batt (15)	Bus (11)	
200 \$	PV1 (60)	WT1 (60)	Batt1 (1)	Bus (2)	7.131
	PV2 (178)	WT2 (239)	Batt (37)	Bus (11)	

Active loss, voltage sag, voltage swell, THD voltage, voltage unbalance and energy contribution of unbalanced 33-bus network by considering battery cost variations for two HDG are illustrated as Figs. (6.36) - (6.41).

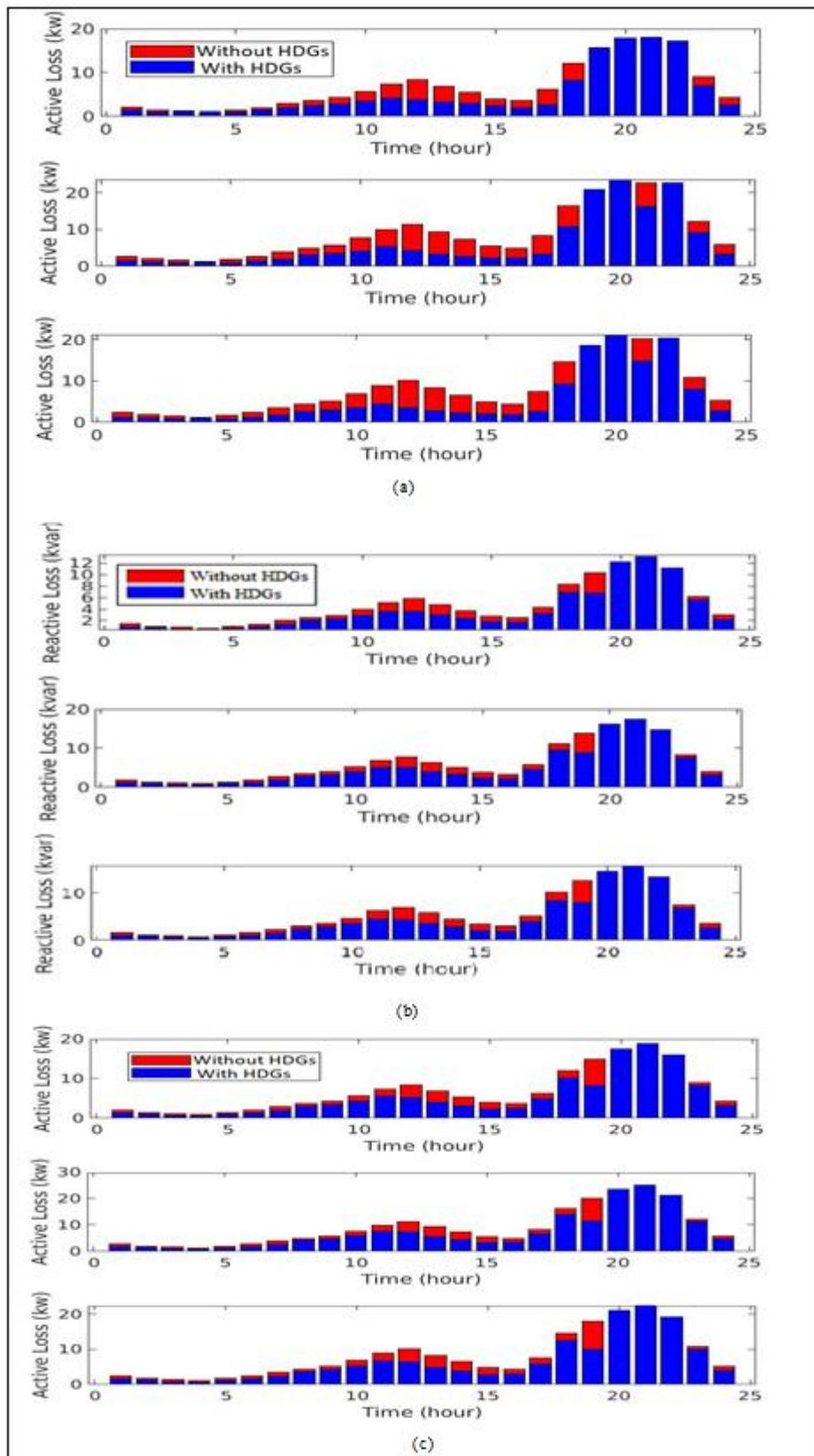


Fig. 6.36. Active loss of unbalanced 33-bus network by considering battery cost variations
a) 50\$, b) 100\$ (base study) and c) 200\$ [Two HDG]

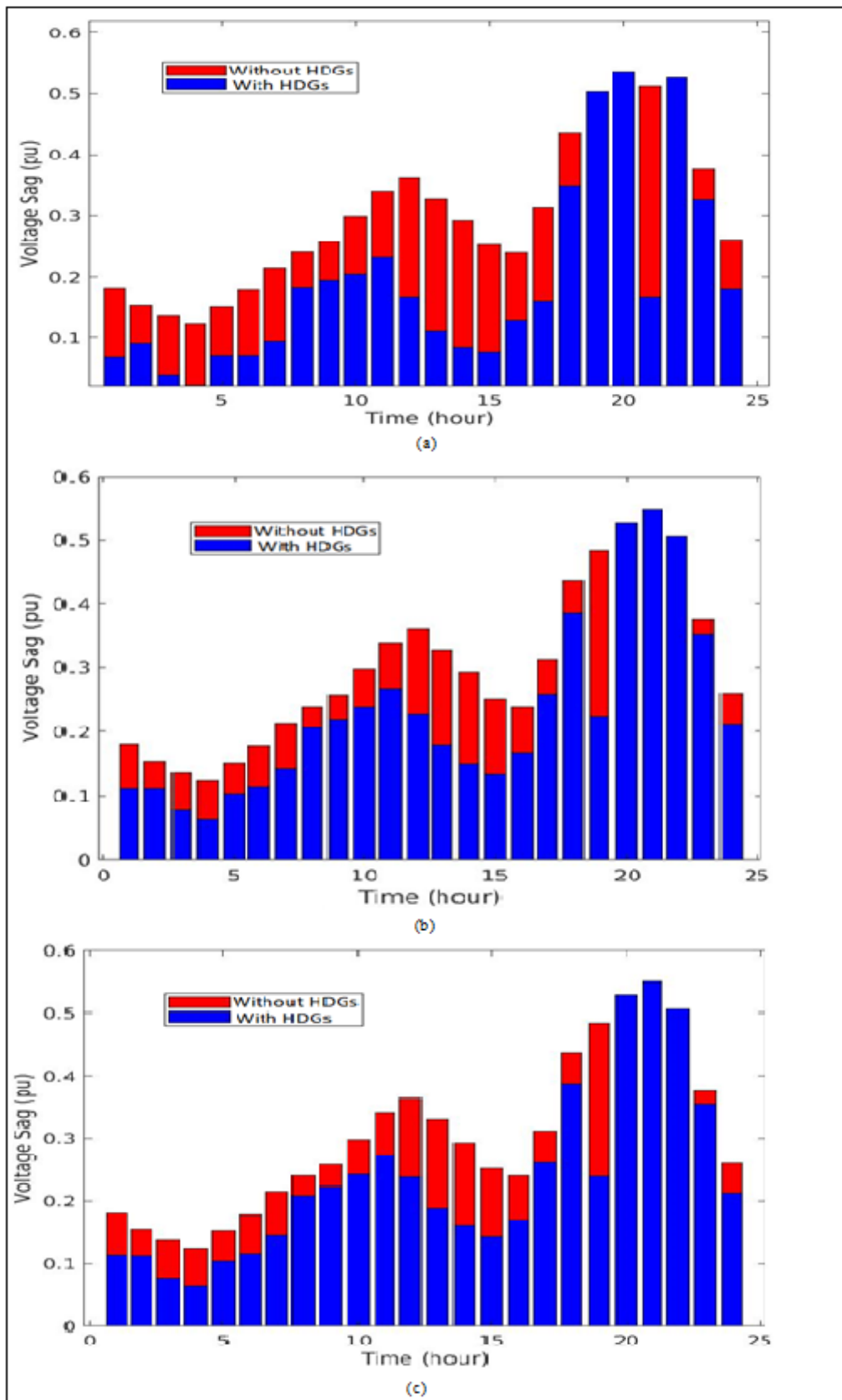


Fig. 6.37. Voltage sag of unbalanced 33-bus network by considering battery cost variations

a) 50\$, b) 100\$ (base study) and c) 200\$ [Two HDG]

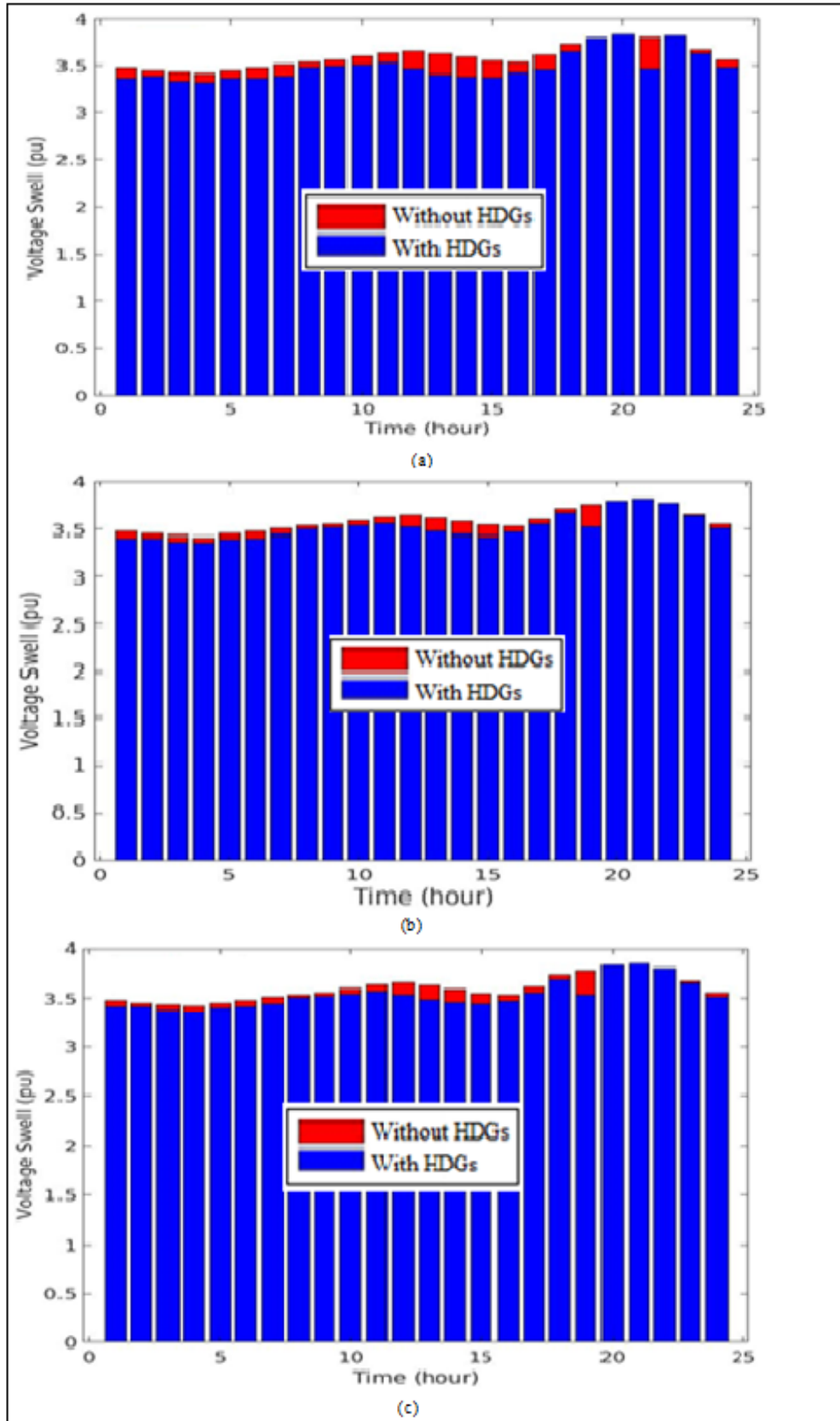


Fig. 6.38. Voltage swell of unbalanced 33-bus network by considering battery cost variations
a) 50\$, b) 100\$ (base study) and c) 200\$ [Two HDG]

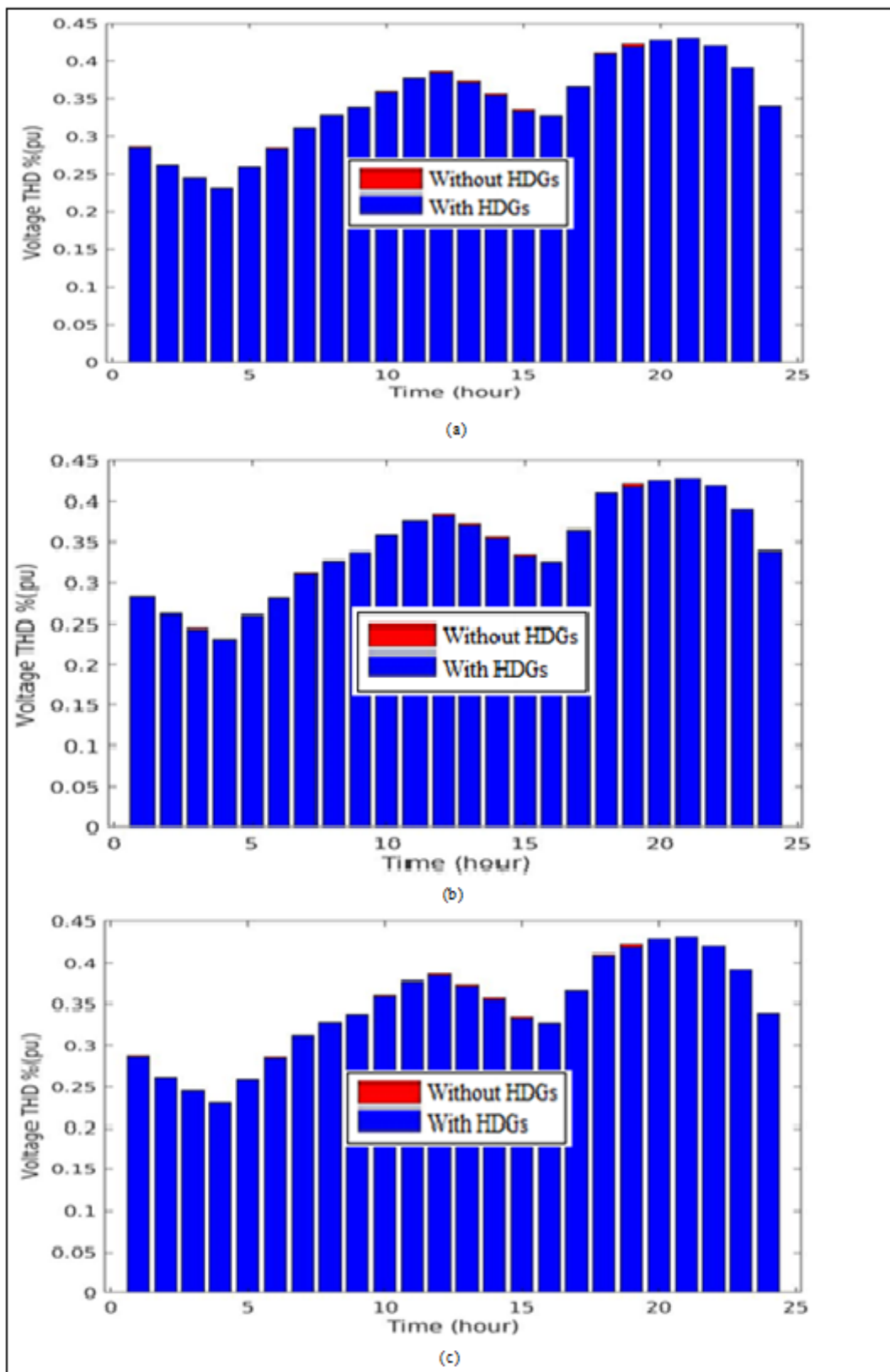


Fig. 6.39. Voltage THD of unbalanced 33-bus network by considering battery cost variations

a) 50\$, b) 100\$ (base study) and c) 200\$ [Two HDG]

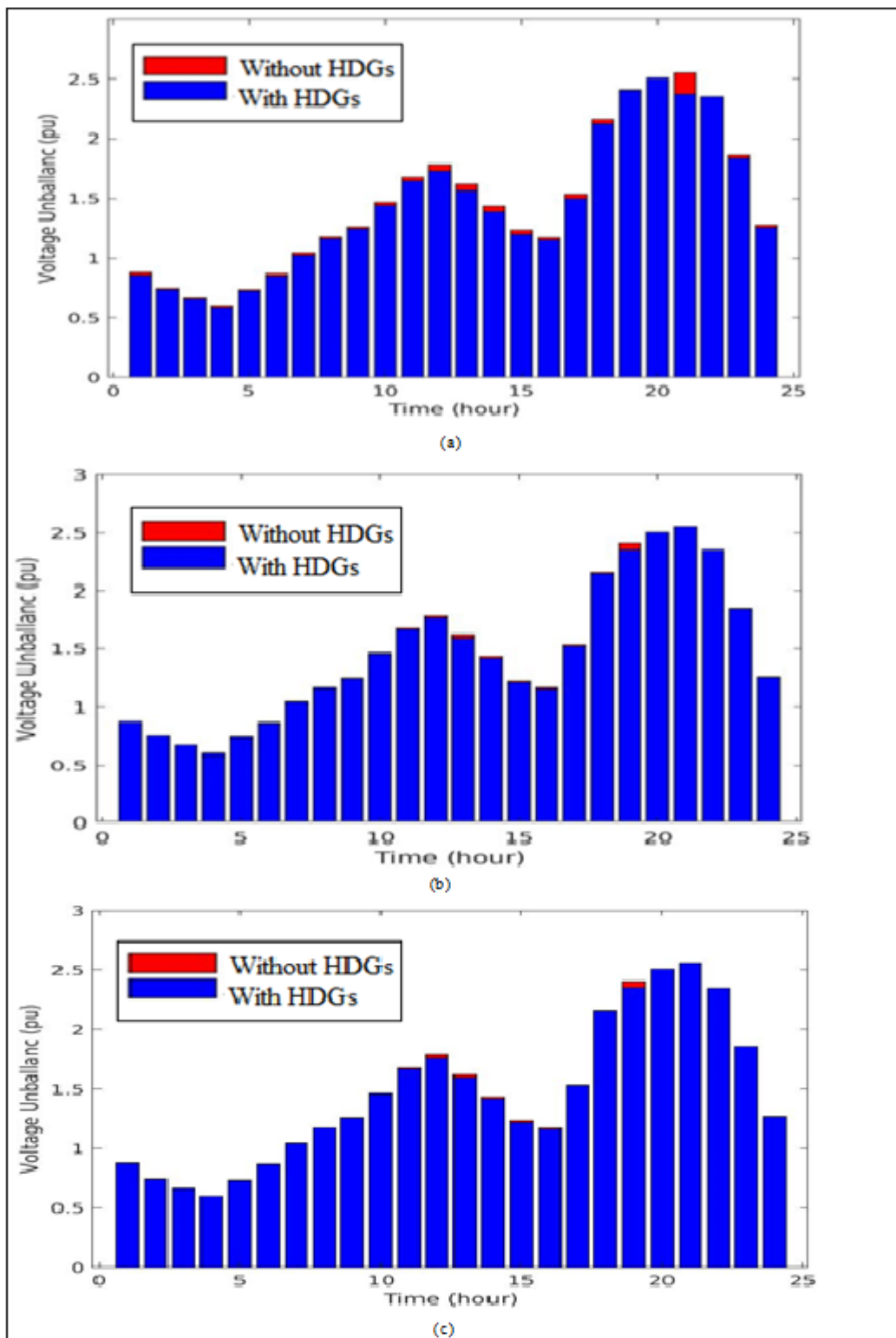
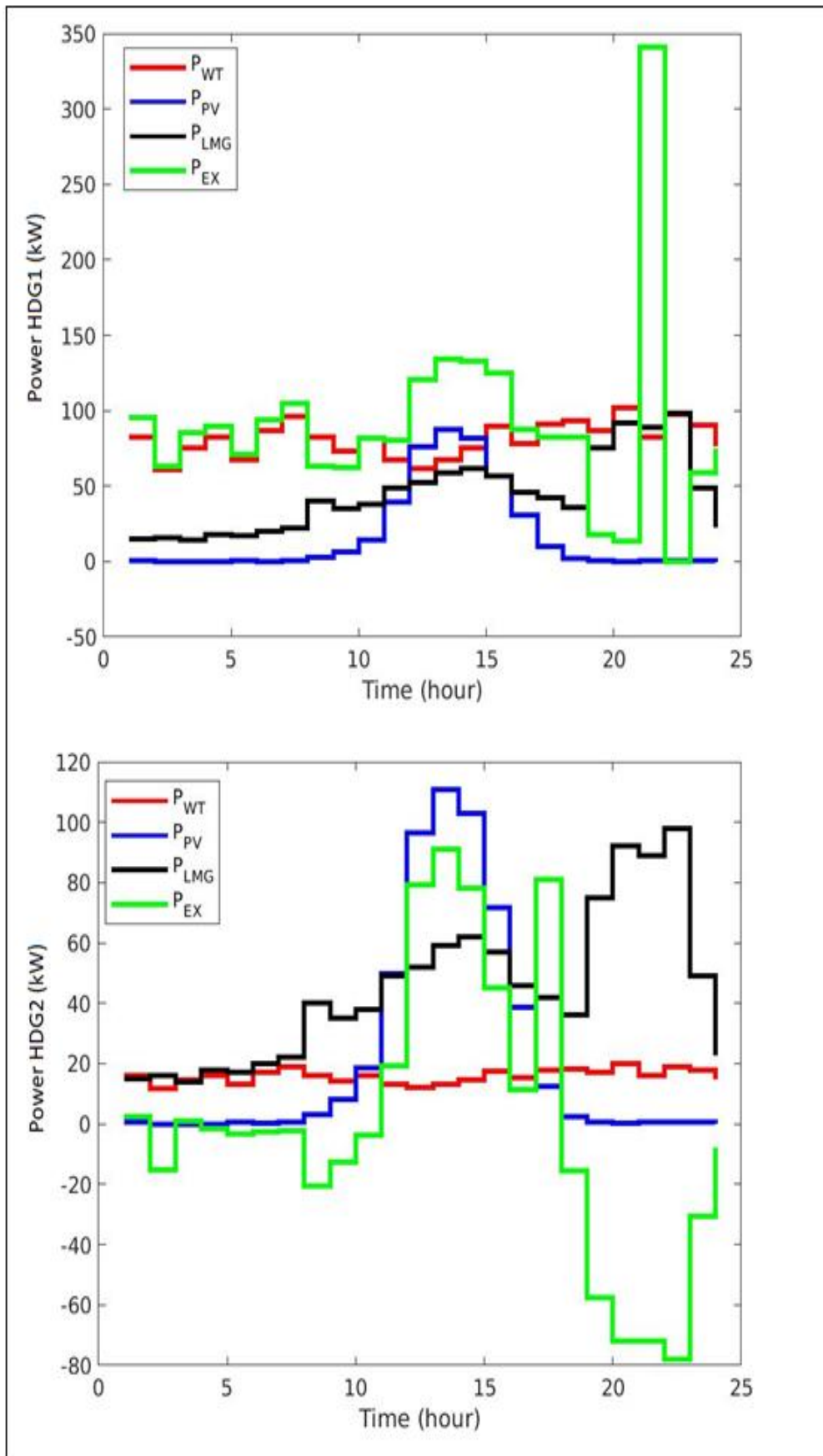
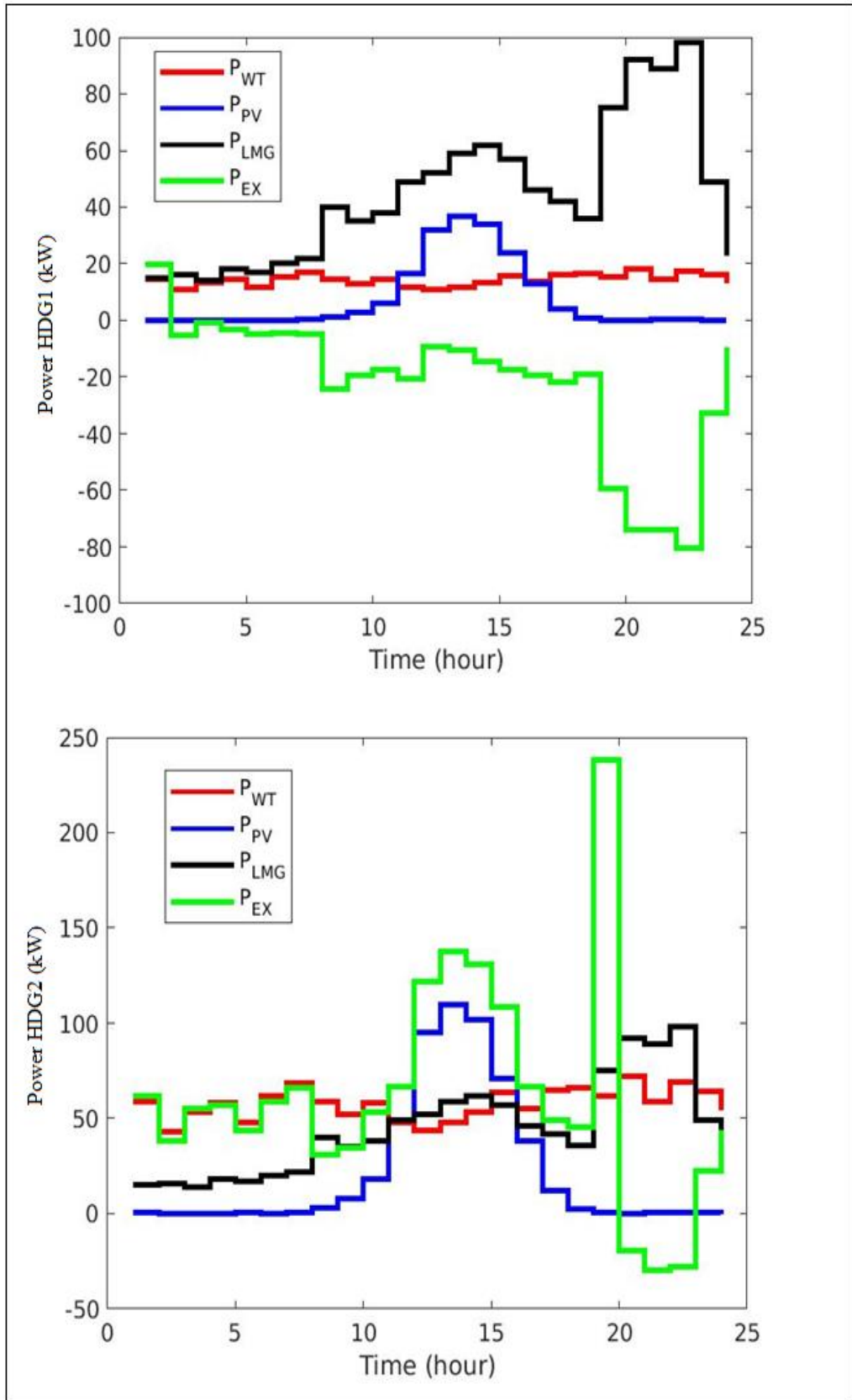


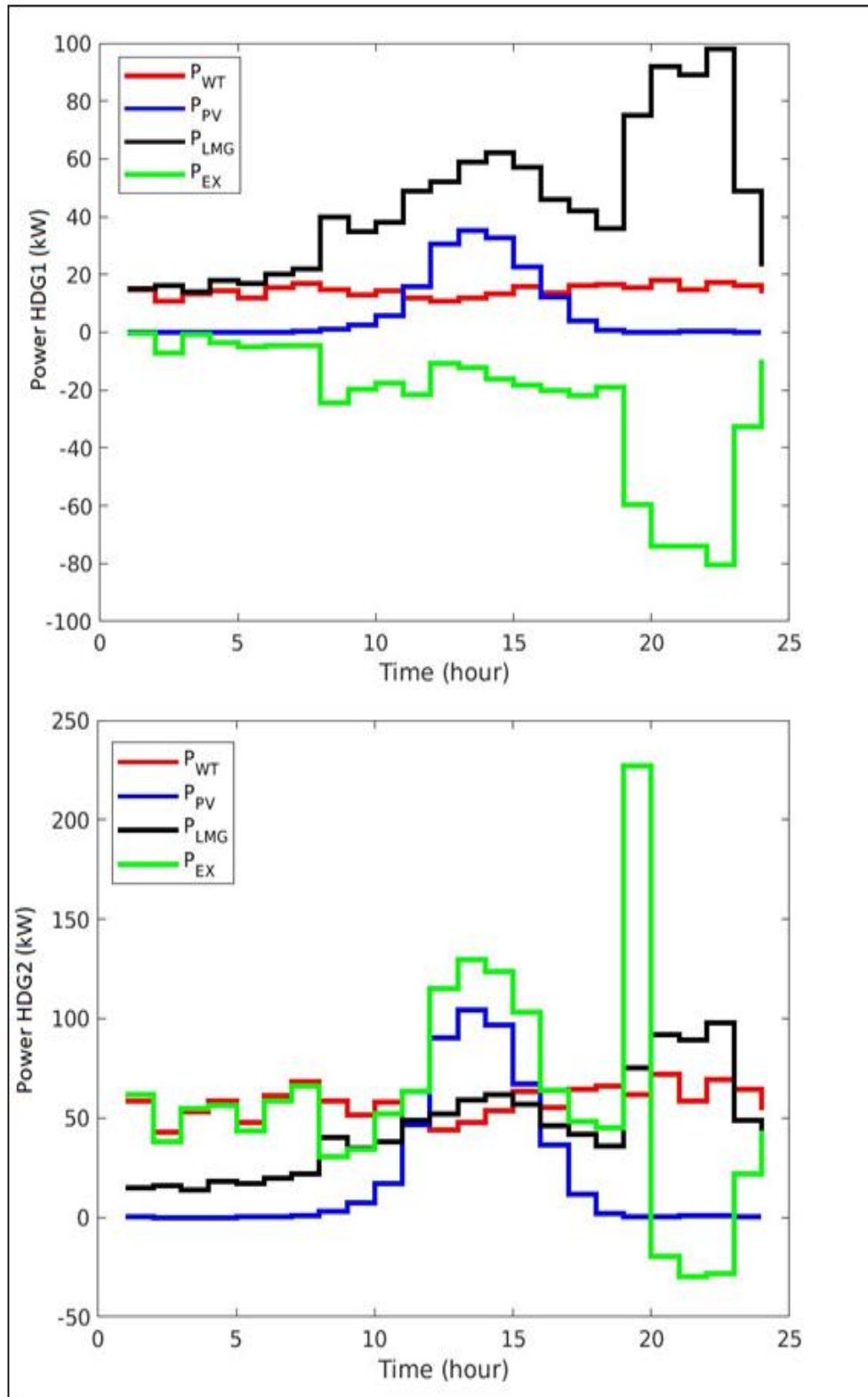
Fig. 6.40. Voltage unbalance of unbalanced 33-bus network by considering battery cost variations a) 50\$, b) 100\$ (base study) and c) 200\$ [Two HDG]



(a)



(b)



(c)

Fig. 6.41. Energy contribution of units considering battery cost variations

a) 50\$, b) 100\$ (base study) and c) 200\$ [Two HDG]

6.2.4.12 Results of Scenario 12 (Superiority of HCSADE to past researches)

In this subsection, the capability of the proposed HCSADE approach due to reducing network loss is compared with some of other methods. In this thesis, the obtained power loss by using the proposed method is equal to 1094.136 kW for 24 hours. Average value of the power loss for one hour is 45.589 kW. In [153], the adaptive colony optimization algorithm (AACO) is used for network reconfiguration with objective of loss reduction in unbalanced 33-bus network and in [154] a network reconfiguration is implemented to reduce the loss cost. In this study, a combined GA and fuzzy genetic algorithm (FGA) is used to solve the network reconfiguration problem. In [155], the reconfiguration of the unbalanced 33-bus distribution network is presented to improve reliability and reduce losses using Modified Heuristic Approach (MHA). A comparison of the proposed HCSADE with AACO, FGA and MHA methods are presented in Table (6.37). The results show that the proposed HCSADE, based on PVWTBAHDG design and placement in the network has the lowest losses. Also, the best amount of THD is obtained with the proposed HCSADE in comparison with the obtained amount in FGA method.

Table 6.37. Comparison to last research for unbalanced 33-bus network

Objective function	Ploss (kW)	$\sum THD$
HCSADE	45.589	8.234
AACO [153]	143.870	--
FGA [154]	148.69	13.307
MHA [155]	142.71	--

6.3 Conclusion

In this chapter, the design and placement of HDG including solar and wind energy resources based on a battery bank system is implemented to reduce losses and improve the PQ in the unbalanced 33-bus distribution network. The design of HDG is done to reduce energy costs including initial investment costs and maintenance and operation costs. Furthermore, Decision variables including location and number of solar panels,

wind turbines, and battery banks are selected and HCSADE method is used based on crossover and mutation operators. Simulation results show that a proper selection of size and site of the HDG in the distribution network can reduce power loss and improve PQ. Also, the results indicate that multi-objective optimization is an appropriate option to show the effective impact on all PQ indices. Besides, the performance and superiority of the HCSADE algorithm over CSA and DE methods as well as other methods in the past studies are confirmed. Also, the results show that by incensing the number of HDG in the network a further improvement in PQ is accrued. Furthermore, by increasing network demand the amount of power loss is increased and PQ is improved.

Chapter7. Conclusion and suggestion

7.1 Conclusion

Advances in technology and the global trend towards the use of renewable energy have introduced distributed generation units in the distribution network as one of the sources of energy supply. Further, some factors such as reliability improvement, pollution and loss reduction have expanded the influence of distributed generation resources in the distribution network. These resources are sited at the end of the network and close to the customers. Also, the generation of these resources is associated with very low pollution and the cost of their primary fuel is minimal. In recent years, renewable energy sources based on distributed generation resources have been widely welcomed by network operators, as these types of resources can provide clean and intelligent generation to meet the demand. One of the best methods to improve power system network characteristics is the use of renewable resources in the distribution network. The use of Photovoltaic-Wind Turbine-Battery Hybrid Distributed Generation (PVWTBAHDG) systems is a highly desirable option for exploiting the distribution networks with the aim of improving network distribution features and in particular, improving network Power Quality (PQ). Non-optimal application of PVWTBAHDG systems may have undesirable effects on network PQ indices, and it will worsen the indices. Therefore, in order to improve the PQ indices, based on the design and application of PVWTBAHDG systems, the optimal location and capacity of this type of system should be determined in the distribution network. The design of PVWTBAHDG systems refers to optimal capacity of the system components, including the PV panels, wind turbines and the capacity of the battery bank. Therefore, in this thesis, the effect of applying the PVWTBAHDG systems on active power losses and PQ indices of radial distribution network has been evaluated. In this research, the PQ indices used include voltage sag, voltage swell, Total Harmonic Distortion (THD) and voltage unbalance. So, the main objective of the problem is to improve the PQ indices of the distribution network. In addition, the optimal application of PVWTBHDG systems, which is an optimization problem with multiple factors, is that traditional methods cannot solve this problem desirably due to its complexity. For this reason, the use of artificial intelligence methods based on intelligent methods of optimization, which has been welcomed in recent years has been proposed in this research for optimization problem solution. In this thesis, a meta-heuristic algorithm named Hybrid Crow Search Algorithm-Differential Evolution (HCSADE) is used to solve the optimization problem. The proposed method is implemented on an unbalanced 33-bus

network. The problem is done as single and multi-objective optimization based on the weighted coefficients method. The simulation results included active power losses, voltage sag, voltage swell, harmonics and voltage unbalance and these parameters are investigated before and after optimization of PVWTBAHDG systems in the network. The effect of increasing the PVWTBAHDG load demand, as well as increasing the network load, is also evaluated for the problem solution. The performance of the proposed HCSADE is compared with the conventional Crow Search Algorithm (CSA) and Differential Evaluation (DE) methods. Furthermore, in order to verify the proposed method, the results are compared with the previous studies. The variations in solar radiation, ambient temperature and wind speed, the HDG load curve with a 100 kW peak and normalized load of network are considered. Also, the technical data for the PV panel, wind turbine and batteries are presented.

The simulation strategies of design and placement of HDGs in unbalanced 33-bus distribution network are presented for different scenarios. Comparison of the single and multi-objective HDG placement shows that the lowest loss is achieved with the objective of loss reduction as single objective. Considering this objective function has positive effect on the improvement of all PQ indices. The size and location of the HDG system, which has a negative effect on the reduction of losses for each of the objective functions of improving the voltage sag, the voltage swell, the THD and the voltage unbalance in the optimized single objective. However, the worst effect on reducing losses in the objective function is voltage unbalance reduction, while the optimization method has done most of the effort to reduce the voltage unbalance and has achieved the desired result and obtained the best response for the voltage unbalance, but active power loss of the network has increased dramatically and resulted in a loss of 6333 kW in 24 hours. The lowest voltage sag is achieved under the voltage sag objective function. It has been observed that the voltage sag objective function has a positive effect on other PQ indices but increases the network losses rather than the base value. The lowest voltage is obtained when the voltage swell is considered as a single-objective function in this case. However, it has been observed that only the objective function of the voltage swell has a positive effect on the THD voltage and voltage unbalance and reduces them rather than the base value, but has a negative effect on voltage sag as well as system cost and power loss. In the single objective of THD reduction, the lowest THD is obtained. The objective function of THD has a positive effect on voltage swell and voltage unbalance and has negative effect on

other indices. The objective function of voltage unbalance improves all PQ indices but increases cost and power loss rates. Also, the best value of the voltage unbalance is obtained in this case. In multi-objective optimization, all objective functions are integrated and normalized. The results show that by considering a multi-objective problem, all indices are improved. Therefore, multi-objective optimization is a more realistic and precise viewpoint to solve a problem that has met all the objectives. The results shows that in the case of the design and placement of two HDGs based on multi-objective optimization using the HCSADE method without considering the cost of HDG, the value of the objective function is reduced, which is to further improve the indices of loss and PQ. Also, the results were clear that the cost of using the two HDGs is higher than one HDG optimal application. It can be seen that all indices have improved beyond the voltage unbalance versus the use of one HDG in condition of two HDG applications. Also, the simulation results showed that the HCSADE method provides lower losses and better PQ indices than CSA and DE methods. It is observed that reducing HDG load demand reduces the cost of the HDG system, and the PQ indices do not change much. Thus, reducing the HDG load demand has more effect on reducing HDG design costs. Also, the increase in network load has led to an increase in losses. The PQ indices have also been increased in comparison with the base state. In scenarios of different combination of HDG system the results show that the combination of PV/WT/Batt/HDG has a lower cost for improving network PQ indices in comparison with other combination of HDG system. Also, the capability of the proposed HCSADE approach to reduce unbalanced 33-bus network losses was compared with some of other methods. In [153], the adaptive colony optimization algorithm (AACO) is used for network reconfiguration with objective of loss reduction in unbalanced 33-bus network and in [154] a network reconfiguration is implemented to reduce the loss cost. In this study, a combined GA method and fuzzy logic (FGA) method is used to solve the network reconfiguration problem. In [155], the reconfiguration of the unbalanced 33-bus distribution network is presented to improve reliability and reduce losses using Modified Heuristic Approach (MHA). A comparison of the proposed HCSADE with AACO, FGA and MHA methods are presented in Table (6.37). The results show that the proposed HCSADE, based on PVWTBAHDG design and placement in the network has the lowest losses. Also, the best amount of THD is obtained with the proposed HCSADE in comparison with the obtained amount in FGA method.

7.2 Suggestion for future work

In this thesis, the design and optimal placement of PVWTHDG based on battery storage are presented with objective of PQ improvement. According to the thesis finding, suggestions for future work are presented as follows:

- Design and optimal placement of PVWTBAHDG by considering reliability improvement of customers;
- Application of PVWTBAHDG and electric vehicles to improve PQ in the distribution system;
- Optimal placement of PVWTBAHDG with network configuration with the aim of PQ improvement;
- Optimal placement of PVWTHDG with fuel cell storage with objective of PQ improvement;
- An integrated hybrid power supply for PVWTBAHDG applications fed by nonconventional energy sources;
- Reliability investigation of electric distribution system with nano-grid architectures using PVWTBAHDG; and
- Control of PVWTBAHDG/ fuel cell with PQ indexes ride-through capability.

References

- [1] T. Ackermann, G. Andersson, and L. Söder, “Distributed generation: a definition,” *Electric Power Syst. Res.*, vol. 57, no. 3, pp. 195–204, 2001.
- [2] P. P. Barker and R. W. De Mello, “Determining the impact of distributed generation on power systems. I. Radial distribution systems,” in *2000 Power Engineering Society Summer Meeting (Cat. No.00CH37134)*, 2002.
- [3] J. A. P. Lopes, N. Hatziargyriou, J. Mutale, P. Djapic, and N. Jenkins, “Integrating distributed generation into electric power systems: A review of drivers, challenges and opportunities,” *Electric Power Syst. Res.*, vol. 77, no. 9, pp. 1189–1203, 2007.
- [4] P. Bajpai and V. Dash, “Hybrid renewable energy systems for power generation in stand-alone applications: A review,” *Renew. Sustain. Energy Rev.*, vol. 16, no. 5, pp. 2926–2939, 2012.
- [5] Y. Naderi, S. H. Hosseini, S. Ghassem Zadeh, B. Mohammadi-Ivatloo, J. C. Vasquez, and J. M. Guerrero, “An overview of power quality enhancement techniques applied to distributed generation in electrical distribution networks,” *Renew. Sustain. Energy Rev.*, vol. 93, pp. 201–214, 2018.
- [6] Y. Ch, S. K. Goswami, and D. Chatterjee, “Effect of network reconfiguration on power quality of distribution system,” *Int. j. electr. power energy syst.*, vol. 83, pp. 87–95, 2016.
- [7] P. C. Chen, R. Salcedo, Q. Zhu, F. De Leon, D. Czarkowski, Z.P. Jiang, V. Spitsa, Z. Zabar, and R.E. Uosef, “Analysis of voltage profile problems due to the penetration of distributed generation in low-voltage secondary distribution networks,” *IEEE trans. power deliv.*, vol. 27, no. 4, pp. 2020–2028, 2012.
- [8] N. Gupta, A. Swarnkar, and K. R. Niazi, “Distribution network reconfiguration for power quality and reliability improvement using Genetic Algorithms,” *Int. j. electr. power energy syst.*, vol. 54, pp. 664–671, 2014.
- [9] B. Sultana, M. W. Mustafa, U. Sultana, and A. R. Bhatti, “Review on reliability improvement and power loss reduction in distribution system via network reconfiguration,” *Renew. Sustain. Energy Rev.*, vol. 66, pp. 297–310, 2016.
- [10] K. M. Jagtap and D. K. Khatod, “Novel approach for loss allocation of distribution networks with DGs,” *Electric Power Syst. Res.*, vol. 143, pp. 303–311, 2017.
- [11] H. HassanzadehFard and A. Jalilian, “Optimal sizing and location of renewable energy based DG units in distribution systems considering load growth,” *Int. j. electr. power energy syst.*, vol. 101, pp. 356–370, 2018.

- [12] A. Ali, D. Raisz, and K. Mahmoud, "Optimal oversizing of utility-owned renewable DG inverter for voltage rise prevention in MV distribution systems," *Int. j. electr. power energy syst.*, vol. 105, pp. 500–513, 2019.
- [13] M. J. Vahid-Pakdel and B. Mohammadi-ivatloo, "Probabilistic assessment of wind turbine impact on distribution networks using linearized power flow formulation," *Electric Power Syst. Res.*, vol. 162, pp. 109–117, 2018.
- [14] A. Y. Abdelaziz, Y. G. Hegazy, W. El-Khattam, and M. M. Othman, "Optimal allocation of stochastically dependent renewable energy based distributed generators in unbalanced distribution networks," *Electric Power Syst. Res.*, vol. 119, pp. 34–44, 2015.
- [15] P. Hou, W. Hu, M. Soltani, and Z. Chen, "Optimized placement of wind turbines in large-scale offshore wind farm using particle swarm optimization algorithm," *IEEE Trans. Sustain. Energy*, vol. 6, no. 4, pp. 1272–1282, 2015.
- [16] Y. Ghiassi-Farrokhfal, F. Kazhmiaka, C. Rosenberg, and S. Keshav, "Optimal design of solar PV farms with storage," *IEEE Trans. Sustain. Energy*, vol. 6, no. 4, pp. 1586–1593, 2015.
- [17] G. V. K. Murthy, S. Sivanagaraju, S. Satyanarayana, and B. H. Rao, "Optimal placement of DG in distribution system to mitigate power quality disturbances," *International Journal of Electrical and Computer Engineering*, vol. 7, no. 2, pp. 266–271, 2014.
- [18] A. Askarzadeh, "A novel metaheuristic method for solving constrained engineering optimization problems: Crow search algorithm," *Comput. Struct.*, vol. 169, pp. 1–12, 2016.
- [19] A. Y. Abdelaziz and A. Fathy, "A novel approach based on crow search algorithm for optimal selection of conductor size in radial distribution networks," *Eng. Sci. Technol. Int. J.*, vol. 20, no. 2, pp. 391–402, 2017.
- [20] P. Rocca, G. Oliveri, and A. Massa, "Differential evolution as applied to electromagnetics," *IEEE Antennas Propag. Mag.*, vol. 53, no. 1, pp. 38–49, 2011.
- [21] G. Oliveri, P. Rocca, and A. Massa, "Differential evolution as applied to electromagnetics: Advances, comparisons, and applications," in *6th European Conf. on Antennas and Propagation (EUCAP)*, IEEE, Mar.2012, pp. 3058-3059.
- [22] A. Bin Humayd, "Distribution system planning with distributed generation: Optimal versus heuristic approach," University of Waterloo, 2011.
- [23] H. L. Willis and W. G. Scott, *Distributed power generation—planning and evaluation*. New York: Marcel Dekker, 2000.
- [24] R. Viral and D. K. Khatod, "Optimal planning of distributed generation systems in distribution system: A review," *Renew. Sustain. Energy Rev.*, vol. 16, no. 7, pp. 5146–5165, 2012.

- [25] N. Hadisaid, J. F. Canard, and F. Dumas, "Dispersed generation impact on distribution networks," *IEEE Computer Applications in Power*, vol. 12, no. 2, 1999.
- [26] J. A. Greatbanks, D. H. Popovic, M. Begovic, A. Pregelj, and T. C. Green, "On optimization for security and reliability of power systems with distributed generation," in *2003 IEEE Bologna Power Tech Conf. Proceedings*, Bologna Italy, Jun.2004.
- [27] M. T. Doyle, "Reviewing the impacts of distributed generation on distribution system protection," in *IEEE Power Engineering Society Summer Meeting*, 2003.
- [28] *Photovoltaics, D.G. and Storage, E., IEEE Application Guide for IEEE Std 1547™, IEEE Standard for Interconnecting Distributed Resources with Electric Power Systems*, IEEE 1547™, 2009.
- [29] O. Ekren and B. Y. Ekren, "Size optimization of a PV/wind hybrid energy conversion system with battery storage using simulated annealing," *Appl. Energy*, vol. 87, no. 2, pp. 592–598, 2010.
- [30] M. Moradi and M. Mehrpooya, "Optimal design and economic analysis of a hybrid solid oxide fuel cell and parabolic solar dish collector, combined cooling, heating and power (CCHP) system used for a large commercial tower," *Energy (Oxf.)*, vol. 130, pp. 530–543, 2017.
- [31] A. Aali, N. Pourmahmoud, and V. Zare, "Exergoeconomic analysis and multi-objective optimization of a novel combined flash-binary cycle for Sabalan geothermal power plant in Iran," *Energy Convers. Manag.*, vol. 143, pp. 377–390, 2017.
- [32] R. Amirante, E. Distaso, and P. Tamburrano, "Novel, cost-effective configurations of combined power plants for small-scale cogeneration from biomass: Design of the immersed particle heat exchanger," *Energy Convers. Manag.*, vol. 148, pp. 876–894, 2017.
- [33] CIGRE Workgroup C6.01. "Development of dispersed generation and consequences for power systems," in *CIGRE Final report*, 2003.
- [34] J. Zhu, K. Cheung, D. Hwang, and A. Sadjadpour, "Operation strategy for improving voltage profile and reducing system loss," *IEEE trans. power deliv.*, vol. 25, no. 1, pp. 390–397, 2010.
- [35] H. Renner and L. Fickert, "Costs and responsibility of power quality in the deregulated electricity market." *Graz*, 1999.
- [36] H. D. Mathur, "Enhancement of power system quality using distributed generation," in *2010 IEEE International Conf. on Power and Energy*, Kuala Lumpur Malaysia, Nov.2010, pp. 567-572.

- [37] A. Woyte, V. V. Thong, R. Belmans, and J. Nijs, "Voltage fluctuations on distribution level introduced by photovoltaic systems," *IEEE trans. energy convers.*, vol. 21, no. 1, pp. 202–209, 2006.
- [38] C. L. T. Borges and D. M. Falcão, "Optimal distributed generation allocation for reliability, losses, and voltage improvement," *Int. j. electr. power energy syst.*, vol. 28, no. 6, pp. 413–420, 2006.
- [39] R. Billinton and R. N. Allan, *Reliability evaluation of engineering systems*. New York: Plenum press, 1992.
- [40] N. Jenkins, R. Allan, P. Crossley, D. Kirschen, and G. Strbac, *embedded Generation*. London, The Institution of Engineering and Technology, 2000.
- [41] R. A. Walling, R. Saint, R. C. Dugan, J. Burke, and L. A. Kojovic, "Summary of distributed resources impact on power delivery systems," *IEEE trans. power deliv.*, vol. 23, no. 3, pp. 1636–1644, 2008.
- [42] *IEEE Standard for Distributed Resources Interconnected with Electric Power Systems*, IEEE P1547, 2002.
- [43] M. Thomson, "Automatic voltage control relays and embedded generation," *Power Eng. J.*, vol. 14, no. 2, pp. 71–76, 2000.
- [44] C. L. Masters, "Voltage rise: the big issue when connecting embedded generation to long 11 kV overhead lines," *Power Eng. J.*, vol. 16, no. 1, pp. 5–12, 2002.
- [45] S. Repo, H. Laaksonen, P. Jarventausta, O. Huhtala, and M. Mickelsson, "A case study of a voltage rise problem due to a large amount of distributed generation on a weak distribution network," in *2003 IEEE Bologna Power Tech Conf. Proceedings*, Bologna Italy, Jun.2004.
- [46] O. Badran, S. Mekhilef, H. Mokhlis, and W. Dahalan, "Optimal reconfiguration of distribution system connected with distributed generations: A review of different methodologies," *Renew. Sustain. Energy Rev.*, vol. 73, pp. 854–867, 2017.
- [47] S. Dahal and H. Salehfar, "Impact of distributed generators in the power loss and voltage profile of three phase unbalanced distribution network," *Int. j. electr. power energy syst.*, vol. 77, pp. 256–262, 2016.
- [48] P. Kayal and C. K. Chanda, "Placement of wind and solar based DGs in distribution system for power loss minimization and voltage stability improvement," *Int. j. electr. power energy syst.*, vol. 53, pp. 795–809, 2013.
- [49] A. Safaei, B. Vahidi, H. Askarian-Abyaneh, E. Azad-Farsani, and S. M. Ahadi, "A two step optimization algorithm for wind turbine generator placement considering maximum allowable capacity," *Renew. Energy*, vol. 92, pp. 75–82, 2016.

- [50] H. S. Ramadan, A. F. Bendary, and S. Nagy, "Particle swarm optimization algorithm for capacitor allocation problem in distribution systems with wind turbine generators," *Int. j. electr. power energy syst.*, vol. 84, pp. 143–152, 2017.
- [51] S. S. Tanwar and D. K. Khatod, "Techno-economic and environmental approach for optimal placement and sizing of renewable DGs in distribution system," *Energy (Oxf.)*, vol. 127, pp. 52–67, 2017.
- [52] K.-Y. Liu, W. Sheng, Y. Liu, X. Meng, and Y. Liu, "Optimal siting and sizing of DGs in distribution system considering time sequence characteristics of loads and DGs," *Int. j. electr. power energy syst.*, vol. 69, pp. 430–440, 2015.
- [53] F. Ugranlı and E. Karatepe, "Optimal wind turbine sizing to minimize energy loss," *Int. j. electr. power energy syst.*, vol. 53, pp. 656–663, 2013.
- [54] G. Mokryani and P. Siano, "Optimal siting and sizing of wind turbines based on genetic algorithm and optimal power flow," in *Renewable Energy Integration*, Singapore: Springer Singapore, 2014, pp. 125–144.
- [55] G. Mokryani and P. Siano, "Optimal wind turbines placement within a distribution market environment," *Appl. Soft Comput.*, vol. 13, no. 10, pp. 4038–4046, 2013.
- [56] M. Dorigo and G. Di Caro, "Ant colony optimization: a new meta-heuristic," in *Proceedings of the 1999 Congress on Evolutionary Computation-CEC99 (Cat. No. 99TH8406)*, 2003.
- [57] P. Azad and N. J. Navimipour, "An energy-aware task scheduling in the cloud computing using a hybrid cultural and ant colony optimization algorithm," *Int. j. cloud appl. comput.*, vol. 7, no. 4, pp. 20–40, 2017.
- [58] "A concise overview of applications of ant colony optimization," *Wiley encyclopedia of operations research and management science*, 2010.
- [59] M. C. Pimentel Filho, E. G. M. de Lacerda, and M. F. Medeiros, "Capacitor placement using ant colony optimization and gradient," in *2009 15th Int. Conf. on Intelligent System Applications to Power Systems*, Curitiba Brazil, Nov. 2009.
- [60] M. Kefayat, A. Lashkar Ara, and S. A. Nabavi Niaki, "A hybrid of ant colony optimization and artificial bee colony algorithm for probabilistic optimal placement and sizing of distributed energy resources," *Energy Convers. Manag.*, vol. 92, pp. 149–161, 2015.
- [61] I. A. Farhat, "Ant colony optimization for optimal distributed generation in distribution systems," *Proceedings of World Academy of Science, Engineering and Technology*, no. 80, p. 495, 2013.

- [62] M. Mahdavi, M. Fesanghary, and E. Damangir, "An improved harmony search algorithm for solving optimization problems," *Appl. Math. Comput.*, vol. 188, no. 2, pp. 1567–1579, 2007.
- [63] D. Karaboga and B. Basturk, "A powerful and efficient algorithm for numerical function optimization: artificial bee colony (ABC) algorithm," *J. Glob. Optim.*, vol. 39, no. 3, pp. 459–471, 2007.
- [64] J. J. Jamian, W. M. Dahalan, H. Mokhlis, M. W. Mustafa, Z. J. Lim, and M. N. Abdullah, "Power losses reduction via simultaneous optimal distributed generation output and reconfiguration using ABC optimization," *J. Electr. Eng. Technol.*, vol. 9, no. 4, pp. 1229–1239, 2014.
- [65] A. El-Zonkoly, "Optimal placement and schedule of multiple grid connected hybrid energy systems," *Int. j. electr. power energy syst.*, vol. 61, pp. 239–247, 2014.
- [66] Y., Tan and Y. Zhu, "Fireworks algorithm for optimization," in *Intern. Conf. on swarm intelligence*, Springer, Berlin, Heidelberg, June 2010, pp. 355-364.
- [67] A. M. Imran, M. Kowsalya, and D. P. Kothari, "A novel integration technique for optimal network reconfiguration and distributed generation placement in power distribution networks," *International Journal of Electrical Power & Energy Systems*, vol. 63, pp. 461–472, 2014.
- [68] P. Civicioglu, "Backtracking Search Optimization Algorithm for numerical optimization problems," *Appl. Math. Comput.*, vol. 219, no. 15, pp. 8121–8144, 2013.
- [69] E. S. Ali, S. M. Abd Elazim, and A. Y. Abdelaziz, "Ant Lion Optimization Algorithm for optimal location and sizing of renewable distributed generations," *Renew. Energy*, vol. 101, pp. 1311–1324, 2017.
- [70] J. Dolezal, P. Santarius, J. Tlustý, V. Valouch, and F. Vybiralík, "The effect of dispersed generation on power quality in distribution system," in *CIGRE/IEEE PES Int. Symp. Quality and Security of Electric Power Delivery Systems*, Montreal QC Canada, Oct.2003, pp. 204-207.
- [71] S. A. Papathanassiou and N. D. Hatziargyriou, "Technical requirements for the connection of dispersed generation to the grid," in *2001 Power Engineering Society Summer Meeting*, Jul.2001, pp. 749-754.
- [72] F. M. Gatta, F. Iliecto, S. Lauria, and P. Masato, "Modelling and computer simulation of dispersed generation in distribution networks. measures to prevent disconnection during system disturbances," in *2003 IEEE Bologna Power Tech Conf. Proceedings*, Bologna Italy, Vol. 3, Jun.2003.

- [73] A. Bhowmik, A. Maitra, S. M. Halpin, and J. E. Schatz, "Determination of allowable penetration levels of distributed generation resources based on harmonic limit considerations," *IEEE trans. power deliv.*, vol. 18, no. 2, pp. 619–624, 2003.
- [74] T. Gonen, *Electric Power Distribution Engineering*, 3th ed. New York: McGraw-Hill, 2015.
- [75] T. Hiyama, M. S. A. A. Hammam, T. H. Ortmeyer, J. Janczak, Pillegi, and T. J. Gentile, "Distribution system modeling with distributed harmonic sources," IEEE, " *Trans. Power Delivery*, vol. 4, pp. 1297–1304, 1989.
- [76] B. Bhandari, K.-T. Lee, G.-Y. Lee, Y.-M. Cho, and S.-H. Ahn, "Optimization of hybrid renewable energy power systems: A review," *Int. J. Precis. Eng. Manuf.-Green Technol.*, vol. 2, no. 1, pp. 99–112, 2015.
- [77] T. Markvart, A. Fragaki, and J. N. Ross, "PV system sizing using observed time series of solar radiation," *Sol. Energy*, vol. 80, no. 1, pp. 46–50, 2006.
- [78] B. Ai, H. Yang, H. Shen, and X. Liao, "Computer-aided design of PV/wind hybrid system," *Renew. Energy*, vol. 28, no. 10, pp. 1491–1512, 2003.
- [79] W. Kellogg, M. H. Nehrir, G. Venkataramanan, and V. Gerez, "Optimal unit sizing for a hybrid wind/photovoltaic generating system," *Electric Power Syst. Res.*, vol. 39, no. 1, pp. 35–38, 1996.
- [80] K. Kusakana and H. J. Vermaak, "Hybrid renewable power systems for mobile telephony base stations in developing countries," *Renew. Energy*, vol. 51, pp. 419–425, 2013.
- [81] H. Yang, L. Lu, and W. Zhou, "A novel optimization sizing model for hybrid solar-wind power generation system," *Sol. Energy*, vol. 81, no. 1, pp. 76–84, 2007.
- [82] A. Kaabeche and R. Ibtouen, "Techno-economic optimization of hybrid photovoltaic/wind/diesel/battery generation in a stand-alone power system," *Sol. Energy*, vol. 103, pp. 171–182, 2014.
- [83] H. Yang, W. Zhou, L. Lu, and Z. Fang, "Optimal sizing method for stand-alone hybrid solar-wind system with LPSP technology by using genetic algorithm," *Sol. Energy*, vol. 82, no. 4, pp. 354–367, 2008.
- [84] A. Askarzadeh, "Developing a discrete harmony search algorithm for size optimization of wind-photovoltaic hybrid energy system," *Sol. Energy*, vol. 98, pp. 190–195, 2013.
- [85] Y. A. Katsigiannis, P. S. Georgilakis, and E. S. Karapidakis, "Multiobjective genetic algorithm solution to the optimum economic and environmental performance problem of small autonomous hybrid power systems with renewables," *IET Renew. Power Gener.*, vol. 4, no. 5, p. 404, 2010.

- [86] A. Askarzadeh, "Distribution generation by photovoltaic and diesel generator systems: Energy management and size optimization by a new approach for a stand-alone application," *Energy (Oxf.)*, vol. 122, pp. 542–551, 2017.
- [87] R. Dufo-López and J. L. Bernal-Agustín, "Multi-objective design of PV–wind–diesel–hydrogen–battery systems," *Renew. Energy*, vol. 33, no. 12, pp. 2559–2572, 2008.
- [88] M. Sharafi and T. Y. ELMekkawy, "Multi-objective optimal design of hybrid renewable energy systems using PSO-simulation based approach," *Renew. Energy*, vol. 68, pp. 67–79, 2014.
- [89] Z. Shi, R. Wang, and T. Zhang, "Multi-objective optimal design of hybrid renewable energy systems using preference-inspired coevolutionary approach," *Sol. Energy*, vol. 118, pp. 96–106, 2015.
- [90] S. Ahmadi and S. Abdi, "Application of the Hybrid Big Bang–Big Crunch algorithm for optimal sizing of a stand-alone hybrid PV/wind/battery system," *Sol. Energy*, vol. 134, pp. 366–374, 2016.
- [91] H. R. Baghaee, M. Mirsalim, G. B. Gharehpetian, and H. A. Talebi, "Reliability/cost-based multi-objective Pareto optimal design of stand-alone wind/PV/FC generation microgrid system," *Energy (Oxf.)*, vol. 115, pp. 1022–1041, 2016.
- [92] A. Maleki and F. Pourfayaz, "Optimal sizing of autonomous hybrid photovoltaic/wind/battery power system with LPSP technology by using evolutionary algorithms," *Sol. Energy*, vol. 115, pp. 471–483, 2015.
- [93] M. J. Hadidian-Moghaddam, S. Arabi-Nowdeh, and M. Bigdeli, "Optimal sizing of a stand-alone hybrid photovoltaic/wind system using new grey wolf optimizer considering reliability," *J. Renew. Sustain. Energy*, vol. 8, no. 3, p. 035903, 2016.
- [94] S. Berrazouane, K. Mohammedi, and S. Alem, "Design and optimal energy management strategy for stand-alone PV-battery-Diesel systems using cuckoo search algorithm," in *3th Int. Conf. on Systems and Control*, Algiers Algeria, Oct.2013, pp. 230-235.
- [95] A. K. Bansal, R. Kumar, and R. A. Gupta, "Economic analysis and power management of a Small Autonomous Hybrid Power System (SAHPS) using biogeography based optimization (BBO) algorithm," *IEEE Trans. Smart Grid*, vol. 4, no. 1, pp. 638–648, 2013.
- [96] S. Leva and D. Zaninelli, "Hybrid renewable energy-fuel cell system: Design and performance evaluation," *Electric Power Syst. Res.*, vol. 79, no. 2, pp. 316–324, 2009.
- [97] C. V. T. Cabral, D. O. Filho, A. S. A. C. Diniz, J. H. Martins, O. M. Toledo, and L. de V. B. Machado Neto, "A stochastic method for stand-alone photovoltaic system sizing," *Sol. Energy*, vol. 84, no. 9, pp. 1628–1636, 2010.

- [98] G. Mousavi and S. M., “An autonomous hybrid energy system of wind/tidal/microturbine/battery storage,” *International Journal of Electrical Power and Energy Systems*, vol. 43, no. 1, pp. 1144–1154, 2012.
- [99] Z. W. Geem, “Size optimization for a hybrid photovoltaic–wind energy system,” *Int. j. electr. power energy syst.*, vol. 42, no. 1, pp. 448–451, 2012.
- [100] N. M. M. Razali and A. H. Hashim, “Backward reduction application for minimizing wind power scenarios in stochastic programming,” in *2010 4th Int. Power Engineering and Optimization Conf. (PEOCO)*, Shah Alam Malaysia, un.2010, pp. 430-434.
- [101] E. Koutroulis and D. Kolokotsa, “Design optimization of desalination systems power-supplied by PV and W/G energy sources,” *Desalination*, vol. 258, no. 1–3, pp. 171–181, 2010.
- [102] B. Abu-Hijleh, “Use of hybrid PV and wind turbine–grid connected system in a local Emirati home in Dubai-UAE,” *Energy procedia*, vol. 100, pp. 463–468, 2016.
- [103] H. Gharavi, M. M. Ardehali, and S. Ghanbari-Tichi, “Imperial competitive algorithm optimization of fuzzy multi-objective design of a hybrid green power system with considerations for economics, reliability, and environmental emissions,” *Renew. Energy*, vol. 78, pp. 427–437, 2015.
- [104] B. Mangu, S. Akshatha, D. Suryanarayana, and B. G. Fernandes, “Grid-connected PV-wind-battery-based multi-input transformer-coupled bidirectional DC-DC converter for household applications,” *IEEE J. Emerg. Sel. Top. Power Electron.*, vol. 4, no. 3, pp. 1086–1095, 2016.
- [105] C. Baglivo, D. Mazzeo, G. Oliveti, and P. M. Congedo, “Technical data of a grid-connected photovoltaic/wind hybrid system with and without storage battery for residential buildings located in a warm area,” *Data Brief*, vol. 20, pp. 587–590, 2018.
- [106] S. Khisa, R. Ebihara, and T. Dei, “Dynamics of a grid connected hybrid wind-solar and battery system: Case study in Naivasha-Kenya,” *Energy Procedia*, vol. 138, pp. 680–685, 2017.
- [107] “Forecast International's Energy Portal, Renewable Energy,” Aug. 15, 2014. Accessed on: Feb. 23, 2021. [Online]. Available: <http://www.fi-powerweb.com/Renewable-Energy.html>
- [108] K. Moslehi and R. Kumar, “A reliability perspective of the smart grid,” *IEEE Trans. Smart Grid*, vol. 1, no. 1, pp. 57–64, 2010.
- [109] J. L. Bernal-Agustín, R. Dufo-López, and D. M. Rivas-Ascaso, “Design of isolated hybrid systems minimizing costs and pollutant emissions,” *Renew. Energy*, vol. 31, no. 14, pp. 2227–2244, 2006.

- [110] A. K. Kaviani, G. H. Riahy, and S. M. Kouhsari, "Optimal design of a reliable hydrogen-based stand-alone wind/PV generating system, considering component outages," *Renewable energy*, vol. 34, no. 11, pp. 2380–2390, 2009.
- [111] B. O. Bilal, V. Sambou, P. A. Ndiaye, C. M. F. Kébé, and M. Ndong, "Optimal design of a hybrid solar–wind-battery system using the minimization of the annualized cost system and the minimization of the loss of power supply probability (LPSP)," *Renewable Energy*, vol. 35, no. 10, pp. 2388–2390, 2010.
- [112] H. Borhanazad, S. Mekhilef, V. Gounder Ganapathy, M. Modiri-Delshad, and A. Mirtaheri, "Optimization of micro-grid system using MOPSO," *Renew. Energy*, vol. 71, pp. 295–306, 2014.
- [113] B. Jyoti Saharia, H. Brahma, and N. Sarmah, "A review of algorithms for control and optimization for energy management of hybrid renewable energy systems," *J. Renew. Sustain. Energy*, vol. 10, no. 5, p. 053502, 2018.
- [114] D. Emad, M. A. El-Hameed, M. T. Yousef, and A. A. El-Fergany, "Computational methods for optimal planning of hybrid renewable microgrids: A comprehensive review and challenges," *Arch. Comput. Methods Eng.*, vol. 27, no. 4, pp. 1297–1319, 2020.
- [115] R.C. Dugan, H.W. Beaty, and S. Santoso, *Electrical Power Systems Quality*, 3th ed. New York: Tata McGraw Hill Education, 2012.
- [116] *Electromagnetic compatibility (EMC) - Part 2-5: Environment - Description and classification of electromagnetic environments*, IEC TR 61000-2-5:2017, 2017.
- [117] *IEEE Recommended Practice for Monitoring Electric Power Quality*, IEEE Std 1159-1995(R2001), 1995.
- [118] *Electromagnetic compatibility (EMC) Part 4-11: Testing and measurement techniques – Voltage dips, short interruptions and voltage variations immunity tests*, IEC 61000-4-11:2004, 2004.
- [119] M. F. McGranaghan, D. R. Mueller, and M. J. Samotyj, "Voltage sags in industrial systems," *IEEE Trans. Ind. Appl.*, vol. 29, no. 2, pp. 397–403, 1993.
- [120] *Electromagnetic compatibility (EMC) - Part 2: Environment - Section 1: Description of the environment - Electromagnetic environment for low-frequency conducted disturbances and signaling in public power supply systems*, IEC TR 61000-2-1:1990, 1990.
- [121] *Semiconductor converters – General requirements and line commutated converters – Part 1-1: Specification of basic requirements*, IEC 60146-1-1: 4.0, 2009.
- [122] *Electromagnetic compatibility (EMC) - Part 2-2: Environment - Compatibility levels for low-frequency conducted disturbances and signaling in public low-voltage power supply systems*, IEC 61000-2-2:2002, 2002.

- [123] *The New IEEE Standards Dictionary of Electrical and Electronics Terms*, IEEE 100-1992, 1993.
- [124] *Power Quality Measurement Methods*, IEC 61000-4-30 77A/356/CDV, 2001.
- [125] *Electromagnetic compatibility (EMC) - Part 4: Testing and measurement techniques – Section 15: Flickermeter - Functional and design specifications*, IEC 61000-4-15:1997, 1997.
- [126] *compatibility (EMC) - Part 3-3: Limits - Limitation of voltage changes, voltage fluctuations and flicker in public low-voltage supply systems, for equipment with rated current ≤ 16 A per phase and not subject to conditional connection*, IEC 61000-3-3:2013/AMD1:2017, 2017.
- [127] *Flickermeter - Functional and design specifications*, IEC TS 60868:1986, 1986.
- [128] *National Electrical Code*, ANCI/NFPA70-1993, 1993.
- [129] *International electromagnetic vocabulary, part 161: electromagnetic compatibility*, 1989. IEC60050-161:1990, 1990.
- [130] *IEEE Recommended practice for emergency and standby power systems for Industrial and commercial applications*, IEEE Standard 446-1987, 1987.
- [131] J. Lamoree, J.C. Smith, P. Vinett, T. Duffy, and M. Klein, “The impact of voltage sags on industrial plant loads,” In *First Int. Conf. on Power Quality*, PQA, Oct.1991.
- [132] G. E. Beam, E. G. Dolack, and C. J. Melhorn, “Power quality case studies-voltage sags: The impact on utility and industrial customers,” *Electric Power Research Inst*, no. EPRI-TR-104581, p. 9311343–, 1995.
- [133] C. Becker *et al.*, “Proposed chapter 9 for predicting voltage sags (dips) in revision to IEEE Std 493, the Gold Book,” *IEEE Trans. Ind. Appl.*, vol. 30, no. 3, pp. 805–821, 1994.
- [134] *IEEE Recommended Practice for the Design of Reliable Industrial and Commercial Power Systems*, ANSI/IEEE std.493-1990, 1991.
- [135] F. H. Silveira, S. Visacro, and R. E. Souza, “Lightning performance of transmission lines: Assessing the quality of traditional methodologies to determine back flashover rate of transmission lines taking as reference results provided by an advanced approach,” *Electric Power Syst. Res.*, vol. 153, pp. 60–65, 2017.
- [136] *IEEE Recommended Practice for Emergency and Standby Power Systems for Industrial and Commercial Applications*, IEEE 446-1995, 1996.
- [137] Westinghouse Electric Corporation. Electric Utility Engineering Dept. *Electric Utility Engineering Reference Book: Distribution Systems*. Vol. 3. The Corporation, 1965.
- [138] L. E. Conrad and M. H. J. Bollen, “Voltage sag coordination for reliable plant operation,” *IEEE Trans. Ind. Appl.*, vol. 33, no. 6, pp. 1459–1464, 1997.
- [139] *IEC standard voltages*, IES60038:2009, 2009.

- [140] A. Robert and J. Marquet, "Assessing voltage quality with relation to harmonics, flicker and unbalance," In *Int. Conf. on Large High Voltage Electric Systems*, vol. 2, Aug.1992, pp. 36-203.
- [141] "interharmonics in power systems, IEEE INTERHARMONIC TASK FORCE," *CIGRE*, vol. 05, no. CIRED2CC02.
- [142] *Electromagnetic compatibility (EMC) - Part 4-15: Testing and measurement techniques– Flickermeter - Functional and design specifications*, IEC 61000-4-15:2010, 2010.
- [143] *Electromagnetic compatibility (EMC) – Part 3-7: Limits – Assessment of emission limits for the connection of fluctuating installations to MV, HV and EHV power systems*, IEC/TR 61000-3-7, 2008.
- [144] T. G. S. Roman and J. R. Ubeda, "Power quality regulation in Argentina: flicker and harmonics," *IEEE trans. power deliv.*, vol. 13, no. 3, pp. 895–901, 1998.
- [145] *IEEE Recommended Practice and Requirements for Harmonic Control in Electric Power Systems*, IEEE Std 519-2014, 2014.
- [146] *IEEE Recommended Practice for Establishing Transformer Capability When Supplying Nonsinusoidal Load Currents*, C57.110-1986, 1988.
- [147] R. D. Henderson and P. J. Rose, "Harmonics: the effects on power quality and transformers," *IEEE Trans. Ind. Appl.*, vol. 30, no. 3, pp. 528–532, 1994.
- [148] J. Arrillaga and N.R. Watson, 2004. *Power system harmonics*, 2th ed. England, John Wiley and Sons, 2004.
- [149] *Electromagnetic compatibility (EMC) - Environment - Compatibility levels for low-frequency conducted disturbances and signalling in public low-voltage power supply system*, IEC 61000-2-2:2002/AMD2:2018, 2018.
- [150] *Electromagnetic compatibility (EMC) - Part 3-2: Limits - Limits for harmonic current emissions (equipment input current ≤ 16 A per phase)*, IEC 61000-3-2:2018, 2018.
- [151] *Electromagnetic compatibility (EMC) - Part 2-4: Environment - Compatibility levels in industrial plants for low-frequency conducted disturbances*, IEC 61000-2-4:2002, 2002.
- [152] T. Ma, H. Yang, and L. Lu, "A feasibility study of a stand-alone hybrid solar–wind–battery system for a remote island," *Appl. Energy*, vol. 121, pp. 149–158, 2014.
- [153] A. Swarnkar, N. Gupta, and K. R. Niazi, "Adapted ant colony optimization for efficient reconfiguration of balanced and unbalanced distribution systems for loss minimization," *Swarm Evol. Comput.*, vol. 1, no. 3, pp. 129–137, 2011.
- [154] H. R. Esmaeilian and R. Fadaeinedjad, "Optimal reconfiguration and capacitor allocation in unbalanced distribution network considering power quality issues," in *22nd Int. Conf. and Exhibition on Electricity Distribution (CIRED 2013)*, Stockholm, Jun. 2013.

- [155] S. Ghasemi, "Balanced and unbalanced distribution networks reconfiguration considering reliability indices," *Ain Shams Eng. J.*, vol. 9, no. 4, pp. 1567–1579, 2018.